A Review of Structural Health Monitoring Literature: 1996-2001

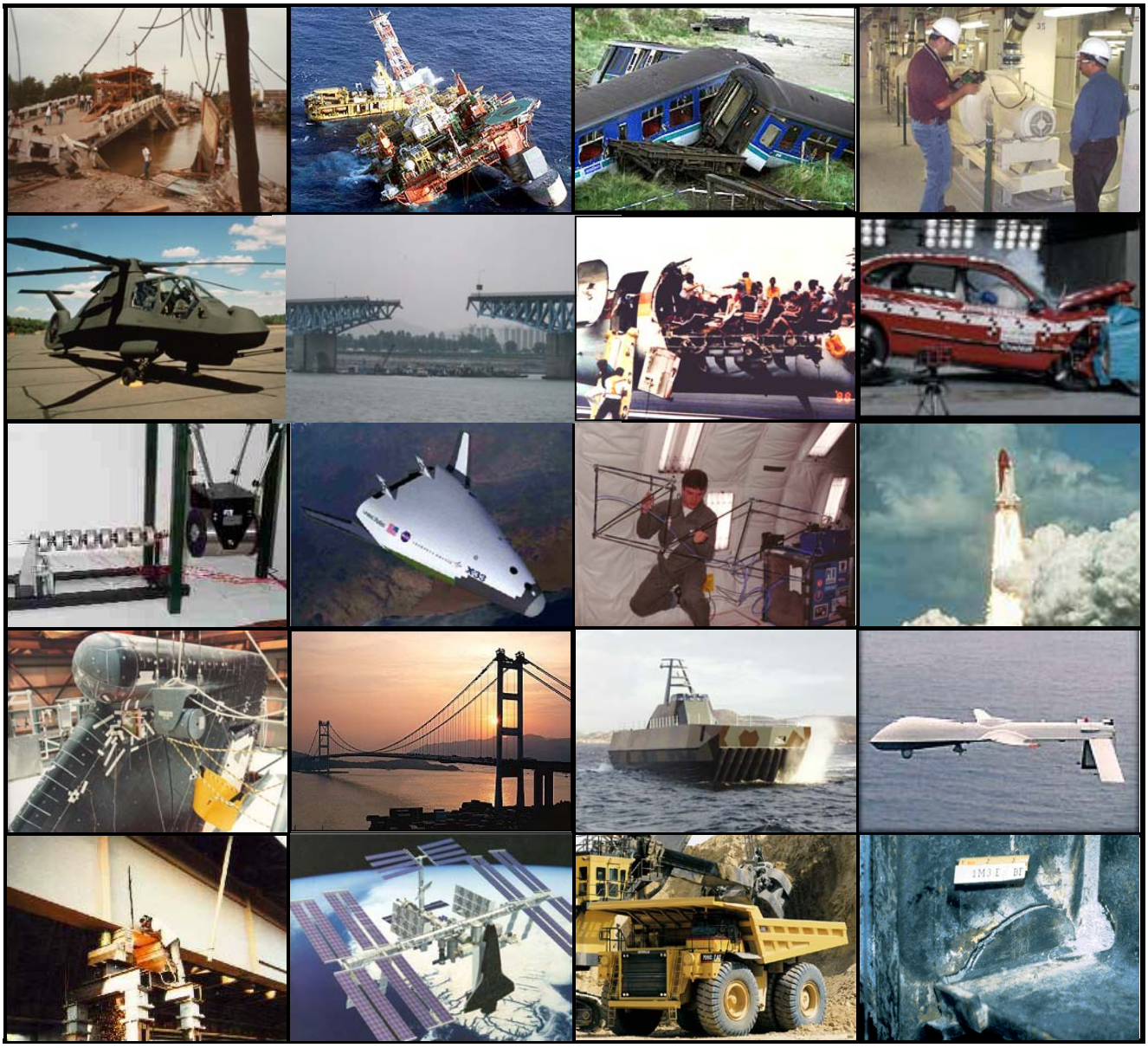

Los Alamos National Laboratory is operated by the University of California for the United States Department of Energy under contract W-7405-ENG-36.

Cover: These photos show civil infrastructure, aircraft, and mechanical systems where structural health monitoring system can be deployed. Starting from the top left, the structures are:

1. Bridge failure from soil liquefaction during a 1990 earthquake in the Philippines.
2. The failure of the Heidrun offshore oil platform near Brazil (Courtesy of Conoco, Inc.)
3. The 1250 BST Londonderry to Belfast train came off the line as it was approaching the Downhill tunnel near Castlerock, UK on June 4th, 2002. (Courtesy of BBC news)
4. Intel Pentium III fabrication facility in Rio Grande, New Mexico. Unpredicted shut-down of this facility can cast Intel $10-15 US million dollars per hour. (Courtesy of Intel, Inc.)
5. Boeing-Sikorsky Rah-66 Comanche Stealth Helicopter. Recently, Health & Usage Monitoring Sysme (HUMS) for rotorcraft has been initiated by Boeing, Sikorsky, Bell, NASA, US Army & Navy, and FAA. (Courtesy of United Technologies, Inc.)
6. One span of the Sung-Soo Grand Bridge over the Han River in Seoul, South Korea fell into the river, killing 20 people and injuring about 30 people. This bridge had pin connections at the span connection points and the linkage pins broke up due to heady traffic. (Courtesy of Seoul National University)
7. 1988 Aloha Airlines failure from fatigue cracks in fuselage connections.
8. The offset crash test performed on TOYOTA AVALON. The air bags of modern automobiles are deployed when the built-in Micro-Electro-Mechanical System (MEMS) accelerometers sense impacts beyond a certain threshold value. Similar MEMS accelerometers can be used for vibration-based damage detection applications. (Courtesy of Toyota, Inc.)
9. A five degrees-of-freedom spring-mass system tested at Los Alamos National Laboratory as part of Los Alamos Dynamics Summer School Program (www.lanl.gov/projects/dss).
10. Lockheed-Martin X-33 Reusable Launch Vehicle (NASA concept art: Courtesy of NASA)
11. Zero-gravity test of a lightweight space truss structure conducted at University of Houston. (Courtesy of University of Houston)
12. Space Shuttle Launch (NASA Photo: Courtesy of NASA)
13. Modal Test of Space Shuttle Vertical Stabilizer (Courtesy of University of Houston)
14. The Golden Gate Bridge in San Francisco. A comprehensive inspection of the Golden Gate Bridge main cables and associated north and south anchorages and tie-downs has been completed at a cost of $226,900 in 1998. (Courtesy of Golden Gate Bridge, Highway and Transportation District)
15. The surface-effect fast patrol boat is a pre-series fast patrol boat built by Kvaerner Mandal in Norway. The fiber optic sensor data were acquired as part of a joint research effort between the Norwegian Defense research Establishment and the Naval Research Laboratory. These data were previously analyzed by LANL staff. (Courtesy of Navel Research Laboratory)
16. The unmanned aerial vehicle Predator, manufactured by General Atomics Aeronautical Systems of San Diego, has been recently modified to carry guided missiles. The additional weight poses increased stress concentration near the connection of the wings to the fuselage. Therefore, General Atomics and US Air Force have shown interest in monitoring operation load conditions and aerodynamics of the UAV Predator. (Courtesy of ABC news)
17. Simulated damage was introduced to one girder of the I-40 bridge in New Mexico as part of an FHWA-funded structural health monitoring study.
18. Concept of Space Shuttle docked to International Space Station (NASA Concept Art, Courtesy of NASA)
19. Caterpillar's 789C is designed for hauling in mining and construction applications. Many of Caterpillar's equipment products have some form of load monitoring systems. (Courtesy of Caterpillar Inc.)
20. A fracture damage to the welded connection in a moment-resisting steel frame caused by 1994 Northridge Earthquake. Many buildings in North California experienced similar damage, but some damage was undetected until it was discovered by accident. (Courtesy of Stanford University)

CONTENTS

TABLE OF FIGURES

A Review of Structural Health Monitoring Literature: 1996–2001

by

Hoon Sohn, Charles R. Farrar, Francois M. Hemez, Devin D. Shunk,
Daniel W. Stinemates, and Brett R. Nadler

ABSTRACT

This report is an updated version of the previous literature review report (LA-13070-MS) entitled "Damage Identification and Health Monitoring of Structural and Mechanical Systems from Changes in Their Vibration Characteristics: A Literature Review" by S.W. Doebling, C.R. Farrar, M.B. Prime, and D.W. Shevitz. This report contains new technical developments published between 1996 and 2001 in the discipline of structural health monitoring. The reviewed articles first are organized following the statistical pattern recognition paradigm reported in Farrar and Doebling (1999). This paradigm can be described as a four-part process: (1) Operational Evaluation, (2) Data Acquisition, Fusion, and Cleansing, (3) Feature Extraction and Information Condensation, and (4) Statistical Model Development for Feature Discrimination. The reviewed articles are then categorized by type of applications, which include beams, truss, plates, bridges, aerospace structures, and composite structures. Other useful resources for the structural health monitoring (SHM) community such as SHM-related projects, web sites, conferences, and technical journals are listed. This report concludes by summarizing the current state of the art of SHM technologies and by identifying future research areas necessary to advance the SHM field.

1. INTRODUCTION

1.1 Objectives and Scope

This review summarizes structural health monitoring studies that have appeared in the technical literature between 1996 and 2001. The primary purpose of this review is to update a previous literature review (Doebling et al. 1996) on the same subject. A condensed version of this previous review was published in the *Shock and Vibration Digest* (Doebling et al. 1998). As with these previous documents, this summary will not address structural health monitoring applied to rotating machinery, often referred to as *condition monitoring.* Condition monitoring of rotating machinery is somewhat mature having made the transition from a research topic to actual practice. This subject has its own body of literature and its own conferences that are for the most part distinct from those associated with general structural health monitoring. The readers are referred to numerous books on this subject, samples of which are included at the end of this review's reference list. In addition, local nondestructive testing techniques are not covered in this review. Instead, this review, as well as the previous one, focuses on more global structural health monitoring methods.

This review begins by defining the term *damage* as it is used in the context summarized herein. Next, the structural health monitoring process is defined in terms of a statistical pattern recognition paradigm (Farrar and Doebling 1999). The use of this paradigm in the literature review represents a significant change in the way this review is organized compared to the previous one. The critical issues for this technology that were identified at the completion of the previous review are then briefly summarized. In the first part of the review, the literature is summarized in terms of how each study fits into the statistical pattern recognition paradigm. In the second portion, the literature is summarized with respect to the various applications that have been reported. Particular attention to the success obtained in identifying damage is made in this portion of the review. This review concludes by attempting to summarize progress that has been made with regard to critical issues identified in the previous review and identifies new issues as they become apparent from the literature reviewed herein.

1.2 Definition of Damage

In the most general terms, damage can be defined as changes introduced into a system that adversely affects its current or future performance. Implicit in this definition is the concept that damage is not meaningful without a comparison between two different states of the system, one of which is assumed to represent the initial, and often undamaged, state. This review is focused on the study of damage identification in structural and mechanical systems. Therefore, the definition of damage will be limited to changes to the material and/or geometric properties of these systems, including changes to the boundary conditions and system connectivity, which adversely affect the current or future performance of these systems. As an example, a crack that forms in a mechanical part produces a change in geometry that alters the stiffness characteristics of that part. Depending on the size and location of the crack and the loads applied to the system, the adverse effects of this damage can be either immediate or may take some time before they alter the system's performance. In terms of *length scales*, all damage begins at the material level and then under appropriate loading scenarios progresses to component and system level damage at various rates. In terms of *time scales*, damage can accumulate incrementally over long periods of time such as that associated with fatigue or corrosion damage accumulation. Damage can also result from scheduled discrete events such as aircraft landings and from unscheduled discrete events such as an earthquake or enemy fire on a military vehicle.

The basic premise of most damage detection methods is that damage will alter the stiffness, mass, or energy dissipation properties of a system, which in turn alter the measured dynamic response of the system. Although the basis for damage detection appears intuitive, its actual application poses many significant technical challenges. The most fundamental challenge is the fact that damage is typically a local phenomenon and may not significantly influence the lower-frequency global response of a structure that is normally measured during vibration tests. Stated another way, this fundamental challenge is similar to that found in many engineering fields where there is a need to capture the system response on scales of widely varying length, and such system modeling has proven difficult. Another fundamental challenge is that in many situations damage detection must be performed in an *unsupervised learning* mode. Here, the term *unsupervised learning* implies that data from damaged systems are not available. These challenges are supplemented by many practical issues associated with making accurate and

repeatable dynamic response measurements at a limited number of locations on complex structures often operating in adverse environments.

Environmental and operational variations, such as varying temperature, moisture, and loading conditions affecting the dynamic response of the structures cannot be overlooked either. In fact, these changes can often mask subtler structural changes caused by damage. For instance, Farrar et al. (1994) performed vibration tests on the I-40 Bridge over the Rio Grande in New Mexico, USA, to investigate if modal parameters can be used to identify structural damage within the bridge. Four different levels of damage are introduced to the bridge by gradually cutting one of the bridge girders as shown in Figure 1. The change of the bridge's fundamental frequency is plotted with respect to the four damage levels as shown in Figure 2. Because the magnitude of the bridge's natural frequency is proportional to its stiffness, the decrease of the frequency is expected as the damage progresses. However, the results in Figure 2 belie the intuitive expectation. In fact, the frequency value increases for the first two damage levels and then eventually decreases for the remaining two damage cases. Later investigation revealed that, besides the artificially introduced damage, the ambient temperature of the bridge played a major role in the variation of the bridge's dynamic characteristics. Other researchers also acknowledged potential adverse effects of varying operational and environmental conditions on vibration-based damage detection (see Figure 3) (Cawley 1997, Ruotolo and Surace 1997b, Helmicki et al. 1999, Rohrmann et al. 1999, Cioara and Alampalli 2000, and Sohn et al. 2001).

(a) Introduction of damage in one of the bridge girders by electric saw cutting.

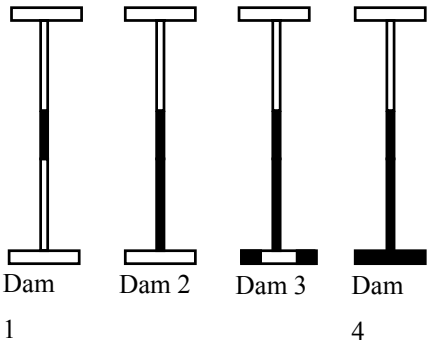

(b) Four levels of damage introduced at the girder (the shaded area represents a reduced cross-section).

Figure 1. Damage Detection Study of the I-40 Bridge over the Rio Grande in New Mexico, USA.

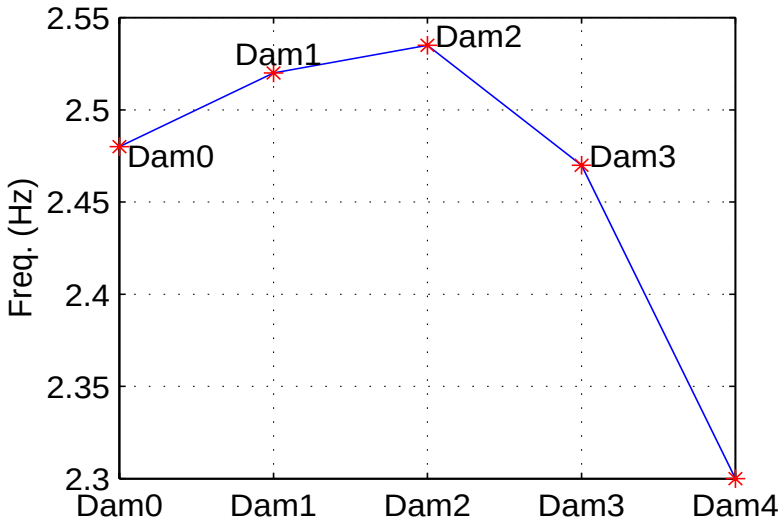

Figure 2. The fundamental frequency change of the I-40 Bridge as a function of the four damage levels shown in Figure 1.

1.3 Structural Health Monitoring Process

The process of implementing a damage detection strategy for aerospace, civil, and mechanical engineering infrastructure is referred to as *Structural Health Monitoring (SHM)*. *Usage monitoring* (UM) attempts to measure the inputs to and responses of a structure before damage so that regression analysis can be used to predict the onset of damage and deterioration in structural condition. *Prognosis* is the coupling of information from SHM, UM, current environmental and operational conditions, previous component and system level testing, and numerical modeling to estimate the remaining useful life of the system.

This review will summarize literature that primarily addresses the SHM problem. The SHM process involves the observation of a system over time using periodically sampled dynamic response measurements from an array of sensors, the extraction of damage-sensitive features from these measurements, and the statistical analysis of these features to determine the current state of the system's health. For long-term SHM, the output of this process is periodically updated information regarding the ability of the structure to perform its intended function in light of the inevitable aging and degradation resulting from operational environments. After extreme events, such as earthquakes or blast loading, SHM is used for rapid condition screening and aims to provide, in near real time, reliable information regarding the integrity of the structure.

The authors believe that the SHM problem is fundamentally one of statistical pattern recognition. Therefore, the damage detection studies reviewed herein are summarized in the context of a statistical pattern recognition paradigm (Farrar and Doebling 1999). This paradigm can be described as a four-part process: (1) Operational Evaluation, (2) Data Acquisition, Fusion, and Cleansing, (3) Feature Extraction and Information Condensation, and (4) Statistical Model Development for Feature Discrimination. The process is described in detail below.

1.3.1 Operational Evaluation

Operational evaluation answers four questions regarding the implementation of a structural health monitoring system:

1) What are the economic and/or life safety motives for performing the monitoring?
2) How is damage defined for the system being monitored?
3) What are the conditions, both operational and environmental, under which the system to be monitored functions?
4) What are the limitations on acquiring data in the operational environment?

Operational evaluation begins to define why the monitoring is to be done and begins to tailor the monitoring to unique aspects of the system and unique features of the damage that is to be detected.

1.3.2 Data Acquisition, Fusion, and Cleansing

The data acquisition portion of the structural health monitoring process involves selecting the quantities to be measured, the types of sensors to be used, the locations where the sensors should be placed, the number of sensors, sensor resolution, bandwidth, and the data acquisition/storage/transmittal hardware. This process is application specific. Economic considerations play a major role in these decisions. Another consideration is how often the data should be collected. In some cases, it is adequate to collect data immediately before and at periodic intervals after a severe event. However, if fatigue crack growth is the failure mode of concern, it is necessary to collect data almost continuously at relatively short time intervals.

Because data can be measured under varying conditions, the ability to normalize the data becomes very important to the SHM process. For instance, the measured fundamental frequency of the Alamosa Canyon Bridge in New Mexico varied approximately 5% during a 24-hour test period. Because the bridge is approximately aligned in the north and south direction, there was a large temperature gradient between the west and east sides of the bridge deck throughout the day. *Data normalization* is a procedure to "normalize" data sets so that signal changes caused by operational and environmental variations of the system can be separated from structural changes of interest, such as structural deterioration or degradation. One of the most common procedures is to normalize the measured responses by the measured inputs. When environmental or operating-condition variability is an issue, the need can arise to normalize the data in some temporal fashion to facilitate the comparison of data measured at similar times of an environmental or operational cycle. An alternative is to normalize the data by direct measurements of the varying environmental or operational parameters. Sources of variability in the data-acquisition process and with the system being monitored need to be identified and minimized to the extent possible. In general, not all sources of variability can be eliminated. Therefore, it is necessary to make the appropriate measurements so that these sources can be statistically quantified.

Data fusion as a discipline emerged as a result of defense organizations attempting to formalize procedures for integrating information from disparate sources (Klein 1999). The objective was to determine battlefield situations and assess threats on the basis of data coming in from numerous different sources. The philosophy of data fusion was quickly recognized to have broader applications. The purpose of data fusion is to integrate data from a multitude of sensors with the objective of making a more robust and confident decision than is possible with any one sensor alone. In many cases, data fusion is performed in an unsophisticated manner, as when one examines relative information between various sensors. At other times, such as those provided by artificial neural networks, complex analyses of information from sensor arrays are used in the data-fusion process.

Figure 3. The measured fundamental frequency of this Alamosa Canyon Bridge in New Mexico varied approximately 5% during a 24-hour test period. This variation emphasizes the importance of data normalization. (Sohn et al. 2001)

Data cleansing is the process of selectively choosing data to accept for, or reject from, the feature selection process. The data cleansing process is usually based on knowledge gained by individuals directly involved with the data acquisition. Manual signal processing techniques such as filtering and decimation can be viewed as data-cleansing procedures applied to data acquired during dynamic tests.

1.3.3 Feature Extraction and Information Condensation

The area of the SHM that receives the most attention in the technical literature is feature extraction. Feature extraction is the process of identifying damage-sensitive properties, derived from the measured vibration response, which allows one to distinguish between the undamaged and damaged structure. The best features for damage detection are typically application specific. Numerous features are often identified for a structure and assembled into a feature vector. In general, a low-dimensional feature vector is desirable. It is also desirable to obtain many samples of the feature vectors. There are no restrictions on the types or combinations of data contained in the feature vector. As an example, a feature vector may contain the first three resonant frequencies of the system, the time when the measurements were made, and a temperature reading from the system.

A variety of methods is employed to identify features for damage detection. Past experience with measured data from a system, particularly if damaging events have been previously observed for that system, is often the basis for feature selection. Numerical simulation of the damaged system's response to postulated inputs is another means of identifying features. The application of engineered flaws, similar to ones expected in actual operating conditions, to laboratory specimens can identify parameters that are sensitive to the expected damage. Damage-accumulation testing, during which structural components of the system under study are subjected to a realistic loading, can also be used to identify appropriate features. Fitting linear or nonlinear, physical-based, or nonphysical-based models of the structural response to measured data can also help identify damage-sensitive features.

The implementation and diagnostic measurement technologies needed to perform SHM typically produce a large amount of data. Almost all feature extraction procedures inherently perform some form of data compression. Data compression into feature vectors of small dimension is necessary if accurate estimates of the feature's statistical distribution are to be obtained. In addition, condensation of the data is advantageous and necessary, particularly if comparisons of many data sets over the lifetime of the structure are envisioned. Because data may be acquired from a structure over an extended period of time and in an operational environment, robust data-reduction techniques must retain sensitivity of the chosen features to the structural changes of interest in the presence of environmental and operational variability. Note that the data-fusion process previously discussed can also be thought of as a form of information condensation.

1.3.4 Statistical-Model Development for Feature Discrimination

The portion of the structural health-monitoring process that has received the least attention in the technical literature is the development of statistical models to enhance the SHM process. Almost none of the hundreds of studies summarized in Doebling et al. (1996, 1998) make use of any statistical methods to assess if the changes in the selected features used to identify damaged systems are statistically significant. Statistical model development is concerned with the implementation of the algorithms that operate on the extracted features to quantify the damage state of the structure. The algorithms used in statistical-model development usually fall into three categories. When data are available from both the undamaged and damaged structure, the

statistical pattern-recognition algorithms fall into the general classification referred to as *supervised learning*. *Group classification* and *regression analysis* are supervised learning algorithms. *Unsupervised learning* refers to the class of algorithms that are applied to data not containing examples from the damaged structure. In general, some form of *outlier analysis* (Barnett and Lewis 1994) must be applied for unsupervised SHM.

The damage state of a system can be described as a five-step process along the lines of the process discussed in Rytter (1993). The damage state is described by answering the following questions:

1) Is there damage in the system (existence)?
2) Where is the damage in the system (location)?
3) What kind of damage is present (type) ?
4) How severe is the damage (extent)?
5) How much useful life remains (prognosis)?

Answers to these questions in the order presented represents increasing knowledge of the damage state. The statistical models are used to answer these questions in an unambiguous and quantifiable manner. Experimental structural-dynamics techniques can be used to address the first two questions in either an unsupervised or supervised learning mode. To identify the type of damage, data from structures with the specific types of damage must be available for correlation with the measured features and, hence, a supervised learning approach must be taken. Analytical models are usually needed to answer the fourth and fifth questions unless examples of data are available from the system (or a similar system) when it exhibits varying damage levels. Therefore, the fourth and fifth questions must be addressed in a supervised learning mode. In general, the fourth and fifth questions cannot be addressed without first identifying the type of damage present. Estimates of the future system loading are also necessary to completely address the fourth and fifth questions.

Finally, an important part of the statistical model development process is the testing of these models on actual data to establish the sensitivity of the selected features to damage and to study the possibility of false indications of damage. False indications of damage fall into two categories: (1) False-positive damage indication (indication of damage when none is present), and (2) False-negative damage indications (no indication of damage when damage is present). Although the second category is detrimental to the damage detection process and can have serious implications, false-positive readings also erode confidence in the damage detection process.

1.4 Summary of Previous Review

Doebling et al. (1996, 1998) provide one of the most comprehensive reviews of the technical literature concerning the detection, location, and characterization of structural damage through techniques that examine changes in measured structural-vibration response. The report first categorizes the methods according to required measured data and analysis techniques. The analysis categories include changes in modal frequencies, changes in measured mode shapes (and their derivatives), and changes in flexibility coefficients derived from measured mode shapes and modal frequencies. Methods that use numerical model updating and the detection of nonlinear response are also summarized. The applications of the various methods to different types of engineering problems are categorized by type of structure and are summarized. The types of structures include beams, trusses, plates, shells, bridges, offshore platforms, other large civil structures, aerospace structures, and composite structures. The report concludes by summarizing critical issues for future research in the area of damage identification as described below.

One issue of primary importance is the dependence on prior analytical models and/or prior test data for the detection and location of damage. Many algorithms presume access to a detailed finite element model (FEM) of the structure, while others presume that data sets from the undamaged structure are available. Often, the unavailability of this type of data can make a method impractical for certain applications. Although it is doubtful that all dependence on prior models and data can be eliminated, certainly steps can and should be taken to minimize the dependence on such information.

Almost all of the damage-identification methods reviewed in this previous report rely on linear structural models. Further development of methods that have an enhanced ability to account for the effects of nonlinear structural response has the potential to enhance this technology significantly. An example of such a response would be the opening and closing of a fatigue crack during cyclic loading either in an operational situation or in the case of a forced-vibration test. Many methods are inherently limited to linear model forms, and therefore cannot account for the nonlinear effects of such a damage scenario. Another advantage of methods that detect nonlinear structural response is that they can often be implemented without detailed prior models if the structure's response can be assumed to be previously linear in its undamaged state.

The number and location of measurement sensors is another important issue that has not been addressed to any significant extent in the previously reviewed literature. Many techniques, which appear to work well in example cases, actually perform poorly when subjected to the measurement constraints imposed by actual testing. Techniques considered for implementation in the field should demonstrate that they could perform well under the limitations of a small number of measurement sensors and under the constraint that the sensor locations be determined *a priori*.

An issue that is a point of controversy among many researchers is the general level of sensitivity that modal parameters have to small flaws in a structure. Much of the evidence on both sides of this disagreement is anecdotal because it is only demonstrated for specific structures or systems and not proven in a fundamental sense. This issue is important for the development of SHM techniques because the user of such methods needs to have confidence that the damage will be recognized while the structure still has sufficient integrity to allow repair. A related issue is the discernment of changes in the modal properties resulting from damage from those caused by natural variations in the measurements. A high level of uncertainty in the measurement will prevent the detection of a small level of damage.

With regard to long-term health monitoring of structures such as bridges and offshore platforms, the need to reduce the dependence upon artificial excitation mechanisms is noted by many researchers. The ability to use vibrations induced by ambient environmental or operating loads for the assessment of structural integrity is an area that the previous review identified for further investigation.

The literature also has scarce instance of studies where different health-monitoring procedures are compared directly by applying them to a common data set. Some data sets, such as the NASA 8-Bay data set and the I-40 Bridge data set, have been analyzed by many different authors using different methods, but the relative merits of these methods and their success in locating the damage have not been directly compared in a sufficiently objective manner.

Overall, it was the opinion of the authors at the time of completion of the previous review that sufficient evidence exists to promote the use of measured vibration data for the detection of damage in structures, using both forced-response testing and long-term monitoring of ambient signals. It is clear, though, that the literature in general needs to be more focused on the specific applications and industries that would benefit from this technology, such as the health monitoring of bridges, offshore oil platforms, airframes, and other structures with long design life. Additionally, research should be focused more on testing of real structures in their operating environment, rather than laboratory tests of representative structures. Because of the magnitude of such projects, more cooperation will be required between academia, industry, and government organizations. If specific techniques can be developed to quantify and extend the life of structures, the investment made in this technology will clearly be worthwhile.

Friswell and Penny (1997) discuss some limitations of various SHM methods. In their opinion, the most significant limitations of SHM methods are the systematic error between a model and a structure as well as the nonstationarity of the structure. The limitation with low frequency vibration data manifests itself in the ability to locate damage considering the global nature of the modal parameter and the local nature of the damage. Also, they state that it is necessary to test any method on both simulated and real data. In conclusion, the authors give their opinion that robust identification techniques able to locate damage on realistic data sets are still a long way from reality.

Aktan et al. (1999) cite some critical issues for SHM, particularly with civil infrastructure, which need to be resolved for deploying reliable SHM systems. Among these issues, the authors state that an integrated approach between academia, government, and industry is needed as well as an engineering approach that goes beyond the realm of any one branch of the engineering disciplines. It is also noted that there are considerable differences in the policies and programs of various Department of Transportation branches throughout the United States. Furthermore, organizations that can enhance integration between the design and performance of structures are greatly needed. The authors state the need for standards that govern sensor calibration and documentation of stochastic information regarding the measurement of certain environmental parameters. The authors emphasize a need for reliable standards for retrofitting structures to ensure that the retrofit accomplishes its desired task of strengthening the structures. Finally, Aktan et al. (1999) question whether only one damage-sensitive feature or a vector of various features is suitable for practical SHM systems. They cite a number of possible causes of damage, and the inherent nonstationarity of those causes implies that both local and global approaches to SHM must be investigated simultaneously.

2. OPERATIONAL EVALUATION

In the next four sections (Sections 2-5), the reviewed articles are categorized based on their relevancy to the four-step process of the statistical pattern recognition paradigm previously described: (1) Operational Evaluation, (2) Data Acquisition, Fusion and Cleansing, (3) Feature Extraction and Information Condensation, and (4) Statistical Model Development for Feature Discrimination. Then, the papers are again summarized according to the specific applications in Section 6. This section starts with papers that specifically address operational evaluation issues.

2.1 Economic and/or Life-Safety Issues

Economic and life-safety issues are the primary driving force behind the development of structural health-monitoring technology. Cawley (1997) notes that pipeline corrosion is a major problem for the oil, chemical, and petrochemical industries. The cost associated with removal of pipe insulation for visual inspection is prohibitive, thus motivating research into the use of Lamb waves for the detection of corrosion under insulation. Furthermore, Halfpenny (1999) mentions the oil industry's need for rapid fatigue analysis in the 1980s when large jacket platforms were being designed and fatigue of these structures was an important issue. Frequency-based methods were investigated because the dynamic wave and wind-load frequency data were readily available.

Garibaldi, Marchesiello, and Gorman (1999) state the need for accurate numerical models for bridge applications in which some modal frequencies are closely spaced. The authors note that the closely spaced frequencies can get obscured during the modal analysis of measurement data from limited measurements on the bridge-span sides and can lead to poor analysis results. Furthermore, because of the inaccessibility of the bridge's underdeck or the cost of closing the bridge to instrument measurements on the roadway, it is difficult to take dynamic measurements under the bridge or in the middle of a lane traversing the bridge.

There is a great emphasis placed on optimizing designs to reduce the weight of some structures and yet still provide required strength. The aerospace industry as well as the shipbuilding industry concentrates a lot of its efforts on design optimization. Wang and Pran (2000) use the

latter industry as an example to explain why SHM systems are becoming even more important for structures, which have reduced strength capacity as a tradeoff with weight reduction.

Noting that the number of aircraft is increasing each year worldwide, Boller (2000) discusses various issues related to SHM of the aircraft to ensure the reliability of these aircraft. He notes that the number of civil and military aircraft that were 15 years or older was approximately 4,600 worldwide in 1997, while the number older than 25 years was 1,900. Those numbers increased to 4,730 and 2,130 by 1999, respectively. Boller also notes that some military aircraft are over 40 years old with a service life of 50 years. He also mentions that the primary damage in aircraft structures results from fatigue cracks initiated at holes of joints and fasteners. Some safety-motivated programs such as the Aircraft Structural Integrity Program (ASIP) and Supplemental Structural Inspection Program (SSIP) are mentioned in this very general overview of aircraft SHM.

Likewise, Graue, and Reutlinger (2000) provide a general overview of SHM for reusable rocket launchers. They discuss various nondestructive inspection techniques such as thermography, shearography (surface stress monitoring), and laser ultrasonics. The authors mention different sensor systems that are being investigated to monitor fuel systems, the turbo machinery, and the thrust chamber of the launchers. Graue and Reutlinger state that in-flight sensor data can aid the ground inspection of the rocket launchers and reduce the cost of inspection while improving operational reliability.

Sikorsky and Stubbs (1997) discuss the goals of bridge management systems including SHM that the American Association of State Highway and Transportation Officials (AASHTO) intend to implement. In particular, the authors advocate a quality-management initiative directed toward the construction stage of bridge structures coupled with modal-based nondestructive damage evaluation (NDE) throughout the lifespan of the bridges. These goals are to help engineers and decision makers determine when and where to spend funds so that structural safety is enhanced, the existing infrastructure is preserved, and the needs of commerce and the motoring public are satisfied. This topic is also discussed in another article (Sikorsky 1997).

In another article, Sikorsky (1999) discusses an evaluation system of the California Department of Transportation (CALTRANS) for reliability, durability, and serviceability of a structure. This

evaluation system enables upper management to assess the costs of repair and maintenance of bridges and highways and to allocate resources efficiently. Sikorsky suggests a loss function, L_{ij}, as a function of a structure's change in stiffness or boundary conditions,

$$L_{ij} = m_i[k_j^{current} - k_j^{baseline}] \ ,$$

where m_i is a loss coefficient related to the *i*th failure mode or *i*th hazard, which has been previously defined, and $k_j^{current}$ and $k_j^{baseline}$ are the current and baseline stiffness of the *j*th element, respectively. This formula allows one to evaluate the economic loss in quantitative terms when a structure is repaired or monitored for damage. The lost function, L_{ij}, represents an expected loss when the *j*th system component fails to resist the *i*th failure mode. Then, when deciding on whether or not to implement a SHM scheme, the following corporate performance measure (CMP) of the SHM scheme can be used,

$$\text{CPM} = \frac{Capacity}{\sum_{i=1}^{n}\sum_{j=1}^{m}[C_{ij} + L_{ij}]} \ ,$$

where the *Capacity* term in the numerator gives a measure of the structure's remaining usage and C_{ij} represents the cost of the structure's component *j* to resist the *i*th failure mode or hazard. The result of Sikorsky's analysis is a methodology that provides a logical connection between the allocation of resources and structural deterioration.

Helmicki et al. (1999) estimate the U.S. investment in infrastructure at $20 trillion and state that inadequacies in the nation's transportation system may be reducing the annual growth rate in gross domestic product by as much as 1%. Therefore, the annually compounding economic impact of the nonoptimal operation and maintenance of our civil infrastructure may reach a significantly higher level than that of a major natural disaster such as an east coast hurricane. Helmicki et al. also state that the U.S. Department of Transportation estimates a $100 billion backlog for bridge repair. The authors then proceed to discuss some opportunities and issues for adapting information technology to civil SHM.

British Petroleum states that the economic benefit of a SHM system for one of their offshore oil platforms was a savings of £50 million. Indeed, Solomon, Cunnane, and Stevenson (2000), relate that the structure's platform jacket standing 180 m above the sea floor weighed 21,000 tons and supported a 30,000-ton topside. The dynamic loads on the jacket from the waves were severe enough to allow the measurement of the waves' impact and the structure's response, including bending moments and accelerations. This system operated for six years, and the result was that the structure was indeed designed too conservatively. Subsequent structures were therefore designed less conservatively with a cost savings.

According to Wang, Satpathi, and Heo (1997), the Federal Highway Administration estimates that nearly 35% of all bridges in the United States (236,000 out of 576,000) are either structurally or functionally deficient. The cost of repair or rebuilding lies in the billions of dollars. Effective SHM methods could reduce this cost while providing higher levels of safety for users during repair or assessment.

Chang (1999) mentions that approximately 44% of the aircraft in the U.S. Air Force are 20 years old or older. Some aircraft, such as the EF-11A, require over 8,000 man hours of maintenance per year. In addition, Chang quotes that the cost of maintaining an F-18 is approximately $35 million per year based on 33 hours of flight per aircraft per month. The automation of just one logistics function could result in an approximate savings of $100,000 per year in manpower and equipment.

Bartelds (1997) states that the direct costs of carrying out preventive inspections and the indirect costs associated with interrupted service provide a strong stimulus for developing a SHM system for aircraft. A SHM system for aircraft can reduce the repair and maintenance costs in two ways. First, the direct costs related to the repair can be reduced by detection damage at a very early stage. Alternatively, the repair can be postponed until the next scheduled major overhauls to reduce indirect costs. Furthermore, a recent study of modern fighter aircraft inspection programs reveals that about 40% of the current inspection time can be saved by using smart monitoring systems. However, the author believes that safety requirements do not justify the development of SHM systems because the current design and certification standards already guarantee an extremely high level of structural reliability.

2.2 Definition of Damage

In many studies reviewed in Doebling and Farrar (1997), damage has been intentionally introduced into a structure in an effort to simulate damage without having to wait for such a damage to occur. In other cases, the authors postulate a damage-sensitive feature and then develop an experiment to demonstrate the effectiveness of this feature. In these cases, there is no need to formally define damage. Most laboratory investigations fall into this category. When a SHM system is deployed on an *in situ* structure, it is imperative that the investigators first clearly define and quantify the damage that they are looking for; then, that they can increase the likelihood that the damage will be detected with sufficient warning, and to make optimal use of their sensing resources.

Cawley (1997) uses Lamb waves to detect corrosion in pipelines. Not only does Cawley specify the type of damage, but he also quantifies the extent of detectable damage. In particular, the extent of damage is quantified as a value relative to the dimension of the pipe diameter and the pipe wall thickness, producing a dimensionless measure of damage extent. This definition of the damage to be detected directly influences many parameters in the test procedure.

Increasing recent demands for lightweight structures and high strength-to-weight ratio materials have motivated the use of anisotropic reinforced laminated composites. Zak et al. (1999) note that delamination is one of the most important failure modes for these composite materials. Such defects might be caused by poor process control during manufacturing, impact loading, or other hazardous service environments. The delamination also substantially reduces the stiffness and the buckling load capacity, which, in turn, influences the structure's stability characteristics. The effects of the contact forces between delaminated layers, the delamination length, and the delamination location on changes in natural frequencies of a plate are investigated. Jacob, Desforges, and Ball (1997) define four failure modes for carbon-fiber composites, namely fiber breakage, matrix cracking, fiber splitting, and delamination. The authors employ wavelet transforms of acoustic emission signals to identify these modes of failure.

Ruotolo and Surace (1997a and c) look for damage in the form of multiple cracks in test beams and note that there has not been much work in damage detection for beams with multiple cracks. More specifically, the authors introduce cracks into the cantilever beam in one or two locations.

On the other hand, some authors such as Rytter and Kirkegaard (1997) define damage simply as reduction in a bending stiffness, EI. Here, I is the moment of inertia of the beam's cross section, and E is the elastic modulus. Rytter and Kirkegaard then analyze the time history data from a four-story structure subjected to earthquake loading in the laboratory. The stiffness reduction of beams and columns are investigated in this study. Likewise, Mares et al. (1999) perform a similar analysis using the numerical model of the four-story structure that Rytter and Kirkegaard (1997) studied.

Onate, Hanganu, and Miquel (2000) conduct finite-element simulations of damaged concrete and reinforced concrete structures such as a nuclear-containment shell, a housing building, and the domes of St. Mark Basilica. The authors' interest is focused on the complex behavior of concrete, including concrete cracking, tension stiffening, and nonlinear multiaxial material properties. Particularly, finite element techniques are developed to permit a more rational analysis of cracking. They first define a local damage index as follows:

$$d_n = \frac{S_n - \overline{S}_n}{S_n} = 1 - \frac{\overline{S}_n}{S_n} \ ,$$

where S_n is the original cross section area, and $\overline{S}_n$ is the effective resisting area after crack formation. The local damage index, d_n, represents the surface density of cracking, and it is initially zero when the concrete is in its intact state. Based on this local damage index, a modified constitutive relation between stress and strain can be formulated. The modified constitutive model accounts for the reduction of the moment resisting area caused by the cracking, and the different response in tension and compression is taken into account. The damage index needs to be estimated at every stage of the deformation process. The authors claim that the progress of the damage index can be experimentally characterized from Young's modulus, tension and compression limit strength, and specific fracture energy obtained from uniaxial tests. Second, a global damage index is defined in terms of internal energies,

$$D = 1 - \frac{\overline{U}}{U} \ ,$$

where $\overline{U}$ and U are the total energy of the structure corresponding to the damaged and undamaged states. The state of the structure with regards to its final failure mechanism is estimated by the global-damage index, and the failure mechanism is identified by observing the local damage indices. For example, as damage progresses, the global-damage index approaches unity. If the global-damage index is governed by only a fraction of the substructures and becomes independent of the rest of the substructures, the damage region of the structure can be isolated.

Maeck, Abdel Wahab, and De Roeck (1998) present a sensitivity-based, model-updating technique to calculate the stiffness degradation of a damaged reinforced concrete beam,

$$S\,\Delta P = \Delta\theta \ ,$$

where $\Delta\theta$ is the discrepancy between the analytical and experimental modal parameters, ΔP is the perturbation of the design parameters to be estimated, and S is the Jacobian or sensitivity matrix consisting of the first derivative of the analytical modal parameters with respect to the design parameters. To simplify the above sensitivity-based updating, the authors develop a damage function that describes the damage pattern along the beam length using only a few representative parameters. In particular, the stiffness degradation is assumed to be of the following form:

$$E = E_o[1-(1-\alpha)\cos^2 t] \text{ and } t = \frac{\pi}{2}\left(\frac{x}{\beta L/2}\right)^n \ ,$$

where E_o is the initial Young's modulus; L is the length of the beam; x is the distance along the beam measured from the center line; α , β , and n are the damage parameters to be updated; and α represents the level of stiffness reduction at the center of the beam. No damage is present when α equals 1. The relative length of the damaged zone with respect to the length of the beam is characterized as β . The exponent n characterizes the variation of the Young's modulus from the beam's center to the end of the damaged zone. If n is larger than one, a flat damage pattern is produced. Otherwise, a steep pattern is obtained. The authors claim that using this damage function not only reduces the design parameter but only represents a realistic damage pattern.

2.3 Environmental and/or Operational Constraints

The effects of environmental variability on the measured dynamics response of structures have been addressed in several studies. Doebling and Farrar (1997) develop a statistical procedure that propagates variability in measured frequency response function (FRF) data and estimates the uncertainty bound of the corresponding modal properties. This study also shows the modal analysis results of Alamosa Canyon Bridge in New Mexico. The modal testing was performed at 2-hour increments for 24 hours. The first mode frequency was shown to vary approximately 5% during the 24-hour cycle and to be closely related to the temperature differential across the deck of the bridge.

Using an analytical model of a cantilever beam, Cawley (1997) compares the effect of crack formation on the resonant frequency to that of the beam's length. In this study, the crack is introduced at the fixed end of the cantilever beam, and the length of the beam is varied. This study is part of a general discussion on the limitations of using modal properties for damage diagnosis. His results demonstrate that the resonance-frequency change caused by a crack, which is 2% cut through the depth of the beam, is 40 times smaller that that caused by a 2% increase in the beam's length. The implication here is that changes in the structure's surroundings or boundary conditions such as thermal expansion can produce more significant changes in resonant frequencies than damage. Then, the authors propose to use the Lamb waves instead of vibration measurements to discern damage from a change in the boundary condition. In Lamb wave testing, the measurements are limited to the short time period between the generation of the wave and the onset of the first reflection signal at the boundaries. For an example of a beam, a wave is generated at one end of the beam, and the first echoes from the other end of the beam are monitored. Therefore, the sensitivity to the boundary conditions is reduced by excluding multiple reflections signals from the boundaries. Any additional reflection signals arriving before the boundary reflection would indicate the presence of damage. This Lamb wave testing is applied to detect delamination in a composite plate and corrosion under insulation in a chemical pipeline system.

Ruotolo and Surace (1997b) is one of the first few papers that explicitly acknowledges the possibility of having multiple baseline configurations. The authors note that structures under test can be subjected to alterations during normal operating conditions, such as changes in mass. To cope with this situation, a damage-detection method based on singular-value decomposition (SVD) is proposed to distinguish between changes in the working conditions and the onset of damage. Let $\mathbf{v}_i$ be the feature vector collected at n different normal configurations (i = 1, 2, …, n). When a new feature vector $\mathbf{v}_c$ is collected, the whole feature vectors can be arranged in a matrix **M**,

$$\mathbf{M} = [\mathbf{v}_1 \, \mathbf{v}_2 \ldots \mathbf{v}_n \, \mathbf{v}_c] \; .$$

If the structure is intact, the new feature vector $\mathbf{v}_c$ will be closed to one of the existing feature vectors $\mathbf{v}_i$, and the rank of the matrix **M** estimated by SVD should remain unchanged by adding $\mathbf{v}_c$ to **M**. On the other hand, if the structure experiences damage, the rank of the matrix **M** will increase by one.

Based on the premise that a unique frequency pattern exists for any given damage scenario, Williams and Messina (1999) identify the location and extent of damage by updating a finite-element model so that the finite-element model can match the measured resonance as closely as possible. The authors acknowledge the limitation of this approach when measurement errors and environmental effects result in frequency changes that mask the presence of damage. Because the lower modes are more susceptible to the environmental factors and less sensitive to damage, the environmental effect particularly becomes a significant problem when only a few lower modes are used.

Staszewski et al. (1999) demonstrate that temperature and ambient vibrations can have negative effects on the performance of piezoelectric sensors employed in composite plate tests. The authors show that detection of the delamination caused by impacts can be obscured by such temperature rises and vibrations. In particular, when an impact with 4 J of energy is combined with thermal heating, this thermal heating produces remarkable spikes at 0.5 kHz and 1.0 kHz of the strain spectrum. Although these spikes do not result in delamination, comparable spikes can be produced by 24 J of impact, which can definitely cause delamination.

Garibaldi, Marchisiello, and Gorman (1999) describe a situation in which operation constraints of a bridge testing can obscure damage-detection results. The authors state that the bridge testing using traffic excitations suffers from a lack of sufficient instrumentation. When normal traffic is used as an excitation source, only exterior sides of the bridge's main span can be instrumented, and other places (such as locations under the vehicle path or on the bottom of the deck) are rarely accessible unless a truck with a special crane is available. The limitation of measurement points becomes a bigger problem when closely spaced modes exist. To cope with this situation, they propose to use Canonical Variate Analysis to discern overlying modes and frequencies.

Wang and Pran (2000) briefly mention the issue of sensor installation. Their discussions focus on the mounting of fiber-optic Bragg grating sensors. Because the fiber-optic sensors are immune to electromagnetic fields and resistant to the harsh corrosive environment, the authors apply the fiber-optic sensors to the hull monitoring of a Norwegian naval vessel, which is conducted as part of the Composite Hull Embedded Sensor System (CHESS) project. One goal of the CHESS project is design verification. Modern ship design is based on finite element analysis (FEA) and the wave loading is estimated by means of scale-model tests, standard design rules, and computer simulation of various sea states. Then, the simulated response from FEA can be compared with the actual measurement data. For the complete design verification, the test data need to be recorded under various environmental and operational states of the vessel. The motions of the ship and the wave profile can be registered by a motion reference unit, a global positioning system (GPS) unit, inertial navigation system, and a wave radar. Finally, the authors address the need for developing onboard signal processing techniques for characterizing the hull response parameters and sea states.

Sohn and Farrar (2000) apply statistical-control charts, which are commonly used for quality control of manufacturing processes such as a chemical process, to damage diagnosis of a bridge column tested in a controlled laboratory environment. The objective is to identify the formation of a plastic hinge at the bottom of the column using acceleration time histories. The damage-sensitive features employed in this study are coefficients of an auto-regressive time prediction model, and the prediction model is estimated from measured time series data. The authors successfully identify the location of plastic hinges but also state that further investigation into the

influence of environmental effects is needed because the authors haven't attempted to distinguish damage from changes in the environment when both are present at the same time.

Calcada, Cunha, and Delgado (2000) make a brief description of the objectives of a research program underway at the University of Porto, Portugal, concerning the experimental and numerical assessment of the dynamic effects of road traffic on bridges. Although the detail of the numerical model is not provided in the authors' paper except that it is stochastic, the authors do mention that a new bridge over the Tagus River in Santarem, Portugal, has been used to experimentally verify the approach, and some preliminary results are provided. In addition, the authors perform a model-updating procedure to further increase the fidelity of the bridge model. The authors propose to consider different vehicle types with varying axles and suspension systems, various pavement roughnesses, and different traffic loads with varying traffic speeds in the numerical model.

When SHM methods are applied during extreme events such as seismic events, earthquake loading poses certain problems for SHM methods, which commonly rely on an accurate characterization of input excitations. Seismic excitations are transient in nature, and this transient behavior limits the performance of most SHM methods that are based on the stationary stochastic-excitation assumption. Furthermore, an earthquake excites only the low-frequency modes of a structure, and lasts for a short time period. Sakellariou and Fassois (2000) attempt to address these problems. First, a time prediction model using an output error estimator (Ljung 1999) is fit to the data obtained from a normal state of the structure. Then, this system identification procedure is repeated for the data obtained from a current state of the structure. Third, a statistical hypothesis test is conducted on the prediction-model parameters associated with the normal and current states. If the model parameters of the current state deviate significantly from these of the normal condition, the fault-detection algorithm signals the existence of defects. Finally, fault localization and magnitude estimation are based on a geometric formulation of fault mode hyperplanes (see Sadeghi and Fassois 1998 for details). The fault-mode hyperplanes are predetermined. When a hyperplane associated with the current state of the structure is computed, the fault mode is identified by comparing the distance between the current hyperplane and all the existing ones. The identified fault mode has the minimal

distance to the current hyperplane. Fault magnitude is estimated by measuring the distance between the current hyperplane and the hyperplane of the selected fault mode.

Cioara and Alampalli (2000) monitor three bridges in New York State from March 1993 to April 1995. Modal parameters are estimated to observe the effect of environmental conditions and structural deterioration over a long period of time. Normal traffic provides excitation sufficient for the identification of modal parameters. The response-time series generated by vehicle traffic consist of two components: (1) a free decay component of the bridge response and (2) a forced-response component induced by the applied excitation. Because the forced-response component is very complicated for use in modal-parameter identification, the authors use a variant of the random decrement technique (RDT) to remove the forced component and to keep only the free-decay component of the response signal. Then, modal parameters are estimated from the free-decay time series. The authors conclude that the variation of the modal parameters is attributed to environmental conditions such as temperature and humidity.

Pirner and Fischer (1997) separate mechanically induced loadings from thermally induced ones in a TV tower in Prague, Czechoslovakia. The researchers note that it is impossible to directly distinguish these loadings using time histories alone. They note, however, that temperature changes produce major and slowly changing stresses, while wind loads produce faster changes. The authors are then able to infer the temperature-induced loadings from a curve relating the number of stress cycles to the stress magnitude.

Helmicki et al. (1999) measure the effects of environmental stresses in a steel-stringer bridge while also recording traffic loads by means of a weigh-in-motion roadway scale. Those environmental stresses include those caused by the variation in temperature throughout the day and traffic-induced stresses. The foundation and substructures are instrumented with embedded concrete strain and temperature gauges, welded-pile strain gauges, and inclinometer conduit soil-pressure sensors. Relevant atmospheric effects at the site are monitored with a weather station. The steel structure is instrumented with weldable foil and vibrating wire-strain gauge mounted on the beams and intermediate crossbeams. A total of 642 channels of sensor data are available for bridge monitoring. Data transmission is wireless, and the data are collected at a central PC.

Some fabrication stresses were determined to range from 3 ksi to 15 ksi. These stresses are typically caused by heat cambering in the stringer web at midspan, dead load in the stringer flange at midspan caused by deck placement, and dead-load stresses in the cross beams caused by pouring of the deck. The authors find that the integral abutments and the welded connections for cross beams and bearing plates are responsible for inducing significant local stresses. Longitudinal stresses of approximately 850 psi are measured at the top rebar layer, and lateral stresses of approximately 550 psi are measured at the bottom rebar layer. These stresses are caused by concrete shrinkage, which results in a significant amount of cracking at the top and bottom deck surfaces. Finally, thermal stresses of up to 6 psi are observed in the stringer flange at the abutment from the daily temperature cycle. An important conclusion of these studies is that these stresses far exceed environmental stresses and stresses caused by recorded traffic, yet they are not explicitly in bridge design. Further information regarding the measurement of environmental data is discussed in Catbas et al. (1999) where the authors talk about related software and hardware issues.

Doebling, Farrar, and Cornwell (1997) measure temperatures to ascertain their effects on modal properties of the Alamosa Canyon Bridge in New Mexico, USA. A total of 52 data sets are recorded during the six days of testing. A series of modal tests are conducted every 2 hours over a 24-hour period to assess the change of modal properties as a function of ambient environmental conditions. In addition, various levels of attempted damage are introduced to the bridge, but the permitted alternation in the bridge does not result in noticeable changes in the modal properties.

Based on a three-year's continuous monitoring of the Westend Highway Bridge in Berlin, Rohrmann et al. (1999) seek to formulate a mathematical description of thermally induced frequency changes in the context of the SHM of bridges. The Westend Bridge is an eight-span, prestressed concrete bridge, which is 243 m long and consists of three-cell box girders. The bridge is supported by seven reinforced-concrete columns of hollow cross sections. The bridge abutments are reinforced-concrete crosswalls, and the bridge is built on a slab foundation. They note that temperature changes cause changes not only in the material properties of a structure but also in the reaction forces of supports when the structure is obstructed from expanding or contracting. A regression analysis of measured data shows that the frequencies of the first 12 modes vary between 0.75×10^{-2} Hz and 4.3×10^{-2} Hz per 1^{o}C change in the bridge

temperature. The results of the experiment show that the natural frequencies are linearly dependent on the measured temperatures. Specifically, they define the frequency change Δf as a function of the mean temperature T_o and temperature gradient ΔT as follows:

$$\Delta f = a_0 T_o + a_1 \Delta T \ ,$$

where the coefficients a_0 and a_1 are determined from a regression analysis of the measured frequency-temperature data.

Park, Cudney, and Inman (1999a) observe that with conventional modal-based SHM, changing environmental and operational conditions alter the structure's vibration signals. This change in environmental and operational conditions often leads to false assessments of structure damage. To overcome this problem, the authors use a piezoelectric transducer (PZT) bonded to the structure as an actuator and sensor, and compute the electrical impedance (or the transfer function) of the PZT. Then, the electrical impedance is shown related to the mechanical impedance of the localized region of the structure, and consequently is used to monitor the changes of local structural properties such as stiffness, mass, and damping. The nature of localized high-frequency excitation forces produced by the PZT makes this impedance method attractive to local damage diagnosis. The impedance method has been successfully applied to SHM of composite reinforced-concrete walls and to a quarter-scale bridge section. The size of the bridge is 1.8 m tall and has a weight of over 250 kg. Four PZT sensor/actuators are bonded on the critical connections to actively monitor the bridge. Three different operational and environmental conditions are imposed on the bridge to assess whether the impedance-based method can successfully identify damage in the presence of these changing conditions. The investigated operational and environmental variations include (1) natural variations of the signal over a long time period, (2) the bridge impacted by a hammer, and (3) a mass of 15 kg added near the joints being measured. Damage is induced by loosening various bolts 1/8 of a turn. With the proposed damage metric, the PZT sensors/actuators nearest the damage location detect the damage without affecting the other PZTs away from the damage location. Park et al. (1999) further develop a compensation technique to minimize the effect of environmental conditions, particularly keeping in mind the temperature effect, on the impedance-based technique.

Park, Cudney, and Inman (1999) discuss the application of mechanical impedance monitoring as a means of damage detection for high-temperature structures. The authors tested a bolted joint structure subject to a temperature range of 482°C to 593°C using high temperature piezolectric sensors. The bolted joint structure was heated in a temperature-controlled oven. Once a steady state temperature was reached, baseline readings were taken for seven days before inducing damage. This procedure was done to compare day-to-day impedance variations, which proved to be minimal. Impedance was then monitored in a damaged state, which was induced by loosening the bolt slightly. The bolt was kept fairly tight to simulate damage in its incipient stage. The baseline impedance measurements varied much more at these high temperatures than the authors had seen in previous room temperature tests. However, these variations were small compared to the variations seen for the damaged high-temperature case, thus showing that mechanical-impedance monitoring is a candidate for damage detection for high-temperature applications.

Pardo de Vera and Guemes (1997) perform a study to determine the effect of ambient temperature on PZT sensors. PZT sensors rely on the electromechanical coupling between the electrical impedance of the PZT and the local mechanical impedance of the structure being monitored. Using a ceramic PZT sensor, the authors computed the electrical impedance for a $4 \times 30 \times 115$ mm composite specimen at various temperatures. The authors found that, as temperatures increased, the overall response spectrum shifted to lower frequencies. The authors compensated for this temperature effect by experimentally studying how temperature affects the expansion and piezoelectric properties of the PZT materials and the structure.

Based on experimental data obtained from the Alamosa Canyon Bridge in New Mexico, Sohn et al. (1998a) indicate that the effects of environmental changes can often mask subtler structural changes caused by damage. In particular, the fundamental frequency of the Alamosa Canyon Bridge varied about 5% as a result of ambient temperature variation during 24-hour vibration tests. The authors examine a linear adaptive filter that may discriminate the changes of modal parameters as a result of temperature changes from those caused by structural damage or other environmental effects. Experimental study from the Alamosa Canyon Bridge indicates that a linear filter of four temperature inputs (two time and two spatial dimensions) can reproduce the variation of the frequencies with respect to the time of day. From this linear filter, a confidence

interval of the fundamental frequency for a new temperature profile is established to discriminate the natural variation due to temperature from other effects.

Zhang et al (1999) state that although acoustic emissions (AEs), which are ultrasonic waves emanating form the formation or propagation of a crack in a material, will indicate the onset of damage under well-controlled laboratory conditions, the AEs in real applications are often buried by a wider variety of other strong interferences and noises. Such interferences and noises include fretting (generated by rubbing of two component surfaces), hydraulic noise, and electromagnetic interference. Most of these noises are transient and have characteristics similar to AE signals. The authors address the problem of detection and isolating AE signals from measured data. A special linear model is fit to the measured data, and statistical tests on the prediction residual errors are performed to detect transient responses in additive noise signals. At the time of publication, the authors were further working on a classification technique to decide if the identified transient signal corresponds to AEs.

To summarize this section, SHM based on vibration signature will not be accepted in practical applications unless robust techniques are developed to explicitly account for these environmental and operational constrains/conditions of the systems to be monitored. Compared to the previous literature review, more researchers become aware of the importance of these issues when a SHM system is deployed in field. However, there are little proven techniques able to address these issues properly.

2.4 Data Management

Seeing a deficiency in modern management methods in the bridge and highway infrastructure, Aktan et al. (2000) set out to present and discuss the issues prerequisite to creating a meaningful and successful health-monitoring system. His proposal entailed the implementation of an integrated-asset management that would facilitate a cost-effective optimization of operational performance and life-cycle preservation with an encompassing data network. The data components would include event-based, intermittent and on-line monitoring, and would combine temporal data collection and spatial-position-based data. A management system would diagnose the useful life only in collaboration with sensing damaged and undamaged states of systems.

The author adds that inventories of existing structure and infrastructure safety-related information are limited in detail. For example, critical welds may be monitored and determined to be damaged, but with accurate information regarding the bridge safety values, the bearing load of a bridge is found to be within safety values. As such, the authors suggest that the infrastructures be reevaluated with appropriate system identification allowing for effective health monitoring.

3. DATA ACQUISITION AND SIGNAL PROCESSING

The actual implantation of a structural health-monitoring system typically starts with designing a proof-of-concept experiment. First, an excitation mechanism for vibration testing should be determined. Then, the physical quantities to be measured, the type and number of sensors, and the sensor placement should be decided. Next, the issue of data acquisition should be addressed, such as how often the data should be collected, how to select the resolution and dynamic rages of the measured quantities, which antialiasing filter should be applied, and so on. Finally, the recorded data should be transmitted safely to central monitoring facilities or to interested users of the data. These issues are tackled in this section. However, it should be noted that the selection of data acquisition and signal-processing strategies is application specific, and economic considerations play a major role in these decisions. It is also the authors' belief that a proper selection and design of data acquisition systems and signal processing procedures should be eventually based on *a prior* numerical simulation of the test systems.

3.1 Excitation Methods

The excitation methods fall into the two general categories of ambient and forced excitation methods. During ambient excitation, the input to a system is not generally measured. In contrast, excitation forces are usually applied in a controlled manner and measured when the forced excitation method is employed. In this review, local excitations such as an excitation using a piezoelectric actuator is addressed in an independent section separated from the conventional forced excitation. Whether or not the measurements of the excitation forces are available makes a difference for the subsequent system-identification procedures. Many structural parameters, such as modal frequencies, modal damping, and mode shapes can generally be identified without the need for a precise measurement of the excitation forces. However, these situations usually require that the nature of the excitation be well characterized (e.g., broadband white noise, impulse, etc.) even if the actual loading event is not measured. On the other hand, there are many other structural parameters, such as mode participation factors that require excitation during the time the system is to be monitored. The decision regarding the measurement of the excitation forces is determined both by the damage-sensitive features that will be identified and by the practicality of measuring the excitation force on a particular structure. For example, during a

modal test of a frame structure in a laboratory, the applied loads from an impact hammer, a shaking table, or a shaker are readily measured using standard instrumentation. However, during a field test of a highway bridge under loading from high-speed traffic, it is far less clear how to accurately measure all of the loads imparted to the structure from the traffic. Additionally, the bridge will see environmental loads such as wind and thermal gradients that may be difficult to characterize. In summary, there are many situations where measuring the excitation forces on a structure are both practical and useful, and there are other situations where it is both impractical and not useful. In either case, some meaningful information with respect to structures can be extracted from the data, but whether the trade of additional testing cost for the additional information is worthwhile is a case-specific decision.

3.1.1 Forced Excitation

In the forced-excitation testing of structures, a wide variety of forcing techniques is used, including actuators, shakers, step relaxation, and various methods of measured impact (see Figure 4). For most of the forced-vibration tests, the input-forcing function is well characterized and system-identification techniques for determining the modal characteristics (resonant frequencies, mode shapes, and modal-damping ratios) of the structures subjected to measured inputs are well established. One advantage of the forced-vibration test is that the input force is typically strong enough to dominate other noise disturbance, resulting in a strong signal to noise ratio. Furthermore, local excitation can be employed to excite only a localized region of the whole system. This employment of the local excitation facilitates the extraction of features sensitive to local structural responses rather than the global behavior of the system and often mitigates the environmental and operation effects, which tend to be global phenomena.

As part of the corrosion-detection study for a pipe specimen, Cawley (1997) uses a 5-cycle 64-kHz tone burst modified by a Hanning window as an input signal for the Lamb wave testing. The tone bursts were generated with piezoelectric transducers. The author points out that it is necessary for Lamb wave testing to control the signal input to the structure very carefully to avoid problems caused by exciting multiple modes and dispersion.

(a) A hydraulic shaker: larger force capacity than electrodynamic shaker but limited high-frequency capability.

(b) Mechanical eccentric mass shaker: generates sinusoidal excitation, but difficult to apply in vertical direction.

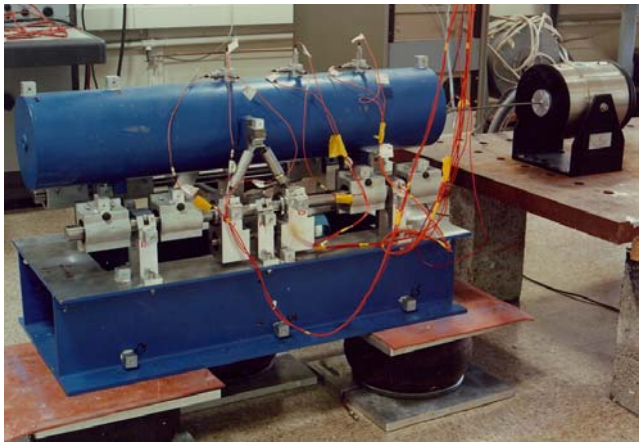

(c) An electrodynamic shaker.

(d) Impact excitation with an impact hammer.

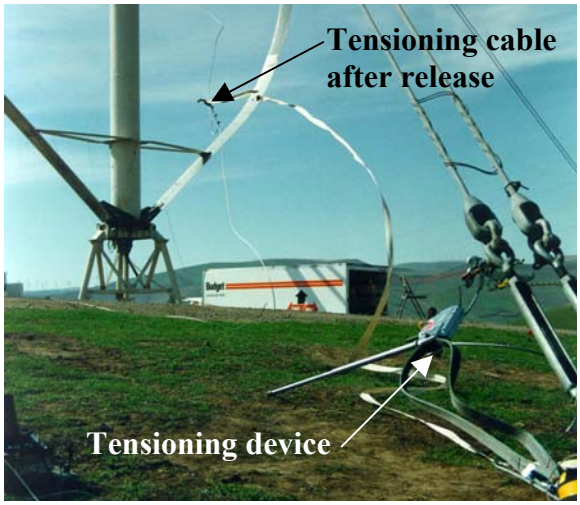

(e) Step-relaxation applied to a wind turbine.

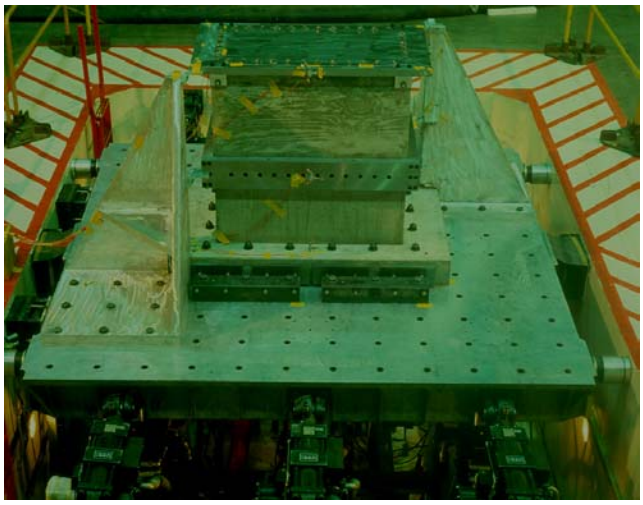

(f) A hydraulic multiaxis shake table.

Figure 4. Different types of forced excitation methods.

In another SHM study using Lamb waves, Wilcox et al. (1999) note that the dispersion, attenuation, sensitivity, and excitability characteristics of thick plates depend on the appropriate selection of Lamb wave mode and frequency. A steel plate is tested to determine spatial-resolution capabilities of Lamb waves in dispersive media. A measure called the maximum resolvable distance (MRD) is used for the best spatial resolution of damage that can be achieved for a given optimal-input signal. For the plate tested, the authors determine that the optimal frequency thickness for 7-cycle tone bursts is 1.61 MHz-mm. The authors note that the MRD does not improve for higher modes, which is surprising because a better resolution normally attributes to higher-frequency waves (smaller wavelength). The authors trace this fact to the need for longer-lasting tone bursts to compensate for increasing dispersive effects at higher frequencies. Attenuation effects are tested on a steel plate immersed in water. Attenuation effects for shear waves in the plate are generally less than for longitudinal waves because water can be assumed to be ideally inviscid. The wavelengths produced by transducers generally need to be 5 to 10 times the wavelength of the Lamb wave so that a well-collimated beam can be generated. They note that modes with small amounts of out-of-plane surface displacements have low attenuation and are hard to excite with out-of-plane surface forces. Therefore, angle incidence techniques as well as interdigital transducers would not be good methods to be used with low attenuation Lamb wave modes. The authors suggest the use of shearing piezoelectric devices for the application of the steel plates immersed in water.

Worden et al. (2002) state that a practical complication of Lamb wave inspection mainly lies in the propagation characteristics of the elastic waves. The propagation is typically characterized by the product of the wave frequency and the sample thickness, or frequency-thickness product (FT). For a low value of this parameter (typically less than 1 MHz-mm in aluminum media), only the fundamental symmetric, S_0, and antisymmetric, A_0, modes can propagate. As the FT product increases, so does the number of allowed modes. However, these higher modes have widely different phase velocities and often experience considerable phase-velocity dispersion as a function of the FT value. Note that damage diagnosis is much simplified if a known single mode of the Lamb waves is generated over a nondispersive region of the FT product.

Zak et al. (1999) study the vibration of a laminated composite plate with closing delamination. A finite element model is also constructed considering contact forced between delaminated layers, and the delamination is modeled by three separate plate elements. The results of the numerical simulations are validated using the experimental data from the laminated composite plates. A harmonic excitation and impulse are used for the experiment.

Rytter and Kirkegaard (1997) perform a vibration test of a full-scale, four-story reinforced concrete building at the European Laboratory for Structural Assessment (ELSA). This building is subjected to an earthquake generated by a pseudo-odynamic testing method. Readers interested in the details of the experiment are referred to Negro et al. (1994). The experimental data are used to validate vibration inspection techniques based on a multilayer-perceptron neural network and a radial-based function network. The relative changes in the modal parameters are used as inputs of the networks to detect the bending stiffness change at the output layer.

Zimmerman (1999) performs a total of 55 modal tests on a vertical stabilizer assembly (VSA) of the Space Shuttle Orbiter, extracting Ritz vectors at 56 measurement points to analyze damage to the VSA. The design of VSA is identical to the original Columbia Space Shuttle Orbiter design. An MB500 shaker with a root mean square force input of 100 N is used, providing 25 ensembles of burst random excitation to the VSA. To minimize unnecessary feedback from the stabilizer to the shaker, the shaker is suspended 10 ft above the excitation point from a platform. The sensor locations and shaker input are similar to the configuration of the Shuttle Modal Inspection System (SMIS). A scanning laser vibrometer is used to obtain additional measurements.

3.1.2 Ambient Excitation

Ambient excitation is defined as the excitation experienced by a structure under its normal operating conditions. All structures are consistently subject to ambient excitation from various sources. The input force is generally not recorded or cannot be measured during dynamic tests that use ambient excitation. Because the input is not measured, it is not known if this excitation source provides input at the frequencies of interest, how stationary the input is, or how uniform the input is over a particular frequency range. Even when measured input excitation (forced excitation) is used, ambient vibration sources are often still present, producing undesirable and

often unavoidable extraneous inputs to the structure. For the development of online, real-time SHM, the use of ambient excitation, however, provides an attractive means of exciting the structure. This type of excitation is a particularly attractive alternative to forced vibration tests during dynamic testing of bridge structures because bridges are consistently subject to ambient excitation from sources such as traffic, wind, wave motion, pedestrians, and seismic excitation. Except for seismic excitation, the input force is generally not recorded or cannot be measured during dynamic tests that use ambient excitation. The use of ambient vibration often provides a means of evaluating the response of the structure to the actual vibration environment of interest.

Pedestrian loading is generated by people walking across the bridge. This excitation method seems limited to footbridges and small-scale bridges and is unappreciable to typical road bridges or large-scale bridges. This type of excitation is often employed to study the psychological perception of pedestrians and passengers in stopped vehicles to bridge vibrations. It is suggested that human sensitivity to vibrations is most closely related to acceleration rather than deflection. Brownjohn (1997) reported ambient vibration tests of a footbridge in Singapore using a person walking and jumping on the bridge as the excitation source. The analysis of the bridge's response to the pedestrian inputs showed that the "bouncy" response was caused almost entirely by two modes near 2 Hz (symmetric and asymmetric vertical modes) that coincided with the typical frequency of normal pedestrian footfall.

Some details of forced and ambient excitation methods applied to long span bridges are given in Felber (1997). Forced and ambient excitation methods are compared, and test results with both methods are shown to be useful for finite element model updating. Although the article addresses system identification rather than damage assessment issues, some results presented are useful for the latter problem. Therefore, a brief description of this article is given here. Felber notes that the interpretation of measured data is a considerable task because a large amount of time histories is recorded during a vibration test. Furthermore, a long-span bridge often has closely spaced bending and torsional modes making it difficult to separate these modes. To overcome these difficulties, Felber introduces the Averaged Normalized Power Spectral Density (ANSPD) as,

$$ANSPD(f_k) = \frac{1}{l}\sum_{i=1}^{l} PSD_i(f_k) \Big/ \sum_{k=1}^{n} PSD_i(f_k) \ ,$$

where f_k is the kth discrete frequency, n is the number of discrete frequencies, PSD_i is the power spectral density at the ith sensor location, and l is the number of total sensors. Felber applies this ANSPD method to a recent seismic assessment of the Port Mann Bridge in British Columbia, Canada. Details of that study are not given here because the example is a pure system identification problem.

Recent advances in modal parameter estimation techniques based on output-only data are worthwhile to mention here because a structure would be more likely excited by freely available ambient excitation sources for the development of a continuous structural health monitoring system. Peeters and De Roeck (2000) presents an overview of these output only, based on modal parameter extraction techniques such as the complex mode identification function, the instrumental variable method, and stochastic subspace identification. He also points out the similarities between the conventional polyreference time-domain identification method, the instrumental variable method, the eigensystem realization algorithms, and the statistical subspace identification methods.

(a)

(b)

Figure 5. Examples of ambient excitations, which are defined as the excitations experienced by a structure or system under its normal operating conditions. This type of excitation has been particularly a very attractive alternative to forced vibration tests during dynamic testing of bridge structures because bridges are consistently subjected to ambient excitation from sources such as traffic, wind, wave motion, pedestrians, and seismic excitation. Except for seismic excitation, the input force is generally not recorded or cannot be measured during dynamic tests that utilize ambient excitation.

3.1.3 Local Excitation

As mentioned earlier, local excitation methods are a subset of the forced excitation techniques. However, because the local excitation tends to excite a specific region of a structure rather than the whole system and this excitation needs special types of actuators, the local excitation is addressed in a separate section.

An impedance-based method is introduced by Park, Cudney, and Inman (1999a). In this SHM technique, a piezoelectric transducer (PZT) is used for both actuation and sensing of a structure's response. The electrical impedance (or the transfer function) of the PZT is directly related to the mechanical impedance of the bonded structure, and consequently is related to structural properties such as stiffness, mass, and damping. Then, a damage metric is defined as the sum of the squared differences of the impedance between the current and undamaged states of the structure over the frequency content of interest. When this damage metric becomes larger than a predetermined damage threshold value, the current state of the system is categorized into a damaged state. The authors note advantages of an impedance-based technique for SHM over the conventional techniques based on modal parameter extraction. First, the technique is not based on any numerical model. The nature of high-frequency excitation, which is typically above 30 kHz, makes this technique very sensitive to local changes within the structure. Finally, this technique can be implemented for continuous online SHM without requiring costly, scheduled base inspections.

Giurgiutiu and Rogers (1997) discuss the use of an Electro-Mechanical Impedance (EMI) technique to detect incipient damage within a structure. The EMI technique relies on the electro-mechanical coupling between the electrical impedance of the piezoelectric materials and the local mechanical impedance of the structure adjacent to the PZT materials. The PZT materials are used both to actuate the structure and to monitor the response. From the input and output relationship of the PZT materials, the electrical impedance is computed. When the PZT sensor-actuator is bonded to a structure, the electrical impedance is coupled with the local mechanical impedance. The authors claim that small flaws in the early stages of damage are often undetectable through global vibration signature methods, but these flaws can be detected using

the PZT sensor-actuator, provided that the PZT sensor actuators are near the incipient damage. Giurgiutiu et al. (2000) apply the method for health monitoring of aging aerospace structures.

Ayres et al. (1996) demonstrate the ability of the Electro-Mechanical Impedance (EMI) technique to detect damage within a bridge joint. The authors installed two $0.635 \times 0.635 \times 0.025$ cm piezoelectric (PZT) sensor/actuators onto a quarter-scale truss bridge joint. The joint consisted of three W sections, four C channels, for 0.635 cm plates, over 7 m of 7.62×7.62 cm angle steel, and more than 200 bolts. In their experiments, the authors simulated damage within the structure by loosening various numbers of the bolts on the structure. The EMI technique successfully detected damage that was located near the PZT sensors.

Pardo de Vera and Guemes (1997) discuss the use of piezoelectric (PZT) materials for damage detection. As mentioned above, this method relies on the electromechanical coupling between the electrical impedance of the PZT and the local mechanical impedance of the structure being monitored. The authors propose an active-sensing PZT that acts as both an actuator and a sensor. To accomplish this active sensing, the authors attach an electronic bridge circuit to the active sensor so that a single sensor can distinguish the actuating signal and the response signal. To test the active-sensing system, the authors bonded a $0.2 \times 10 \times 20$ mm piezoceramic to a $4 \times 30 \times 115$ mm composite specimen. After the initial response was measured from the undamaged structure, the response was measured from three different damage cases. The damage was introduced by drilling a hole 35 mm from the PZT active sensor and varying the diameter of the hole. A damage index factor defined as the difference between the transfer functions from the undamaged and damaged cases displayed a linear relationship with the size of the hole. The authors claim that this test demonstrates that the active-sensing PZT can be used to detect and determine the relative magnitude of a hole within a structure.

Chen et al. (1997) discuss the use of active tagging for damage detection in glass-fiber reinforced polymer (GFRP) composite C-channels. In this method, the GFRP composite is “tagged” by embedding ferromagnetic particles into the composite matrix. An alternating magnetic field is then passed over the tagged composite channel that causes the tagging particles to vibrate. This active tagging can be used to identify vibration characteristics such as natural frequency and damping of the composite piece that in turn can be used for damage prognosis.

Wang and Chang (2000) present an active diagnostic technique for identifying impact damage in composites. This method uses a built-in network of piezoelectric elements that act as both actuators and sensors for detecting impact damage. A signal generator produces diagnostic signals that are emitted from the piezoelectric ceramic wafers, and the waves propagate through the material and are measured by the other wafers. Damage is identified by analyzing differences in sensor measurements, which are mainly caused by a change in local material properties, before and after the damage is introduced. The differences can be related to the location and size of the delamination. The arrival times of waves to each sensor are recorded, and this information is used to determine the damage location. The center location of damage is determined by using an optimization algorithm to minimize the error of estimated distances among all the paths between the center of damage and the sensor locations. The size of the delamination can be estimated by using a similar minimizing algorithm that incorporates parameters of the composite material. Experiments were conducted on various graphite/epoxy plates with four piezoelectric wafers mounted on the surface with conductive epoxy. Damage was introduced to the plates by means of a quasi-static impact. The optimal spacing between the actuators and sensors were determined to be 12.7 to 20.32 cm. Damage location and size estimated with the described technique were comparable with x-ray images of the damaged plates. The estimated damage centers were within 5.08 mm of the actual ones in 68.8% of the cases, and 90.1% were within 10.16 mm. The presented technique often overestimated the actual size of the damage.

Lin (1999) develops a printed circuit film layer of piezoceramic materials, which can be embedded into composite structures or surface mounted on metallic structures (see Figure 6). The piezoceramic materials serve as both sensors and actuators allowing passive and active sensing diagnostics. In passive sensing mode, the response of structures are passively recorded when the system is subjected to an unknown external excitation. The active sensing diagnostic uses the built-in actuators as well as the sensors to generate controlled internal excitation and to measure the corresponding structural response. Because the response signals of a structure are often affected by operational and environmental variations of the structure, the employment of a known excitation force makes the subsequent signal processing and system identification much easier. The layer has a thickness of less than 0.08 cm and a temperature tolerance of up to 200^{o}C. This temperature tolerance is above the curing temperature for most composites. Lin claims that the layer has little to no effect on the mechanical properties of the composite. As an example, the

author points to tests comparing the tensile strength of composites with and without the sensor network layer. The tests show no difference in failure loads between the two.

Lichtenwalner and Sofge (1998) present a similar active sensing system called Active Damage Interrogation (ADI) developed at the Boeing Company—Phantom Works Division utilizing an array of piezoelectric transducers attached to or embedded within a structure for both local excitation and sensing. The structure is excited by multiple actuators across a desired frequency range. Then, the structure's dynamics are characterized by measuring the transfer function between each actuator/sensor pair. Statistical pattern analysis of the transfer function deviation is used to identify, locate, and assess damage within the structure. This technique is applied to detect delamination initiated by low velocity impact in a McDonnel Douglas Explorer rotorcraft composite flexbeam, which is a glass-epoxy composite structure linking the rotorblades to the helicopter hud. Lichtenwalner et al. (1998) also show that this ADI system is very effective in identifying simulated fastener failures in a metallic structural test article. Finally, the authors state that several issues need to be addressed before field implementation of the ADI system. These issues include the development of more robust and reliable damage interrogation algorithms to optimize overall damage detection, localization and assessment performance, and evaluation of environmental variation effects on the ADI system such as temperature, humidity, and accumulated load cycles.

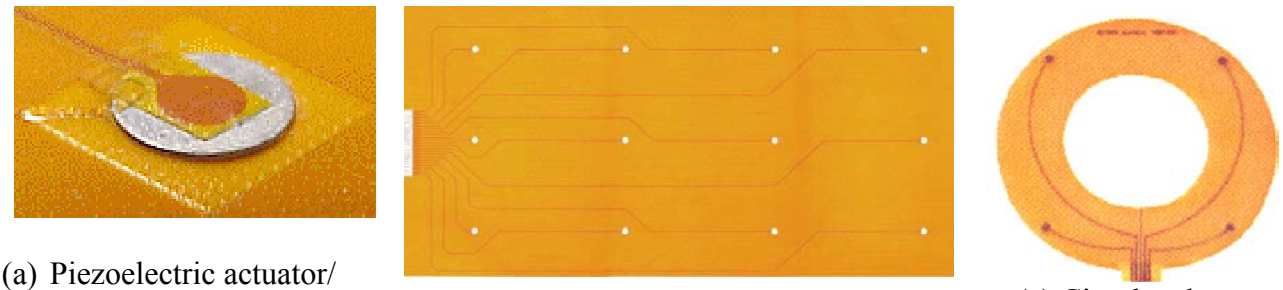

(a) Piezoelectric actuator/ sensor

(b) Rectangular shape sensor network

(c) Circular shape

Figure 6. An embedded network of distributed piezoelectric actuators/sensors: this thin film of sensor/actuator network can be either surface mounted or embedded into composite structures. (Courtesy of Acellent Technologies, Inc.)

3.2 Sensing Structural Response

The premise of vibration-based SHM is that perturbations in a structural system will cause changes in measured vibration signals. Therefore, physical quantities most relevant and sensitive to the structural properties of interest should be selected for monitoring purposes. Kinematic quantities typically measured in vibration testing include accelerations, strain, and displacement. In addition, the measurements of temperature, humidity, and wind are required to quantify the environmental conditions of the system. Based on the physical quantities to be monitored, the type of sensors is subsequently selected. For example, because piezoelectric accelerometers and other AC-coupled sensors produce zero offset errors when trying to follow a slow motion, displacements computed by double-integrating these accelerometer readings may not be reliable estimates. Other considerations include the number of sensors, sensor placement, and so on.

3.2.1 Strain

Wang and Pran (2000) employ fiber-optic strain gauges to monitor the vertical bending, horizontal bending, torsion, vertical shear force, and longitudinal compression forces developed in a Norwegian Fast Patrol Boat's hull. The ultimate goal of these measurements is the calculation of global bending moments to which the shop's hull is exposed. The researchers would then have the ability to characterize the forces exerted on the hull. Based on a finite element simulation with 722,000 degrees of freedom, the global moments and forces are determined to be the best features to characterize the wave loading on the hull. Wang and Pran (2000) use wavelet transformation techniques to analyze the transient strain readings from the sensors and to find that the vertical bending modes dominate the signals from the ship's hull.

Rizkalla, Bemokrane, and Tadros (2000) describe a project to remotely monitor the performance of three bridges in Canada that are repaired with fiber reinforced polymer (FRP) composites. Specifically, the researchers are interested in measuring the strains developed in the FRP composites used for prestressing the girders and for reinforcement of the deck slab and barrier walls. They utilize fiber-optic sensors and electric-based temperature sensors to accomplish this task. In particular, Fiber-Optic Bragg Grating (FBG) sensors are used to monitor the strains in the Carbon FRP reinforcement of the girders and deck slab of one bridge as well as the glass

FRP reinforcement of the barrier walls. A total of 63 FBG sensors and 2 multi-Bragg sensors are glued to the Carbon FRP bars. These sensors located at the girders' midspan are used to monitor the maximum strains, and others located at the girder ends are used to evaluate the transfer length of the prestressing tendons. Because of the relatively high prestressing strain (about 8,800 microstrain) and the limited full range of the FBG sensors (10,000 microstrain), most of the sensors are installed after tensioning the prestressing tendons, while some are installed beforehand to measure the initial prestressing strains of the Carbon FRP and steel tendons. In addition, 22 electric-based temperature sensors are installed to compensate for the thermally induced strains. Finally, 26 electric resistance strain gauges are used at locations near some of the FBG sensors to compare the performance of the FBG sensors with that of the conventional electric strain gauges. The strains are recorded using a fiber grating strain indicator, a 32-channel multiplexing unit for quasi-static strain measurements, and a 24-channel multiplexing unit for temperature measurements, respectively. The researchers find that traffic-induced loads have a negligible effect on the bridge girder strains in comparison to the thermally induced loads. In fact, they demonstrate the necessity of measuring temperatures to account for the significant thermal effects because these effects on the measured strains are dominant. In addition, the conventional strain gauges' performance deteriorates quite rapidly as a result of moisture, while the FBG sensors' performance remains acceptable.

Similar studies comparing conventional and fiber-optic strain gauges for bridge SHM can be found in Kim and Paik (1997). In this paper, the authors state that Fabry-Perot optical fiber sensors show a high resolution of approximately 0.12 microstrain. Strains measured on the bridge were found to correlate with the velocity of a truck traversing the bridge during experiments. In particular, a 30-ton truck traverses the bridge at velocities between 10 km/h to 60 km/h. Changes of strain are observed depending on the truck velocity, although the temperature effects that Rizkalla, Bemokrane, and Tadros (2000) measured are not really considered. According to Rizkalla, Bemokrane, and Tadros, the strains caused by the temperature effects dominate the traffic-induced strains. Therefore, Kim and Paik's results should be reinterpreted in light of this temperature dependence of strains. Kim et al. (1997a) install Fabry-Perot fiber-optic sensors on the Sungsan Bridge in Seoul, Korea for strain measurement. The authors found similar resolution capabilities as Kim and Paik (1997) found in their work.

Todd, Johnson, and Vohra (2000) develop a strain sensing system to provide high-resolution, low-noise data, which can be analyzed and processed with a number of existing damage detection techniques. The authors demonstrate their system on a clamped plate where damage is inflicted by loosening the clamping bolts. Eight impact tests are conducted on the plate, four with the bolts fully tightened and four with the bolts loosened. Impact locations vary for each test performed. Fiber Bragg Grating (FBG) sensors are used to measure strains at 16 locations. The sensing system uses four diodes as light sources along with two scanning Fabry-Perot filters, two photo detectors, six couplers, and a laptop computer. Following along the same lines, Todd et al. (1999) apply FBG sensors to the I-10 bridge in southern New Mexico as well as to the Viaduc Des Vaux Bridge under construction near Lausanne, Switzerland. They demonstrate that FBG sensors can be useful in monitoring traffic-induced loads as well as loads inherent during the construction phase.

Yamaura et al. (1999) state that recent advances in the fiber-optic technology of Brillouin Optical Time Domain Reflectometry (BOTDR) allow the measurements of distributed strain over distances of 20 km. They describe a particular BOTDR system developed by Nippon Telegraph and Telephone (NTT) Corporation in Japan. Light of a given frequency, ω, is shifted a small amount, $\Delta\omega$, by an optical frequency shifter and is passed to the test fiber as a pulse of frequency, $(\omega+\Delta\omega)$. Some of the light is backscattered and returns to the input side of the optical fiber where it is combined with light from the original source of frequency, ω. The resulting light wave is sent to the detector. By ensuring that the frequency shift, $\Delta\omega$, of the optical frequency shifter is the same as the Brillioun frequency shift, $\Delta\omega_{br}$, only the Brillouin backscattered light from the backscattered process is detected. Therefore, it is possible to measure the Brillouin spectrum of the optical fiber in each longitudinal position by measuring the output of the optical frequency shifter. As $\Delta\omega_{br}$ changes in proportion to the strain of the optical fiber, the distribution of the strain along the optical fiber can be continuously measured. The spatial resolution of the BOTDR used in their study is 2 m, and the strain sensitivity is 0.02%. A 3,000 × 1,000 × 25 mm plate of mild steel is used to test a BOTDR fiber (AQ8602) made by ANDO Electric Company. The optical fiber of 1 km total length is looped back on itself at 2 m intervals and bonded at 200 mm intervals with either epoxy resin or cyanoacrylate. A 2-m length of wire style displacement gauge is installed on the backside of the steel plate. An 800-ton

test rig is used to undertake the tensile test, and tension is recorded as the load increased in 50-ton steps to a maximum load of 700 tons. The authors detect the presence of strain in the absence of an applied load. This strain is a result of the gluing process and could be an important calibration issue for the use of BOTDR fiber optics in SHM. Based on their results, Yamaura et al. conclude that it is possible to measure deformations of steel structures with the BOTDR fibers and that there is no difference in measurement precision between the different glues used. For strain measurements in small areas, the aforementioned BOTDR fibers must be modified by decreasing the spatial resolution of the BOTDR fiber. The authors do so by looping the fibers, with the loop diameter of 60 mm, chosen to minimize transmission loss of light for their particular test. The looped ends are free to move by fixing the fiber at only 2 points. Tests are undertaken on an acrylic plate with cracks simulated by separating the plate at its center. The crack-induced strains are successfully measured.

Following along the same lines, Oka et al. (1999) present their development of a Brillouin Optical Time Domain Reflectometry (BOTDR) fiber sensor. They note that BOTDR optical fibers are used extensively in communication applications and that the very same fibers are used to measure strains in concrete structures. Those fibers incorporate a soft core to prevent excessive strains in the core region and fiber failure in communication applications. On the other hand, full strain transfer to the fiber core is desirable for strain measurements. The researchers give requirements of BOTDR fiber sensors for concrete strain measurements. Among these requirements, the fibers must withstand forces from concrete pouring and curing as well as be easily connected to other fibers. In addition, the fibers must remain intact when cracking occurs. In response, Oka et al. (1999) develop a fiber consisting of a glass core, ultraviolet curable resin coat, teflon tube, and glass-fiber-reinforced plastic (GFRP) coat. Finally, a chemical fiber string is wound spirally around the sensor to fix it firmly to the concrete. The diameter of the fiber is 2 mm. The researchers subject their fiber sensors to tensile tests and note that the fibers can measure strains of more than 1%. Another important observation is that the inner fiber does not slip through the GFRP coating. Further tests on a $5.2 \times 1.5 \times 0.3$ m reinforced concrete slab confirm the reliability of the BOTDR fiber sensors. It remains to be seen whether the BOTDR fiber sensor can be put into practice in an actual construction environment.

Kurashima et al. (1997) also investigate the performance of BOTDR fiber-optic sensors. The authors mounted fiber-optic sensors on the surface of a 10 × 0.4 × 0.5 m reinforced concrete beam. Traditional electrical resistance strain gauges were also mounted on the surface of the beam. The beam was then subjected to two-point flexure using a 5-ton load. The authors found that the distributed strain measurements from the BOTDR sensors provided $\pm 3 \times 10^{-5}$ accuracy. The authors also showed that the sensors could detect an induced strain change of less than ± 100 to 150×10^{-6}.

Westermo and Thompson (1997) discuss the development of a passive, peak strain sensor technology for SHM of bridges and buildings. The technology is based on the irreversible magnetic property changes that occur in a class of steel alloys when strained. The authors test the device on a three-story, wood frame house that sits on a 30 degree slope and is 100 m away from the Hayward fault in Northern California. Analyses of the structure indicate that a structural mechanism most vulnerable to damage is the in-plane shear resistance of the framed walls. The upper floor dead load and lateral load are entirely supported by the first level framed walls. These walls have no diagonal bracing; and their shear rigidity comes only from the wallboard. Therefore, damage from lateral loads will most likely "rack" or rotate the walls in-plane. The authors, therefore, decide to monitor this rotation as an indicator of damage. To do so, the authors mount their strain gauge diagonally between the stud and the cover plate or top beam. An accelerometer is also mounted on the structure to trigger the monitoring system when a seismic event occurs. The strain sensors have a sensitivity of roughly 2% of full dynamic scale and are sensitive to out-of-plane rotations, which would indicate the wall "racking" failure. The system is continuously operating in the absence of significant seismic activity.

Structural health monitoring projects are sometimes limited by the high cost of sensors and associated signal conditioning. Satpathi et al. (1999) discuss the development of a low-cost strain gauge sensor. In their work, the authors test the use of small patches of thin film piezoelectric material, polyvinyldene fluoride (PVDF), as strain gauges. The authors note that PVDF has several advantages over other piezoelectric materials including cost, high elastic compliance, and ability to be mounted in tight locations. To validate the use of PVDF patches as strain gauges, the authors examined parameters such as sensitivity to strain and effects of temperature. The authors employed a standard cantilever beam test to study the aforementioned parameters.

The PVDF sensors showed excellent strain sensitivity at room temperature and were easily calibrated using the cantilever beam test. To study the effects of temperature, the cantilever beam tests were performed at various temperatures ranging from –5°C to 26.2°C. The results showed that the PVDF strain sensitivity is a linear function of temperature, thus making it easy to compensate for.

Lhermet et al. (1998) discuss the development of an electromagnetic sensor that can be used to monitor the stress state within certain types of steels. Some ferromagnetic materials are subject to a phenomenon known as magnetostriction, in which the magnetic permeability of the material changes as a function of the stress within the material. The magnetic permeability of a material can be measured indirectly by using a charge coil placed next to or around the material. Therefore, the varying current or voltage can be related to the stress quantity. The authors used this idea to develop a sensor that can monitor the stress within bridge cables and a certain type of steel reinforcements for concrete. The authors used finite element analysis to aid in the design and construction of a prototype sensor. The sensor was fit with a magnetic shield to isolate it from external dynamic and static magnetic fields. The sensor was installed on a section of the bridge cable that was subsequently subjected to tensile forces. During the test, various conditions such as the external magnetic field and temperature were varied to determine the sensitivity of the sensor to the environment. The sensor turned out to be very insensitive to changing environmental conditions. At the time of the paper, field tests of the sensor on an actual bridge and in a prestressed concrete structure were planned.

The identification of impact intensity and location on a composite plate can ensure the integrity of the fiber and matrix when damage is not readily detectable. Tracy et al. (1998) use an array of piezoelectric sensors to measure strain time histories. The measured time histories are compared with the responses simulated from a finite element model of the composite plate. The difference between the measured and analytical responses is minimized by varying impact intensities and locations in the numerical model. A combination of impact intensity and coordinates results in the minimum difference between the measured and analytical responses and is selected as the best-fit estimate of the impact. The nonlinear figure-of-merit solution for the impact force and location is found through an iterative process involving a smoothing algorithm with a backward filter. Each piezoelectric sensor measures two orthogonal in-plane strains. A quantity for strain,

invariant to the orientation of the sensor placement, is computed and the response of the plate model is generated based on Kirchhoff's thin plate theory.

3.2.2 Displacement

Martin et al. (1999) compare various types of piezoelectric transducers for their effectiveness in detecting damage in carbon fiber reinforced polymer (CFRP) composite materials. The transducers are two low profile transducers, 200 μm thick PZT ceramic sensor, a high temperature piezoelectric polymer composite, and a standard bulk PZT transducer. The authors compare the performance of the bulk PZT transducers with those of the low-profile transducers. They find that the low-profile transducers are not as durable as the bulk transducers and that the low-profile transducers are more sensitive to the type of mounting employed. The authors also compare piezoelectric transducers that are mounted on the panel surface or internally. The test is performed on a 275 × 275 mm, 16-layer composite plate. Using adhesive, the transducers are bonded to the composite panel at equal distances from the center of the panel. The panel is simply supported on four corners. Stress waves in the panel are generated by artificial acoustic emission techniques. The response of the internally mounted transducers to stress waves is better than that of the surface-mounted transducers. This better response is attributed to the fact that the internally mounted transducers are coupled better to the composite than the surface mounted transducers. However, the internally mounted transducers are not as effective at detecting acoustic emission as surface mounted transducers because the dominant measured stress waves in thin CFRP composites propagate at the surface. The surface-mounted transducers are three times as sensitive to surface-generated waves as are the internally mounted transducers, and the surface-mounted transducers do not cause internal stress concentrations, as do the internally mounted transducers.

Global Positioning Systems (GPS) have advanced to the point that they are capable of recording displacements at rates of up to 10 samples per second with an accuracy of 1 cm horizontally and 2 cm vertically. Celebi (1999) proposes using GPS displacement measurements for the SHM of structures with long periods. He notes that displacement readings of structures are necessary to accurately record building drift ratios, which can be used to determine if a building has been overstressed. Celebi states that a drawback of using accelerometer measurements to obtain those

displacements is the integration errors introduced when the displacement is calculated from the accelerations. To test the feasibility of using GPS for such measurements, the author uses cantilever steel bars to simulate the dynamics of tall buildings. Each bar has a 4-second period in the weak direction, corresponding to a 30- to 40-story building and has a GPS unit fixed to its free end. That unit is capable of sampling both east-west and north-south displacements at 10 Hz. The bars are set into motion by initially displacing their free ends. A test is also conducted on an actual 44-story building in Los Angeles, California, where the GPS unit is placed on the building's roof. Limited details about this experiment are provided. Celebi (1999) concludes that GPS measurements hold promise for the SHM of building structures. However, GPS technology is not designed to provide local measurements that would be needed to assess crack extent and location.

Stanbridge, Khan, and Ewins (1997) use mode shapes as a feature for detecting damage in a 175 × 175 × 1 mm plate. The damages are a saw cut in the plate and a fatigue crack. The authors use a Continuously Scanning Laser Doppler Vibrometer (CSLDV) for this application. The CSLDV functions essentially as an interferometer, detecting the instantaneous difference in the wavelength of laser light directed at and scattered from the plate. First, the heterodyne demodulation of the signal, which arrives from the initial undamaged plate, is considered the baseline signal. Then, the demodulation signal of a new signal from a plate of an unknown condition is compared with the baseline signal. Defects should appear as discontinuities in the displacement amplitude-time plot of the incoming signal. The authors state that at a distance of 2 m from the plate, the plate does not need to be polished for the CSLDV measurements. A coat of white paint, however, will help reduce unwanted specular reflection. The authors discuss obtaining spatial mode shapes from scanning with the CSLDV along a line. They note that problems can arise when a line scan ends abruptly. If the scan varies in time sinusoidally, these difficulties disappear. Because line scans may not detect defects that run along the scan line, the authors propose circular scans and perform a 10 mm-diameter scan of the plate. The authors state that because the spectrum of the CSLDV measurements before demodulation contains the frequency of the mode shape with corresponding symmetrical sidebands, only a Fourier transform of the incoming undemodulated signal is necessary. One shortcoming of the Fourier transform approach is that this method requires the digitization of the signals, whereas the

demodulation requires only the reference light signal to analyze the incoming signal in an analog fashion.

Other examples of using Laser Doppler vibrometry (LDV) to measure displacements include Zak et al. (1999) and Zimmerman (1999). Zak et al. use LDV to measure the dynamics response of composite plates subject to impulse excitation, and Zimmerman uses a scanning laser vibrometer to characterize the dynamic response of a Vertical Stabilizer Assembly for the Space Shuttle Orbiter. A commercial product of such a LDV is shown in Figure 7. LDV is a noncontact vibration measurement technique using the Doppler effect. The LDV permits measurement of not only velocity but also direct displacement and can operate at distances of hundreds of meters. Laser vibrometers are typically two-beam interferometric devices, which detect the phase difference between an internal reference and the measurement beam. The measurement beam is focused on the target and scattered back to the interferometer.

Figure 7. In-plane measurement on a printer drive using a laser Doppler vibrometer. The LDV permits velocity or displacement measurements of hot, miniature or soft surfaces, even under water, without mass-loading. (Courtesy of Polytec, Inc.: www.polytec.com)

Structures are composed of several structural components. Motion between the structural elements can redistribute loads and even lead to failure. Monitoring the relative motion between structural elements might provide a means to examine the integrity of the structure. Su (1998) discusses the use of time domain reflectometry (TDR) to monitor relative displacements between structural elements within a concrete structure. Coaxial cables are embedded into adjacent concrete blocks, and an electromagnetic pulse is sent down the cable for monitoring. If two adjacent structural members move relatively, the cable at the interface between the elements will be distorted. This distortion in the cable will create a reflection of the electromagnetic pulse. The location of the distortion can be determined from the time delay of this reflection. A single coaxial cable can be used to monitor several joints between different structural elements. In his work, Su embedded a coaxial cable into 5 sequential concrete blocks, and two blocks were displaced to simulate movement within a structure. The TDR technique was able to accurately detect the location of the movements.

Jenkins et al. (1997) introduce a static deflection based damage detection method as an alternative approach to frequency response function based approaches. They argue that the frequency response functions are relatively insensitive to many instances of localized damage such as fatigue crack or notch, which results in very little changes in the system mass or inertia. A closed form equation and finite element models for a fixed-free 2 degree-of-freedom (DOF) beam motivate their results. The beam is a 457 mm by 13 mm square steel beam with a transverse cut made at 64 mm from the fixed end. Various cut depths were tested for a static deflection tip load and natural frequencies. The 2 DOF model is subjected to a cut that induces a 10% stiffness decrease, yielding an 11% static deflection increase, while the frequency change is limited to less than 7%. Accordingly, as the number of DOFs increases, the frequencies of the system become less sensitive to damage, while the sensitivity of the static deflection to damage remains the same. The authors uphold their statement that the static deflection is a valid tool. This is achieved by using finite element models to show that static deflection is more sensitive than frequency for cases of longitudinal and torsional damage.

3.2.3 Acceleration

Zimmerman (1999) extracts Ritz vectors from static and dynamic tests performed on the Vertical Stabilizer Assembly (VSA) of the Space Shuttle Orbiter. The Ritz vectors represent an alternative to mode shapes spanning the response space of dynamic systems. To validate the Ritz vector extraction procedure, the author performs a static test using 10 linear variable differential transducers (LVDT) mounted along the front edge of the VSA and a dynamic test using 56 accelerometers.

Many SHM studies use commercial piezoelectric accelerometers to measure the dynamic response of the test structures. Examples of such studies include Doebling and Farrar (1997) and Ruotolo and Surace (1997c). Ruotolo and Surace (1997c) use a total of 11 accelerometers mounted along a cantilever beam to calculate Frequency Response Functions, from which resonant frequencies can be extracted.

3.2.4 Temperature

Rizkalla, Bemokrane, and Tadros (2000) directly measure temperatures and use these measurements to calculate thermally induced strains in bridges. In fact, they monitor strains in reinforced bridges with Fiber Bragg Grating (FBG) sensors and note the importance of separating thermally induced strains from those strains caused by possible damage in fiber reinforced polymer reinforcements.

Foedinger et al. (1999) further give details of the development of their Fiber Bragg Grating (FBG) thermal strain sensors. When the Bragg grating is illuminated using broadband light, a narrow wavelength component is reflected at the Bragg grating. The reflection wavelength is linearly sensitive to both strain and temperature changes in the grating location. For surface mounted FBG sensors, there are no transverse strain sensitivity effects. For embedded FBG sensors, transverse strains must be taken into account because they account for 10% to 15% of the measured strains. The authors develop a variant of the classical FBG sensor to remove the effects of these transverse strains. This sensor consists of an inner 80 μm diameter fiber with Bragg gratings spliced between standard 125 μm diameter optical fiber, and surrounded by a thin, hollow silica tube. The outer tube is designed to isolate the grating from the transverse

strains, provided that the magnitude of the transverse strains do not cause the outer tube to make contact with the 80 μm inner fiber.

Tennyson and Mufti (2000), on the other hand, discuss a method for directly canceling the effects of thermally induced strains in FBG sensors when measurements of these thermal strains are not sought. In this method, the wavelength shift, $\Delta\lambda = \lambda - \lambda_o$, caused by the thermal effect is analytically calculated as

$$\frac{\Delta\lambda}{\lambda_o} = (GF)\,\varepsilon + \beta\,\Delta T \ ,$$

and

$$\beta = \beta_0 + GF\,(\alpha_s + \alpha_0) \ ,$$

where β is the apparent thermal strain/degree temperature change, ε is the strain, ΔT is the temperature gradient, *GF* is the FBG gauge factor, β_o is the thermooptic response of the FBG at fabrication (typically 10 to 25 microstrain per degree Celsius), and α_s and α_o are the thermal expansion coefficients of the substrate and sensor, respectively. The temperature compensation is provided by an equivalent unbonded length of optical fiber mounted next to the strain sensor. The authors note that one particular benefit of using fiber-optic sensors is their reliability in hostile environments by citing the same bridge experiment that Rizkalla, Bemokrane, and Tadros (2000) undertake.

Moerman et al. (1999) also recognize the importance of canceling the effects of thermally induced strains in Fiber Bragg Grating (FBG) sensors. Furthermore, they compare electric strain gauges with FBG gauges during tensile tests of rebars and creep and shrinkage measurements of prisms. A 200-m-long optical link is provided to an optical spectrum analyzer to demonstrate the possibility of a remote SHM. The Bragg grating sensors are shown to be more linear and sensitive over their operating ranges than the electric strain gauges. One problem that the researchers encounter is fiber breakage when the tested material cracks. They conclude that this problem needs to be addressed before FBG sensors can be used in practical applications.

Hot spots and partial discharges along a power transmission line may lead to extensive damage requiring costly repair and creating an unsafe environment. Therefore, the temperature and electrical load within a power transmission line must be continuously monitored. However, direct measurement of the temperature within a power cable is not a simple task because the high electric and magnetic fields created by the power lines render the majority of temperature measurement sensors useless. Teral et al. (1998) propose a new method for measuring temperature along a power transmission line. Current temperature measurement is based on "anti-Stokes" Raman back-scattered light. When photoluminescent, or "Raman-active" molecules are exposed to a high temperature, the molecules are exited from the ground energy state of the molecular system. When pulsed light is injected into a fiber-optic sensor that runs along the transmission line, this Raman effect causes some of the light to be reflected. This reflected light can be detected using Optical Time Domain Reflectometry (OTDR). The authors claim that this method has two main drawbacks, which are low reflection intensity and inability to detect rapid temperature changes. They propose that this method can be improved by using a fiber-optic sensor core that has a substantially higher index of refraction. The authors suggest that using a core doped with a heavy metal ion increases the reflection intensity of the pulse light.

3.2.5 Wind

Lau et al. (1999) discuss some aspects of the Wind and Structural Health Monitoring System (WASHMS), implemented by the highway department in Hong Kong to monitor the Tsing Ma, Kap Shui Mun, and Ting Kau bridges. The bridges are deemed wind sensitive by the highway department. WASHMS contains the following components. The sensory system consists of 756 sensors to measure wind velocities, temperatures, accelerations, weights of vehicles, strains, and displacements. Signal amplifiers and interfacing equipment are included in this portion of WASHMS. The data acquisition system consists of a personal computer controlling outstation units installed on the bridge decks. The data acquisition system collects and digitizes the signals from the sensors and transmits them via fiber-optic connections to the next portion of WASHMS, the data processing and analysis system. This system contains workstations that archive, analyze, display, and record data. Finally, the processed data are forwarded to a central

computer for system operation and control, the final portion of WASHMS. Temperature variations in the bridges are measured to determine thermally introduced stresses at critical locations. Traffic jams can be observed with the help of installed video cameras, and seismic loadings are assessed based on an AASHTO's multimode spectral analysis procedure applied to the measured ground motions. Noting that bridge cables usually carry over 90% of the total vertical load acting on cable-supported bridges, the authors relate that WASHMS monitors cable tensions to assess the global health of the bridges. Specifically, WASHMS calculates the natural frequencies, mode shapes, and modal damping ratios of the cables to evaluate the cable tensions. The authors further note that the damping ratio is inversely proportional to the vibration amplitude, but directly proportional to the critical wind speed for the onset of wind-induced vibrations. To conclude, Lau et al. (1999), note that these environmental parameters measured by WASHMS indicate that the bridges have been conservatively designed. Detailed information regarding the measurements of wind, traffic, and thermal loads can be found in Solomon, Cunnane, and Stevenson (2000) and Wong et al. (2000). The latter authors also provide the bridges' displacements, accelerations, strains, and cable forces as well as relationships between wind loads to wind speed. Furthermore, comparisons between measured loads and design loads are given.

3.2.6 Other Measurement Quantities

Moisture has an important influence on the lifetime of concrete structures. In fact, water acts as a transport agent for damaging ions such as chloride, sulfate, carbonate, and ammonium. Corrosion of steel rebars is also an important factor in assessing the useful life of concrete structures. Wiese et al. (1999) have developed a fiber-optical moisture sensor to monitor the moisture content of concrete. Their measurement system consists of a plastic optical fiber, a light source, and a high-resolution microspectrometer as well as a sensor. The sensor contains a polymer matrix that is attached directly to the concrete. An indicator dye is injected into that matrix, and the water content in the matrix affects the absorption spectra of the dye. As light from the source passes through the optical fibers to the sensor, the microspectrometer determines which wavelengths of light are absorbed by the polymer matrix/dye in the sensor. In this way, the moisture content of the concrete to which the sensor is directly attached can be determined. Without moisture, the

sensor shows a peak wavelength in the absorption spectrum of 602 nm. The peak wavelength is shifted about 40 nm to 562 nm when the water content in the sensor matrix is 28% by weight. The researchers confirm the long-term stability of the sensing system as well as the reproducibility of results when the moisture content of test specimens is wetted and dried in a cyclic manner. They also testify that the system can monitor the drying process of concrete.

Solomon, Cunnane, and Stevenson (2000) discuss the deployment of a manometer-like, fluid-based level sensing system to measure bridge deck profiles. Temperature and fluid damping compensation is provided for accurate measurements of the deck profile. The authors note that the system has been verified by crosschecking the bridge deck profiles against the low-frequency component of the displacement derived from accelerometers, and the static deflection is determined to be fairly accurate.

Park, Cudney, and Inman (1999b) discuss using piezoelectric materials as sensing and actuating devices to detect changes in the mechanical impedance of a massive, dense structure as an indicator of damage. When a piezoelectric material is bonded to a mechanical structure, the electrical impedance of the piezoelectric sensor/actuator is directly related to the mechanical impedance of the structure. The authors note that this technique has been studied for several different applications, but never for massive, dense structures. In this investigation, the authors use piezoelectric sensors to monitor the mechanical impedance of a header pipe that is 431.8 mm in diameter, 50.8 mm thick, and 82.55 mm long. Baseline impedance readings were taken before inducing any damage in the structure. To induce damage, a hole was drilled into the structure. To increase damage, the hole was deepened. Several different hole depths, hole locations, and excitation frequencies were analyzed. The results of the tests proved that this technique was able to successfully detect damage within a massive structure.

Structural health monitoring sensors for civil structures need to be durable so that they can withstand the harsh construction and service environment. Lin et al., (1999) discuss the feasibility of using electrical time domain reflectometry (ETDR) sensors to detect crack damage within a concrete structure. The ETDR technique can be thought of as a “closed loop radar” system. Signals are sent into ETDR sensors (a coaxial cable) by a step generator. If there are any impedance discontinuities along the length of the sensor, such as those caused by strain

concentration, part of the input step signal is reflected. The ETDR sensors have several advantages over their fiber-optic counterparts, including higher durability, precise distributed sensing capability that can pinpoint the location of damage, multiple sensing capability along a single sensor line, and uniform sensitivity along the entire length of the cable. The authors tested the ETDR technique using concrete specimens fit with the ETDR sensing cables. The concrete specimens were 558.8-mm-long beams with rectangular cross sections (50.8 mm × 76.2 mm). The concrete beams were reinforced near the bottom with two steel rods to prevent brittle fracture during the test. The beams were loaded in a 3-point bending until failure. Readings were taken from the ETDR during the loading process. In each case, the ETDR sensors were able to accurately depict the strain along the length of the beam and detect any cracks that formed during the loading process.

Shinozuka et al. (2000) demonstrated the applicability of Synthetic Aperture Radar (SAR) imaging technology to the monitoring of urban area damage caused by a destructive earthquake. This technique involves using a SAR antenna to shoot a bundle of rays at a region, such as a building or a group of buildings. Then, the reflected rays are collected and evaluated to form a SAR image. The image processed after some extreme events such as an earthquake can be analyzed and compared to a predamage image to identify regions affected by the earthquake. This information can then be disseminated to an emergency management agency to help the allocation of rescue crew and resources. The method was demonstrated with a numerical simulation experiment, and continuing work is underway to expand the method to an actual urban environment. The authors claim that the SAR imaging can be operational under various weather conditions and at any time of the day.

Schueler et al. (1997) discuss using electrical conductivity changes within a carbon fiber reinforced polymer (CFRP) to detect damage. The carbon fibers within a CFRP are electrically conductive and are surrounded by an insulating polymer. The conductivity of CFRP composites display high anisotropic conductive behavior, with the conductivity being much higher in the direction of the carbon fibers than in other directions. As fiber bundles within the composite are severed or broken as a result of damage, conductivity paths through the sample are destroyed, resulting in lower conductivity/higher resistance. The conductivity is also sensitive to damage in the form of delamination. The current transfer between adjacent piles is reduced as they are

delaminated, also resulting in an increase in electrical resistance. The authors propose using a technique known as Electrical Impedance Tomography (EIT) to locate damage within a CFRP structure. In this method, several electrodes are connected to the edge of the CFRP structure. An electrical current is injected into the sample through two of the electrodes, and the potential difference between all other neighboring electrodes is measured. By repeating this process for different combinations of current injecting electrodes, the potential and current distributions within the sample can be obtained. From this information, local increases in the electrical resistance can be used to pinpoint damage. The authors created $52 \times 52 \times 0.16$ mm CFRP specimens to test this method and used 16 razor blades pressed into the edges of the specimens for electrodes. After testing the undamaged specimen, a 5 mm diameter hole was drilled into the specimen in various locations. The authors found that this method successfully located the hole.

Shinozuka and Rejaie (2000) propose a method to use satellite, aerial, and other remotely sensed pre- and postdisaster imagery data to detect major regional or individual structural damage in near real time. The three steps identified for the detecting change in a sequence of images in this study are tracing correspondent pairs, categorizing types of damage and change, and scene registration. First, a sequence of at least two images of a scene is analyzed to detect changes. To trace corresponding pairs in a sequence of images, the location of each specific point of interest is identified in each of the multiple images. By doing this, the corners of objects can be tracked, and deformations of the objects such as buildings or other structures can be computed. Difficulties in this step arise when different illumination conditions exist at the time each image is taken. Also, when large deformations occur, it is difficult for automated algorithms to track points from one image to another. The second step is the recognition of the type of change in a scene. For example, the construction of a new building in a scene will be detected as a change, but it should not be categorized as structural damage. One challenge requiring further investigation is detection of damage on partially visible surfaces. In this study, the first two steps of the algorithm are user-assisted rather than completely automated. The third step is to locate the identified damage on a map using Geographical Information System (GIS) and Global Positioning System (GPS) capabilities. This step is not a part of the near real-time damage identification, but it is an important step for deploying immediate rescue missions to the damaged structure.

Lin et al. (2000) evaluate the effectiveness of the electrical time domain reflectometry (ETDR) technique in monitoring shear deformation and detecting shear crack damages in concrete beams. The ETDR technique derives information from the reflections of a voltage pulse sent through a transmission medium. It is a well-developed technique that has been widely used in electrical engineering applications. The method can measure the deformation of the whole structure as well as pinpoint the location of disturbances. The authors use an embedded high-sensitivity coaxial sensor prototype to monitor the transverse shear response of a concrete cylinder. The capacitance of the cable is increased in the sheared section, where the diameter of the cable changes. The authors claim that the maximum capacitance change occurs at the center of the shear couple where the cable is deformed the most.

Melvin et al. (1997) discuss the Integrated Vehicle Health Monitoring (IVHM) system, which provides reliable and low-cost maintainability for the X-33 Reusable Launch Vehicle (RLV). This paper focused on the distributed sensor systems for onboard IVHM implementation. The Bragg grating fiber-optic sensors will be used for measuring strain and hydrogen concentration. Palladium is known to react with hydrogen forming hydride, and the Bragg grating sensors bonded to palladium deform due to strains in the reacting palladium. The Bragg grating sensors measure this strain monitoring the concentration of hydrogen. Roman techniques will be used for temperature measurement. This method depends on the intensity ratio of the Stokes and anti-Stokes wavelengths in the Raman backscattered signal, which is temperature dependent. Acoustic emission sensors will be used to locate cracks and monitor their growth. The fatigue crack initiation and growth are detected by analyzing the elastic waves that are generated by the sudden release of strain energy as the crack propagates. The IVHM system employs 16 single mode optical fibers, which have 20 to 25 Bragg gratings per fiber, for strain and hydrogen detection on the hydrogen tank, and two multimode temperature fibers on each fuel tank, and four acoustic transducers on the hydrogen tank. These sensors must be able to survive the temperature ranges from –252°C to 121°C and withstand launch and reentry environments.

Feng et al. (2000) develop an electromagnetic (EM) imaging technology for detecting voids and debonding between fiber reinforced polymer (FRP) composite jackets and reinforced concrete columns. Retrofitting RC columns with FRP composite jackets has been demonstrated to enhance structural performance. However, debonding between the jacket and column caused by

seismic damage or poor workmanship can considerably weaken the column, and such damage can remain visually undetected. The proposed damage detection technique is to send a continuous EM wave at the reinforced column and detect the reflected wave energy. A fraction of the wave energy is reflected at each dielectric interface between adjacent layers (e.g., between air and jacket, jacket and column, etc.). An air gap between the jacket and column will form an additional interface, and the energy reflected at this interface should be detectable as evidence of debonding damage. The technique was unsuccessful when plane EM waves were used, so a dielectric lens was used to focus the wave on the bonding interface of the jacketed column. The time gating technique was used to remove unwanted reflections caused by unavoidable obstacles different from air voids. The modified EM wave technique was successfully demonstrated in laboratory tests to detect voids and debonding in a jacketed column with no rebar. Detecting voids in the column with rebar was still under investigation at the time of publication.

3.2.7 MEMS Technology for Sensing Motion

Microelectromechanical systems (MEMS) are miniature electromechanical sensor and actuator systems developed from the mature batch-fabricated processes of Very Large System Integration (VLSI) technologies. Advances in MEMS technologies have led to dramatic reductions in size, power consumption, and cost for wireless communications. Their small size allows them to be used in applications where conventional sensors and actuators would be intrusive. Because of the economies of scale achievable from the conventional chip manufacturing processes, they can be mass produced and copiously applied in a cost-effective manner. Furthermore, they consume very little power, on the order of 500 μW to 40 μW. One example of MEMS wireless sensor modules is shown in Figure 8.

Varadan and Varadan (1999) discuss applications of MEMS sensing to aircraft structures, noting that the small size of these MEMS sensors allows for minimal aerodynamic disruption of the structure. Many MEMS sensors are used in applications where one attempts to measure Lamb, Love, or Rayleigh waves. Varadan and Varadan cite such applications for aircraft SHM.

Figure 8. An example of MEMS wireless sensor modules, which incorporate a wireless telemetry system, on-board microprocessor, sensors, and batteries into a package about a cubic inch in size. (Courtesy of Berkeley Sensor & Actuator Center, University of California: Berkeley www-bsac.eecs.berkeley.edu)

It should, however, be noted that reliability and measurement accuracy are still problems that must be addressed for successful implementation of MEMS technologies to SHM. While MEMS sensing technologies are appropriate for local SHM applications, such as those that identify crack initiation, propagation, and corrosion, deploying a large number of MEMS devices over a large area in a cost-effective manner is a difficult problem. MEMS technologies can make this type of SHM system possible.

Varadan and Varadan (2000) further discuss MEMS-based SHM. In particular, the authors talk about *in situ* aircraft SHM and relate that the biggest single factor in implementing such a system is the sensor wiring. In the authors' opinion, advances in wireless data transmission must first be made before practical SHM systems can be implemented. They note that wires are prone to breakage and vandalism and that wiring is not amenable to moving systems. Finally, the authors mention a MEMS device that incorporates both gyroscopic and acceleration measurement capabilities in one. A reduction in the signal processing load and power requirements is the main advantage of such a sensor.

Vandiver (1997) discusses some SHM techniques related to damage detection in U.S. Army missile systems, such as the determination of propellant separation. Vandiver mentions that Lockheed Martin and System Excelerator participates in a health monitoring prototype development program called the Missile Advanced Remote Monitoring System. A PATRIOT launcher is instrumented with three axis MEMS accelerometers, a humidity sensor, and an

ambient temperature sensor. Numerous shock, vibration, humidity, and temperature data are remotely transmitted over a cellular phone. The author anticipates that, with the miniaturization of electromechanical components and advances in micropackaging, MEMS will play a major role in the future health monitoring of missile structures.

Jones et al. (1999) discuss using silicon-based MEMS technology for damage detection in carbon fiber reinforced polymer (CFRP) composites. The authors claim that silicon-based microsensors can be used for the detection of impacts as well as the presence of damage. The authors describe some serious drawbacks of optical MEMS and surface acoustic wave (SAW) devices, including the cost and complexities involved with signal conditioning. The authors claim that these problems can be remedied through the use of silicon-based, movable element, micromachined transducers. The authors performed a series of experiments in which the microsensors were embedded into a CFRP composite plate. The first series of experiments determined the response of the sensors to low energy impact tests. This study was accomplished by dropping a brass ball bearing on the plate from various heights. The second series of experiments was aimed at determining the response of the sensors to low energy, high frequency acoustic emission within the CFRP panel. This second study was accomplished by fracturing a 0.5 HB pencil lead against the panel and recording the response of the microsensors. The results of the experiments show that low energy impacts on the order of 10 μJ are easily detected with the silicon-based, movable element, microsensors. The low energy (10 μJ), high frequency (10 kHz to 150 kHz) acoustic emission events were detected up to a distance of 13 cm.

One of the main problems with installing sensors within structures for health monitoring is connecting the sensors to outside power sources and data acquisition modules. Gause et al. (1999) discuss the initial testing of Remotely Queried Embedded Microsensors (RQEM). The RQEM system consists of sensor tags and a sensor tag reader. The sensor tag reader has the capability of remotely interrogating the sensor even when the strain sensor is buried up to one inch beneath composite material. The sensor tag is actually powered by the reader itself. Initial testing of the RQEM system showed that more development is needed before these sensors can be used to monitor strain effectively. However, the experimental test performed did demonstrate that the RQEM sensors were very robust and held up well under harsh conditions. Two RQEM sensors were installed on a mast structure of the Spruance Class destroyer to determine the

ability of RQEM sensors to withstand a strong electromagnetic interference (EMI) environment. Both sensors remained operational over the 6-month testing period. RQEM sensors were also installed on the access panels of an AV-8B Harrier T1 Jet to test the robustness of the sensors under heavy vibration conditions. At the time of the paper, the sensors had accumulated over 50 hours of flight time with no degradation of functionality.

Ruffin (1999) discusses the use of microelectro-mechanical systems (MEMS) for structural health monitoring of missile systems. The Remote Readiness Asset Prognostic/Diagnostic System (RRAPDS) will use MEMS technology to remotely monitor several components of missile systems to reduce costs and prevent problems.

3.2.8 Fiber-Optic Sensors

Fiber-optic sensors are gaining attention in the field of structural health monitoring. In Section 3.2.1, the use of fiber-optic sensors for strain measurement has been addressed. Here, more applications of fiber-optic sensors to measuring strain, displacement, temperature, and other physical quantities have been further addressed.

Giles et al. (1999) conducted a study to determine the feasibility of using a distributed fiber-optic sensor for health monitoring in composite structures. By using an optical sensor in which the entire length of the fiber has the capability to detect damage, the number of sensors needed for the structure is greatly reduced. A stress distribution along the fiber will create a perturbation of the birefringence in the fiber, which can be detected and monitored. The authors note that there are several issues that must be monitored closely when embedding the optical sensors into the composite. The optical sensors must not degrade the mechanical properties of the host composite, and they must maintain sound contact with the composite for accurate stress transfer to the sensor for reliable measurements. The coating on the fiber must provide good bonding to the composite structure as well as provide protection from the environment. During the experiment, the authors found that a polyimide coated HiBi silica fiber provided the best bonding conditions to the host composite. The fibers were embedded into a carbon fiber/Epoxy (Hexcel T800/924) wing skin structure that was 1.8 m long by 0.76 m wide. The authors performed a series of tests that included stressing and impacting the skin structure by various means.

The results showed that the distributed fiber-optic sensors could detect strain changes within the structure. The sensors were also capable of detecting impacts within a few centimeters.

Seim et al. (1999) used fiber-optic Bragg grating strain sensors for health monitoring of a historic bridge near Portland, Oregon. The Horsetail Falls Bridge is an 18.3-meter reinforced concrete slab span type bridge, consisting of three 6.1-meter spans. The bridge was built in 1914 and was not designed for the traffic loads that it is currently subjected to. To increase the load-carrying capacity of the bridge, the Oregon Department of Transportation used fiber reinforced plastic composite (FRPC) strengthening. Twenty-eight fiber-grating sensors were placed on the bridge in order to monitor the performance of the FRPC additions and the existing concrete structure. After the sensors were positioned, a 26,000-pound dump truck was moved to various locations on the bridge to ensure that the sensors were functioning properly. In parallel with this activity, more rigorous laboratory tests based on this structure are scheduled. Finite element models of the FRCP-reinforced bridge are also being developed. Data taken from the bridge will be used to validate the laboratory work and finite element models.

Austin et al. (1999) discuss the use of fiber-optic Bragg grating sensors to monitor fatigue crack growth and delamination within hybrid laminates. Hybrid laminates consist of alternating layers of fiber-reinforced plastic (FRP) and aluminum alloy. These laminates have good fatigue characteristics as well as high strength-to-weight ratios. A common failure mechanism for hybrid laminates is fatigue crack growth, which is confined to the alloy laminae, and delamination between the composite and alloy layers near the crack. The authors claim that embedded Bragg grating fiber-optic sensors can be used to monitor the strain in the layers near a fatigue crack. To test this, the authors constructed a rectangular hybrid plate of 152 mm × 350 mm × 1.46 mm. The test piece consisted of a panel made from four composite plies and two 8,090 aluminum-lithium alloy plies. A hole of a 6.35 mm diameter was drilled in the center of the specimen to simulate a fastener hole. The test specimen was fit with an array of 40 Bragg grating fiber-optic sensors near the fastener hole. The specimen was then loaded with a sinusoidal waveform at a frequency of 10 Hz, and strain measurements were taken from the fiber-optic sensors at a frequency of 200 Hz. The peak-to-peak load amplitude was 25.2 kN. The test results show that the fiber-optic sensors can indeed be used to monitor fatigue crack growth and delamination in hybrid laminates.

Takeda et al. (1999) discuss the use of plastic optical fibers to detect transverse cracks within FRP structures. The use of the plastic optical fibers is justified because the plastic optical fibers are much cheaper and easier to install than conventional silica fiber counterparts. Also, the plastic optical fibers have similar coefficients of thermal expansion and elasticity characteristics as the parent FRP structure, resulting in good bondage between the parent material and the optical fibers. However, the plastic optical fibers have much greater light attenuation than silica fibers, limiting their use to short distance transmission. Because transverse cracks in 90° plies of cross-ply FRP laminates generally do not grow into the 0° plies, the plastic optical fibers are embedded along reinforced fibers in the 0° plies so that transverse cracks do not cut the optical fibers. The authors then tested the FRP materials in several configurations of tension and bending while observing surfaces for crack initiation with a video microscope. The authors found that the optical intensity transmitted through the plastic optical fibers decreased linearly with increasing strain when no cracks were present. As cracks began to form, however, the power transmitted through the fibers decreased drastically in a nonlinear fashion. After each test, it was confirmed that the plastic fiber-optic sensors were still in one piece. From the experiments, the authors concluded that the presence of cracks near the sensors resulted in a nonlinear reduction in the optical power transmitted.

Typical electrical strain gauges, such as resistive type, piezoelectric, semiconductor, and capacitance gauges, are small and very accurate strain measuring devices. However, they generally have a small dynamic range, gauge factors of less than 5, and are affected by environmental conditions such as moisture and temperature. Gregory et al. (1999) discuss the development of an optical waveguide sensor with the capability to monitor strains up to 2,000 microstrain that are not affected by temperature. The sensor consists of a flexible, hollow, glass tube, an absorptive layer deposited on the outside of the glass tube, and another layer of high optical reflection. A light source is introduced into one end of the tube via fiber optics. The transmitted light is then read by another fiber-optic sensor at the opposite end of the tube. As the tube is subjected to strain and bends, the outgoing light will have a lower intensity than the incoming light. This intensity reduction is related to the curvature radius of the tube. Thus, strain measurements can be made with this system. The authors tested several different configurations of this sensor in a four-point bending test and found that a glass tube first coated

with polyimide, then with aluminum, could read strains up to 2,500 microstrain (actually higher than the desired design objective of 2,000 microstrain) and had a gauge factor of approximately 490. These results show that optical waveguide sensors are extremely sensitive and have the ability to measure large deformations.

Cohen et al. (1999) discuss the development of a fiber-optic sensor system that will detect wear of water lubricated shaft bearings on Naval marine propulsion systems. The sensor system helps eliminate the amount of downtime needed for traditional inspection methods. These bearings are comprised of nitrile rubber staves that support a shaft, which has a copper nickel sleeve. By embedding plastic fiber optics within the nitrile rubber staves, the amount of wear present within the staves can be detected. As the sacrificial fiber-optic sensors wear, their optical power transmission characteristics change. The plastic fiber-optic sensors are chosen because of the similarity of their material properties with the host nitrile rubber. Currently, a simple underwater indicator is being considered for monitoring wear, and this indicator requires a diver with a light source to inspect the fiber-optic sensors occasionally. At the time of the report, work was underway to develop a means to route the fiber-optic sensors to the ships' onboard data systems for real-time measurement.

Lo and Shaw (1998) discuss the development of a corrosion sensor that is made of a Bragg grating fiber. The sensor is divided into two parts; one that measures corrosion and the other that measures temperature. This corrosion sensor is first fabricated by prestressing an ordinary Bragg grating fiber. While the fiber is under stress, the fiber is partially coated with a metal film such as copper. When this prestress on the fiber is released, the residual stress will remain within the part of the fiber coated with the metal film. As this metal coating is corroded and wears out, the stress within this section will change and the change of optical intensity can detect the stress change. However, temperature variations can also create changes in the optical intensity of the Bragg grating that could influence the stress and the corrosion measurements. This potential influence is why the "free" end of the fiber is used as a temperature sensor. The temperature measurements from the uncoated part can be used to compensate the temperature effect on the readings taken from the metal-coated part of the Bragg grating fiber.

Kwon et al. (1998) use Michelson fiber-optic sensors for health monitoring of a truss bridge. A Michelson fiber-optic sensor is designed so that the magnitude and direction of the measured strain can be determined. The authors found that these sensors were susceptible to signal noise problems and did not produce desirable results.

Vurpillot et al. (1997) discuss the use of fiber-optic sensors to monitor the displacement of the Versoix Bridge in Switzerland. The system that the authors used for measurement uses a measurement fiber that is mounted to the surface of the bridge and a reference fiber, which is free. The reading unit measures the difference of length between the two fibers. The resolution of this monitoring system is approximately 2 μm.

Huang et al. (1997) discuss the use of multimode fiber-optic sensors to aid in the selection of the pavement structure for the Humen Bridge in China. Because the Humen Bridge is a sea bridge subject to a very adverse environment, the quality of the pavement and its resistance to weather induced damage are keys to the performance of the bridge. The authors developed an annular test structure, 10 m in diameter, covered with five different pavement types. Each pavement sample is 100 mm thick and consists of 4 layers, including a steel plate, a waterproof layer, a protection layer, and a surface layer. The authors mounted eight multimode optical fibers to the surface layer of each sample. To test the samples, the authors continuously ran two sets of 5,000-kg wheels over the test samples for a period of three months. A multimode optical fiber produces a speckle pattern at the output when a light source is launched. The pattern is a result of interference and coupling of the different modes propagating down the fiber. The intensity and phase of each mode is modulated when the fiber is vibrated. Damage to the pavement samples caused a decrease in the pavement rigidity that tends to reduce the natural frequencies of the pavement system. The authors used this frequency decrease to successfully detect the onset of damage in the pavement samples that allowed them to choose the most robust pavement structure to be used for the Humen Bridge.

Furrow, Brown, and Mott (2000) developed an optical fiber system for monitoring strain in composite bridge decks. The system was designed to monitor deformation or strain in real time as well as periodically over a period of years. The extrinsic Fabry-Perot interferometer (EFPI) was selected as the most suitable sensor system to measure displacement in this study.

The authors' investigation showed that the EFPI sensor was the only sensor sensitive to the axial strain components and was relatively insensitive to temperature variations. In a scale model test of the composite bridge, the EFPI sensors were attached to the surface of a specimen to demonstrate the measurement capabilities of the sensors. Next, two three-point bend tests were performed on the composite bridge test specimens. Each bridge specimen was composed of a top face sheet, a bottom face sheet, and a support structure made up of triangular sections. Sensors were embedded in both face sheets and in the support structure. In both cases, the sensors embedded in the top and bottom face sheets were damaged during installation, and no data could be taken from them. The sensors in the supports survived installation, and the measurements agreed with those from electrical strain gauges and were as expected. Finally, two 3.048×6.096 m composite bridge decks were instrumented for field testing. Again, the face sheet sensors were damaged and were unusable. The sensors in the support structure were operational. Data were taken for about six hours on two days, one week apart, with the composite bridge installed into an on ramp of a truck weighing station. The data were consistent from one week to the next. A slight drift in the data was observed, and further testing was planned to determine if this variation was caused by increasing temperature throughout the day or actual permanent damage to the bridge deck.

Kwon et al. (2000) use 3×3 fiber-optic Michelson interferometric sensors to detect failure in reinforced concrete beams. The sensor is constructed with a 3×3 fiber-optic coupler in the middle. Two photo detectors and a laser diode are coupled to the ports on one side, and sensing fibers are coupled to two of the ports on the other side. The third port is immersed into index matching liquid. The sensor can measure the magnitude and direction of structural strain. The fiber-optic sensors and electrical strain gauges were attached to the surface of a rebar before the concrete was poured to form the beams for experiments. The beams were loaded in bending until fracture occurred. The authors found that the measurements from the fiber-optic sensors did not match the measurements from the electrical strain gauges. However, the fiber-optic sensors were successful in detecting the failure of the beam.

Satori et al. (2000) developed polyamide coated, small-diameter optical fibers for composite plate monitoring. The advantage of the small 50 μm diameter fibers over normal 125 μm optical fibers is that they do not cause strength deterioration in composites because of their less intrusive nature. The thinner fibers were tested and found to have similar tensile strength to that of the normal fiber, with the same mechanical reliability. The transmission loss in the small-diameter fibers was somewhat higher, but the authors contend that this is not a problem because the length of embedded sensors will be at most several hundred meters. The authors fabricated the polyamide coated fine optical fibers by a fiber drawing process. The fibers were then treated with hydrogen loading under high atmospheric pressure for more effective photosensitivity. Next, the outer polyamide layer was partially etched away by chemical solvent, and Bragg gratings in the fibers were fabricated using the beam scanning method. Finally, the optical fibers were annealed to suppress the wavelength shift. To connect the small-diameter fiber to the normal fiber, which is more suitable for connection with the light source or detector, the authors investigated a special connection method, and the average light loss at the connector was found to be 0.35 dB.

Lloret et al. (2000) present a method for long-term monitoring of structures using existing SOFO deformation sensors. The SOFO optical fiber sensors, which are based on a Michelson interferometer, have been successful for measuring deformations that occur slowly over time. Each sensor consists of two optical fibers. One is installed in mechanical contact with the structure to be monitored, while the second, the reference fiber, is placed loose in a pipe for temperature compensation. Deformation of the structure is measured based on the difference of length changes between the two fibers. The lengths of the fibers are measured by interferometry. Based on the SOFO sensors, the authors further developed a monitoring system to monitor the dynamic behavior of structures, which requires a much higher sampling rate. To use the SOFO sensors to measure the dynamic behavior, the radio frequency (RF) amplitude modulation of a broadband source was employed. Although the dynamic monitoring system was validated with experimental tests, further work is needed to achieve the desired sampling rate.

Okabe et al. (2000) apply fiber Bragg grating (FBG) sensors for detecting transverse cracks in carbon fiber reinforced plastic (CFRP) cross-ply laminates. Because the FBG sensors are sensitive to nonuniform strain distribution along the length of the gratings, they have the potential for detecting damage that causes such strain in composite materials. To detect

transverse cracks, an FBG sensor was embedded in 0^o ply on the border of the 90^o ply where the transverse cracks appear. The reflection spectrum was measured at various tensile stresses, and the change in the spectrum was analyzed. It was found that the transverse cracks could be detected from the change in the form of the reflection spectrum.

Borinski et al. (2000) discuss the use of optical fiber sensors in the harsh environment associated with high-performance aircraft. Fiber-optic sensors are ideal for such environments because they are tolerant to extreme temperatures, electromagnetic interference, shock, and vibration. Furthermore, the fiber-optic sensors are suitable for aircraft, which contains inflammable fuel, because they are not a spark source and add negligible weight to aircraft. The authors present sensor designs based on the extrinsic Fabry-Perot interferometer (EFPI) for measuring pressure, acceleration, and skin friction. Each of the sensors has been fabricated and tested.

Elvin and Leung (1997) discuss the use of fiber-optic sensors for the detection of delamination in cantilever beam-type composite structures. Specifically, the authors propose using a system that consists of two fiber-optic sensors. One of the fibers will be embedded within the composite structure, while the other fiber will serve as a reference fiber outside of the structure. When a moving point load is applied to the structure, the reading from the embedded fiber will change. As the point load is moved over a delaminated region, the total extension of the embedded fiber will jump significantly, and the phase difference between the lights from the output of the embedded fiber and the reference fiber will be shifted. By noting the position of the load, the magnitude of the change in total extension as well as the phase shift, the position, and relative magnitude of the delamination can be determined.

Davis et al. (1996) discuss the use of fiber-optic Bragg grating (FBG) sensors to monitor static loads as well as modal response of a bridge section. The authors installed 48 FBG sensors on a full-scale single-lane bridge section in a controlled laboratory setting. The bridge section was 12.2 × 3.4 m and contained a 15.24-cm-thick concrete deck. The deck was supported by three longitudinal steel I-beams. Thirty FBG sensors were attached to the rebar in the deck section before the concrete was poured. The remaining sensors were attached to the underside of the I-beams. Right after the concrete was poured, the sensors recorded strain information at a rate of 6 samples per minute for 250 minutes. After that, the sensors recorded strain once an hour during

the 38-day concrete cure cycle. After the curing cycle, a series of static tests were performed on the intact structure by loading the structure at various positions. One of the I-beams was then incrementally cut with a torch to simulate damage, and the tests were repeated. Comparison of the strain measurements from the intact and damaged structures showed a significant change in strain patterns. The authors then used the same array of the FBG sensors to perform modal analysis on the structure. Two sets of dynamic measurements were taken. The first set was taken after the I-beam had been cut and the second set was taken after the cut had been repaired by welding. The bridge was excited with a 222-N shaker located on the center of the concrete deck. The authors found a noticeable difference in the modal behavior of the bridge in the damaged and undamaged states.

Staszewski, Read, and Foote (2000) discuss the methodology of the intelligent signal processing used for the passive impact damage detection system based on fiber-optic sensors. To obtain information about the energy and location of impacts, more advanced signal processing is required than is needed for operational load monitoring systems, even though they use the same basic sensors. The authors describe the signal processing methodology, including data preprocessing, feature extraction and selection, pattern recognition, and optimal sensor placement. Impact experiments were performed on a composite wingbox structure to demonstrate the technique. The structure was instrumented with fiber Bragg grating sensors calibrated to produce voltage proportional to strain. Data corresponding to impacts that do not cause damage were collected, and then the structure was subjected to a series of damaging impacts. Signal denoising was performed with the orthogonal wavelet transform, followed by feature extraction analysis and statistical pattern recognition analysis.

Rao et al. (1997) report on a wavelength-multiplexed fiber-optic sensor system based on the combination of a Fiber Bragg Grating (FBG) and an all-fiber Fabry-Perot interferometric (FFPI) sensor. The FFPI, formed by wiring two FBGs with the same central wavelength, is interrogated using low coherence interferometry to minimize the interferometric phase noise in order to achieve high sensitivity. The change in the optical path of the FFPI is used for high sensitivity vibration measurement, while the wavelength-shift of one of the two FBGs is used for temperature measurement. Strain is measured by the wavelength shift of another FBG sensor, which is arranged in tandem near the FPPI and has a different central wavelength to the FPPI.

Multiple sensor pairs are wavelength-multiplexed to facilitate quasi-distributed measurement for static-strain, temperature, and vibration measurement.

The Composite Hull Embedded Sensor System (CHESS), a joint program between the U.S. Naval Research Laboratory and the Norwegian Defense Research Establishment, is described in a paper by Wang and Pran (2000). The CHESS ship hull monitoring system is based on a flexible modular design, which allows one to take advantage of distributed computation technology when computationally intensive signal processing tasks are necessary. CHESS is an ideal system for fiber-optic sensors because fiber-optic sensors are often used in applications requiring distributed sensing. In the CHESS system, each sensing unit is functionally integrated with control and local digital signal processing. Wang and Pran explain that the sensors must be synchronized for real-time signal processing. The various signal processing modules used employ a common data interface and structure. Data communication between modules is based on TCP/IP sockets, allowing data to be passed between signal processing modules running on different computers in the network.

Johnson et al. (1999) also discuss the CHESS program. Global ship hull bending is recorded with Bragg grating sensor pairs, local strain concentrations are monitored with Bragg grating rosettes, and the vibrational response of the ship's water jet propulsion system is measured with a small array of longitudinally bonded gratings. Large dynamic strain responses caused by wave slamming are also monitored. The authors' analyses of the measured data show that the Fiber Bragg Gratings are well suited to measuring low-frequency, high-amplitude strains encountered in hull bending as well as the small, high-frequency vibrations present in the propulsion system.

3.2.9 Sensor Placement

Side et al. (1997) discuss issues of the optimal sensor placement for a simple 300 × 300 × 3 mm rectangular plate numerical model clamped on two opposing edges and simply supported on the other two opposing edges. Damage is simulated with the aid of a finite element model and is introduced by severely reducing Young's modulus. Drawing on earlier work, the authors measure shear strains as the most effective data for diagnosis (Staszewski, Worden, and Tomlinson 1998). The authors train a neural network and then use a genetic algorithm to

determine the optimal placement of sensors. The efficiency of the algorithm is confirmed through an exhaustive search of all possible sensor locations, in which the optimal solution is only slightly different from that calculated from the genetic algorithm.

Staszewski et al. (2000) employ a genetic algorithm to determine the optimal sensor locations for impact location and amplitude identification on a composite plate. A box-like structure composed of aluminum channels and a composite plate was used as the test specimen to simulate the skin panel of an airplane. The impacts to the composite plate were applied on the top surface, while the bottom surface was instrumented with 17 piezoceramic sensors to record strain data. Using the time after impact of maximum response and the magnitude of response as inputs to the neural network, the trained neural network was used to identify the impact location and estimate the impact level. The objective of the general algorithm was to select the optimal sensor configuration composed of three sensors out of 17 sensors. The best sensor configuration was chosen by minimizing the percentage errors in the impact level prediction at the given sensor locations. This genetic algorithm (GA) turned out to generate suboptimal fail-safe sensor placement. The performance of this suboptimal sensor configuration was compared with the optimal sensor placement found by an exhaustive search.

Said and Staszewski (2000) found the optimal sensor placement for the same test structure in a slightly different manner. The same genetic algorithm is used, but the optimal solution is found by maximizing the overall mutual information within selected sensors. Based on information theory, the mutual information assesses the information content of sensor data by eliminating arbitrary dependences between features obtained from the selected sensor locations. The sensors selected by this method are located closely to the fixed boundaries. The authors state that this observation matches well with the practice where the most difficult regions for amplitude detection are near the boundaries because these regions have relatively small detections compared with the central area of the plate.

A powerful and important concept for determining optimal sensor location for damage detection can be found in Shannon's principle of mutual information (Cover and Thomas 1991). If there are two sets of measurement locations, *A* and *B*, the mutual information, $I(a_i, b_j)$, represents the amount of information learned by a_i about b_j,

$$I(a_i, b_j) = \log_2 [\frac{P_{AB}(a_i, b_j)}{P_A(a_i) P_B(b_j)}] \ ,$$

where a_i and b_j are the measurements from the sensor locations *A* and *B*, respectively, $P_{AB}(a_i, b_j)$ is the joint probability density for measurements *A* and *B*, and $P_A(a_i)$ and $P_B(b_j)$ are the individual probability densities for *A* and *B*, respectively. If the measurement of a_i is completely independent of the measurement of b_j, $I(a_i, b_j)$ becomes zero and is then averaged over all sensor locations, resulting in the average mutual information between *A* and *B*. The optimal sensor location is determined by minimizing the information between sensors.

Heylen and Trendafilova (2000) use the concept of average mutual information between measurement location sets to find the optimal sensor spacing on a rectangular plate. Finite element simulations of the plate are performed, and damage is a simple 70% reduction in the stiffness of two elements. The authors consider only equally spaced sensor configuration but with different spacing between the sensors. They then determine the sensor spacing, which minimizes the mutual information between the sensors. The sensor selection procedure does not depend on the damage configuration or the damage detection method. Average errors between the actual and estimated stiffness are approximately 7%. These average errors are achieved with the optimally spaced sensors and the sensors with less than the optimal spacing. On the other hand, average errors of approximately 28% are obtained using the sensor sets whose spacing is greater than the optimal sensor spacing.

Following along the same lines, Papadimitriou, Katafygiotis, and Yuen (1999) propose a sensor placement technique to improve the quality of the model parameter estimates. The optimal sensor configuration is selected by minimizing the information entropy measuring the uncertainties in the model parameter estimates. The uncertainties in the parameter estimation are attributed to limitations of the mathematical models, the presence of measurement errors, and unknown excitations. The object function for the optimization is based on the prediction errors between the model and measured responses. The difference between measured and model response time histories is considered to be a specific realization of a stochastic process taken from a class of probabilistic models, parameterized by a given parameter set. Here, the

uncertainty in the parameter set is quantified using probability density functions (PDFs), which measure the relative plausibility of each model chosen beforehand to describe the input-output relation of the structure. Baye's Theorem is used to process new measurements and update the PDF that is used to quantify the uncertainties in the parameter set. The object function is then minimized with response to different sensor numbers and configurations using a genetic algorithm. In a similar study, Beck, Chan, and Papadimitriou (1998) apply the method to a nine-story uniform shear building represented by a spring-mass model. The authors find that optimal sensor placement strongly depends on the type of excitation, i.e., broadband ambient, impulsive, or forced harmonic excitations, and the structural parameterization scheme employed. Another similar study was performed by Beck, Papdimitriou, Au, and Vanik (1998).

Schulz et al. (1998) address the issue of damage resolution as a function of spatial distribution of sensors. They show that damage can be located within a spatial resolution equal to the distance between sensors on a structure. The technique proposed by the authors requires the measurement of the frequency response functions corresponding to both translational and rotational modes. Furthermore, excitation forces must be applied at points where the response of the structure is measured. Assuming that the structure's force-to-displacement transfer function, H, is known for the undamaged state, Schulz et al. partitions the transfer function matrix into sections corresponding to the measured displacements, H_{11}, and those unmeasured. A damage vector, d, is then defined as the difference between the measured force vector and the H_{11}^{-1} matrix multiplied by the vector of measured displacements. Physically, this damage index represents unbalanced forces near damage. That is, if damage occurs, the damage vector will have nonzero entities only at the DOFs connected to the damaged elements. This damage index is used to locate damage within the spatial resolution of sensors. A finite element simulation of a cantilever beam is employed to verify this method. The finite element model of the beam consists of 15 elements, 15 rotational and 15 translational DOFs. Five percent linear stiffness reduction in one element is successfully detected, and this procedure is repeated for all 15 elements successively. Results indicate that, for all damage cases, the damage is correctly bounded between the closest measurement nodes. However, when only translational degrees of freedom are used, the method is not always robust.

Ettouney et al. (1999) discuss determining optimal sensor locations for structural health monitoring for structures that are subject to multiple loading conditions. The authors touch on existing methods for determining optimal sensor locations for single loading conditions. The authors claim that a structure will have a different optical sensor configuration for each loading case that it is subjected to. Because it is not practical to outfit a structure with a network of sensors for each possible loading case it may see, an optical sensor location for the multiple loading cases must be developed. The authors present a goal programming method to handle conflicting optimal sensor configurations for different loading cases. This programming consists of assigning weighting factors to each loading condition. For their work, the authors used design factors for the corresponding loading condition as weighting factors in the goal programming scheme. The authors apply the method to numerical models of two different structures subject to multiple loading conditions. The first structure was a simple steel tower subject to its own weight as well as wind loads. The second structure was a suspension bridge subject to its own weight as well as horizontal seismic loads.

3.2.10 Other Issues

Wang and Pran (2000) discuss the use of fiber-optic strain gauges based on the Bragg grating principle. They explain that fiber-optic sensors are ideal for distributed sensing because many sensing channels can be integrated into a single fiber. The performance of the fiber-optic strain gauges is compared to that of a conventional electrical strain gauge, and it is noted that the conventional sensors suffer from electromagnetic noise. Wang and Pran state that Bragg fiber-optic strain gauges can receive signals at frequencies of many kHz but are limited to measuring strains up to 2,000 microstrain because the sensing range is limited by the sensors' passband.

Efforts by the Japanese government to utilize fiber-optic sensor systems are detailed by Mita (1999). Mita uses the Raman optical time domain reflectometry sensor as a means for measuring temperatures during concrete curing. In addition, soil temperatures around underground natural gas tanks are monitored to ensure that the soil remains frozen there. It is noted that fiber-optic sensors are cost-effective for applications requiring distributed sensing and that these sensors are minimally intrusive when embedded into materials such as concrete and composites.

Solomon, Cunnane, and Stevenson (2000) discuss the instrumentation of the Tsing Ma Bridge in Hong Kong. The authors relate that 52 wind components are measured using 21 anemometers, 438 platinum resistance thermometers are installed on the bridge, and load plate sets are placed into the carriageway to measure traffic loads. An additional 121 inertial navigation-grade servo-accelerometers and a dual-fluid system for displacement measurements are installed. This latter measurement system consists of pressure sensors placed along a system of interconnected fluid-filled pipes, and the displacement is derived from the differential pressure between reference and measurement points. The authors caution that temperature effects must be carefully accounted for because they affect the readings. Temperatures in the pipes are measured at 15 locations throughout. A total of 364 resistance strain gauges are also installed on the bridge to measure strains. A dual-fault-tolerant, fiber-optic network was chosen for communication between the logging outstations and the central computers. The outstations gather measurement information from nearby sensors and forward it to the central computers. The authors emphasize the need for minimizing the amount of wires because of economic considerations.

A discussion of fiber-optic sensors based on Optical Time Domain Reflectometry (OTDR) for the SHM of concrete structures is discussed in Leung et al. (1997). The method is based on the backscattered power in a fiber as a function of time. In straight portions of the fiber, the loss is caused by absorption and scattering, whereas in the curved portion, the loss depends on the fiber curvature. In principle, when cracks form, the fiber will bend and backscattered power will change. Leung et al. develop a model of signal loss versus crack opening. They note that high sensitivity implies high signal loss at cracks, while low sensitivity sensors may not detect small cracks. Tests are conducted on laboratory scale specimens. A sensor rod with a fiber-optic cable wound around it is cast into a beam, which undergoes a three-point bending test. Additionally, the sensor is tested in a notched beam. A displacement transducer is placed near the notch and a plot of signal loss versus displacement is constructed. Although the optical measurements are affected by noise, results indicate that cracking can be detected with the sensor rod.

Diagnosing the health of sensors is an important issue for SHM applications. Hickinbotham and Austin (2000) present a method for automating the detection of sensor defects and claim that their method is the only such method. The researchers apply their diagnostic tool to sensors on airframes. They note that the structural health of airframes is often monitored by an analysis of

the frequency of occurrence matrix (FOOM) produced after each flight. Each cell in the FOOM records a stress event of a particular severity. These matrices are used to determine the amount of an aircraft's useful life that has been consumed. During the monitoring of the FOOMs, there are two types of sensor defects. Electromagnetic current faults cause a random addition of stress counts, and the second type of fault is a shift in the response of a sensor. Sensor faults are detected by examining the variability of FOOMs from normal flight conditions. A number of statistical measures are applied to sets of example FOOMs and are used as inputs to a novelty detector. This novelty detector identifies any unusual flight, providing that changes are evident in the measurements. Sensor data from 80 flights were provided, and data from 40 of these flights were used as training data. Sensor fault data are simulated by adding noises or drafting the remaining 40 data sets. With results from these flights, the authors conclude that the novelty detector can be successfully used to detect abnormal sensor data.

Paolozzi, Felli, and Capanero (1999) are exploring the use of interferometric optical fibers embedded into aluminum plates and shells to measure temperature variations in those structures. They note that the foremost application of such aluminum plates and shells is found in the aerospace industry and that temperature is an important factor in fatigue analysis. The authors also state that optical fiber sensors are more appropriate for taking global measurements because the quantities measured are actually integrated over the length of the fiber. Because of the severe environment to which the fiber is subjected during casting, research in embedding these fibers into aluminum has concentrated on developing optimal fiber coatings that can withstand temperatures of between 700^{o}C to 750^{o}C. Furthermore, it is noted that a good bond between the metal and the coating is essential for good strain coupling. Based on testing, the authors find that aluminum coated fibers seem to be the best, but caution that further testing is needed to characterize the aluminum-polyimide interface. The authors also devise a means for embedding optical fibers into aluminum plates that they call the *collamination* method. In this method, the optical fiber is embedded between two very thin aluminum sheets (about 150 μm). It is important that these sheets be very clean for proper fiber/metal bonding, and so they are ultrasonically degreased in an Inibisol bath. The research performed to date reports positive results on simple fiber integrity tests only, and the authors caution that additional testing is required before the success of collamination can be established.

Catbas et al. (1999) note that a practical issue in SHM is coordinating the data from various sensors, especially when those sensors are measuring different quantities and have different communication and hardware requirements. For example, a typical instrumentation system deployed on a bridge might monitor wind velocity with a frequency of 1.0 Hz as well as traffic-induced strain and acceleration with a frequency of 75 Hz. In addition, those measurements might not be collected simultaneously. The researchers are attempting to find an optimum compromise between quality, quantity, and content of data. Some limitations that the authors address may become obsolete because of the continuous improvement of data acquisition and computing.

Matrat, Levin, and Jarlas (1999) have investigated the effects of interfacial debonding between embedded Fiber Bragg Grating (FBG) sensors in composite materials. The responses of debonded FBG sensors are compared with those of fully bonded FBG sensors by means of finite element analysis. In fact, the authors create a finite element model of a 36-piles carbon/epoxy composite with a polymide coated optical fiber embedded in the midplane. The plate thickness is 4.572 mm. The silica glass fiber is 125 μm in diameter and has a 7.5-μm-thick coating. The region of the fiber composite interface is modeled with a refined mesh, and the three-dimensional strain field is determined through a contact analysis for various thermomechanical loadings. The authors observe that the fully debonded fiber/composite interfaces result in the largest strain measurement errors, with axial stresses being in error of approximately 1% to 4% (the latter value is a result of thermal effects) and with transverse stress errors of approximately –75%. The authors postulate that the errors result because the debonded interface cannot transfer the composite stress effectively to the center of the fiber. Additionally, the authors observe nonlinear strain response when combining both thermal and mechanical loading, irrespective of debonding. Although not considered in their paper, the moisture content of the material as well as adhesion capabilities of certain glues under varying environments needs to be considered in FBG sensor debonding. Limited research in the effects of different glues on FBG sensor performance has been performed by Yamaura et al. (1999).

Paolozzi, Ivagnes, and Lecci (1999) examine the mechanical influence of a dense network of embedded optical fibers on carbon fiber/sterocyanate resin composites. Specifically, the researchers conduct interlaminar shear tests, flexural tests, and flatwise tests to estimate the

degradation of bonding between the composite plies and fibers, pull-out tests, and traction tests on composites with embedded optical fibers. These tests, with the exception of the pull-out test, are undertaken according to typical American Society of Testing Materials (ASTM) standards. The pull-out test indicates that the fiber fails by breaking rather than by debonding, thus concluding that the bond strength of the optical fiber with the composite resin is stronger. The strength and elastic modulus of the composite specimens tested are unaffected by the embedded optical fibers. The researchers observe that only the traction strength of the composite specimens tested with optical fibers positioned perpendicularly to the reinforcing fibers degrade to about 50% of the nominal value. The reason for this strength degradation is that the perpendicularly oriented fibers are by necessity kinked to wrap around the reinforcing fibers. This kink could then lead to stress concentrations that affect the traction strength.

Sensor reliability becomes important when measurements are required over a long period of time. Hyland (1997) uses this motivation to discuss some benefits of the Adaptive Neural Control (ANC) network. He states that the ANC architecture is able to effectively deal with applications in which sensors and actuators are defective. In these cases, the ANC network solves an optimization problem under the new constraints, achieving a new network topology that is optimal for the new hardware configuration.

Fiber Bragg Grating (FBG) sensors hold promise for SHM applications, which require distributed sensing at reasonable costs. Yamakawa et al. (1999) perform tensile tests on optical fibers coated with either polymide or ultraviolet-cured epoxy acrylate. Both coated fibers are 125 μm thick. The former exhibits a tensile strength of 1.1 GPa with a maximum strain of 1.5%, while the latter's values are 1.4 GPa and 1.8%. Because 0.2% is the approximate yielding strain of steels, the coated FBG sensors have ample measurement range for steel applications. The authors also perform thermal expansion tests and obtain an expansion rate of 9.8 microstrain/^{o}C, and a compression rate of 6.5 microstrain/^{o}C for both coated fibers. Finally, the authors observe that the FBG sensors indicate slightly smaller strains compared to the values obtained by resistive foil strain gauges when both are glued on identical and identically loaded steel specimens.

Kulcu et al. (2000) review information technology issues for continuous monitoring of the Commodore Barry Bridge. The monitoring system of the bridge consists of over 100 channels of sensors. Of these channels, there are slow speed strain gauges to measure slowly varying environmentally induced strains as well as high-speed strain gauges to measure the effects of traffic. In addition, a camera is used to record traffic pattern images. These gauges are hard wired to a central data acquisition station, in which three slow-speed data acquisition systems, one high-speed acquisition system, and a data control computer are located. All data acquisition systems are integrated under the LabVIEW platform. Finally, the authors talk about data storage, introducing two conceptual databases. One of those databases is Internet-based, and the other one processes all data locally and makes the results available through the Internet.

Lin (1999) describes the SMART (Stanford Multi-Actuator-Receiver Transduction) layer developed for structural diagnostics of composite materials (see Figure 6). The SMART layer is manufactured with the same methods as printed circuit boards. It is a flexible sheet that contains distributed transducers. The SMART Layer is embedded into a composite member, and the transducers it contains can be both actuators and sensors. The layer has a thickness of less than 0.08 mm (0.003 in.) and a temperature tolerance of up to 200^{o}C (400^{o}F). This temperature is above the curing temperature for most composites. Lin claims that the layer has little to no effect on the mechanical properties of the composite. As an example, the author points to tests comparing the tensile strength of composites with and without the SMART layer. The tests show no difference in failure loads between the two.

Particularly attractive sensors for SHM are those based on the piezoelectric thin-film concept. Such sensors can be utilized in situations where distributed sensing is important. The most notable advantage of thin-film sensors is their ability to continuously sense parameters such as strains as opposed to discrete points. Zeng et al. (1999) describes the process of Electrostatic Self-Assembly (ESA) used to fabricate many of these thin-film sensors. The ESA process involves consecutive adsorption of anionic and cationic molecule-based polyelectrolytes onto charged substrates. The choice of particular ions is important for the properties of the piezoelectric thin films. Zeng et al. use asymmetric structured polymers with large dipole moments for the thin film processing. The researchers characterize their films with ultraviolet visible spectroscopy and thickness measurements, while investigating the electrorestrictive and

piezoelectric responses of the films by performing bending deformation experiments. Zeng et al. (1999), demonstrate that multiple films with different piezoelectric coefficients can be fabricated with the ESA process. This fabrication ability is important for MEMS devices where piezoelectric materials are used for actuation as well as for general SHM applications that require different levels of strain measurements.

McKee et al. (1999) described the use of "smart coatings" to detect cracks for use on engine components. These coatings, developed by Innovative Dynamics, Inc., are less than 10 microns thick and contain planar sensors for crack detection called crackwire sensors, which measure crack length by monitoring changes in the resistance of the sensor. These sensors also have the ability to detect plastic deformation as well as crack growth. The authors performed a series of destructive tests on Inconel 718 coupons covered with smart coatings. From the results of the tests, the authors concluded that the smart coatings are effective at detecting cracking as well as plastic deformation.

Development of multipurpose sensors is receiving large amounts of attention in the field of smart structures. Dubow et al. (1999) describe the use of embedded piezoelectric disks as multipurpose sensors. Specifically, the authors embedded pressed or semicrystalline PZT ceramic sensors into various epoxies. The authors show that these sensors could serve three separate purposes: monitoring the cure stage of the epoxy, strain measurements, and dynamic mechanical modulus monitoring. The electrical impedance of the piezoelectric sensors varies with the viscosity during curing as well as the state of strain of the epoxy. By monitoring the impedance, the sensors can be used as cure monitors and as strain gauges. Two or more embedded sensors are used to determine the acoustic velocity of the epoxy. From the acoustic velocity, the dynamic mechanical properties (Youngs modulus, Bulk modulus, and Poisson ratio) can be calculated. In his way, the piezoelectric sensors can be used as dynamic property monitors. Monitoring the dynamic properties of the material can indicate the onset of damage within the material.

Teral et al. (1998) propose a method for measuring lateral forces along a power transmission cable with a specially designed fiber-optic sensor. First, the central core of the fiber would be designed to have a known refractive index. Second, this core would be surrounded with a guiding cladding with a refractive index lower than the previous one. Third, a second guiding

layer with a substantially higher refractive index than the core would surround the first cladding layer. Finally, a cladding with a substantially lower index than the first cladding would surround the second guiding region. A train of interrogating light would be pulsed into the central small core. Any lateral force in the fiber would deflect a fraction of this light into each layer. Because every layer has a different refractive index, the deflected light would arrive at the other end of the fiber with a varying time delay. Because the wave speed of each guiding region is known in advance, the time delay information can be used to locate the lateral force induced in the cable.

3.3 Data Transmission

The objective of instrumentation is to acquire data, and the role of a telemetry system is to transmit the data so that the acquired raw data can be transformed into useful information. Today's conventional monitoring systems are characterized as having instrumentation points wire-connected to the centralized data-acquisition system through coaxial cables [see Figure 9 (a)]. Common sensors output analog signals that need to be sampled and digitized for use in modern discrete signal processing systems. The distance from the sensors to the data-acquisition system can range from 10 to 300 m in practice. As the signal travel distance becomes longer, the analogy signals may become noisy and degrade because of coupled noise sources near the cable path. When the analog signals arrive at the centralized data-acquisition system, an analog-to-digital converter discretizes the analog waveforms. At this stage, the user of the monitoring system can take raw digitized data and extract the relevant engineering quantities from the data.

As the number of instruments increase, the degree of sophistication in the instrumentation and the computational and data-processing needs become far greater. The single largest problem in the conventional wired system is the installation of all instrumentations. Straser et al. (1998) states that the cost of installation approaches 25% of the total cost of a monitoring system, and the installation time consumes over 75% of the total testing time for large-scale structures. With the monitoring system installed, the concern shifts to the cost of maintenance. For *in situ* testing, the repeated changes in temperature and humidity, exposure to rain and direct sunlight rapidly deteriorate the sensors and cables.

There are several technologies that have merged and created the opportunity to develop a monitoring system that has new configurations and characteristics: wireless communication, embedded computational power, and MEMS sensors. Wireless communication can remedy the recurring cabling problem of the conventional monitoring system. Embedded microprocessors or microcontrollers can allow the inequity of distributed computational power and data processing. MEMS sensors can provide compelling performance and an attractive unit price. With the combination of the wireless communication, embedded processors, and MEMS sensors, it is possible to move the data acquisition and a portion of data processing toward the sensors, presenting a departure from the traditional instrumentation configuration. A system architecture view of such a new system is presented in Figure 9 (b). This section presents articles addressing issues related to wired or wireless data transmission.

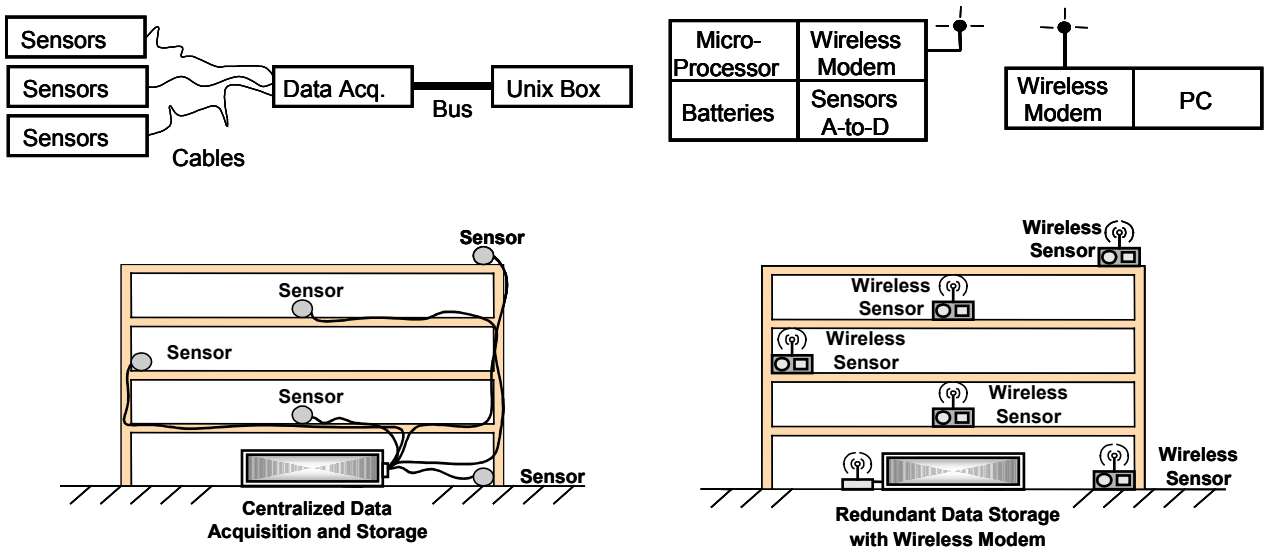

(a) Conventional wired monitoring system (b) Modular wireless monitoring system

Figure 9. Comparison of wired and wireless configurations of a structural health monitoring system (Courtesy of Straser et al. 1998).

3.3.1 Wired Transmission

Mita (1999) briefly addresses a monitoring system developed by Shimizu Corporation in Japan for construction management purposes such as that for erecting buildings. Sensor data are collected and stored in the computer of a local monitoring system. The data are transmitted to a central storage and monitoring server via the Internet. Because most of the server functions are coded in JAVA programming language, the portability of the system is excellent. Mita mentions that a major difficulty is the lack of standard wireless networking systems but points to recent developments as promising to overcome this difficulty.

Todoroki, Shimamura, and Inada (1999) present a study on the use of Ethernet LAN (Local Area Network) to transfer digitized sensor data. The authors note that the use of Ethernet LAN can preclude thick bundles of transmission wires and makes it robust against electromagnetic interference. Other potential benefits of Ethernet LAN in SHM applications are that multiple sensor types are easily interconnected and that changes to the SHM system are easily implementable.

The Ethernet LAN for real-time SHM applications is yet impractical because all stations have an equal chance of sending data and cannot reserve priority. The authors discuss the structure of the Ethernet LAN system, detaining the different layers and byte-structure of data packets as well as the TCP/IP and UDP/IP data transfer protocols. They discuss four types of cables used in the Ethernet, citing the 10-base-5 and 10-base-2 coaxial cables as very noise-resistant. The authors state that using 10-base-5 cables requires repeaters every 500 m if the data transmission length extends beyond 500 m. In this case, the maximum transmission length is 1,500 m. In addition, connecting stations to the 10-base-5 transceivers are needed. Although the 10-base-2 cables are more cost-effective, problems at one connecting station affect the whole network. Finally, the 10-base-F cable, although expensive, is an optical link that is very noise resistant and suitable for outdoor usage. The authors discuss “SmartLink,” a product manufactured by Keithley Corporation, that incorporates 3 channels of strain gauges or 8 channels of voltage measurements. The SmartLink can store 15 kilobits of data in memory, with a maximum recording rate of 33 kHz. The SmartLink is physically 169 × 35 × 28 mm, and uses the UDP/IP protocol. The authors also show a schematic of a SHM system called the Plug & Monitor system

on the Japanese bullet trains. This system incorporates vibration, temperature, optical, and speed sensors as well as cameras under the railroad carriages to confirm the condition of the tracks. Each subnetwork on the train features its own CPU to process data locally and minimize the amount of data transmitted, thereby minimizing chances of data collision. This system does not require structural analysis or experiments to detect damage but only requires the user to plug sensors into the system. The system then automatically constructs the relations between the distributed sensors and judges deviations from the normal measurements. Then, web-based cameras are used to confirm damage. The authors, however, do not specifically state the details of the Plug & Monitor system and only state that the software is written with JAVA for Web portability.

3.3.2 Wireless Transmission

Two practical problems present themselves when implementing a SHM system in the field. First, the infrastructure required to transmit and process data can be prohibitive in an economic sense. Second, massive interconnections from the sensors to the processors require complex configurations of hardware systems. To deal with these problems, Mitchell et al. (2000) propose the use of distributed computing and sensing to detect damage in critical locations. Their system makes use of wireless communication technologies, either Radio Frequency (RF) communication links or commercial wireless cellular phone networks. The proposed system consists of several clusters distributed physically over a structure, which communicate with a central processing unit and amongst themselves through wireless means. Each cluster is composed of a microcontroller, a wireless transmitter, data acquisition circuitry, actuators, and sensors. Each cluster has the capability to individually acquire data and process it locally or simply communicate with the central processing unit. The authors develop a laboratory scale hardware setup for distributed computing and sensing. Their cluster is designed around a Motorola 8051 microcontroller development board. Three-layer network architecture is developed for effective communication between the central processing unit and the individual clusters. The architecture supports the detection and correction of errors introduced by the communication channel through coding techniques and retransmission of data.

Walter (1998) employs a space telemetry system in order to characterize the environments that a system encounters in service. When the system is in service in space, the acquisition of the environmental measurements presents unique challenges. For instance, a satellite system in space is exposed to a wide range of temperatures, charge particles, and electromagnetic radiation, requiring a sensing system, which can cover a broad range of these measurement quantities. Additionally, the measurement through space telemetry is often hampered by limitations in available frequency bandwidths. Based on mechanical shock and vibration specifications listed in environmental design requirements, accelerometers are commonly used to measure inputs and responses in component and structural levels. Considering the fact that launching satellites into low earth orbits costs approximately $10,000 per lb, the size and weight of the measurement system must be minimized. However, for space testing, the more measurement channels the data acquisition/telemetry system has, the more accelerometers, signal conditioners, multiplexers, radio frequency transmission links, and battery power are required. This situation imposes a conflict against to the stated goal of minimizing the total/payload of space vehicles. Furthermore, when multiple measurement channels are available, the numerous sensor readings should be combined into a single output stream so that they can be transmitted over a single radio frequency link to a ground receiving station. Regarding this multiplexing, the author gives a review of time and frequency division multiplexing over radio frequency transmission links. A history of the space telemetry technology evolution can be found in Strock and Rueger (1995).

Straser et al. (1998) propose a civil infrastructure SHM system based on wireless data transfer technology. Specifically, the authors note that long term SHM can provide a benchmark to improve the fidelity of subjective visual inspections, reduce inspection costs by focusing inspection efforts on regions where damage may be located, and decrease the manual inspection periods. They also note that high costs per channel, extensive cabling, signal deterioration over long transmission distances and environmental exposure, and maintenance costs have prohibited the deployment of SHM systems for civil infrastructure. To address these concerns, Straser et al. introduce key design factors such as ease of installation, low costs per unit, and broad functionality. In particular, embedded microprocessors, radio modems, batteries, data acquisition equipment, MEMS accelerometers (Kistler 8352A2) and digital/analog converters (Harris Semiconductor H17188) are specified. A major obstacle for SHM systems providing real-time monitoring is the time synchronization between sensors. To overcome this obstacle, the authors

implement an AM type radio to perform the time synchronization. The prototype system developed includes a PC running network communication software and analysis software to calculate interstory drifts and cumulative normalized Arias intensity. The authors claim that the price of their prototype system in 1997 was less than $1,000.

Mitchell et al. (1999) discuss the application of smart sensors and wireless data transmission over radio frequency (RF) for health monitoring. The use of wireless transmission of structural data eliminates several problems such as extensive transmission cables and damage to instrumentation or computing equipment as a result of harsh environment. The authors develop a smart sensor, which integrates a microcontroller, a sensor, and the RF receiver/transmitter. The microcontroller has the ability to sample signals from several different sensors. This multiplexing ability reduces the total number of data channels needed. To demonstrate the feasibility of the wireless transmission, the authors performed an experiment that consisted of monitoring the variations of the natural frequency for a cantilever beam with a tip mass. To simulate damage (loss of mass), the tip mass was removed. The beam was excited with a chirp signal over a frequency range of 4 Hz to 100 Hz. The excitation and sensor data were transmitted over the wireless channel at a rate of 19,200 bps. This transmission rate was equivalent to a sample rate of 400 Hz. The wireless results proved to give similar results when compared with wired results for the same test setup.

Bennett et al. (1999) discuss monitoring of strains and temperatures within the pavement of a highway using wireless telemetry. The ultimate goal of this monitoring system is to predict a remaining fatigue life of the pavement based on the actual strain measurement rather than the estimated strain values predicted from an analytical model. Previous attempts of *in situ* strain monitoring required extensive cabling, and this resulted in high installation costs, excessive highway damage, and unreliable electrical connections. To overcome these difficulties, the authors developed an instrumented asphalt core with built-in telemetry that can be bonded into the pavement structure of a highway to monitor strains and temperatures using telemetry. The asphalt core is instrumented with two resistive strain gauges and two thermistors for temperature measurement. The strain gauges are aligned with the bottom of the roadbase layer in the pavement structure. The system is set up to record temperatures once every 30 minutes and strains for 10 minutes once a day. The sampling rate for all data channels is set to 100 Hz.

After validating the asphalt core system with several laboratory experiments, the measurement system was installed in an actual highway in the United Kingdom (UK) to monitor strain and temperature data. Plans are in place to install several more of these systems in various locations throughout the UK.

Health monitoring of large civil structures is often difficult, if not impossible, in the event of a natural disaster. During such events, cellular phone lines are under heavy usage, which creates difficulties for wireless data transmission using cellular phone lines. Lovell and Pines (1997) discuss the use of a spread spectrum wireless modem for remote monitoring of large civil structures that avoids these problems. The authors claim that this method avoids the existing cellular infrastructure that can be costly and unreliable during real-life natural disasters. The Federal Communication Commission (FCC) allocated a significant portion of the 900 MHz frequency band to digitally transfer data over short distances. Wireless modems using the frequency spread spectrum range of 902 to 928 MHz can provide immunity from interference by customizing the communication software that handles error detection and flow control for the modem. To validate the system, the authors performed a laboratory experiment on a simple fixed-fixed aluminum beam constructed with a bolted joint at the center of the beam. Strain sensor arrays were positioned on both sides of the joint to monitor changes in mechanical impedance caused by loss of torque load in the bolt, and the sensor readings are connected to a local data acquisition system residing in a notebook computer. A series of tests were performed at various levels of bolt torque preload. Then, a host personal computer (PC), positioned at approximately 30 m from the notebook, was used to remotely instruct a data acquisition system via spread spectrum modems. The wireless modems provided transmission rates of up to 38.4 kbps. Data were successfully transmitted with no communication problems at a range of up to 1.6 km, provided a direct line-of-sight existed between the two modems.

Ihler et al. (2000) discuss the major steps in planning and implementing a modular, wireless sensor system. They also discuss as an example the design of a simplified wireless sensor system based on a crackwire. They identify the following as the major steps to implementing a wireless system: choosing a power supply, frequency selection, signal modulation, and embedding of the sensor pad into a carbone fiber composite substrate. The authors developed a crackwire sensor system for monitoring the structural integrity of aging aircraft. The system consists of two main

parts, the sensor and an RF-module. The sensor is composed of four conducting wires in an epoxy-based substrate. The sensor is paced around a rivet where cracks are expected. As a crack propagates, the conducting wires are broken, leading to an interruption of the circuit. By monitoring which wires have been broken, the local crack growth is monitored. The RF-module consists of a power divider, a rectifier and a voltage-controlled oscillator. To determine the optimum carrier frequency, numerical computations of propagation of RF waves must be conducted. At the time of the article, the proof-of-concept prototype had not yet been constructed and tested.

4. FEATURE EXTRACTION AND INFORMATION CONDENSATION

The area of the SHM that receives the most attention in the technical literature is feature extraction. Feature extraction is the process of identifying damage-sensitive properties, derived from the measured dynamic response, which allows one to distinguish between the undamaged and damaged structures. Almost all feature extraction procedures inherently perform some form of data compression and data fusion. Data compression into feature vectors of small dimension is necessary if accurate estimates of the feature's statistical distribution are to be obtained. Condensation of the data is advantageous and necessary, particularly if comparisons of many data sets over the lifetime of the structure are envisioned. In this section, linear features are first introduced. Then, applications with nonlinear features and features for nonstationary time signals are briefly discussed.

The efficiency of pattern recognition and artificial intelligence necessary in many damage detection methodologies is determined in part by the use of appropriate data preprocessing. Staszewski (2000a) examines various preprocessing techniques that enhance feature extraction and selection. He defines five case studies to which various processes are applied. The first case employs a power spectra analysis for spur gear vibrations while later using a wavelet transform as an alternative approach in the second case. The third and fourth case studies also use wavelets, but for data compression and feature reduction through wavelet patterns. The last study involves less feature-centered analysis, focusing on optimal sensor placement using neural network implementation. The paper is essentially a feature extraction survey, building five case studies around significant numbers of sources for readers of data preprocessing.

4.1 Resonant Frequencies

Zak et al. (1999) examine the changes in resonant frequencies produced by closing delamination in a composite plate. In particular, the effects of delamination length and position on changes in resonant frequencies are investigated. Numerical simulation using finite element formulation is carried out on an eight-layer graphite/epoxy composite plate. As the delamination length grows, some additional vibration modes are observed. The multiples of these additional frequencies are also present when nonlinear effects resulting from contact are taken into account. The numerical

results are validated by performing experimental tests on the eight-layer composite plates of 250 × 90 × 8 mm. The delamination of the plates is introduced in the middle plane in the form of thin Teflon foil. The influence of the delamination length on the first three natural frequencies is examined, and a good agreement between the numerical and experimental results is obtained.

Ruotolo and Surace (1997a and c) claim that most detection techniques for crack damage in a beam are applicable only when there is a single crack in the beam. The authors propose a damage assessment method for identifying multiple cracks in beam structures. The proposed method is based on two optimization techniques: genetic algorithms and simulated annealing. By combining these two optimization techniques, local minima/maxima are avoided and global extrema are sought. Here, the objective function is formed as a function of the difference between the measured and calculated frequencies and mode shapes. The proposed method is then applied to numerical data simulated from a beam with multiple cracks and experimental data measured from three cantilever steel beams with two cracks. For these specific applications, the authors find that simulated annealing is more efficient than genetic algorithms in finding the correct crack locations and depths in less computation time.

Rytter and Kirkegaard (1997) perform a vibration test of a full-scale four-story reinforced concrete building at the European Laboratory for Structural Assessment (ELSA). This building is subjected to an earthquake generated by a pseudo-dynamic testing method. The experimental data are used to validate vibration inspection techniques based on a multilayer perceptron neural network and a radial-based function network. The relative changes in the modal parameters are used as inputs of the networks to detect the bending stiffness changes of the system at the output layer.

Williams and Messina (1999) formulate a correlation coefficient that compares changes in a structure's resonant frequencies with predictions based on a frequency-sensitivity model derived from a finite element model. This approach is termed Multiple Damage Location Assurance Criterion (MDLAC). In this approach, a damage index, δD_i, represents a linear stiffness reduction of the *i*th element of a finite element model, and the damage vector, $\{\delta D\}$, is the collection of all damage indices. Then, the fractional change in the *k*th resonant frequency, δf_k, can be written as a function of the damage indices,

$$\delta f_k = \sum_{j=1}^{m} \frac{\partial f_k}{\partial D_j} \delta D_j \quad ,$$

where *m* represents the number of elements, and

$$\frac{\partial f_k}{\partial D_j} = \frac{\{\phi_k\}^T [K_j] \{\phi_k\}}{8\pi^2 f_k \{\phi_k\}^T [M] \{\phi_k\}} \quad ,$$

is the sensitivity of the *k*th frequency with response to damage at the *j*th element, $\{\phi_k\}$ is the *k*th mode shapes, $[M]$ is the mass matrix, and $[K_j]$ is the stiffness matrix for the *j*th element. The DLAC coefficient computes the correlation between the frequency changes, $\{\delta f\}$, predicted from the finite element model and the actual changes, $\{\Delta f\}$, estimated from the experiment,

$$MDLAC(\{\delta D\}) = \frac{|\{\Delta f\}^T \{\delta f\}|^2}{(\{\Delta f\}^T \{\Delta f\})(\{\delta f\}^T \{\delta f\})} \quad .$$

This MDLAC is similar to the Modal Assurance Criterion (MAC) used for comparing mode shapes and takes the value of 1.0 for an exact pattern match and 0.0 for patterns that are uncorrelated. It should be noted that because the MDLAC is independent of scaling, the frequency change $\{\delta f\}$ and the scaled frequency change $c\{\delta f\}$ produce the same MDLAC value. Furthermore, because of the linear nature of the sensitivity $\partial f_k / \partial D_j$, $\{\delta D\}$ and $c\{\delta D\}$ result in the same MDLAC value. Therefore, the MDLAC provides information about only the relative amount of damage among the elements. The scaling constant *c* can be estimated using either a first order or a second order approach (Messina, Williams, and Contursi 1998). Williams and Messina (1999) undertake a numerical and experimental verification of the MDLAC method. The experiment consists of a number of aluminum rods screwed together to form different configurations. Damage is a 40% reduction in stiffness and is implemented by using smaller diameter rods in some locations. The authors find that the second order approach performs better while the first order approach overestimates the damage severity. It is found that 10 to 15 resonance frequencies are needed to provide sufficient information about damage and that the use of antiresonances can increase the accuracy of the damage estimation. The authors note that, in practice, errors in frequency measurements can alter the apparent frequency change

patterns and affect the ability of the MDLAC approach to give a correct prediction. Furthermore, because the analytical finite element model is unlikely to be an exact match to the real structure, the authors propose model updating procedures to deal with this problem.

Chaudari and Maiti (1999) propose a method for modeling transverse vibration of a geometrically segmented cantilever slender beam using the Frobenius method of solving an Euler-Bernoulli type differential equation. Then, using the first three frequencies, the authors solve an inverse problem to locate and quantify a crack in the beam. Two beam types are investigated. The first beam is composed of three sections. The two end segments have a uniform thickness of different dimensions, and the central section has varying thickness. The second beam consists of two segments, one of which is tapered. Then, a crack is modeled as a rotational spring in the central section of the first beam. Similarly, for the second beam, a crack is modeled in the tapered section. Comparisons of their cracked beam models are made with the closed form solutions available in the literature. While the crack locations estimated from the first three calculated resonant frequencies are fairly accurate, the crack sizes are obtained with errors that can be as large as 21%.

Hanselka et al. (1997) propose an online monitoring technique, which uses an onboard microcontroller to extract modal properties when the structure is in use. For damage diagnosis, the authors solve an inverse eigenvalue problem trying to estimate the stiffness changes from the measured modal properties. First, the authors express the system stiffness matrix as a function of the system connectivity, J_i, and the stiffness scaling factor of each element, α_i,

$$K = \sum_{i=1}^{n} \alpha_i J_i \ ,$$

where α_i is the scaling factor for the *i*th element stiffness and is equal to one when the element is undamaged. The total number of elements is *n*. The authors claim that the scaling factor is estimated from each frequency and mode shape pair of vibration modes. That is, the scaling factor is estimated for *p* different modes: α_i^j ($j = 1,...,p$). However, the details of this inverse problem are not provided in the article. Then, the damage location is identified by the following frequency-based indicator:

$$I_f(i) = \frac{1}{\sum_{j=1}^{p} (\alpha_i^j - \overline{\alpha}_i)^2} \ ,$$

where

$$\overline{\alpha}_i = \frac{1}{p} \sum_{j=1}^{p} \alpha_i^j \ .$$

The computation of the damage index, $I_f(i)$, is repeated for all elements ($i = 1,...,n$), and the damaged element is the one that maximizes the damage indicator, $I_f(i)$. Furthermore, the modal parameters needed in this approach are extracted onboard using a signal processing technique called the MX filter system (Campanile and Melcher 1994). This MX filter system is implemented on a digital signal processing (DSP) chip, and the changes of the modal parameters are traced online.

Todd, Johnson, and Vohra (2000) develop a sensing system that relies on Fiber Bragg Grating sensors. They apply their system to a clamped plate in which damage takes the form of loosened clamping bolts, and they calculate modal frequencies and modal vectors. Eight tests are performed on the plate, four of which are with an undamaged plate and the rest with a damaged plate. From a measured strain time series, the cross spectral matrix is formed and a singular value decomposition is performed on the matrix at each spectral frequency. The first (largest) singular values are selected over the entire frequency band, and the peak detection scheme is used to identify structural modes. Then, the corresponding singular vectors are designated as mode shapes. Six modal frequencies and mode shapes are calculated for the clamped plate. The authors find that the autospectral estimates are fairly well separated among the different damaged cases, although modes 4, 5, and 6 are not excited by the excitation used. The authors apply a statistical hypothesis test to decide whether damage is present or not from the modal properties calculated.

Lew and Juang (2001) present similar approaches to structural damage detection using virtual passive controllers attached to a structure. The first approach utilizes a direct output feedback controller, and the second approach uses a second-order dynamic feedback. The authors formulate the n measured frequencies as functions of the r element stiffnesses. When n is less than r, this inverse problem, which attempts to estimate the element stiffnesses from the measured frequencies, becomes intractable. The first feedback controller based method solves this problem by adding m closed loop feedback controllers, and each of these feedback controllers or loops has n frequencies. Now, the total number of the original system's frequencies and the feedback loop frequencies becomes $n(m+1)$, which is greater than r. Then, the frequency changes are approximated as linear functions of the element stiffnesses using a truncated Taylor expansion, and this inverse problem is solved by a Least Squares projection. The second controller-based method is essentially the same as the first one. In the second method, however, the feedback controllers take the form of second-order dynamic equations. For this case, the total number of the system frequencies with m feedback controllers becomes $2m+n$. The same procedure as the first direct feedback controller method is iterated. The success of the method is demonstrated using the numerical simulations of a 100 × 2.54 × 0.0636 cm cantilever beam. The first 10 frequencies of the beam are used in the first method, and the first 12 frequencies in the second method. In the finite element simulations, the beam is discretized into 15 elements, and damage takes the form of a 5% stiffness reduction. For both methods, measurements are taken at elements 3 and 15. For the first method, the controller is applied either to element 3 or 15. For the second method, two second-order controllers are placed at elements 3 and 15 simultaneously. Both methods converge to the true element stiffness values after 5 iterations when 6 elements have the 5% stiffness reduction. The authors note that the first direct feedback approach is simple, whereas the second-order feedback controller approach offers the flexibility of adjusting the natural frequencies and allows one to increase the number of low frequencies added to the system. In real applications, the two methods can be combined.

Morassi (1997) presents a diagnostic technique based on the determination of some Fourier coefficients of the stiffness variation caused by damage. This study focuses on identifying notches in axially vibrating beams. First, the eigenfunctions of the analytical model are expanded as a series of the eigenfunctions of the undamaged beam, and it is imposed that this analytical model have the same frequencies as the experimentally estimated frequencies of the damaged

structure. This constraint converts the diagnosis problem into solving a system of nonlinear equations where the unknowns are the Fourier coefficients, which represent the stiffness distribution along the beam caused by damage. If the damage is assumed small, these nonlinear equations can be solved iteratively. Alternatively, this problem can be solved by the variational methods shown in Cawley et al. (1979). An experiment on a 4-m-long, free-free axially vibrating steel beam of double T cross-section is undertaken to validate the method. For beams with small notches, the method performs well if only the first 4 frequencies are considered in the expansion. Using the first 6 frequencies, however, causes the model to be less accurate. He claims that the success of damage identification heavily depends on the accuracy of the analytical model employed, and only the frequencies for which the analytical model is validated should be included in the identification process.

Mroz and Lekszynski (2000) conduct a sensitivity analysis of frequencies to the location of additional masses and support locations. By changing boundary conditions and adding supports, they conclude that additional supports do affect the frequencies of the tested cantilever. The use of frequency changes is proposed for SHM because of their sensitivity to varying support locations and cracking. The authors caution that the form of the objective function, which is needed when the number of parameters, i.e., additional masses and support locations are greater than measurements, is important and further study on this topic is warranted.

Leutenegger et al. (1999) developed a model to predict fatigue crack length based on resonant frequencies of a beam. Previous models have assumed linear “open crack” behavior. Unlike previous models, this model included the nonlinear effect that arises as a result of the cracks opening and closing. According to the authors, a linear model underestimates the crack size because the crack closure during half of the loading cycle will result in a smaller drop in resonant frequency than that of a corresponding open crack. The authors compare results from their nonlinear model and a linear model with experimental data. The comparison shows excellent agreement between the nonlinear model results and the experimental data. The comparison also shows the improved accuracy obtained using the nonlinear model instead of the linear model.

4.2 Frequency Response Functions

Mares et al. (1999a) propose a damage location procedure based on rigid body constraints. They simulate a crack in a two-dimensional finite element model of a cantilevered beam, which they discretize into 10 elements along the length of the beam. Frequency responses are calculated for the beam's damaged and undamaged states. A crack is introduced at the third element from the fixed end, and an external load, which would prevent any deformation of the cracked element when the beam is vibrating in one of its normal modes, is calculated. In other words, when the external load is applied at the damaged element, there is no difference in the frequency response functions between the damaged and undamaged state of the cantilever beam. On the other hand, if the load is applied to the other elements that are undamaged, there is a change in the frequency response function. The authors then apply this constraining load to one element at a time and solve a set of equations describing the dynamics of the whole beam. The equations that the finite element model solves for the whole beam are given by

$$\det(N^T H(\omega)\, N) \ ,$$

where $H(\omega)$ is the frequency response function, N is an n by 2 matrix describing the rigid body modes of the elements, and n is the number of nodes. Because the model is two-dimensional, there are only 2 rigid body modes for each element, one translational and one rotational,

$$N^T = [0 \cdots I \; -R^T \cdots 0]^T \ .$$

Here, the only nonzero matrix entries are the 2 by 2 matrices, I and $-R^T$, corresponding to the nodal forces applied to constrain the element translationally and rotationally. Thus, there are many different N matrices constraining different elements one at a time. If the external loads area is applied to the actual damage element, then the determinant in the above equation becomes zero. Therefore, by assuming different N matrices, the damaged element can be located. However, this method would be computationally too intensive for structures with many elements.

Agneni, Balis Crema, and Mastroddi (2000) use the measured frequency response functions (FRFs) for model updating and damage detection. The mass and stiffness matrices are estimated from the FRFs. The Fast Fourier Transform (FFT) of the original time signal into the frequency domain distorts the estimation of the FRF when the time signal is truncated at the end of the time window. The authors investigate the effect of the truncation on the FRF. Numerical simulations on an aluminum beam supported at both ends are undertaken to point out the effects of data truncation. The authors evaluate the mass and stiffness matrices from the calculated FRFs and investigate the effects of truncation on these matrix terms. It is shown that truncation can cause a significant change in the FRF even when no damage is present and can conceal the effects caused by damage. The authors note that the truncation effects depend not only on the time window size used in the FFT calculation but also on the decay rate of various modes. Therefore, consideration must be given to these facts when using FRFs in damage detection applications.

Assuming that the structure's frequency response function, H, is known for the undamaged state, Schulz et al. (1998) define a damage vector, d, as the difference between the force vector, f, and the H^{-1} matrix multiplied by the vector of measured displacements,

$$d = H^{-1}x - f \ .$$

Physically, this damage index represents unbalanced forces near damage. That is, if damage occurs, the damage vector will have nonzero entities only at the DOFs connected to the damaged elements. This damage index requires that the excitation forces be known. When the excitation forces are unknown, a new damage indicator is developed by combining the unbalanced damage force and the unknown external force,

$$r = d + f = H^{-1}x \ .$$

Note that f and x are obtained from the damaged state of the structure, and H is obtained from the undamaged state. Furthermore, the force, f, is assumed to be random and uncorrelated but not necessarily known. Finally, a damage indicator matrix, D, is then formulated as D,

$$D^2 = \frac{1}{f_2 - f_1}\int_{f_1}^{f_2} R \circ R^* \, df \ ,$$

where R is the expectation of $r \times r^*$, * is the complex conjugate transpose operation, f_1 and f_2 are the lower and upper cutoff frequencies of the frequency bandwidth, and ∘ denotes element-by-element multiplication. If the damage is between DOFs i and j, then D_{ij}^2 becomes nonzero. Therefore, damage can be located using this damage indicator. When the complete degrees of freedom of the model are not measured, a model reduction technique such as the Guyan reduction method could be employed to approximate the unmeasured coordinates. The authors demonstrate the method on finite element models of fixed-fixed and fixed-free beams. Damage was modeled as a 25% reduction in beam stiffness while a random force is applied to one element. Damage is successfully located, and it is observed that the rotational degrees of freedom are more sensitive to the damage than the translational.

Lopes, Pereira, and Inman (2000) relate the electrical impedance of the piezoelectric material to the frequency response functions of a structure. The frequency response functions are extracted from the measured electric impedance through the electromechanical interaction of the piezoceramic and the structure. A piezoelectric patch is bonded on a section of a clamped-free aluminum beam measuring $500 \times 30 \times 5$ mm, and an analytical model of the beam with piezoelectric material is derived using a generalized Hamilton's principle. The authors find that the stray piezoelectric effects can alter the FRFs significantly, and it is speculated that the piezoelectric effects are more recognizable because of the structure's small size. The authors reduce the beam's stiffness by 5%, 10%, 15%, 20%, and 25%, and normalize the effects of each stiffness reduction by considering the percentage differences in the natural frequencies between the damaged and undamaged structures. However, the method presented does require that the damage location be known because the piezoelectric patch measures the electrical impedance in the localized regime.

Balis Crema and Mastroddi (1998) correlate measured Frequency Response Function (FRF) with mass, stiffness, and viscous and hysteretic damping matrices. They claim that it is possible to identify structural properties directly from the measured FRF data and to detect possible local stiffness or mass variations. The structural parameters are estimated by constructing inverse problems at different frequencies and input-output pairs. The authors perform numerical

simulations on truss and beam structures such as airplane wings to validate the approach. As always, it is found that noise can corrupt the resolution.

Trendafilova (1998) uses the frequency response functions or the displacement transfer functions as damage-sensitive features. First, the differences between the response functions of the healthy and the damaged structures are summed up over all possible combinations of the input and response pairs at each frequency, and this computation forms a vector of the differences estimated at different frequency values. Next, the dimension of this feature vector is reduced by removing these degrees of freedom (DOFs) and frequency areas for which the differences between the damaged and undamaged structures are smaller than a certain threshold value. Finally, the discriminant functions for damage localization and quantification are constructed, and the associated damage classifier is built.

Monaco, Calandra, and Lecce (2000) also use the frequency response functions (FRFs) as damage-sensitive features. The goal of their experiments was to obtain a low complexity procedure for determining the reliability of the damage identification indices. The damage indices chosen for their work are the averages of the differences between integer healthy and damaged structure's FRFs. Each FRF was averaged sixteen times to cut off all noise resulting from factors with a characteristic time lower than the acquisition time. Experiments were performed on two structures, a "light structure" and a "heavy structure," with the same experimental setup. Three different types of damage were introduced to the structures: added masses, cuts, and constraint yielding. The damage indices presented successfully identified very small structural damages (less than 1% added mass and cuts of increasing length and thickness) in each case. The authors claim that the capabilities of the technique could be extended to quantify and localize damage.

Chouaki and Ladeveze (2000) introduce the notion of visibility of damage in a structure. Simulations of an eight-bay cantilever truss modeled with three-dimensional beam and joint elements are used to validate their SHM procedure. A 3% uniformly distributed noise level has been added to the simulations, and less than 33% of the degrees of freedom are measured. The response of the structure is simulated in the frequency range of 0 to 45 Hz, and the method uses the first 13 frequencies. An error metric is introduced in the following manner. A weighted

integral of all 13 frequencies is taken, and the contribution of all the substructures to the integral is calculated as the total error. If the error of each substructure is greater than 0.8 times the total error, which is integrated over all frequencies and substructures, the substructure is considered damaged. With their simulations, the authors are able to localize a broken tension member in the second bay from the fixed end of the truss. A shortcoming of the method is realized if the global error metric does not surpass the noise level. In addition, the authors use their results to update their model and detect mismodeled joints.

4.3 Mode Shapes (MAC and CoMAC)

Natke (1997) uses changes in natural frequencies and mode shapes to detect damage in a finite element model of the cable-stayed steel bridge consisting of 5 spans: 31 m, 64 m, 171 m, 64 m, and 31 m. Damage is simulated by removing the bottom flanges of the longitudinal girders in the end spans. Such a damage scenario is extreme, and the results of such a simulation reflect this situation. In fact, the second vertical bending mode shows a 23% reduction in the corresponding frequency, and the MAC values of the mode shapes differ significantly from unity. Natke justifies performing a linear modal analysis of the bridge because of the high pretension of the cables, which generally cause the bridge to perform in a nonlinear fashion. This high pretension essentially ensures that the cables always carry most of the load from the bridge deck, preventing any bilinear stiffness effects of the entire bridge.

Doebling and Farrar (1997) examine changes in the frequencies and mode shapes of a bridge as a function of damage. This study focuses on estimating the statistics of the modal parameters using Monte Carlo procedures to determine if damage has produced a statistically significant change in the mode shapes. Stanbridge, Khan, and Ewins (1997) also use mode shape changes to detect saw-cut and fatigue crack damage in flat plates. They also discuss methods of extracting those mode shapes using laser-based vibrometers.

Another application of SHM using changes in mode shapes and participation factors can be found in Ahmadian, Mottershead, and Friswell (1997). The authors propose a damage detection procedure that uses measured displacements of a structure and an existing analytical model to locate faults. When damage occurs in substructures or likewise a small part of a larger structure,

the substructure's modes will be changed but the modes of other substructures will be unaffected. In fact, damage in a particular substructure changes the participation factors of the higher modes of this substructure, but not the higher modes of the other substructures. This observation is used by the authors to formulate the following approach to damage detection. Damage localization is based on the weighted scalar product of Δu, which is the difference between the measured and predicted displacement vectors of a particular substructure, with φ, which is the vector of higher mode shapes of that substructure,

$$\varphi^T M \Delta u \ ,$$

where M is the substructure mass matrix. This weighted scalar product must be zero for an undamaged substructure. Finite element calculations are performed to verify the usefulness of the method. It is noted by the authors and demonstrated through the finite element simulations that the method is capable of handling problems of truncation and random noise in the measured displacements.

Ettouney et al. (1998) discuss a comparison of three different structural health monitoring techniques applied to a complex structure. All three of the techniques are based on knowing the mode shapes and natural frequencies of the damaged and undamaged structure. A finite element model was used to extract modes of up to 250 Hz for this work. The first method is based on monitoring the change of the stiffness matrix of the structure. The stiffness matrix of an undamaged structure can be computed from the measured modal parameters, and the stiffness matrix for the damaged structure can also be computed using the mode shapes and natural frequencies obtained from the damaged structure. The change in the stiffness matrix of the damaged and undamaged states can then be used for damage detection. In a similar fashion, the flexibility matrices can be computed from the measured modal parameters of the damaged and undamaged structures. Then, the flexibility change between the damaged and undamaged states can be used for damage detection. The third method is the damage index (DI) method described by Stubbs et al. (1999). Unlike the previous two methods, damage is identified at structural element levels rather than at nodal degrees of freedom in this method. Ettouney et al. (1998) applied all three methods to a complex steel structure. The overall dimensions of the structure were approximately $3 \times 21 \times 21$ m and consisted of 241 structural elements and 78 structural

connections. The structure was modeled using finite elements. Mode shape and natural frequency information was extracted from the analytical models of the damaged and undamaged conditions. Damage was introduced into the model by altering the modulus of elasticity for selected structural elements. All three methods were able to detect the relative location of the damaged elements with acceptable accuracy. However, it is questionable whether these methods can work in real-world applications because the number of mode shapes and natural frequencies, which can be identified from experimental modal analysis, are often limited.

4.4 Mode Shape Curvatures

Maeck and De Roeck (1999) apply a direct stiffness approach to damage detection, localization, and quantification for a bridge structure. The direct stiffness calculation uses experimental frequencies and mode shapes in deriving the dynamic stiffness of a structure. The method makes use of the basic relation that the bending stiffness of a beam is equal to the bending moment divided by the corresponding curvature, which is the second derivative of the bending deflection. Changes in the dynamic stiffness, given by changes in the modal curvature, indicate the presence of damage. A particular advantage of using either modal curvatures or their derivatives as features is that the modal curvatures tend to be more sensitive to local damage than do modal displacements. Maeck and De Roeck validate their approach using the Z24 prestressed concrete bridge in Switzerland and a reinforced concrete beam, which are both gradually damaged. The authors note that when a central difference approximation is used for the calculation of curvatures from mode shapes, this approximation results in unwanted oscillations and inaccurate values. Therefore, they use a weighted-residual penalty-based technique to account for the inherent inaccuracies of the measured mode shapes. This technique, which resembles a finite element technique, approximates the curvatures from the measured mode shapes by minimizing an objective function. Maeck and De Roeck first divide the structure into a number of elements separated by nodes that correspond to the measurement points. Each of the nodes has three degrees of freedom; a displacement, a rotation, and a curvature. Then, the authors minimize an objective function, which consists of the differences between (1) the measured and approximated mode shapes, (2) the first derivative of the measured mode shapes and approximated rotations, and (3) the second derivative and the approximated curvatures. The continuity of rotation and

curvature is enforced by the last two terms in the objective functions. They note that the advantages of this approach are that direct curvatures are available and that boundary conditions can be imposed. A drawback is that penalty factors for the last two terms must be imposed so that the penalty factors are large enough for computational effectiveness and small enough to avoid numerical difficulties. A similar study is reported in Maeck, Wahab, and De Roeck (1998) where the authors estimate the stiffness degradation of a damaged reinforced concrete beam using the direct stiffness approach.

Ho and Ewins (1999) present a numerical evaluation of the Damage Index method, which is defined as the quotient squared of a structure's modal curvature in the undamaged state to the structure's corresponding modal curvature in its damaged state. That quotient depends, of course, on which mode is chosen. The first 3 mode shapes from a numerical model of a cantilever beam are used to calculate the Damage Index. The damage takes the form of a thickness reduction in the beam. The authors find that the performance of the Damage Index is highly susceptible to the presence of noise in the mode shape. For the simulation, the noise level is assigned in terms of the percentage of the maximum amplitude of the mode shapes. When the noise level is 1%, the Damage Index locates damage correctly for the severest cases of damage, a 50% reduction in beam thickness. The authors show that noise is amplified in the Damage Index because curvature is the second derivative of the mode shape, and the curvature is squared. In fact, the standard deviation of the modal curvature is approximately twice that of the corresponding mode shape. In addition, the standard deviation of the curvature squared increases to about $4\sqrt{2}\,n^2$ after squaring. Here, n is the assigned noise level. The authors discuss acceptable noise levels to obtain a certain confidence in the Damage Index results and to give an example of a noise level of 0.15% to have a 99% chance of identifying damage. The authors also determine that the sparser the measurement points are, the worse the performance of the Damage Index becomes. The authors note that a 33% measurement of the complete DOFs is the minimum requirement for sensor placement beyond which damage is incorrectly located in the cantilever beam. Below the 33% measurement, the Damage Index shows damage in two locations when in fact there is only one location. Finally, it is shown that damage severity cannot be correctly ascertained with the Damage Index, regardless of the noise level or the damage test case.

In another paper by Ho and Ewins (2000) the authors state that higher derivatives of mode shapes are more sensitive to damage, but the differentiation process enhances the experimental variations inherent in those mode shapes. To overcome this difficulty, the authors attempt to derive a mode shape-based feature that is sensitive to damage while relatively insensitive to experimental variation. The authors propose changes in the mode shape slope squared as a feature. Specifically, the first derivative of the mode shape is calculated and then squared. Change in this quantity is used as the damage-sensitive feature. To compute the derivative of the mode shape, a local polynomial is fit through every four consecutive measurement points and the resulting polynomial is differentiated. They note that this way of computing mode shape derivatives is subject to smaller variations than those with a finite difference approximation, which is typically used to calculate the derivatives. The proposed method is demonstrated on cantilever beams that measure 10 × 20 × 1,000 mm, and the damage is made by a 2-mm-wide saw cut at five different levels ranging from 10% to 50% of the beam's depth. Finite element models of the beams are created, and changes of the first 3 natural frequencies are calculated. Experimental results indicate that the higher derivatives of mode shapes are more promising than mode shapes themselves as damage-sensitive features, but also indicate that false damage indications can be observed at mode shape nodal points where the measurement qualities are relatively poor. The authors state that the mode shape derivative near boundaries could produce false positive indications of damage. They recommend that the use of derivatives of mode shapes for damage diagnosis be scrutinized more closely.

Wang et al. (2000) evaluate the damage index method by reviewing the formulation of the method, examining the traditional assumptions step by step, and then applying the method to numerous damage cases of a concrete bridge finite element model. The evaluation was undertaken because, in the authors' experience, the damage index suffers from some unresolved problems that limit its effectiveness. First, the sensitivity of the method to damage can change as a function of damage location because of the variation in modal strain energy. Therefore, it cannot be assumed that the damage index will respond in a uniform manner to localized damage at an arbitrary location. Second, it is traditionally assumed that the normalized damage measure behaves as a standardized normal random variable. However, because the damage index formulation is explicitly a deterministic one, the authors state that the damage should be related to an energy criterion. To test the feasibility of using the damage index to locate damage, tests

were conducted with a finite element model of a bridge. Damage was introduced to the model by reducing some element's elastic modulus. The results obtained agree with results from the authors' previous work that show excellent identification for large states of damage (more than 10% to 20% stiffness decrease). The authors draw the following conclusions. First, without regard to location or damage magnitude, the method correctly located damage states approximately 70% of the time. The method is most successful near the center of the structure and suffers considerably near the abutment. Second, further theoretical numerical studies are necessary to determine if the damage index variable is normally distributed as it is assumed to be.

Kim et al. (1997b) extend the damage-index method for structures in which no information for the undamaged, or baseline, structure exists. The authors present a method that can be used to estimate modal parameters of an undamaged structure using data from the current damaged structure and a corresponding finite-element model. The authors develop a finite-element model (FEM) of the structure in question and extract modal information from the model. Modal information is also extracted experimentally from the current damaged physical structure. From this, the authors create an object function that is the norm of the fractional changes in the eigenvalues between the initial FEM and the physical structure. The authors claim that the stiffness parameters for an undamaged baseline model can be determined by minimizing this object function. The authors tested this methodology on a truss bridge with a steel frame. The ridge structure is 12.19 m high and supports a 5.89-m roadway. The bridge has had several repairs to damage over its service life. The authors performed vibration testing on the bridge to extract modal parameters. The authors used the above methodology to estimate a baseline model for the bridge, and the baseline model is subsequently used to locate damage. The results from the estimated baseline model were in good agreement with actual conditions.

Garcia et al. (1998) extract modal parameters using the autoregressive moving-average (ARMA) prediction model in the time domain and the classical frequency response function (FRF) in the frequency domain. The authors claim that modal parameter extraction using the FRF is very user-dependent because the estimation of modal parameters depends heavily on the knowledge and ability of the analysts. The ARMA method is a promising technique in that this approach removes the erroneous user interface associated with the FRF technique. To compare the two

methods, the authors fit a simply supported aluminum channel with 13 accelerometers, a force transducer, and a 0.907-kg shaker. Different stages of damage were introduced into the channel by saw cuts of various depths. Both modal extraction techniques were combined with the damage index (DI) method to locate damage. The first 5 modes were extracted from the experiment of the beam. Comparison of the results revealed that the ARMA technique was successful in determining the 4th and 5th mode shapes and in locating damage. The ARMA method was not, however, successful in reproducing the first mode of the channel.

In a similar study, Garcia and Osegueda (1999) use parameters of an autoregressive moving-average (ARMA) model for damage diagnosis to eliminate the need to estimate modal parameters and to minimize user interface associated with the modal parameter extraction procedure. The experimental setup consisted of a pinned-pinned aluminum channel instrumented with 13 accelerometers, one force transducer, and a shaker. ARMA models are constructed at each accelerometer location individually. Then, a characteristic curve of each ARMA coefficient is generated by fitting the ARMA coefficients from all accelerometers as a function of beam length. The cubic spline curve-fit is used, and the beam is divided into 60 elements. This step is repeated for all ARMA coefficients. Now, by treating the characteristic curves as pseudo mode shapes, the damage index described in Section 4.4 is computed for each of the ARMA coefficients and each of 60 elements. Using a vector of damage indices corresponding to all ARMA coefficients at each element as an input to a Bayesian classification algorithm, two-category damage classification is conducted for each element revealing potential damage locations. The authors report only partial success in finding the correct locations of damage and have a difficult time in identifying multiple damages.

4.5 Modal Strain Energy

Zhang, Qiong, and Link (1998) propose a structural damage identification method based on element modal strain energy, which uses measured mode shapes and modal frequencies from both damaged and undamaged structures as well as a finite element model to locate damage. The element modal strain energy ratio (SER_{ij}), which is the *i*th modal strain energy in the *j*th element stiffness divided by the total strain energy of the ith mode, is defined as

$$SER_{ij} = \frac{\phi_i^T k_j \phi_i}{\phi_i^T K \phi_i} = \frac{\phi_i^T k_j \phi_i}{\omega_i^2} \ ,$$

where k_j is the *j*th element stiffness matrix, K is the system stiffness matrix, and ϕ_i is the *i*th mass normalized mode shape. Then, a damage indicator, β_{ij}, is defined as the difference of the element modal strain energy ratio before and after damage,

$$\beta_{ij} = \frac{\phi_{di}^T k_j \phi_{di}}{\omega_d^2} - \frac{\phi_{ui}^T k_j \phi_{ui}}{\omega_u^2} \ ,$$

where the subscripts *d* and *u* denote the damaged and undamaged structures, respectively. Simulation studies using beam and truss type structures are performed to evaluate the feasibility of this method. The damage takes the form of stiffness reductions in the beam or truss elements, ranging from 40% to 50%. Multiple damage scenarios are introduced into the beam and truss simulations, and 5% noise is included. Modal data from the first five modes are used in the method. As usual, the authors find that their method cannot detect damage in a structure when the damage is located in an element not sensitive to modal parameter changes. However, the strain energy method has demonstrated some ability in locating multiple damage regions. Finally, the authors compare their method with the Element Frequency Sensitivity, Subspace Rotation Vector, and the Local Frequency Change Ratio methods of damage identification. These other methods give mixed results as to their abilities to locate damage in various elements.

Worden et al. (1999) present another strain energy study using a damage index approach. An aluminum plate stiffened with stringers is tested. Damage is introduced as saw cuts in the outside stringer. Nine levels of damage are investigated and the depth of the cut ranges from 10% to 90% of the plate thickness. Nineteen accelerometers are located on the plate for modal analysis. However, only 9 measurements along the damaged stringer are used to calculate mode shapes, essentially producing a one-dimensional formulation of the strain energy method. The diagnostic used is an integrated version of the modal curvature, f_{ij}, defined as

$$f_{ij} = \int_{a_{j-1}}^{a_j} dx \left(\frac{d^2\varphi_i}{dx^2}\right)^2 \Bigg/ \int_0^L dx \left(\frac{d^2\varphi_i}{dx^2}\right)^2 \ ,$$

where *i* represents the mode number, *j* represents an element number, L is the length of the stringer along which the curvatures are calculated, φ is the mode shape, *x* is the position along the damaged stringer, and *a*'s correspond to the integration limits. A damage index, β_k, is formulated as the quotient of the sum of damaged f_{ij}'s over all modes to the sum of undamaged f_{ij}'s over all modes. By a careful selection of modes, the damage index is able to detect a saw cut corresponding to 70% of the stringer thickness and locate it with an accuracy of less than 21 mm over a 725-mm-long stringer.

Carrasco et al. (1997) discuss using changes in modal strain energy to locate and quantify damage within a space truss model. The authors constructed a scaled-down model of a space truss structure that contained 12 bays with interior cross bracings. The model was instrumented with accelerometers and force transducers so that modal information for each structural element as well as global modal information could be extracted. Five baseline tests were performed on the structure with no damage to obtain baseline modal parameters. The baseline tests were followed by 18 tests with various damage scenarios. This method is based on the fact that damage in a structural member causes changes in the modal strain energy. The total modal strain energy for each structural element can be computed using experimental mode shapes extracted from the damaged and undamaged cases. Changes in the modal strain energy between the damaged and undamaged scenarios will be localized around the damaged structural elements. The authors also claim that the magnitude of the changes can be used as an indicator of the overall magnitude of the damage. Results of the test showed that this method did very well at localizing damaged elements within the truss structure.

Choi and Stubbs (1997) develop two methods for detecting damage in two-dimensional plates. The first method is based on changes in local compliance, while the second method is based on changes in local modal strain energy. For each method, the two-dimensional plate is discretized into several elements for analysis, and classical plate theory is used to develop a damage index for each element within the plate. For the compliance method, the damage index involves the ratio of the pre- and postdamage flexural rigidities for each mode of vibration. For the modal strain energy method, the damage index involves the ratio of the modal strain energy pre- and postdamage for each mode of vibration. To validate the two approaches, the authors developed a

finite element model (FEM) of a 304.8 × 304.8 × 15.24 cm plate. The FEM was used to perform a free vibration analysis of the plate to determine modal parameters for both damaged and undamaged cases. To simulate damage, the stiffness of certain elements within the FEM was reduced by 50% to 75%. The modal information produced by the FEM was fed into the compliance and modal strain energy algorithms. Results showed that the compliance method provided slightly better results in predicting and locating damage within the plate.

4.6 Dynamic Flexibility

Bernal (2000a) mentions that changes in the flexibility matrix are sometimes more desirable to monitor than changes in the stiffness matrix. Because the flexibility matrix is dominated by the lower modes, good approximations can be obtained even when only a few lower modes are employed. Such would be the case when one tries to infer mode shapes from a limited set of measurements. Bernal outlines a state-space realization procedure to identify the modes at sensor locations and presents closed form solutions for computing mass normalized mode shapes when classical damping is assumed. He then illustrates the process with a numerical example of a 39 DOF truss. The truss structure is outfitted with 9 sensors on the unsupported joints of the lower chord and excited with random white noise. The truss dissipation mechanism utilizes Rayleigh damping with a magnitude of 5% of critical damping in the two modes, which have the largest modal mass in the vertical direction. The author obtains accurate results identifying the modes, even for modes that exist in regions with high modal densities.

Reich and Park (2000) focus on the use of localized flexibility properties for structural damage detection. The authors choose flexibility over stiffness for several reasons, including the facts that (1) flexibility matrices are directly attainable through the modes and mode shapes determined by the system identification process, (2) iterative algorithms usually converge the fastest to high eigenvalues, and (3) in flexibility-based methods, these eigenvalues correspond to the dominant low-frequency components in structural vibrations. A structural flexibility partitioning technique is used because when the global flexibility matrix is used, there is an inability to uniquely model elemental changes in flexibility. The strain-based substructural flexibility matrices measured from before and after a damage event are compared to identify the location and relative degree of damage.

Topole (1997) discusses the use of the flexibility of structural elements to identify damage. Many structural health-monitoring techniques rely on the fact that structural damage can be expressed by a reduction in stiffness. A reduction in stiffness corresponds to an increase in structural flexibility. Topole indicates that there are certain instances where it is advantageous to use changes in flexibility as an indicator of damage rather than using stiffness perturbations. Topole develops a sensitivity matrix that describes how modal parameters are affected by changes in the flexibility of structural elements. From this information, he develops a scalar quantity for each structural element, which indicates the relative level of damage within the element. The proposed method was applied to a theoretical structure that consisted of a principal mass supported by 4 bays of elastic truss elements connected by elastic joints. Topole investigated four damage scenarios, including damage at a single element or joint as well as damage at several locations. Reducing the stiffness of a truss member or joint simulated damage. The proposed method worked well at locating and quantifying damage for the single location scenarios. However, the method provided erroneous results for cases where damage was introduced in multiple locations.

The unity check method, proposed by Lin (1998) for locating and quantifying damage using modal parameters, is an addendum to his previous work (Lin 1990). This unity check method starts from the fact that the product of a stiffness matrix and a flexibility matrix produces a unity matrix at any stage of damage,

$$\mathbf{F}_d \ \mathbf{K}_d = \mathbf{I} \ ,$$

where $\mathbf{K}_d$ is the stiffness matrix for the damaged structure, $\mathbf{F}_d$ is the corresponding flexibility matrix, and $\mathbf{I}$ is the identity matrix, respectively. The stiffness matrix for the damaged structure $\mathbf{K}_d$ can be represented using the stiffness matrix of the baseline structure $\mathbf{K}_u$ and the unknown change of stiffness caused by damage, $\Delta\mathbf{K}$,

$$\mathbf{K}_d = \mathbf{K}_u - \Delta\mathbf{K} \ .$$

Furthermore, the flexibility matrix of the damaged structure can be estimated from the natural frequencies and mode shapes measured during a modal test of the damaged structure,

$$\mathbf{F}_d = \Phi_d \ \Lambda_d^{-2} \ \Phi_d^{\mathrm{T}} \ ,$$

where Φ_d is the mode shape matrix, and Λ_d is a diagonal matrix where each diagonal entity is a natural frequency. By substituting the second equation of this paragraph into the first equation of this paragraph, one obtains the following equation,

$$\mathbf{F}_d \ \Delta\mathbf{K} = \mathbf{F}_d \ \mathbf{K}_u - \mathbf{I} \ .$$

Assuming that the stiffness matrix of the baseline structure has been satisfactorily verified by a model test, the only unknown term in the above equation is the stiffness perturbation, $\Delta\mathbf{K}$. The damage location and damage amount are estimated by solving the above equation using the least squares technique.

4.7 Damping

When compared to frequencies and mode shapes, damping properties have not been used as extensively as frequencies and mode shapes for damage diagnosis. Crack detection in a structure based on damping, however, has the advantage over detection schemes based on frequencies and mode shapes in that damping changes have the ability to detect the nonlinear, dissipative effects that cracks produce. Modena, Sonda, and Zonta (1999) show that visually undetectable cracks cause very little change in resonant frequencies and require higher mode shapes to be detected, while these same cracks cause larger changes in the damping. In some cases, damping changes on the order of 50% are observed. Their study focuses on identifying manufacturing defects or structural damage in precast reinforced concrete elements. The peculiar dynamic response of reinforced concrete justifies the use of damping and nonlinear responses as damage-sensitive features. They propose two new techniques based on changes in damping to detect cracking. The first method, which is applicable for a classically damped system, estimates stiffness reductions based on the measurements of the modal damping variations and the bending curvatures. On the other hand, the second method involves distinguishing between the viscous and friction components of damping and identifying the damage through friction detection and characterization. These techniques are employed to locate cracks in a 1.20×5.80 m precast hollow floor panel excited with stepped sines and shocks, and the diagnosis results are compared with those of frequency and curvature based approaches.

Kawiecki (2000) measures damping of a 90 × 20 × 1 mm metal beam and metal blanks used to fabricate 3.5-in. computer hard disks. He notes that damping can be a useful damage-sensitive feature. A pair of 0.25-mm-thick piezoelements are surface bonded at two locations on both sides of the specimen. Then one pair is excited out of phase using a sinusoidal sweep signal and the resulting elastic wave is picked up by the other transducer pair located at the other end of the specimen. Modal damping is determined using the half-power bandwidth method applied to the measured FRF within the frequency range of 5 kHz to 9 kHz. The author claims that the presented approach will be particularly suitable for structural health monitoring of lightweight and microstructures.

During vibration tests of prestressed reinforced concrete hollow panels, Zonta, Modena, and Bursi (2000) observe that cracking in reinforced concrete specimens results in a frequency splitting in the frequency domain and the beat phenomenon of the free decay signals in the time domain. The authors claim that crack formation in prestressed reinforced concrete triggers a nonviscous dissipative mechanism making damping more sensitive to damage, and they propose to use this dispersive phenomenon as a feature for damage diagnosis. They note that the dispersion cannot be represented by the standard linear model of a single degree of freedom system. With a skew-symmetric damping operator, however, a linear model can still be used to describe the situation. In fact, for the single degree of freedom system, this operator corresponds to an imaginary damping. Moreover, the presence of the dispersive phenomenon admits that the oscillator has a variable stiffness, and this variability is proportional to the frequency. For a continuous system, this operator corresponds to a mixed second-order differential operator in the wave equation. The authors recognize the need for further research into using the dispersion phenomenon for damage detection because additional effects such as hysteresis and other nonclassical dissipative mechanisms must be considered.

4.8 Antiresonance

Williams and Messina (1999) compared the measured frequencies with these predicted from a finite element model to locate damage and quantify the size of the damage. The Multiple Damage Location Assurance Criterion (MDLAC) method is used for this comparison.

The MDLAC computes the correlation between the frequency changes, $\{\delta f\}$, predicted from the finite element model and the actual changes, $\{\Delta f\}$, estimated from the experiment,

$$MDLAC(\{\delta D\}) = \frac{|\{\Delta f\}^T \{\delta f\}|^2}{(\{\Delta f\}^T \{\Delta f\})\,(\{\delta f\}^T \{\delta f\})} \ .$$

This MDLAC is similar to the Modal Assurance Criterion (MAC) used for comparing mode shapes and takes the value of 1.0 for an exact pattern match and 0.0 for patterns that are uncorrelated. This MDLAC method only requires the measurement of a few frequency changes between the undamaged and damaged states of the structure, and the accuracy of the damage predictions is further improved by including antiresonances into the criterion. Specifically, the authors use antiresonances in the Multiple Damage Location Assurance Criterion (MDLAC) method to detect damage in a simulated truss structure, in which stiffness reductions of 25% in some elements constitute damage. They conclude that the incorporation of antiresonance data into the MDLAC algorithm improves the accuracy of the damage predictions by increasing the size of the damage-related frequency change database without increasing the test frequency range.

4.9 Ritz Vectors

The Ritz vectors represent an alternative to mode shapes spanning the response space of dynamic systems. Ritz vectors (or Lanczos vectors) have been shown to be very effective for dynamic and earthquake analyses, eigenvalue problems, and model reductions. However, very few studies have applied Ritz vectors to damage detection or system identification problems because of the difficulty of extracting Ritz vectors from vibration testing. Zimmerman (1999) presents a system identification procedure, which extracts Ritz vectors from measured vibration test data. From the measured frequency response functions or impulse response functions, a state-space representation of the dynamic system is first obtained using the Eigensystem Realization Algorithm (Juang and Pappa 1985). Next, the Ritz vectors are recursively extracted from the estimated state matrices. These Ritz vectors are then used in the Minimum Rank Perturbation Method (Zimmerman and Kaouk 1994) to locate and quantify damage. The proposed approach is demonstrated using a finite element simulation of a 32 DOF truss structure with 2% modal

damping in all modes. Damage is simulated simply as a 50% reduction in one strut's stiffness without including nonlinear effects. Zimmerman (1999) shows both analytically and numerically through the truss simulation that the first three Ritz vectors contain more information about the damage in the truss than the lowest three modal vectors and conclude that the Ritz vectors tend to be more sensitive to damage than modal vectors. In addition, the experimental extraction procedure of the Ritz vectors is successfully demonstrated, indicating that the error between the extracted and analytical Ritz vectors is less than 2.5%. Motivated by the fact that Ritz vectors tend to be more sensitive to damage than traditional mode shapes, Zimmerman extracts Ritz vectors from the measured dynamic response data of a Vertical Stabilizer Assembly (VSA) of the Space Shuttle Orbiter to verify the results of the truss simulation. The author shows that the first three Ritz vectors are very different from the first three mode shapes and furthermore demonstrates that Ritz vectors can offer a clearer picture of damage than modal vectors can. Finally, Zimmerman performs a test on a cantilever beam to further validate his claims regarding the advantage of using Ritz vectors.

Sohn and Law (1999a) propose another procedure for Ritz vector extraction based on the measured flexibility matrix. The flexibility matrix is represented as a function of the modal parameters. Noting that only a few lower modes and modal frequencies are identified for most modal analyses, the authors divide the flexibility matrix into two parts, a modal flexibility and a residual flexibility. The modal flexibility is constructed from the measured modal parameters while the residual flexibility is the contribution of the unmeasured dynamic modes to the full flexibility matrix. The first Ritz vector is simply a static deflection associated with the assumed spatial load distribution and is computed by multiplying the modal flexibility matrix with the spatial load distribution. In a recursive fashion, consecutive Ritz vectors are extracted by assuming that the product of the previous Ritz vector and the mass matrix is a load so that the product multiplied with the modal flexibility matrix gives the next Ritz vector. Sohn and Law (1999b) indicate that their method of Ritz vector extraction is able to generate different sets of Ritz vectors from arbitrary load patterns while the state-space method of Ritz vector extraction only identifies those vectors corresponding to a specific load pattern employed in the experiment. The method is tested on a grid-type bridge model consisting of two parallel girders and six evenly spaced cross beams connecting the girders. The girders are steel rectangular tubes, and the cross beams are C-shaped members. The frequency response functions (FRFs) in the range

from 0 Hz to 100 Hz are estimated. Rational polynomial techniques are employed to extract the first 6 frequencies and mode shapes from the FRFs. A finite element model of the bridge is also constructed to compare the analytically and experimentally extracted Ritz vectors. The authors extract the Ritz vectors from the vibration data of the bridge using both the state-space and flexibility approaches, and use the Modal Assurance Criterion to quantitatively compare the experimentally extracted Ritz vectors with the analytically calculated ones.

Sohn and Law (1998b) further incorporate load-dependent Ritz vectors into a Bayesian probabilistic framework for damage detection damage in a structure. The Bayesian approach searches for the most probable damage event by comparing the relative probabilities for different damage scenarios, where the relative probability of a damage event is expressed in terms of the conditional probability of the damage event, given the estimated Ritz vector sets from the structure. Based on numerical examples of an eight-bay three-dimensional truss structure and a five-story frame structure, the authors claim that load-dependent Ritz vectors are in general more sensitive to damage than the corresponding modal vectors and that structural elements of interest can be made more observable using the Ritz vectors generated from particular load patterns.

Burton, Farrar, and Doebling (1998) present two methods of determining the stiffness change of a damaged structure using lower vibration modes. The authors assume *a priori* knowledge of the undamaged structure's stiffness matrix, mass matrix, frequencies and mode shapes. Furthermore, the damage locations are also assumed as known. The first method uses damage Ritz vectors to expand the measured mode shapes to the complete dimension of the associated finite element model. Then, the expanded mode shapes are combined with an iterative residual-based scheme for estimating the stiffness changes and updating the expanded mode shapes. Rather than mode expansion, the second method uses a reduced system model, the dimension of which is the same as the number of measured modes. An updating procedure is then proposed that iteratively determines the stiffness property changes of the full-scale system and then transforms those results to the reduced set of measured coordinates. The authors find that both methods converge quickly and accurately for a simple spring-mass model.

4.10 ARMA Family Models

Sohn and Farrar (2000) apply statistical process control techniques to vibration-based damage diagnosis. First, an Auto-Regressive (AR) mode is fit to the measured acceleration time histories from an undamaged structure,

$$y(t) = \sum_{j=1}^{3} \varphi_j y(t-j) + e(t) \ ,$$

where $y(t)$ is the measured time history at time t, φ_j is the AR coefficients to be estimated, and $e(t)$ is the prediction error term. The coefficients of the AR model are selected as the damage-sensitive features for the subsequent control chart analysis. Then, the AR coefficients obtained from subsequent new data are monitored relative to the baseline AR coefficients. Any significant deviation from the baseline of AR coefficients would indicate either a change in environmental conditions or damage. Several projection techniques such as principal component analysis and linear/quadratic projections are also applied to transform the time series from multiple measurement points into a single time series in an effort to reduce the dimensionality of the data and enhance the discrimination between features from undamaged and damaged structures. Finally, the statistical procedure combined with the AR time prediction model is applied to vibration test data acquired from a concrete bridge column as the column is progressively damaged.

Bodeux and Golinval (2000) demonstrate the use of Auto-Regressive Moving-Average Vector (ARMAV) models on the Steel-Quake structure at the Joint Research Center in Ispra, Italy. The Steel-Quake structure is used to test the performance of buildings during earthquakes. The authors use the state-space formulation for a multidegree of freedom structure subject to ambient excitations, which can be expressed as

$$x[n] = Ax[n-1] + W[n] \ ,$$

where $x[n]$ is the observed vibration vector at the nth discrete time point, A is the matrix containing the different coefficients of the autoregressive (AR) part of the model, and $W[n]$ is a matrix containing the moving average (MA) terms, which are related to the external and white

noise excitations. Bodeux and Golinval note that the *r*th natural frequency ω_r and damping ratio ξ_r can be extracted from the associated eigenvalue τ_r of the AR matrix *A*,

$$\omega_r = \frac{|\ln(\tau_r)|}{\Delta t} \text{ and } \xi_r = -\frac{\mathrm{Re}(\ln(\tau_r))}{|\ln(\tau_r)|} ,$$

where Δt is the discrete time interval and Re denotes the real part of a complex number. It is noted that, in general, the ARMAV models contain a larger number of eigenvalues than the actual frequencies of the system. Therefore, only a subset of the estimated eigenvalues will be associated with the structural modes. The distinction between these physical and nonphysical modes is performed by a stability diagram, which traces the physical modes by changing the AR model order. Bodeux and Golinval (2000) use a method known as the Prediction Error Identification Method to calculate the model parameters. This method treats the system stochastically and seeks to minimize the following prediction error, $\varepsilon[n|\theta]$,

$$\varepsilon[n|\theta] = x[n] - \hat{x}[n|n-1,\theta] ,$$

where θ is a vector of AR and MA coefficients to be determined, and $\hat{x}[n|n-1,\theta]$ is the predicted response at time *n,* given the previous responses up to $n-1$ and the assumed model parameters θ. Bodeux and Golinval (2000) detect damage in the Steel-Quake structure using changes in the frequencies estimated by the ARMAV technique. Their statistical approach is based on the mean and sample standard deviation of the estimated natural frequencies. They assume that the structure is damaged if the 99% confidence interval of the newly obtained frequencies does not overlap with the 99% confidence interval of the associated baseline frequencies.

Sakellariou and Fassois (2000) formulate a fault identification and detection model that they call an Output Error (OE) model. With this model, the researchers attempt to address problems associated with seismic excitations such as nonstationarity, limited length, and limited frequency content of the excitations. For a particular six-story structure subjected to earthquake excitation, the OE model takes the form

$$\frac{\partial^2 x_6[t]}{\partial t^2} = \frac{B(c)}{A(c)} x_0[t] + e[t] \ ,$$

where $x_0[t]$ and $x_6[t]$ represent the ground displacement and the displacement of the sixth story at time *t*, respectively, $e[t]$ is an error term that accounts for the nonstationary noise, and $B(c)$ and $A(c)$ are polynomials having the following form:

$$A(c) \equiv 1 + a_1 c + ... + a_{n_a} c^{n_a} \text{ and } B(c) \equiv b_0 + b_1 c + ... + b_{n_b} c^{n_b} \ ,$$

where the backshift operator c^n is defined as

$$c^n x[t] = x[t-n] \ .$$

The authors claim that a main advantage of such a model is that it does not assume any particular representation of noise. The a_i and b_i coefficients are determined by minimizing a quadratic functional of the output error. This method is demonstrated using numerical simulations of the six-story building. First, the a_i and b_i coefficients corresponding to various prespecified fault modes are calculated and compressed. The compressed features are considered hyperplanes in a higher dimensional space. The distance between these hyperplanes and a new hyperplane from a new data set is used to determine the particular fault mode for the new data set. A problem with such a method is that it requires a set of fault modes to be predetermined before the method can be used. The need for this prior fault simulation is a shortcoming of this method. Nevertheless, Sakellariou and Fassois (2000) test their method and find that, with their simulations, a 5% stiffness reduction in any given building story can be detected and the magnitude of the stiffness reduction quantified.

Heyns (1997) uses a multivariate Auto-Regressive Vector (ARV) model to detect and locate damage in a cantilever beam with two different widths. Heyns notes that this ARV approach does not require artificial excitation or measurement of the input forces. Mode shape changes are extracted from the AR model, and curvatures are calculated from the mode shape changes. The curvatures are determined to be more sensitive to damage than are mode shapes. Damage is simply defined as a reduction in the beam's stiffness, and the damage apparently does not result

in nonlinearity. Heyns simulates different levels of damage at different locations to verify the AR model's effectiveness. Although noise has adverse effects on the proposed method, it is still possible to accurately identify the damage location in this simulation. Furthermore, Heyns states that considerably less data are needed for this method than for traditional modal analysis.

De Stefano, Sabia, and Sabia (1997) use Auto-Regressive Moving-Average Vector (ARMAV) models to obtain modal parameters of a three-span bridge girder with unknown random excitation. In general, the estimation of the autoregressive (AR) and moving average (MA) coefficients in the ARMAV models requires solving a complicated nonlinear optimization problem. To avoid this problem, the authors first fit an ARV model to the data and compute the AR coefficients and prediction errors. Next, the authors use the prediction errors as estimates of the unknown inputs to the ARMAV model. Then, the AR and MA terms are found by means of a least squares approach. This process is repeated a few times until convergence is reached. Finally, the modal properties are estimated from the ARMAV model.

Loh and Lin (1996) compare the dynamic characteristics of a seven-story, reinforced-concrete building identified from four recorded seismic data (Whittier, Landers, Big Bear, and Northridge earthquakes). The modal frequencies, damping, and modal participation factors of the building are estimated using time domain system identification techniques. When the system is assumed to be linear time invariant, an Autoregressive with Exogenous Inputs (ARX) model or Auto-Regressive Moving Average model with Exogenous Inputs (ARMAX) is used to extract modal parameters. However, when a structure undergoes damage during an earthquake, the structure becomes time-variant. In fact, the authors find that natural frequencies estimated from some earthquakes do not coincide with the frequencies extracted from other earthquakes. The authors speculate that the time variance of the system during earthquakes causes instant changes in the building's parameters. Because it is observed that the building is damaged during the earthquakes, a forgetting factor is introduced into the ARX and ARMAX models to decrease the weights of previous time history values when estimating modal parameters. A decreasing exponential function of time is used as a forgetting factor to impose continuously decreasing weights to previous measurements. Furthermore, recursive identification methods, such as the adaptive forgetting through multiple models (AFMM) method and the recursive least squares method, are introduced to identify the modal properties of time varying systems. The authors

claim that the AFMM method provides more reliable modal parameters than the recursive least squares method for rapidly changing dynamic systems.

Although the common theme in feature extraction for structural health monitoring has been detecting anomalies in modal parameters, Loh et al. (2000) sought to estimate modal parameters with an Adaptive Fading Kalman Filter (AFKF) and Nonlinear Autoregressive Moving Average (NARMA) models. The RMS error between the experimental response and the ones estimated from these AFKF and NARMA models would signify damage. The advantages of the method are in the time domain tracking where one of two adaptation algorithms aids in recursive identification of nonlinear parameters. The authors list the inaccuracies in system identification in two classes, uncertainty caused by the nonlinear response and the incompleteness of the model. Their initial step is to test for nonlinearity of a structural model using a Hilbert transform followed by an identification of the mode shapes. Taking raw seismic data from the Kobe earthquake, they develop a basic system model with a stiffness matrix and joint rotation. Their most common model uses a variable forgetting factor algorithm to evaluate the nonlinear characteristics through a linear model. The model parameters are then found with a Kalman filter. The AFKF algorithm acts by lessening error-based forgetting factors. In another building example, they are able to identify the time-varying stiffness and damping of the first floor. The NARMA model is an analytical model that represents nonlinearity. They feed a training model with different input data and find that feeding different inputs is more satisfactory than feeding output data to learn the behavior of a healthy structure. Damage would be shown as large deviations from the network output versus true response.

4.11 Canonical Variate Analysis (CVA)

It is important to be able to distinguish closely spaced modal frequencies and mode shapes for vibration-based damage detection if one uses these modal quantities as features. The situation in which some modal frequencies degenerate can also complicate the detection process, if not lead to erroneous results, especially when a limited set of measurement data are available in the field. Garibaldi, Marchesiello, and Gorman (1999) propose using Canonical Variate Analysis (CVA) to extract mode shapes to overcome this problem. They note that choosing the correct model order is not straightforward and is a deficiency with such a method. The authors suggest using a

Modal Assurance Criterion (MAC) approach to determine the correct CVA order. The order of the CVA model, which gives the maximum MAC between two consecutive mode shapes, is chosen. Garibaldi, Marchesiello, and Gorman (1999) then simulate a three-span bridge with two coincident modal frequencies and the associated mode shapes to validate their approach. They urge that structure symmetry be utilized, in addition to making better use of limited measurements. In fact, for their bridge simulation, which had on each side nine equally spaced accelerometers, the authors add and subtract accelerometer measurements from the opposite side of the bridge. By doing so, the authors are able to separate the closely spaced flexural and torsional modes.

Garibaldi et al. (1999) compare the ARMAV and CVA-BR (Hermans and Van der Auweraer 1998) system identification techniques in the field of bridge monitoring. These two methods both allow extracting the dynamic characteristics of a system from output-only measurements. The ARMAV technique requires relatively short time histories for modal parameter identification, but suffers from the non-Gaussianity of the signals. To alleviate the effect of the non-Gaussianity, a signal preprocessing using a moving time window is employed. However, the design of an optimal time windowing scheme presents a considerable challenge. On the other hand, the CVA-BR needs longer time records but allows the extraction of higher modes compared to the ARMAV. The CVA-BR also provides several quality control indices such as the stabilization diagrams for frequencies, dampings, and MAC values.

4.12 Nonlinear Features

Brandon (1997 and 1999) states that, although the nonlinear response of a mechanical system has often been overlooked in structural health monitoring, nonlinear identification can provide valuable information for structural health monitoring. Although the author does not conduct any experiments or numerical simulations, he illustrates nicely the situation in which one could lose valuable information when linearizing time series, which are inherently nonlinear. This loss of information often occurs when one discards the time series data and focuses mainly on the spectral data. The author advocates the use of time-domain system identification techniques such as ARMA models and autocorrelation functions to retain important nonlinear information.

In a similar study, Brandon et al. (1999) investigate the effects of various cracks on a polyethylene cantilever beam. In particular, variations in the frequency response functions of the beam with a severe open crack condition contradict the expected reduction in resonant frequency. Nevertheless, the authors observe the expected results when the cantilever is excited with low amplitude sources. That is, a less severely damaged beam exhibits an expected reduction in the measured frequencies while the beam with a more severely cracked opening contracts the expectation. In addition, the authors state that a beam with a crack, which is neither open nor closed but at its equilibrium position, suffers degradation of its frequency response function with increasing bandwidth. The authors claim that this aspect can be potentially used as a feature for crack detection.

Tsyfansky and Beresnevich (1997) attempt to detect and quantify fatigue cracks in a beam by identifying nonlinear properties of a geometrically nonlinear system. First, the bending modes of the beam are excited with harmonic loading at a frequency, which is one-third of the beam's natural frequency. This harmonic excitation frequency is chosen because it is known to maximize the appearance of even-numbered harmonic components in the frequency spectrum as a result of cracking. Then, the Fourier spectrum of the beam's response is analyzed, and the presence of the superharmonic (above the harmonic excitation frequency) frequencies is determined. The size of the fatigue crack is determined based on the ratio of the second superharmonic amplitude to the first one. The relationship between this spectral ratio and the crack size is established based on predetermined calibration curves. It is also noted that this calibration curve is independent of the level of the external harmonic excitation simplifying the diagnosis. The researchers claim that the sensitivity of their method to damage is 10 times greater than conventional methods based on linear vibration procedures. Tsyfansky and Beresnevich (1997) test their method by simulating the dynamics of a cracked beam, in which the crack is modeled by assuming a bilinear stiffness for the beam at the crack location.

Todd et al. (2001) analyze certain properties of chaotic responses of a structure to look for subtle changes caused by damage. First, a structure is excited using a low-dimensional deterministic chaotic input. Then, attractors are reconstructed from the measured input and output time series by means of the embedding theorem. Here, the attracter is defined as an invariant subspace of the full state space, and the stability and dimension of the attracter are exploited as indicators of

damage. Specifically, the ratio of output attractor variance to input attractor variance is used as a damage-sensitive feature. This attractor variance ratio increases as damage progresses. The technique is demonstrated on a five degree-of-freedom spring-mass system, which is vertically suspended with elastic cables and connected to a vertical shaker through a force transducer. To simulate damage, the spring connecting masses 2 and 3 was reduced about 15%. Todd and Nichols (2002) also apply the same technique to a beam structure subject to boundary damage controlled by a special elastic clamp.

Adams and Farrar (2002) distinguish linear and nonlinear types of damage by modeling the dynamic transmissibility in a frequency domain with an autoregressive exogenous (ARX) model. The main premise of this work is that the harmonic response of a nonlinear system at a specific frequency is correlated with the input at that frequency and the response(s) at sub- and superharmonics of that frequency. For instance, a quadratic nonlinearity such as $\cos^2 \omega t = (1 + \cos 2\omega t)/2$ results in sub and superharmonics components at 0 and 2ω. Based on this premise, the frequency domain ARX model is constructed as follows:

$$Y(\omega_k) = B(\omega_k)U(\omega_k) + A_{-1}(\omega_{k-1})\ Y(\omega_{k-1}) + A_1(\omega_{k+1})\ Y(\omega_{k+1})\ ,$$

where $Y(\omega_k)$ is the response spectrum at frequency ω_k, and $B(\omega_k)$ is the exogenous term describing the conventional linear transfer function. This exogenous coefficient characterizes the linear nature of the damage, and $A_{-1}(\omega_{k-1})$ and $A_1(\omega_{k+1})$ are the autoregressive coefficients that characterize the nonlinear nature of damage. Here, the correlation between different frequency components is a consequence of nonlinear feedback. The magnitudes of the exogenous and autoregressive terms are used as features. The probability density functions of these features are estimated using the normality assumption of the features. Then, damage is identified using shifts of the mean on class-conditional densities of the features. This technique is demonstrated on a three-story building model consisting of unistrut columns and aluminum floor panels. The structure was instrumented with 37 accelerometers and was excited with an electrodynamic shaker at the base. Damage was imposed in the form of a reversible reduction in a bolt preload.

4.13 Time-Frequency Analysis

In contrast to the Fourier analysis, the time-frequency analysis can be used to analyze any nonstationary events localized in time domain. Vill (1947) notes that there are two basic approaches to time-frequency analysis. The first is to divide the signal into slices in time and to analyze the frequency content of each of these slices separately. The second approach is to first filter the signal at different frequency bands and then cut the frequency bands into slices in time to analyze their energy content as a function of time and frequency. The first approach is the basic short term Fourier transform, also known as spectrogram, and the second one is the Wigner-Wille Transform. Other time-frequency analysis techniques include, but are not limited to, wavelet analysis and empirical mode decomposition combined with Hilbert transform. This section intends to collate in one place different approaches and some recent advances in the field of time-frequency analysis for damage detection.

Bonato et al. (1999) extract modal parameters from structures in nonstationary conditions or subjected to unknown excitations using time-frequency and cross-time-frequency techniques. First, the time-frequency estimator for the amplitude ratio between two different measurement points $AR(t,f)$ is computed using wavelet transforms,

$$AR(t,f) = \sqrt{\frac{D_i(t,f)}{D_j(t,f)}} \ ,$$

where $D_i(t,f)$ is the Wigner-Ville wavelet transform of a signal recorded from the *i*th measurement points, *t* is the time variable, and f is the frequency variable. In a similar way, the time-frequency estimator for the phase difference between two different measurement points becomes

$$PH(t,f) = phase\left(\frac{D_i(t,f)}{D_j(t,f)}\right) .$$

It is observed that, if there is a structural mode at a specific frequency value, the amplitude and phase estimates should be constantly present at that frequency throughout the whole time interval. Based on this observation, the standard deviations of the amplitude and phase estimates are computed with respect to the time axis, and the standard deviation of the amplitude and phase estimators are plotted as a function of frequency,

$$g(f) = \int_0^T AR(t,f)^2\,dt \text{ and } h(f) = \int_0^T PH(t,f)^2\,dt \ ,$$

where $g(f)$ and $h(f)$ are the standard deviations of the amplitude and phase estimates, respectively. In a frequency value where a single mode component is predominant, the amplitude and the phase estimates tend to be constant in time. Therefore, these structural modes can be identified by searching the minima of the above standard deviations. The authors show that the phase estimator remains steadier over time than does the amplitude estimator, thus providing better estimates of modal frequencies. The proposed approach is applied to a numerical model of a three-story shear building.

Gaul and Hurlebaus (1999) use wavelet transforms to identify the location of impacts on a plate structure. A smart structure composed of an isotropic steel plate and distributed piezoelectric film sensors (PVDF) is tested. When an impact is applied to the plate, the plate generates dispersive flexural waves, and the embossed PVDF sensors measure the strain caused by the flexural waves. The wave propagation of the flexural waves is analyzed with the aforementioned wavelet transform. In particular, the maximum of the wavelet magnitude with different frequency content leads to the arrival time of the waves to each PVDF sensor. The time lag between the instant of the impact and the recording of the signals and the group velocity of the flexural waves are then obtained by solving a system of four nonlinear equations. These equations are derived from relationships that exist between the coordinates of the four different sensors and the arrival time of waves at these sensors. From the group velocity, the authors determine the wave number, which is defined as the integral of the reciprocal of the group velocity over a certain frequency range. Gaul and Hurlebaus claim that their technique is able to locate the coordinates of the impact location within 10% of accuracy.

Valente and Spina (1997) use the Gabor wavelet transform to model the nonsymmetric behavior of the opening and closing of a crack in a simply supported steel I-beam. The authors introduce a constitutive model composed of a symmetric and antisymmetric part. These parts are distinguished by examining the peaks of the Gabor Transform. The authors show that the antisymmetric part, which represents the effects of the crack, is uniquely associated with the spectral peak at zero frequency. Valente and Spina confirm their analysis with experiments on full-scale beams in both the undamaged and damaged cases. The damage causes the beam to exhibit bilinear stiffness behavior, whereas the beam with a closed crack had the original stiffness and the beam with an open crack had a reduced stiffness. In fact, only the first mode dynamics of the beam are analyzed.

Jacob, Desforges, and Ball (1997) discuss the use of wavelet coefficients as features for damage identification. Because material damage in composites often produces high frequency acoustic emissions, the authors apply wavelet transformation to the acoustic emission time signals to identify the failure mode of the material. These authors compare wavelet coefficients from Coifet, Daubechies, Symmlet, and Vaidyanathan wavelets when these various wavelets are used to decompose an impact-type waveform. The authors note that the Daubechies, Symmlet, and Vaidyanathan wavelets produce a good representation of the signal with a limited number of low scale coefficients. However, this ability to represent the waveform does not necessarily lead to better classification performance. In fact, all four wavelets investigated have the similar ability to classify the signals. The authors state that the choice of the appropriate wavelet to use will be based on the type of waveform being analyzed.

Naldi and Venini (1997) briefly explore the use of wavelets to detect damage in structural components. The authors numerically simulate damage in a beam constrained in all but the axial direction. The damage is simply a 20% reduction in axial stiffness at one-third the distance from the end. The coefficients of the Daubechies wavelet are used to locate the damage, and a harmonic excitation is applied to the beam. Then, the stiffness reduction, which varies from 50% to almost 0%, is detected using the first seven Daubechies wavelet coefficients in the vicinity of the damage. Second, Naldi and Venini apply the wavelet transforms to another beam that has the same geometry as the first one. However, the second beam is characterized by an elastoplastic behavior with linear isotropic hardening. The onset of plasticity is numerically simulated and the

wavelet analysis is undertaken. This wavelet analysis faithfully reconstructs the plastic regions. Finally, the authors apply the wavelet technique to the plane-strain isotropic hardening system and achieve good results.

Biemans et al. (1999) use Daubechie's wavelet coefficients to detect crack growth in the middle of a $400 \times 150 \times 2$ mm rectangular aluminum plate with 6 piezoceramic sensors mounted symmetrically around the crack. Static loading, sinusoidal loading, and Gaussian white noise are provided by one of the sensors, and the crack growth is monitored by the remaining sensors. The authors demonstrate that classical Fourier analysis can yield misleading results. In fact, some cracks have virtually no effect on frequency components of measured signals. They, however, show that certain Daubechies wavelet coefficients provide a reasonable indicator of crack presence. The logarithm of the variance of the wavelet coefficients is calculated for the undamaged plate, and the mean vector of the logarithms is computed. This mean vector is compared with the same measure applied to damaged plates. A Euclidean distance between the mean vectors of the cracked and uncracked plates is used as a damage-sensitive feature. The feature values from the undamaged plates are used to establish an alarm level above which damage could be considered present. Questions about whether higher frequency excitations could detect smaller crack lengths are left unresolved.

Staszewski et al. (1999) employ the orthogonal wavelet analysis of the strain data taken from piezoceramic devices on a composite specimen to identity impacts, which produce delamination. The high-frequency strain data from the piezoceramic sensors exhibit spiky responses when delamination is formed in a composite panel. The Kurtosis measure of the decomposed signals, which is the normalized 4th order spectral moment, is used to detect the spikes. The Kurtosis estimates taken from the wavelet transform correctly identify delamination resulting from an impact of 24 J while impacts of 4 J cause no damage and no change in the Kurtosis measure. The estimation of the Kurtosis is repeated for the original strain data. However, the characteristics of the Kurtosis remain flat for all energy levels. This result indicates that the orthogonal wavelet transform can extract features, which are related to delamination in the composite materials. The authors do warn that temperature rises and ambient vibrations can have severe effects on the results and can compromise the piezoelectric sensor performance.

Al-Khalidy et al. (1997) apply the Daubechies wavelet transform to detect fatigue damage in a building structure subjected to an earthquake. In this study, the building is modeled with a linear single DOF oscillator, and fatigue damage is modeled as a random impulse in the input signal. The seismic excitation is modeled as a filtered white noise. The time of fatigue occurrence is detected from several signal-to-noise ratios. The sampling rates, signal-to-noise ratio, and the vanishing moments of the wavelets are observed to affect the detectability of the impulse signal. For a lower noise level, increasing the sampling rate improves the detectability of the impulse. In the case of a higher noise lever, the impulse becomes more detectable with a low sampling rate. Furthermore, with an increase of the sampling rate from 8 Hz to 100 Hz, detection of those impulses becomes easier. However, the wavelet coefficient amplitudes become smaller when the sampling rate is increased. Robustness of wavelet analysis to external noise is also investigated, and the performance of wavelet analysis drastically deteriorates even for very low noise levels. Hou, Noori, and St. Amand (2000) use a similar simulation with the Daubechies wavelet to investigate the effectiveness of wavelet analysis for SHM.

Wang and Deng (1999) discuss a structural damage detection technique based on wavelet analysis of spatially distributed structural response measurements. This approach is based on a premise that damage in a structure causes the structural response perturbations at the damage sites and that the local perturbations are often discernable in wavelet components. Comparisons between the Haar and Gabor wavelets are made by conducting static and dynamic simulations on simply supported beams and plates with crack damage. Cracks range in thickness, size, and displacement fields, to which the wavelet analyses are applied and are calculated. In all cases, the methods demonstrate the ability of the wavelets to capture the crack location by exhibiting marked peaks in the spatial scale corresponding to the crack location. The authors reduce the number of measurement points from 1,024 to 62 and then to 31 to assess the sensitivity of the wavelet method. By approximating the displacements at neighboring, unmeasured points, the Haar wavelet analysis is still able to detect crack locations. When 15 measurements are taken, however, no trace of the crack is detected.

Masuda, Yamamoto, and Sone (1999) give a three-step process to identify time varying transfer functions, which represent the instantaneous frequency response functions of linear time varying systems. First, an estimate of the nonstationary spectrum of the input is obtained.

The nonstationary spectrum is estimated with the help of a time-frequency smoothing where the smoothing kernel is defined through a predefined measure of the local nonstationarity of the process. This measure is essentially the Fourier transform of the expectation of the input convolved with itself at time delays. Next, the input is decorrelated by means of the aforementioned nonstationary spectrum. Finally, the nonstationary cross-spectrum between the output observations and the decorrelated input is estimated. The authors apply their method to a simulation of a 4 degrees-of-freedom (DOF) structural system, which has sudden stiffness degradation. This system is subjected to the El Centro earthquake. The time varying transfer function is taken to be the ratio of each DOF's displacement to the ground motion. Identified frequencies agree with the actual frequencies of the system. The authors also test their method on an actual seven-story building subjected to ground motions from the Northridge earthquake. This building suffers severe damage in its concrete-frame columns at the base and middle floors. As a result, the fundamental frequency changes from 0.67 Hz to 0.42 Hz. The authors' analyses indicate that the first frequency changes at about 6 seconds while the second frequency changes at around 10 seconds. The authors note that the changing time of the fundamental frequency is a reasonable result, as the maximum ground acceleration occurs at 5.5 seconds of the earthquake.

Pierce et al. (1997) discuss the use of wavelet analysis to detect delamination in a composite plate. The plate, a mixed carbon/glass fiber panel with dimensions 400 × 300 × 3 mm, contained a 20 × 20 mm void delamination. A fiber-optic sensor was embedded within the structure to monitor Lamb waves within the structure. The Lamb waves were created by an external acoustic source that was mounted onto the surface of the composite. The authors claim that classical Fourier analysis of the data does a good job of detecting penetrating defects such as holes. However, frequency domain analysis does not do an adequate job in detecting delamination damage. The authors state that this is because delaminations do not provide very high reflection coefficients for the Lamb wave. In other words, the reflected portion of an induced Lamb wave is small and is sometimes not distinguishable by traditional frequency domain analysis such as the Fourier transform. In their work, the authors show that by performing a time-frequency analysis using a wavelet transform, delaminations within the composite plate can be detected with good accuracy.

Wavelet analysis has been one of the fastest evolving signal processing tools in the area of damage detection. Staszewski (1998) presents a summary of recent advances and applications of wavelet analysis for damage detection. This includes time-frequency analysis, wavelet spectrum, orthogonal or discrete wavelet decomposition, wavelet-based data compression, denoising and feature extraction, linear and nonlinear system identification, and image processing. The author advocates that the wavelet analysis provide new insight into nonstationary signal analysis with respect to classical time-invariant approaches and seems promising for a wider range of applications. However, the author cautions that most of the recent applications are largely limited to academic research because of the complexity of the mathematical and theoretical background associated with the wavelet analysis.

4.14 Empirical Mode Decomposition

The Empirical Mode Decomposition (EMD) technique is a local and adaptive technique for frequency-time analysis. This technique decomposes the original signal into a series of intrinsic mode functions (IMFs), and the remaining term accounts for truncation error. The IMF is a function that satisfies two conditions. First, in the segment of data being analyzed, the number of extrema and number of zero crossings must either equal or differ at most by one. Second, the mean value of the envelopes defined by the local maxima and by the local minima is zero. The purpose of decomposing the signal into a sum of IMFs is to obtain component signals with well-behaved Hilbert Transforms, and the instantaneous frequency of each IMF has physical significance. Vincent, Hu, and Hou (1999) compare the EMD method with a wavelet analysis for damage detection for a three-story shear building. The building is modeled as a simple 3 DOF system. The structure is monitored for 20 seconds, and damage takes the form of a 10% stiffness loss between the ground and first story at 10 seconds. The instantaneous frequencies calculated from the first five IMFs show a sudden drop at 10 seconds, which correspond to the occurrence time of the damage. It is concluded that although both the EMD and Wavelet methods are effective in detecting the damage, the EMD method seems to be more promising for quantifying the damage level. In fact, the IMFs demonstrate the capability to identify structural frequencies associated with multiple vibration modes. However, the authors caution that, in the case of mode

mixing coupled with disparate time scales in a single IMF, the EMD method may not be appropriate for SHM applications. Otherwise, the EMD method holds promise.

Pines and Salvino (2002) use the Empirical Mode Decomposition (EMD) in conjunction with the Hilbert transform to obtain phase and damping information of time series data obtained from a one-dimensional structure with and without structural damage. The EMD is used to determine the relative phase response between two successive degrees of freedom. As the structural elements become damaged, the nature of the phase and damping response changes between the two successive degrees of freedom. The location and extent of damage are then determined by tracking phase properties between the successive degrees of freedom.

4.15 Hilbert Transform

Natke and Cempel (1997) use the Hilbert transform to convert the equations of motion into new coordinates. The Hilbert transform takes advantage of the fact that damage induces changes in the higher frequencies of a system and has relatively little effect on the system's lower frequencies. Furthermore, over the long term, the lower frequencies do not change much, whereas the higher frequencies do as a result of damage. The authors claim that the new coordinates introduced by the Hilbert Transform handle better the different timescales of the system's life. Key to this ability is the Modulation Theorem. It states that, if two signals have nonoverlapping spectra, i.e., one is lowpass and the other is highpass, the Hilbert transform of the product of the two is equal to the product of the transformation of the highpass signal and the original untransformed lowpass signal.

4.16 Principal Component Analysis or Singular Value Decomposition

An application of Principal Component Analysis (PCA) can be found in Sohn and Farrar (2000) where the authors analyze measurements from a reinforced concrete column that is subjected to static/dynamic testing in a laboratory environment. Their ultimate goal in using PCA is to reduce the amount of data collected from various sensors in such an experiment. Time series data from 39 measurement points on the bridge column are transformed into a single time series by performing PCA. Because there is inevitably a loss of information when multiple time series are

compressed into a single time series, PCA is used to preserve as much information as possible during the compression. Sohn and Farrar (2000) first normalize the original time series by subtracting the mean from each time series and dividing by the standard deviation. Then, the 39 by 39 covariance matrix of the multiple channel measurements is calculated. The eigenvectors of this matrix are the principal components. The eigenvector corresponding to the largest eigenvalue represents the direction along which the most information from the time series is found. In fact, Sohn and Farrar determine that the first principal component contains about 30% of the time series' total information. They project the 39 time series onto the first principal component and use the projected time series for subsequent feature extraction and statistical process control.

Ruotolo and Surace (1997b) note that structures under test can be subjected to alterations during normal operating conditions, such as changes in mass. To cope with this situation, a damage detection method based on singular value decomposition (SVD) is proposed to distinguish between changes in the working conditions and the onset of damage. Let $\mathbf{v}_i$ be the frequency response function (FRF) measured from n different normal configurations (i = 1, 2, …, n). When a new FRF $\mathbf{v}_c$ is collected, all FRFs can be arranged in a matrix **M**,

$$\mathbf{M} = [\mathbf{v}_1 \, \mathbf{v}_2 \ldots \mathbf{v}_n \, \mathbf{v}_c] \ .$$

If the structure is intact, the new FRF $\mathbf{v}_c$ will be closed to one of the existing FRFs $\mathbf{v}_i$ and the rank of the matrix M estimated by SVD should stay unchanged by adding $\mathbf{v}_c$ to **M**. On the other hand, if the structure experiences damage, the rank of the matrix M will increase by one. A numerical example is presented where the FRFs are simulated from the responses of two locations on a cantilever beam. A lumped mass is present in one case to simulate operational variability, and noise is added to the measurements. Ten FRFs from different normal conditions are used to construct **M**. Damage is simulated by reducing the stiffness of one element in the numerical model. An increase in the rank of the matrix **M** is observed when the FRF from the damaged condition is added to the matrix of undamaged FRFs, indicating that the new FRF is independent from the FRFs corresponding to the undamaged system. This increase in the matrix rank is considered indicative of damage in the system.

Bernal (2000b) introduces a method to locate damage that uses a singular value decomposition (SVD) of the flexibility matrix change of a system. Next, a set of load vectors is identified so that the loads do not induce stress fields in the damaged elements. In other words, these load vectors are the basis of the null space of the flexibility matrix change caused by damage. Bernal calls these vectors the Damage Locating Vectors (DLV). The DLVs are computed strictly from the measured data without the knowledge of the damage locations. The DLV method has two drawbacks. It is not useful when the damage does not induce changes in the flexibility at the measured points. In addition, the method may prove ineffective when the damage region is too large compared to the number of sensors. Because the stress level in any element will never be exactly zero, one must establish a threshold stress level for proper damage diagnosis. To this end, Bernal introduces the normalized stress index as the stress in an element divided by the largest stress value over all of the elements. A threshold for the index is then chosen below which an element would be considered damaged. The method is numerically tested on an 8 degree of freedom (DOF) fixed-fixed beam outfitted with accelerometers and on a numerical model of a 10 DOF shear building with an uneven distribution of mass and stiffness. The first simulation's damage is defined as a 25% reduction in flexural stiffness in one element and a 50% reduction of stiffness in another element. The second system's damage is defined as a 25% reduction of stiffness in floor 2 and a 50% reduction in floor 6. In both cases, the DLV method clearly identifies the damage within the resolution of the sensor array.

Manson et al. (1999) employ acoustic emission signals for damage detection. The authors are able to detect and analyze stress waves but could not dissociate the stress waves generated from damage and those from the acoustic emissions of the test apparatus, making the results inconclusive for damage detection at that time. The experimental setup consists of an I-beam subject to three-point bending ranging from 50 kN to 410 kN. They set up the beam with an acoustic emission transducer coupled with a gain amplifier and a low pass filter. Various features are investigated, including rise time, peak amplitude, signal duration, and ring-down count. Two different methods are exercised to reduce the dimensions of the extracted feature data. The first is principal component analysis (PCA), a method of multivariate statistics. From a covariance matrix of the experimental data, a singular value decomposition is used to make a transformation to principal components. This dimension reduction technique eliminates combinations of data that least contribute to the variance of the data. The second method is

nonlinear transformation, or Sammon mapping for minimizing the Sammon Stress. A common approach is to use neural networks; specifically, they use a Radial Basis Function network to implement the mapping. Their results indicate that the inherent dimension of the data was of low dimension and that the PCA method closely matches the nonlinear Sammon mapping. Both are successful in clustering frequencies that could be associated with damage at a later time.

4.17 Finite Model Updating

Yang and Lee (1999) present a two-stage method for damage diagnosis. In order to minimize the nonuniqueness problem caused by incomplete modal data, a substructure technique is first used to detect potential damage regions. By locating the potential damage locations first, the search space may be narrowed to ensure better damage quantification in the second step. Next, the second step of the method involves a minimization process to quantify the damage extent. The authors also address the issue of spatially incomplete measurements. Because the objective function is based on errors between components of the experimental mode shapes and the associated analytical mode shapes only, neither mode shape expansion nor model reduction is required. Yang and Lee test their method with numerical simulations where the experimental data are simulated from a more refined model than the numerical model to be updated. A tapered cantilever beam is analyzed for this study. Damage is simulated as 20% and 40% stiffness reductions of two elements, and the threshold value above which damage is flagged is 5%. The authors claim good results for their diagnostic method. However, they state that the involvement of too many higher modes can actually have adverse effects on damage diagnosis because the inherent modeling error then increases.

Damage detection techniques using finite element model updating require solving an inverse problem using measured test data to detect, locate, and quantify damage. This procedure often leads to updating of a large number of damage parameters, especially when the structure has many structural members. Parameter reduction in damage identification is undertaken by Fritzen and Bohle (1999a). By means of the linear substructure approach, the authors calculate the change in the dynamic stiffness matrix associated with the damage and describe these matrix changes with dimensionless correction parameters. The correlation between residual vectors and parameters is defined as the scalar product between the two. They use this measure in their

parameter reduction. Those parameters that have a high correlation with the residual vectors are considered for updating. After reducing the size of the parameter sets by means of a correlation technique, the resulting system for the model's dynamic equations is solved via Tykhonov-Phillips regularization. Finally, the damage extent is quantified by the stiffness loss in the selected damage parameters. This quantification is done by fitting the model to the experimental data of the damaged bridge. The size of the parameter set is reduced from 1,080 to 9, and the selected parameters are the shell and beam elements encircling the location of the damage. One problem that may arise with the authors' method is that the parameter reduction may indeed choose the most damage-sensitive parameters but may fail to correctly locate the damage. This method is applied to the I-40 Bridge in New Mexico, which is gradually damaged at four levels, and the associated frequency response functions are used for diagnosis.

In a study that closely parallels the aforementioned, Fritzen and Bohle (1999b) compare two parameter reduction methods, namely the QR orthogonal decomposition of the parameter space and Efroymson's criterion (Efroymson 1960) for the SHM of the same bridge. The authors formulate the damage detection strategy exactly as in their earlier work and solve the resulting inverse problem again via Tykhonov-Phillips regularization. The Efroymson criterion investigates whether the addition of a new parameter yields a significant reduction of the residual errors. This procedure is repeated for all parameters, and the solution of the final parameter subset is used for the damage localization. Alternatively, the QR orthogonal decomposition technique can be employed to reduce the original parameter space into a smaller subspace of prominent parameters. In this method, the sensitivity matrix is decomposed into a product of an orthogonal matrix Q and an upper triangular matrix, R. Then, the residual errors can be reformulated using only a subset of the Q matrix columns and the associated subsets of R. Both strategies of parameter reduction led to satisfying results, and the authors are unable to state a preference.

Onate, Hanganu, and Miquel (2000) discuss methods of modeling crack damage in concrete. The authors attempt to account for the various nonlinearities that cracks present. These nonlinear effects include the different material response under tension and compression while the linear effects of stiffness degradation caused by mechanical and physical effects are also considered. In addition, the researchers ensure the appropriateness of a finite element mesh for a model of

concrete involving cracking. To model the cracking in a finite element simulation, the researchers first formulate a constitutive relation between stress and strain that accounts for the reduced area caused by the cracks,

$$\sigma = (1-d)\mathbf{D}\varepsilon \ ,$$

where σ is the stress tensor, **D** is the elastic constitutive matrix, and ε is the strain tensor. The damage indicator *d* is the percent reduction in the cross-sectional area caused by cracking. This constitutive model requires the knowledge of the damage variable *d* at every stage of the deformation process. The formulation of the damage indicator evolution first requires the definition of a scalar norm of the strain tensor τ ,

$$\tau = (\theta + \frac{1-\theta}{n}) \sqrt{\sigma^T \mathbf{D}^{-1} \sigma} \ ,$$

with

$$\theta = \sum_{i=1}^{3} \sigma_i \Big/ \sum_{i=1}^{3} |\sigma_i| \text{ and } \pm\sigma_i = \frac{1}{2}(|\sigma_i| \pm \sigma_i) \ ,$$

where *n* is the ratio between the tension and compression limit strengths, and the stress tensors σ_i are those corresponding to the reduced areas. Finally, a damage criterion is formulated as

$$F(\tau, r) = \tau - r \le 0 \ ,$$

where *r* is the damage threshold value. Damage grows when the norm τ exceeds the current threshold value, and an initial value of the damage threshold r_o is calculated as the ratio of the tensile strength to the square root of the elastic modulus. The authors then formulate an evolution law of the damage parameter *G(r)* as a function of *r*

$$d = G(r) = 1 - \frac{r_o}{r} \exp[A(1 - \frac{r}{r_o})] \ ,$$

where A is a parameter determined from the energy dissipated in a uniaxial tension test of a concrete specimen. Then, a global damage indicator D, which is the percent reduction in global energy caused by damage, is defined,

$$D = 1 - \frac{\overline{U}}{U} = 1 - \frac{\mathbf{a}^T \int_V \mathbf{B}^T (1-d)\sigma \, dV}{\mathbf{a}^T \int_V \mathbf{B}^T \sigma \, dV} \quad ,$$

where V is the material volume, **a** is a displacement vector, and **B** is the matrix relating strains to displacements. Again, the stress tensors are those corresponding to the reduced areas, and $\overline{U}$ and U are the total energy of the structure corresponding to the damaged and undamaged states. The state of the structure with regards to its final failure mechanism is estimated by the global damage indicator. A structure will fail when the global damage indicator D approaches unity. The authors test their method on simulations of a reinforced concrete containment vessel and two buildings.

Park and Reich (1999) use invariance properties of the element or substructural transmission zeros to detect and locate damage in a structure. First, the authors describe a variational method of partitioning the global equations of motion of the structure into substructural equations for the partitioned structure. In particular, the strain frequency response function (FRF) of each element $H_\varepsilon(\omega)$ is computed from the global displacement FRF $H_g(\omega)$,

$$H_\varepsilon(\omega) = SLH_g(\omega)L^T S^T \quad ,$$

where ε denotes strain, ω is the frequency, S is the discrete operator that relates the strains to the displacements, and $H_g(\omega)$ is the global FRF. It is this form of the strain-based localized FRF that is used for damage detection. It is noted that the transmission zeros of this transfer function are not affected by changes in the element stiffness parameters. This invariance property of the transmission zeros is exploited to detect damage. The transmission zeros of a particular substructure are determined for the reference and damaged cases. The variation between the two sets of transmission zeros are determined numerically, and the relative variation of one substructure is compared to those of the other substructures. The substructure with the lowest overall variation is deemed to be the damage location. It should be noted that some possible

shortcomings of this method are as follows. First, it is generally impossible to excite all modes of a structure as well as to cover the whole structure with enough sensors to accurately measure all degrees of freedom. Second, damage detection via the measurement of transmission zeros does not allow for accurate damage prediction when that damage occurs at element boundaries. Park, Reich, and Alvin (1997) demonstrate the usefulness of their method by considering a ten-story building modeled as a plane beam subjected to ground acceleration. However, the authors give few details of that simulation or of the damage case.

Chattopadhyay et al. (1997) present a refined finite element model based on higher order theory to model the dynamic response of delaminated composite beams instrumented with sensors and actuators. The authors note that their model accurately accounts for through-thickness transverse shear deformations as well as nonlinear strains induced by applied electric fields from piezoelectric actuators. The model is verified with experiments performed on Graphite/Epoxy laminates. It is noted that the presence of delamination obstructs the damping capacity of the actuators and the nonlinear actuation effects are more significant for lower stiffnesses. Although the particular finite element method is developed for control applications of composites, the modeling techniques can also be useful for characterizing the behavior of damaged composites with finite element updating procedures.

Ruotolo, Sorohan, and Surace (2000) create three finite element models of a three-dimensional, eight-bay truss and use experimental data from the truss structure to update the models. The first finite element model consists of simple truss elements, the second consists of Euler-Bernoulli beam elements, and the third consists of three beam elements per actual individual truss element. Three beam elements per an actual truss member are used to accurately model the effects of the connectors. Although the researchers do not introduce damage into the truss structure in this work, they note that an accurate numerical model of the structure in its undamaged state is essential for damage detection. The authors use the eigenvalue sensitivity method for model updating. The authors compare natural frequencies of the three updated models with the experimental frequencies and demonstrate that the third model performed the best, giving a frequency error of approximately 0.85%. The first and second models give errors of 3.5% and 2.1%, respectively. These results are verified by applying the Modal Assurance Criterion and

Cross-Orthogonality relations between the experimental and numerically calculated mode shapes.

Lopez-Diez et al. (2000) present the Modified Component Mode Synthesis (MCMS) method for model updating. This variant of the Component Mode Synthesis (CMS) method relates the physical coordinates *x* with generalized coordinates *q* using a transformation matrix T composed of the preselected modes,

$$x = \begin{bmatrix} x_M \\ x_C \end{bmatrix} = \begin{bmatrix} \mathbf{I} & \mathbf{0} \\ \Psi_C & \Phi_N \end{bmatrix} \begin{bmatrix} x_M \\ q_N \end{bmatrix} = \mathbf{T}\, q \ ,$$

where the physical coordinates *x* are partitioned into the master degrees of freedom (DOF), x_M, and the complementary DOF, x_C; $\mathbf{I}$ and $\mathbf{0}$ are the identity and null matrices, respectively; Φ_N is the mode shape matrix corresponding to the master DOFs. Each column of Ψ_C is a static deflection of the complementary DOFs when a unit displacement is imposed on each master DOF, and the deflections of the remaining DOFs are restrained. Finally, q_N represents the generalized coordinates resulting when the master DOFs are fixed. One advantage of the MCMS method over the CMS method is that the MCMS accounts for some dynamic deformations corresponding to the unitary displacements of the master degrees of freedom. The authors compare the performance of the MCMS method with other methods such as the CMS and improved reduced system methods. Indeed, they perform tests on a composite plate and condense an 882 DOF model down to 7 and 9 DOFs, respectively. The MCMS method gives the smallest errors for both cases.

Chen and Ewins (2000) provide a means of determining if the initial finite element model can be refined or not before undertaking finite element model updating. The authors give means to check the convergence properties of model updating as a function of discretization error and to check the configuration error of the model. Discretization errors come from modeling a continuous physical system by a discretized numerical model, and configuration errors arise when the complicated parts in a physical structure are modeled with simplified types of elements. The use of different formulations in the mass matrix construction is closely related to the convergence of the model prediction. In addition, the authors estimate compensation for the

discretization errors to distinguish the discretization errors from the parameter estimation errors. Furthermore, the proposed method of configuration check identifies unsuitable elements that contribute to configuration errors of the model.

Alexiou et al. (2000) state that although detailed models often correlate better with experimental data, there are still needs for techniques that can quantitatively determine among different models which model represents experimental data the best. The authors consider a global shape criterion (GSC) $\chi^s(\omega)$ and a global amplitude criterion (GAC) $\chi^a(\omega)$ to provide shape and amplitude based information in the frequency domain,

$$\chi^s(\omega) = \frac{|H_E(\omega)^T H_A(\omega)|^2}{(H_E(\omega)^T H_E(\omega))(H_A(\omega)^T H_A(\omega))} ,$$

$$\chi^a(\omega) = \frac{2|H_E(\omega)^T H_A(\omega)|}{(H_E(\omega)^T H_E(\omega)) + (H_A(\omega)^T H_A(\omega))} ,$$

where $H_A(\omega)$ and $H_E(\omega)$ are the analytical and experimental frequency response functions (FRF), respectively. The superscript * denotes a complex conjugate. Once such global criteria are defined, the corresponding local criteria are defined by replacing the global FRFs with only the *i*th response and the *j*th input pair of the FRFs,

$$\chi^a_{ij}(\omega) = \frac{2|H^*_E(\omega)H_A(\omega)|_{ij}}{(H^*_E(\omega)H_E(\omega))_{ij} + (H^*_A(\omega)H_A(\omega))_{ij}} ,$$

where $\chi^a_{ij}(\omega)$ is a local amplitude criterion (LAC) and $(A)_{ij}$ is the *i*th row and the *j*th column component of matrix A. Noting that the LAC is a function of frequency between the lower and higher cutoff frequencies, ω_l and ω_h, of the measure frequency bandwidth, the averaged LAC $\overline{\chi}^a_{ij}$ is defined as

$$\overline{\chi}^a_{ij} = \frac{1}{\omega_h - \omega_l} \int_{\omega_l}^{\omega_h} \chi^a_{ij}(\omega)\ d\omega .$$

This averaged LAC can be computed for each response degree of freedom (DOF) with the fixed excitation point. Such a LAC is an alternative to assessing the correlation at each DOF via COMAC. Four different finite element models of an automobile oil pan are used to ascertain the effectiveness of the LAC method and determine which model represents the oil pan the best. The four models have varying degrees of refinement between 212 to 2,380 elements (or between 1,128 to 11,130 DOFs) and the most refined model with 2,380 elements is used as the reference model replacing an actual experiment. The averaged LAC is then computed for 18 nodes common to all models. This LAC criterion is found to be more sensitive than the COMAC criterion. A sensitivity based updating procedure is formulated to estimate the variation of the design parameters,

$$S\,\Delta\varphi = \varepsilon\ ,$$

where φ represents a vector of the design variables that consist of the structure's geometric and material properties, S is the sensitivity matrix of the GSC and GAC with respect to the selected design parameters, and ε is a vector given by

$$\varepsilon = \begin{bmatrix} 1-\chi_s(\omega) \\ 1-\chi_a(\omega) \end{bmatrix}\ .$$

Finally, the change of the design parameters $\Delta\varphi$ is given by

$$\Delta\varphi = S^T W_f S + W_\varphi^{-1} S^T W_\varphi E\ ,$$

where W_f and W_φ are diagonal weighting matrices, and E is a collection of ε's estimated at different frequency values. The oil pan is divided into nine regions, and the design variables are the thickness of the nine regions. Nine modes of the structure exist in the updating frequency range of 200–2,000 Hz. The updating algorithm is applied in a recursive fashion, and convergence is obtained after 13 iterations. The computed thickness changes are within 8% of the nominal values of the reference model.

Beardsley, Hemez, and Doebling (1999) compare two methods of updating nonlinear finite element models with data taken from experiments. The first method simply defines the residue or difference between measured time data and time data obtained from the finite element model. It uses a least squares approach to minimize the objective function, which is itself a function of the residue vector. The authors note, however, that the success of this method is conditioned by the ability of the mathematical model to span the subspace to which the test data belong. The second method uses the same time data, but a different objective function is minimized. The Singular Value Decomposition (SVD) of the time domain data, both measured and numerically generated, is used to define the residual vectors. In effect, the objective function to be minimized is the sum of the distances between the measured and generated singular vectors and the diagonal matrix of the time series' singular values. It should be emphasized that because the system analyzed is nonlinear, time and not frequency data are appropriate. Before performing the numerical optimization, the authors build response surfaces, which are defined as tables of the values of the objective functions evaluated over a range of model parameters. Beardsley, Hemez, and Doebling use results from impact experiments on a hyperelastic polymer to compare the two updating methods. The authors do not observe a significant difference between the two methods and state that the first one requires less computation. However, they also note that the first objective function is less sensitive than the second objective function to an important design parameter (the velocity of impact). Finally, the second method has the ability to filter measurement noise because it incorporates the SVD.

Papadimitriou, Levine-West, and Milman (1997) present an iterative model updating technique for damage detection using incomplete sets of experimental frequencies and mode shapes. Their method involves a least squares minimization of the dynamic unbalanced force residuals. This minimization is subject to quadratic inequality constraints introduced to properly account for the expected measurement and modeling errors. This three step iterative procedure consists of mode shape expansion, damage localization, and damage quantification. Damage localization is based on an element strain energy error between the expanded experimental mode shapes at the current iteration and the analytical mode shapes at the previous iteration. The damage size is then estimated using the expanded mode shapes, and the estimate is iteratively updated until convergence is reached. Modal data simulated from a three-dimensional truss structure are used to assess the advantages, limitations, and overall performance of the method in relation to the

number and location of sensors, the location and magnitude of damage, and the number of the measured modes. The first eight modes in the range of 10 Hz to 200 Hz are used. Damage is a simple 50% reduction in the cross sectional area of three truss members. Two different sensor configurations, one with 99 sensors and the other with only 15 sensors, are used to assess the fidelity of the method for different amounts of sensors. The results indicate the superiority of the method when using more sensors.

Liu and Chen (1996) adopt a spectral finite element method to formulate the equilibrium equation of the truss in the frequency domain. Then, the damage identification problem is formulated as an optimization procedure in which the unbalanced nodal forces in the frequency domain are minimized. A transient response of the structure is used as a feature, and the transient response is represented by the summation of a finite number of waveforms using a discrete Fourier transform. The authors claim that because the spectral finite element method describes a displacement field in a truss element precisely without interpolation, the transient dynamic behavior of a truss element can be computed accurately regardless of the member length. On the other hand, the use of shape functions in the conventional finite element method requires finer discretization of each truss member, and the computation can be costly. The numerical example demonstrates the effectiveness of the spectral finite element approach to identify the element properties of the truss structure such as axial rigidity and mass density.

Many other authors also employ finite element simulations to generate features to be used in damage detection procedures. Ruotolo and Surace (1997a and c) use a finite element simulation of a multicracked cantilever to generate frequencies and mode shapes of the damaged beam and use these in a cost function to be minimized. Furthermore, Rytter and Kirkegaard (1997) simulate the effects of changing stiffness of beams and columns in a building structure. They then use these effects to train a neural network for damage detection.

Choi and Kwon (2000) utilize a finite element model to develop a damage detection system for a steel truss bridge. The numerical model was built based on the design drawings of a real bridge, and it was updated using measurements from static and dynamic loading tests of the real bridge. First, the stiffness of the truss members was adjusted so that the deflections in the model matched those from the static tests. Second, the mass of the truss members was adjusted so that

the natural frequencies obtained from the analytical model matched those from the experimental modal analysis. Then the refined finite element (FE) model was used to determine which truss members had the highest stresses during static analysis. This analysis identified eight truss members as most vulnerable to damage. Based on this observation, stiffness reduction in each of these eight truss members is simulated to generate eight damage cases for the subsequent neural network analysis. The FE model was used to produce strain data as well as mode shapes and natural frequencies used in their neural network damage detection system.

4.18 Wave Propagation

Safak (1997) claims that the investigation of wave propagation in multistory buildings can offer important insight into building dynamics that a classical vibration-based analysis cannot provide because of lack of sufficient sensors. In particular, Safak claims that the wave propagation approach is simpler to implement, more accurate at high frequencies, and is more useful for identifying damage from vibration records. Furthermore, the wave propagation approach incorporates damping more accurately and accounts for the energy absorption by the soil layers under the foundation. He then discusses a wave propagation model for multistory buildings, detailing the formulation of the boundary conditions between the building foundation and the ground to obtain good theoretical estimates of the reflection and transmission coefficients at the building/ground interface. The author states that changes in the wave propagation parameters, namely the reflection and transmission coefficients and the wave travel times, are more sensitive to damage than classical mode shapes and frequencies. To study the problem experimentally, a 17-story steel frame Health Science Building at UCLA in Los Angeles will be outfitted with 72 accelerometers (4 horizontal at every floor and 4 vertical at the basement level) probably to measure the incoming vertical seismic waves. Also, a ten-story reinforced concrete, frame/shear wall Millikan Library at Caltech in Pasadena will be instrumented with 36 accelerometers, 3 horizontal at every floor, and 3 vertical in the basement.

Along similar lines, Pines (1997) applies wave propagation modeling to damage detection in one-dimensional structures. As applied to global SHM, local damage is modeled as a change in the local dispersion relation of individual structural elements. Simulations of a one-dimensional rod are used in the study. The rod deflection is written in terms of a complex spatial shape

function and the wave-mode coordinates. With this relation, the dynamic force-displacement relation is derived. Finally, the global stiffness matrix of the entire structure is assembled, and the simulation is undertaken. The method is applied to a free-free bar with a 10% reduction in stiffness of the first element. Using a Newton-Raphson iteration, the eigenvalues of the damaged transfer function are calculated at the damage state. A slight decrease in these eigenvalues is noticed, and a change in the local wavenumber of element 1 is also noticed in the absence of any noise. An actual experiment is performed where an extra 10 g mass is attached to the bar to cause the system change. The bar is tested with a piezoelectric actuator and accelerometers. A 4% increase in the local wavenumber is observed in the region with increased mass. Pines states that the method requires fewer sensors to capture a one-dimensional structure's dynamics and offers greater sensitivity in detecting local impedance changes in damaged regions. However, the difficulty in measuring wave coordinate variables as well as the need for excitation and measurement at every node of the model require that additional research into the method be performed. Furthermore, more studies with applications to complicated structures need to be considered.

Lovell and Pines (1998) attempt to use wave propagation to detect damage within a bolted lap joint. The authors develop a dynamic analysis technique of a bolted lap joint using continuum wave mechanics and construct an analytical model to predict the scattering of propagated waves at the bolted joint. An analytical description of the transfer function dynamics is also developed based on the displacement wave amplitudes determined from the continuum mechanics equations. The authors then formulate least squares cost functions comparing experimental and analytical frequency response functions at the joint as well as the wave scattering properties of the system. To validate the analytical models, an aluminum plate with the dimension of $3.175 \times 25.4 \times 939.8$ mm was constructed with a central overlapping bolted joint section. The joint was fit with two piezoelectric sensors and two piezoelectric actuators. The joint was first excited to determine the dynamic transfer function response under various bolt preloads. It was then excited to determine the wave scattering properties of the joint under changing bolt preloads. All experimental results were compared to analytical predictions, and the analytical model for wave scattering successfully detected the preload loss in the bolt.

Ma and Pines (2000) further investigate using wave propagation modeling to detect damage in one-dimensional structures by applying the concepts of the Reverberated Transfer Function (RTF) and the Dereverberated Transfer Function (DTF). Wave dynamics generated at natural boundaries and subsequently reflected at geometric boundaries can lead to pole-zero characteristics of a conventional RTF. The DTF is obtained by applying a wave model based virtual controller at these boundaries. The DTF response can be used to locate and quantify damage in a structure. A 3-DOF three-story building structure is modeled as three asymmetric spring mass elements. In the undamaged structure, the virtual controllers at each mass prevent any wave energy from being reflected back. If damage is present, the local controller will not be able to prevent reflection. By examination of the DTF for each mass, the location and amount of stiffness loss in the structure can be determined.

Purekar et al. (1998) and Lakshmanan and Pines (1997) also use wave propagation within a material to identify delamination and crack damage within a composite rotorcraft flexbeam. Using a continuum mechanics approach, the authors develop an analytical model for the flexbeam that has been damaged through delamination. This analytical model predicts how structural waves scatter when they reach the delamination zone. The analytical model includes the effects of wave transmission and reflection components that impinge upon the damaged region. The analytical model also takes into account the transitional effects of waves propagating from an undamaged region into a damaged region and vice versa. From the continuum mechanics models, the authors develop transfer functions for the damaged and undamaged regions. Because structural waves will propagate through a damaged region with a speed different from that of an undamaged region, the authors developed an equation to predict the phase lag that is created when a wave propagates through a damaged region. To verify the analytical model that was developed, the authors tested several thin 46 × 2.5 cm graphite-epoxy composite beams. Delamination damage was introduced into some beams by inserting a Teflon sheet into the composite during the lay-up process. The beams were excited in the flapwise direction using piezoelectric actuators bonded near the root of the beam. Transfer functions from the experimental test and the analytical analysis were compared and found to be in good agreement except for the first mode, where the analytical model failed to provide accurate results. Examination of the experimental data also verified that the both the phase and magnitude of the wave changes as the wave encounters a damaged region.

The propagation of waves in a structure is frequently used for damage detection. If an axisymmetric cylindrical shell or tube is loaded with an axisymmetric load, only axisymmetric wavemodes exist. If there is a nonaxisymmetric defect present, however, antisymmetric wavemodes will arise. Leutenegger et al. (1999) discuss a technique for constructing the dispersion diagrams for analyzing the wave modes in a circular cylindrical shell. In this technique, the time difference of an excitation pulse arrival is measured at two different locations on the structure. From this measurement, the group velocity for the pulse can be calculated. The dispersion diagram can be constructed by measuring the group velocity of a narrow band signal at several different frequencies. Information about damage present in the tube can be drawn from any antisymmetric wave modes that appear in the dispersion diagram.

Focusing on the structural health of concrete, Shah et al. (2000) are able to demonstrate damage detection techniques for a number of structural loading situations, including beam loading, static loading, and elongation and torsion of concrete samples. The dynamic investigation involves the evaluation of through-thickness ultrasonic amplitude transmission in comparison with ultrasonic velocity measurements. An ultrasonic transducer sends a pulse that passes through the distributed damage and is collected by a receiver. The results find that the attenuation of the signal amplitude demonstrates greater change than change in the ultrasonic velocity measurements. A 50% reduction in Young's modulus revealed an 84% change in the peak amplitude from the undamaged state to the damaged state, while only a 9% change is noted in the pulse wave velocity. The beam testing includes a fatigue response at selected modes with an estimated crack length after cyclic loading. The remaining service life is predicted by linearly relating the reduction rate of the measured natural frequencies to the fatigue life of the specimen. The static loading used a solenoid-driven impactor to create a set of stress waves that propagate along the surface and reflect off the opposite surface to reach a set of accelerometers. Stress waves with a frequency content of 0 to 100 kHz are generated and then observed by the first accelerometer that is placed before the induced crack and by the second accelerometer placed after the crack. Following the methodology of their first experiment, the signal amplitude between the first and second accelerometers is found to be more sensitive to the damage than the velocity change.

4.19 Autocorrelation Functions

Feroz and Oyadiji (1997) use autocorrelation functions of dynamic response measurements to investigate damage in bars in which damage is a simple slot. Although the authors use ultrasonic methods, it is illustrative of how the autocorrelation function can be used as a damage-sensitive feature even for global vibration-based damage detection. Experiments are performed on a 16 × 16-mm square section of a steel bar that is 2,440 mm long. The slots are 2 mm in width and range from 2 to 8 mm in depth. An impact excitation is applied at a distance of 915 mm from the slot. The authors use PZT sensors mounted on the bar surface and induce longitudinal stress waves in the bar by means of an impact. Feroz and Oyadiji show that a slot of 10% of the bar depth can be detected using the autocorrelation function as a feature and that, as the slot size increases, the autocorrelation function amplitude increases at the zero time lag.

4.20 Other Features

Sikorsky and Stubbs (1997) describe the application of quality management and modal-based nondestructive damage evaluation (NDE) techniques to improve bridge management. As a means for accomplishing this management, the authors define a feature called the safety index, β, given by

$$\beta = \frac{[\mu_R - \mu_L]}{\sqrt{\sigma_R - \sigma_L}} ,$$

where μ_R and μ_L are the mean resistance or strength of a structure and the mean load to which a structure is subjected, respectively, and σ_R and σ_L are the standard deviation of resistance and the standard deviation of load, respectively. This safety index is calculated for different bridge components. The mean and standard deviation of the structural components' resistances are calculated with the help of modal parameters obtained experimentally. A simulated 500-ft-span truss bridge is subjected to prescribed seismic forces, and the resistances are calculated as a result of the bridge's performance with various levels of simulated damage. The means and standard deviations of the loads can be easily calculated from the specific loading to which the bridge is subjected, such as the earthquake in this paper. The safety index β for each bridge

component is calculated, and control charts of β with control limits of one standard deviation are constructed. However, it is unclear how the authors obtain enough data to construct control charts. The control charts determine which components will require additional attention based on how well their β values stay within the control limits.

Lee and Liang (1999) devise the Energy Transfer Ratio (ETR) as a feature to detect and locate damage. The ETR is the ratio of the modal energy dissipated during one cycle to 4π times the energy of the mode before the cycle. The authors claim that the ETR had a higher signal-to-noise ratio than conventional modal parameters. The change of the natural frequencies is related to the change of the ETR as follows:

$$\frac{\omega_i^h - \omega_i^d}{\omega_i^h} = \frac{\exp(ETR_i^h) - \exp(ETR_i^d)}{\exp(ETR_i^h)} \ ,$$

where ω_i^h and ω_i^d are the *i*th natural frequencies before and after damage, and ETR_i^h and ETR_i^d are the ETRs for the *i*th mode before and after damage, respectively. Suppose that the damage creates a frequency change by a factor of 0.1% and that the initial ETR is 0.001. This damage results in the ETR change of 100% or 1,000 times more change compared to that of the frequency. A $1/6$-scaled highway bridge model is used to test the effectiveness of the ETR in determining damage location. The bridge consists of a 40-in.-wide concrete slab supported by 3 single span parallel steel girders. Measurements are taken at 16 points on the slab in a rectangular grid pattern. Two damage cases are considered. A bearing is first removed to simulate bearing damage. Then, a crack on the tension side of the center span girder is introduced in 3 successive steps. Only small changes in the ETRs occur when measurements are taken at locations away from the damaged location. In contrast, large ETR changes occur near the damage location. Similar conclusions hold for both cases of damage. While the modal frequencies change from 0.1% to 7.8% depending on the damage case, the changes of the ETR range from 30% to 1,892%.

De Callafon (1999) develops an online damage detection technique using so-called model based orthonormal functions. First, the dynamic system to be monitored is approximated by a frequency response function (FRF) or a minimum state space realization,

$$H(z) = D + C(zI - A)^{-1}B = D + \sum_{k=1}^{\infty} CA^{k-1}B\, z^{-k} \ ,$$

where $H(z)$ is the FRF; *A, B, C*, and *D* are the corresponding state space matrices, and *z* is the variable of the *z*-transform. Here, note that the FRF is represented as a linear combination of the orthonormal basis function z^{-k} times the Markov parameter $CA^{k-1}B$. A more generalized Markov expansion of the FRF can be obtained,

$$H(z) = D + \sum_{k=1}^{m} L_k\, V_k(z) \text{ with } \theta^T = [D \ L_1 \ L_2 \cdots L_m] \ .$$

In this equation, only a finite number *m* of expansion coefficient L_k is used to represent the FRF. $V_k(z)$ denotes a set of orthonormal basis functions that can be calculated from the state space matrices, *A*, *B*, *C*, and *D*. Once $V_k(z)$ is computed, the parameter set can be estimated from a simple least squares estimation technique. When a new input/output pair $u(t)/y(t)$ is measured from the structure, the associated parameter set θ is computed from $u(t)$, $y(t)$, and the previously estimated reference $V_k(z)$. If the structure has not been structurally changed since the construction of the reference orthonormal functions, the parameter set of the reference model θ_r will asymptotically equal that of the new data set θ_n. Moreover, it can be shown that the following parameter estimation error ε satisfies a zero mean Gaussian distribution with a covariance matrix *Q*,

$$\varepsilon = \sqrt{N}\,(\theta_r - \theta_n) \ ,$$

where *N* is the data point number of the $u(t)/y(t)$ pair, the covariance matrix *Q* is estimated using the reference orthonormal functions, and θ_r and θ_n are the reference and new parameter sets, respectively. Finally, damage is monitored by performing a *t*-statistic test on the parameter error.

Pai and Jin (2000) present a Boundary Effect Detection (BED) method for locating small structural damages using Operational Deflection Shapes (ODSs) measured by a scanning laser vibrometer. The claimed advantage of the BED method is that it requires no model or historical data to locate damage. The method works by extracting boundary-layer solutions from experimental ODSs using a sliding-window, least-squares, curve-fitting method. In an undamaged system, the high-order ODSs have nonzero boundary-layer solutions only at structural boundaries. Damage in a structure causes nonzero boundary-layer solutions at damage locations. By detecting this, the damage in the structure can be pinpointed. The authors performed experiments on several structures and concluded that the BED method is sensitive and reliable for locating small damage.

Using impulse response, Sophia and Karolos (1997) solve an optimization problem to identify the locations and magnitudes of stiffness reduction within a two-dimensional frame structure model. The objective function is defined as the difference between the Markov parameter (impulse response) measured from the damaged structure and the one obtained from the numerical model of the baseline structure. It is assumed that a state-space representation of the dynamic system is identified from the measured frequency response functions or time series, and the Markov parameters are computed from the estimated state-space matrices. The analytical Markov parameter from the numerical model is represented as a function of the unknown stiffness perturbations, and a quadratic optimization with linear equality and inequality constraints is solved to find the values of the stiffness perturbations that minimize the prescribed objective function. The proposed damage detection method is applied to numerical data simulated from a 10-story, 2-bay steel frame structure model. The model consists of 50 frame elements and 90 DOFs. It is assumed that responses are measured from all DOFs and that the input to the model is known.

Valentin-Sivico et al. (1997) diagnose structural integrity by monitoring the stiffness and damping reduction obtained from the state-space representation of a system. First, a state-space representation is identified from dynamic measurements using an Eigensystem Realization Algorithm. Then, the state-space model is transformed into the physical coordinate system. Because the state-space representation of any dynamic system is not unique, a linear transformation is required so that the first half of the state variables corresponds to displacements

and the second half corresponds to velocities. Finally, the second order differential equations of the system or mass, stiffness, and damping matrices can be extracted from the transformed state-space model. The proposed method is verified on numerical examples. However, the authors caution that the proposed method requires inputs at all measured degrees-of-freedom to transfer the state variables into the meaningful physical coordinates.

Liu and Rao (2000) propose a technique to identify the system stiffness and mass matrices from the measured vibration signals. First, a minimum rank system realization technique is employed to obtain a minimum order state-space representation of the dynamic system based on the system input/output measurements. Second, a transformation matrix, which relates the state-space model of the system to the second order differential equations of motion, is computed. However, because there are infinite numbers of state space models for a given dynamic system, a unique transformation is found by using a canonical representation of the state-space models. Finally, the mass and stiffness matrices can be identified from the equations of motion and compared to the baseline mass and stiffness matrices from the healthy structure to identify damage.

Mehrabi et al. (1998) determine the causes of changes in the measurement state of a structure subject to static loading conditions using a technique called a precursor transformation method (PTM). Based on PTM, the measurement changes such as displacements, strains, and internal forces can be related to causes or precursors through a linear transformation matrix,

$$\Delta \mathbf{P} = \mathbf{C}\, \Delta \mathbf{T} \ ,$$

where $\Delta \mathbf{P}$ is a vector of changes in measured displacements, strains, or internal forces, $\Delta \mathbf{T}$ is a vector of virtual initial strains or temperatures causing the measurement changes, and $\mathbf{C}$ is a precursor transformation matrix relating the causal strains or temperatures to the changes in the measurements. The precursor matrix $\mathbf{C}$ can be estimated by performing finite element static analysis multiple times with unit temperature changes at each degree-of-freedom to generate each column of the $\mathbf{C}$ matrix. For the given $\Delta \mathbf{P}$ and $\mathbf{C}$, $\Delta \mathbf{T}$ is obtained by solving a linear optimization program. Furthermore, it can be shown that the pattern changes in response measurements caused by damage at a certain location is identical to the pattern changes in these measurements associated with a temperature change at the same location. In other words, the damage can be directly estimated from $\Delta \mathbf{T}$ in the above equation. It may be argued that the

measurement changes can be directly related to damage rather than temperature. This formulation, however, results in a precursor transformation matrix, which is a complicated nonlinear function of unknown extent and location of damage.

Gawronski and Sawicki (2000) use a damage-sensitive feature called *sensor norms* to determine damage locations for flexible structures. First, the H_2 norm of a system transfer function, $G(\omega)$, is defined as

$$\| G \|^2 = \frac{1}{2\pi} \int_{-\infty}^{+\infty} tr[G^*(\omega)\ G(\omega)]\ d\omega\ ,$$

where $\| G \|^2$ is the H_2 norm of the transfer function and $tr[\cdot]$ is a trace operation of a matrix. Next, the H_2 norm of the transfer function at the *j*th sensor location is defined as the root-mean-square sum over all modes,

$$\| GS_j \|^2 = \sum_{i=1}^{n} \| G_{ij} \|^2, \qquad j = 1,...,\ s\ ,$$

where $\| GS_j \|^2$ is the *j*th sensor norm and $\| G_{ij} \|^2$ is a component of $\| G \|^2$ corresponding to the *i*th mode response at the *j*th sensor location. Gawronski (1998) shows that $\| G_{ij} \|^2$ can be estimated from the system natural frequencies, modal damping ratios, and the modal displacements at the actuator and sensor locations. Finally, the *j*th sensor index for damage localization is defined as a weighted difference between the *i*th sensor norm of a healthy and a damaged structure, i.e.,

$$Sensor\ Index = | \| GS_j^h \|^2 - \| GS_j^d \|^2 | / \| GS_j^h \|^2\ ,$$

where the superscripts "*h*" and "*d*" are used to denote quantities associated with the healthy and damaged structures, respectively. The location of damage is identified by finding a sensor location, where the sensor index significantly increases.

5. STATISTICAL DISCRIMINATION OF FEATURES FOR DAMAGE DETECTION

The portion of the structural health monitoring process that has received the least attention in the technical literature is the development of statistical models to enhance the SHM process. Statistical model development is concerned with the implementation of the algorithms that operate on the extracted features to quantify the damage state of the structure. In this section, two classes of statistical model development are presented: supervised learning and unsupervised learning. The unsupervised learning can be applied to data not containing examples from the damaged structure, but this approach is inherently limited to level one or level two damage classification, which identifies the presence of damage only. When data are available from both the undamaged and damaged structure, the supervised learning approach can be taken to move forward to higher level damage identification to classify and quantify damage. Often, numerical simulations using an analytical model of a structure are used to augment the scarce test data associated with an undamaged structure.

5.1 Supervised Learning

5.1.1 Response Surface Analysis

Inada et al. (1999) employ response surface analysis for damage identification of carbon fiber reinforced plastics (CFRP) beams and plates. The response surface analysis is used to obtain the approximation relationship between natural frequencies and damage parameters such as damage location and size. For example, a response surface in cubic polynomials relates the damage size to the measured frequencies. The response surface analysis conducts the design of experiments to find the most suitable points for fitting the surface effectively and performs surface regression analysis by the least squares method. In this study, the response surface analysis is applied to simulation data generated from analytical models of CFRP beams and plates. Good agreements between the actual and predicted damage parameters are obtained. However, it should be noted that this response surface analysis requires training data sets from various damage conditions, which might not be obtained easily in real applications.

5.1.2 Fisher's Discriminant

To reduce the amount of data to be analyzed in a given structural health monitoring system, multidimensional feature vectors are often projected onto one-dimensional subspace using linear or quadratic projections. Fisher discrimination is an example of a linear projection and is particularly useful for separating two different distributions from each other. The Fisher discriminant is a linear transformation, which transforms the original multivariate distributions into univariate distributions whose means are as far apart as possible while the variances of those transformed distributions are as small as possible. This linear discrimination assumes that the two original distributions have the same variance. When this assumption does not hold, a more general quadratic procedure can be used. The quadratic procedure, however, is more computationally intensive. Sohn and Farrar (2000) successfully implement linear/quadratic discrimination procedures to the data measured from a concrete bridge column subjected to static/dynamic testing. The authors demonstrate that such a discrimination procedure, coupled with time series and statistical control chart procedures, can be useful in facilitating the damage diagnosis.

Garcia and Stubbs (1997) present several damage classification algorithms based on Bayes' Rule. The classification assigns a new set of features to the class with the highest conditional probability,

$$P(C_i \mid x) > P(C_j \mid x) \text{ for all } j \neq i \ ,$$

where $P(C_i \mid x)$ is the conditional probability of class C_i given a feature vector of x. For the damage classification problem presented, there are only two classes: C_1 = undamaged and C_2 = damaged. In practice, $P(x \mid C_i)$, the conditional probability of obtaining a particular set of features x given the assumption of class C_i, is easier to estimate than $P(C_i \mid x)$. Therefore, using the Bayes' rule, the previous equation can be rewritten as

$$P(x \mid C_i)\ p(C_i) \ > \ P(x \mid C_j)\ p(C_j) \text{ for all } j \neq i \ .$$

If $P(x|C_i)$ is assumed to have a multivariate normal distribution with mean vector m_i and covariance matrix Σ_i, a general quadratic discriminant function can be obtained,

$$\text{If } -\ln|\Sigma_i| - (x-m_i)^T\Sigma_i^{-1}(x-m_i) + 2\ln P(C_i) > -\ln|\Sigma_j| - (x-m_j)^T\Sigma_j^{-1}(x-m_j) + 2\ln P(C_j),$$
$$\text{assign } x \text{ to class } C_i,$$

where $P(C_i)$ is the prior probability of class C_i. From this general quadratic discriminant function, three different types of discriminant functions are evaluated. First, the general quadratic discriminant is simplified by assuming that $P(C_i) = P(C_j)$. Two additional linear discriminant functions are obtained by further assuming that (1) $\Sigma_i = \Sigma_j$ and (2) $\Sigma_i = \Sigma_j = I$. The performance of the three discriminant functions is compared by using a finite element model of a truss structure. For the simulation, the damage index, based on the modal frequencies and mode shapes, is used as the feature fed into the discriminant functions. Among the three discriminants, the simplest form of the linear discriminant outperformed the other two discriminant functions.

5.1.3 Neural Networks

Many damage detection schemes utilize neural networks to detect, localize, and quantify damage in structures. Rytter and Kirgegaard (1997) evaluate two neural networks for damage assessment, namely the multilayer perceptron (MLP) network with back propagation and the radial basis function (RBF) network. Both the MLP and RBF networks consist of one hidden layer in addition to the input and output layers. A finite element model of a four-story building is used for this work. Random damage states are generated through finite element simulations, and are essentially stiffness reductions in beams and columns. The associated relative changes in four lower natural frequencies and two lower mode shapes are used as inputs, and the relative bending stiffness of the beams and columns are used as outputs. Four thousand nine hundred sets of frequencies and mode shapes are randomly calculated for different damage conditions. The two-layer MLP network has 100 nodes in the hidden layer and uses the 4,900 data sets for training, whereas the RBF network utilizes 980 data sets for its training and consists of 980 nodes in the hidden layer. Both networks are validated with additional 700 data sets. It is concluded that the MLP network demonstrates the possibility of being used in connection with vibration-based

inspection, whereas the RBF network completely fails. However, the authors caution that the performance of the RBF network is highly dependent on an appropriate selection of damage cases used in the training.

Loh and Huang (1999) observe that a nonlinear neural network can be regarded as a general type of nonlinear auto-regressive moving-average (NARMA) model, which is a representation of a nonlinear discrete time series. Based on this observation, Loh and Huang model the seismic response of a half-scale five-story steel frame structure with three different networks. The structure is subjected to different levels of peak accelerations. These excitations range from 20% of the El Centro peak ground motion, to 20%, 40%, and 60% of the peak ground motion recorded in the Kobe earthquake. The second floor response of the steel frame structure is predicted using the responses of the first and third floors. The first model is a linear model where the current response of the second floor depends on the past responses at the first and third floors with a time lag of 4. In the second network, the time lag is increased from 4 to 8. The third network differs from the second one in that the current second floor acceleration nonlinearly depends on the first and third floors' accelerations. This nonlinear model is realized with two hidden layers and the hyperbolic tangent activation function. On the other hand, the two linear networks contain no hidden layers. The typical prediction errors are 10%, 8%, and 6% for the first, second, and the third network, respectively. Furthermore, the researchers discover that the nonlinear model is able to predict the structure's behavior during earthquakes if the network is trained using past earthquakes with equivalent peak amplitudes.

Faravelli and Pisano (1997) make use of a feed-forward neural network to detect and locate damage in a numerical simulation of a two-dimensional, nine-bay truss structure. For the generation of training data sets, all possible damage scenarios are simulated assuming that damage occurs in only one element at a time. Because of the symmetry of the structure, damage is considered in only 27 members of the structure instead of all 46 members. Furthermore, only a complete removal of a truss member is considered in this study. The proposed neural network consists of two subneural networks. The first network determines if any of the truss members is damaged and classifies the damaged element into one of the diagonal, vertical, or horizontal element groups. Depending on the classification of the damaged element, the next neural network corresponding to the appropriate element group is called upon to determine which of the

diagonal, vertical, or horizontal elements is actually damaged. Only the three lowest modes of the truss are considered to train the neural networks. All networks have the following characteristics: The two hidden layers of each of the networks contained 30 and 25 nodes, respectively. The networks are trained with a back-propagation algorithm, an adaptive learning rate, and momentum. Essentially, the learning rate is an important factor for the convergence rate of the network and for the convergence to a global minimum of the objective function. The maximum number of iterations used to train the network is 20,000. The performance of the network varies depending on which element group constrains the damage.

Chan et al. (1999) construct an autoassociative neural network to detect changes of cable tension on the Tsing Ma suspension bridge in Hong Kong. The Tsing Ma Bridge has a main span of 1,377 m and an overall length of 2,160 m, making it the world's longest suspension bridge. The authors note that the main cables of a suspension bridge are the most crucial components, and small variations in the cable tensions affect the internal force distributions in the deck and towers influencing bridge alignment. An autoassociative network is realized by a multilayer feed-forward network with a bottleneck layer in the middle. This network is called *autoassociative* because the patterns at the input layer are reproduced at the output later. The bottleneck layer allows one to filter redundant information while retaining the essential information in the output layer. In this study, the first twelve natural frequencies measured from the normal conditions of the bridge are used as the inputs and outputs of the network. Then, a novelty index is defined as the difference between the target outputs and the outputs estimated from the autoassociative network. When the bridge experiences abnormal structural conditions such as the reduction in cable tension, the novelty index is expected to significantly increase. In fact, the novelty index is able to detect the anomaly caused by a 5% reduction in the cable tension. The authors claim that the proposed combination of the autoassociative network and novelty analysis has the ability of discerning between changes caused by damage and natural variations of the system.

Liu, Sana, and Rao (1999) use an autoregressive with exogenous inputs (ARX) model of a cantilever aluminum beam to extract vibration signatures, and employ multilayer, feed-forward neural networks (MFFNN) to locate damage and estimate its size. Because only the first two mode dampings of the beam are accurately estimated, only these modes are excited by two

piezoelectric actuators. Another pair of piezoelectric patches are used as sensors. The Schroeder-phased signal is used as the excitation signal. Damage takes the form of holes 5 in. from the clamped end of the beam. The diameters of these holes are 7/64 in., 5/32 in., and 7/32 in., respectively. The proposed damage diagnosis consists of two MFFNNs. The first network takes the measured frequencies as inputs to locate damage. Then, the second network uses the frequencies and the estimated damage location as inputs to estimate the damage size. Both networks use the tan-sigmoid activation functions for all layers. The neural networks are trained using various damage cases generated by a numerical model of the beam, which is first refined using the measured dynamic characteristics of the actual beam. The authors report that damage location is estimated well, while the damage extents for the two largest damage cases differ from the actual damage extents by approximately 100% and 40%, respectively.

Liu and Sun (1997) use neural networks to identify damage in a simply supported three-span bridge. The neural networks are trained using simulated data from a finite element model of the bridge. The bridge model is discretized into 30 uniform beam elements. Damage is simulated by reducing element stiffness and is located at the middle as well as the sides of the spans. The features used in this study are the maxima and minima of the bridge elongation curves produced by a moving truck traversing the bridge. The authors assume that these elongation curves could presumably be calculated from strain gauge measurements. Five separate neural networks are used to monitor local dynamic characteristics along the total span of the bridge. Nine local elongation curves, calculated at different locations along the bridge, are used as inputs to the five networks. The network outputs are estimated stiffness reductions in terms of percentage. The authors find that damage influences the extreme values of the elongation curves in different ways, depending on the damage location in relation to the elongation curve. However, the authors conclude that these local bridge elongations from a moving truck are effective features for damage detection. Furthermore, a parallel neural network structure like that used in this study can reduce the training time of the network while providing accurate damage assessment and localization capabilities because of the local nature of the multineural network-based SHM system.

Hermann and Streng (1997) introduce problem-specific neural networks for structural damage detection in plate truss structures. Especially, this study evaluates different learning rates, network types, reduction techniques of network topologies, and dimension analysis. First, by applying dimensional analysis, the dimensions of the input and output layers of the network are reduced. Second, the topology of the network is reduced by a pruning algorithm called the Optimal Brain Surgeon. Essentially, this pruning algorithm uses the second derivative of an error function to determine the weight, which leads to the smallest increase of the error function when eliminated. This weight is then eliminated, and the topology complexity is decreased. To demonstrate the effectiveness of their method, the neural network analysis is applied to a two-dimensional, six-bar truss structure subjected to both horizontal and vertical loads. The structural behavior is characterized by horizontal and vertical displacements at three nodal points. The input patterns consist of these six nodal displacements, whereas the percentage stiffness reductions of each element are used as output patterns. An additional two hidden layers are composed of 12 nodes each. The training sets were constructed with the help of finite element simulations. Training of the network for 100,000 epochs reduced the sum squared error from 554.71 to 0.00465 with an average test error of 8.7%. The authors caution that, for the success of the neural network analysis, the training patterns should include a sufficient number of characteristics that distinguish between undamaged and damaged states of the structure.

Using three-layer feed-forward neural networks, Hanagud and Luo (1997) present a composite plate SHM methodology that is based on measured structural dynamic response. Two types of damage, delamination, and stiffness loss caused by impact and transverse cracks, are considered. Analytical models are constructed to predict the dynamic response of the damaged structure. A neural network for delamination uses frequency response functions (FRFs) as inputs and delamination information of the plate as outputs. The network consists of 128 input nodes, 30 hidden nodes, and 18 output nodes. The network is trained using 10 damage cases introduced by using very thin Teflon films between layers during the lay-up process. Delamination is centered in the test specimen, and delamination lengths range from 0 to 18 cm. The second neural network for stiffness deterioration again uses the FRFs as inputs, and the outputs are ratios of the stiffness of the damaged structure to the stiffness of the undamaged structure. The network consists of 128 input nodes, 30 hidden nodes, and 5 output nodes. This network is trained using

16 damage cases. The authors state that the delamination and the stiffness loss are successfully identified.

Employing the previous composite plate used by Hanagud and Luo (1997), the same authors (Luo and Hanagud 1997) propose dynamic learning rate training for neural networks that provides faster convergence than the conventional steepest descent method. The learning rate is adjusted by simply setting the learning rate to certain prespecified values if the error rate falls into certain intervals. Here, an error rate is defined as the ratio of the difference in error functions at two consequent time points. Luo and Hanagud note that, although the fast learning rate is desirable for faster convergence, a fast learning rate with traditional steepest descent methods can result in overshooting near the region of the optimal points. The authors claim that their dynamic learning rate overcomes this difficulty.

Jenq and Lee (1997) utilize a back-propagation neural network with an adaptive learning rate to predict hole defect sizes and locations in glass fiber reinforced plastic (GFRP) composite laminated beams. The initial finite element model is calibrated using the measurement data to ensure the accuracy of the numerical model. Then, five hundred sets of simulations are performed to generate training data sets with various sizes of holes at different locations. The sizes of the holes range from 9 mm to 14 mm, and the location varies from 3 mm to 17 mm from the clamped end. The frequency shifts of the first four modes are used as inputs of the network, and two output nodes correspond to the hole size and location. There is one hidden layer consisting of 15 nodes. After one hundred thousand learning epochs, the sum of squares error is reduced from 10^5 to 10. The averaged errors for predicting the hole diameter and location are 7% and 6%, respectively.

Nakamura et al. (1998) train a neural network to detect damage in a seven-story steel moment-resisting frame building that has a floor plan of 11 m by 13 m and a total height of 23 m. This building was actually damaged during the Kobe earthquake of 1995. The measurements are conducted before and after repairs to the damaged frame are made. Most damage manifests itself as beam-column connection fracture. Data after repair are used to represent the undamaged structure and are used to train the network. Velocity transducers are located at each story, and each story has its own network. Each individual network has as inputs the interstory

displacement and interstory velocity. The output is the interstory restoring force. Two hidden layers, one with 15 nodes and the other with 10 nodes, are used. The network is trained using the random search method, which avoids being trapped in local minima. After training, the root mean square (RMS) prediction errors associated with the undamaged stories remain relatively small. On the other hand, the RMS errors associated with the actually damaged third and fourth stories become fairly large after the earthquake. The authors then calculate the story stiffnesses by means of a least squares approach applied to the phase plane plots of the restoring forces. The stiffnesses of the damaged stories decrease by more than 20%, while those of the undamaged stories decrease by less than 7%. Although the method locates the story where damage occurs, the actual damaged connection of the story is not identified with the method.

Masri et al. (2000) present a nonlinear system identification technique based on neural network approaches for the health monitoring of an unidentified mechanical system, which displays significant nonlinear behavior typically encountered in applied mechanics. First, the network is trained using the vibration measurement from a baseline condition of the system. The four response accelerations and the input excitation are measured from the mechanical system, and the accelerations are numerically integrated to yield velocity and displacement records. Subsequently, the trained network is fed with new vibration signals from the same structure but from damaged conditions. Two damaged cases are obtained by altering the physical parameters of the baseline system. Two different neural networks are investigated in this study. The first network approximates the four system accelerations as a function of the input force excitation, four displacements, and four velocities. The second network maps the displacements, velocities, and accelerations to the system force excitation. The prediction error serves as a damage-sensitive indicator in the underlying structure. If the mechanical system is structurally altered from its baseline condition, the trained network with the baseline data sets will no longer be a good approximation of the system, resulting in larger prediction errors. Based on this premise, the first network produces the output errors increased by about 18% and 44% for the two damage cases investigated. The second network produces a similar result although a smaller dispersion in the prediction errors is observed. Although the authors advocate the efficiency of nonparametric identification approaches such as the proposed neural networks, they also point out the limitations of the nonparametric approaches in locating damage unless *a priori* knowledge is available on damage states and their respective vibration signatures.

Barai and Pandey (1997) adopt two types of neural networks for damage detection of a simulated railway bridge. Vibration signals from the bottom chord notes of the truss bridge model are used as inputs for the neural networks. The first network is a conventional multilayer perceptron (MLP) neural network, and time delay of the dynamic response is introduced in the second time-delay neural network. The vibration signals are simulated by traveling a moving load on the truss bridge at a constant speed. The performance of the two trained neural networks is examined for both complete and incomplete measurements available during the testing phase. Damage is simply introduced by reducing stiffness in one element at a time. The performance of the time-delay neural network is found to be generally better than that of the conventional MLP neural network.

Feng and Bahng (1999) propose a new method for the monitoring of jacketed columns that employs the combination of vibration testing, neural network, and finite element techniques. The authors constructed a small-scale bridge model based on an old design standard, and the columns of the bridge model were retrofitted with carbon fiber composite. A finite element model was constructed to predict baseline vibration characteristics of the bridge, and the predicted responses were compared with the vibration test data taken from the scale model. Damage was then introduced in the bridge model, and vibration tests were repeated for several damage cases. The data taken from the finite element model and the damaged bridge were used to train the neural network using a standard back-propagation algorithm. For the network, the input pattern consisted of the mode frequencies and mode shapes of the columns determined from finite element analysis. The output pattern consists of correction coefficients of element stiffness for the columns. In this way, the trained network is then used to determine the stiffness degradation of the bridge.

Choi and Kwon (2000) developed a damage detection method for a steel truss bridge based on neural network analysis. A finite element (FE) model was constructed and refined based on static and dynamic tests of the real bridge. The static analysis of the FE model identified eight truss members subjected to high stress level, and stiffness in each of these members was reduced to simulate eight different damage cases. Two separate neural networks were developed for damage localization. The first network determined whether the damage was located either to the left or to the right of the bridge's midpoint. The strain readings from seven truss members were generated

from the numerical model and used as inputs to the first network. The output was a binary number corresponding to the left or the right side of the bridge. The value of the binary output tells which half of the bridge is assumed damaged. The inputs to the second neural network were the binary output from the first network, and modal parameters, mode shapes, and natural frequencies were generated from the FE model. There were eight outputs from the second network, and each output indicates the existence of damage at the associated truss member. Damage diagnosis using the neural network system was performed successfully, but the performance of the second network was sensitive to the number of nodes chosen for network construction.

Maseras-Gutierrez et al. (1998) discuss the use of piezoceramic sensors and neural networks to detect impact in composite materials. The authors used two separate neural networks to predict impact location and impact energy for a circularly clamped composite test specimen. The 340 × 340 × 2.5 mm test specimen was a laminate consisting of a carbon fiber fabric and a toughened epoxy resin. The specimen was fit with four piezoceramic sensors for out of plane strain measurement. An instrumented dropweight impact rig was used to perform several impact tests on the specimen that had hydraulically clamped rings of 300 mm internal diameter. A series of four different sets of tests were performed. First, the specimen was impacted at one hundred equally spaced points in order to train the neural networks. Next, the specimen was impacted at thirty random locations to validate the trained neural network. For these first two sets, the impact energy was 0.3 J, which was far below the damage threshold. For the third set, the specimen was impacted once with an energy of 10 J, which produced damage within the specimen. Finally, the second set of random impacts at 0.3 J was repeated. The final two sets of the test were performed to investigate how the performance of the neural networks was affected by damage in the specimen. The standard multilayer perceptron neural networks were used, and the networks were trained with a back propagation learning rule. A trial and error approach was implemented to determine the optimum dimensions for each network. To improve the generalization capacity of the networks, the training data vectors were expanded by copying them and corrupting the copies with different Gaussian noise vectors. The results from the networks showed that the impact location and magnitude could be predicted with acceptable error. Also, the tests showed that damage within the composite structure did not significantly degrade the prediction performance of the networks.

Chang et al. (2000) use an iterative neural network for structural health monitoring. The network is first updated using initial training data sets consisting of assumed structural parameters as target outputs and their corresponding dynamic characteristics as inputs. Then, the structural parameters predicted from the trained neural network are used in finite element analysis to reproduce the measured dynamic characteristics. The network model would go through the second training phase if the simulated dynamic characteristics significantly deviate from the measured ones. After the completion of training, the structural parameters identified from the measured vibration signals are used to infer the location and extent of damage. A large set of training data are generated by simulating various damage cases in a finite element model of the structure, and an orthogonal array is used to generate the representative space of the training data, which can significantly reduce the size of the training data set. Furthermore, a modified back-propagation neural network is devised to overcome possible saturation of the sigmoid function and speed up the training. This iterative neural network approach is verified from numerical and experimental studies of a clamped-clamped T beam. In these examples, three natural frequencies and first mode shape curvature of the beam are used as inputs, and a set of structural parameters, which represent various damage cases, are used as outputs.

Haywood et al. (2001) examined various features extracted from dynamic strain signals to identify impact location and amplitude on a composite plate. Impact tests on a 608 × 304 × 3 mm graphite fiber reinforced epoxy resin composite were conducted. A total of 12 piezoelectric transducers were embedded in the panel. Neural networks were trained using various features as inputs, and the target outputs were the impact coordinates. The examined features include time and frequency domain features. When the peak response of each signal and the position of the peak in time were used as inputs, the average error of the two impact coordinates were 1.2% of the plate area. Because the exact peak response and the time point of the peak response are often difficult to measure, the time envelopes of the signals are estimated using a Hilbert transform. When the peak response and the associated time point were estimated from the envelopes of the signals, the average prediction error decreased to 0.56%. The next network was constructed using the integrals of the real and imaginary parts of the Fourier transform as input features. When this network was tested, the average error of the two impact coordinates corresponded to 1.97% of the panel area. The increased error in the frequency domain analysis was attributed to the time information of the signals lost in the Fourier transform.

5.1.4 Genetic Algorithms

Ruotolo and Surace (1997a and c) formulate an inverse problem that decides the position and depth of cracks in beams using measured modal parameters. Then, this optimization problem is solved by employing a genetic algorithm. The cost function to be optimized is represented as a function of the measured modal frequencies and the associated frequencies computed from a finite element model. Note that the mode shapes are not included in this cost function because the authors conclude that the mode shapes are not sufficiently accurate to be considered in this particular problem. The performance of the genetic algorithm is compared to that of the simulated annealing scheme. Although the crack locations and depths in the cantilever beam are successfully identified, some practical issues still exist. The simulated annealing procedure converges to an accurate global minimum solution faster than the genetic algorithm, but both methods require around 10,000 evaluations of the cost function. As the structure to be monitored becomes more complicated, like whole buildings, the proposed optimization becomes prohibitive. In addition, the solution of the optimization may not be unique. For example, the model cannot distinguish whether a crack is located on the top or bottom portion of the beam. A similar study is done in Ruotolo and Surace (1998) where genetic algorithms, simulated annealing, and eigensensitivity analyses are compared for detecting 4 damage scenarios in a finite element model of a four-story steel frame structure. Simulated annealing detects all damage cases with the fewest runs. In fact, by using the twelve natural frequencies of the four-story building, some damages are correctly diagnosed.

Mares et al. (1999b) construct a cost function as a function of the difference between measured and analytical transmissibilities and minimize the cost function through a genetic algorithm. The transmissibility function, T_{ij}, between the *i*th and *j*th degree of freedom is defined as

$$T_{i,j} = E[\, Y_i Y_j^* \,/\, Y_j Y_j^* \,] \ ,$$

where Y_i is the frequency response function of the *i*th response point, * denotes complex conjugation, and E is the expectation operator. The authors numerically simulate the dynamic behavior of a four-story building with three degrees of freedom (DOFs) on each floor: one in-plane rotation and two orthogonal lateral displacements. They refer to these simulations as

measured data. To improve the performance of the optimization, a small fraction of transmissibility functions are selected from all possible combinations of the transmissibility functions. Those transmissibility functions showing the greatest difference between undamaged and damaged states are chosen as the most sensitive to damage and are used in the formulation of the following cost function, $G(\mathbf{D})$,

$$G(\mathbf{D}) = 1 - \sum_{i,j \in A} \sum_{k=1}^{n} \left| \ln \left\| \frac{T_{ij}^{c}(\omega_k)}{T_{ij}^{m}(\omega_k)} \right\| \right| ,$$

where n refers to the number of frequency lines analyzed, $\mathbf{D}$ is the state-of-damage vector, which is organized so that, for each floor, it contains the reduction in stiffness of the columns and braces, and $T_{ij}(\omega_k)$ corresponds to one of the selected transmissibilities. The superscripts m and c denote measured and calculated quantities, respectively. The first summation in the above equation is performed only for the selected transmissibility functions. The authors use a two-step optimization procedure to obtain the global minimum of this cost function. First, a genetic search is performed on the cost function so that the downhill of the global minimum is determined quickly. Then, a classical gradient-based algorithm is run to refine the solution. By performing this two-step optimization, the accuracy of the solution is improved, and global minima are successfully identified, thus avoiding local minima. Various damage scenarios are simulated by reducing the stiffness of columns and/or braces in the building model. It is concluded that damage in braces is more easily identified that damage in columns.

Krawczuk et al. (2000) apply a genetic algorithm to identify and locate damage in a laminated composite beam. The researchers define damage as delamination and demonstrate the validity of their method with a numerical model. The researchers use an objective function, θ, which is based on changes in natural frequencies and the Damage Location Assurance Criterion (DLAC) defined as

$$\theta(s) = \frac{|\, \boldsymbol{\delta\omega}_m^T \; \boldsymbol{\delta\omega}_s \,|^2}{(\boldsymbol{\delta\omega}_m^T \; \boldsymbol{\delta\omega}_m)\; (\boldsymbol{\delta\omega}_s^T \; \boldsymbol{\delta\omega}_s)} ,$$

where $\boldsymbol{\delta\omega}_m$ is a vector of frequency changes obtained from either simulation or experiment, and $\boldsymbol{\delta\omega}_s$ is the theoretical frequency change vector obtained from an analytical model with assumed damage at location s. A zero value for θ indicates that there is no correlation between the test and analytical model, and the unit value indicates an exact match between the patterns of frequency changes. The position and size of the damage is estimated by maximizing this objective function. Two cases of delamination are investigated. The first case is a delamination equal to 35% of the total beam length, and the second case is equal to 15% of the total length of the beam. Only the first 4 natural frequencies are considered in the objective function. The genetic algorithm approach correctly determines damage for both cases. These results are compared with those from a neural network in which the first 4 natural frequencies are used as inputs, and the onset location of delamination, delamination end location, and the number of the delaminated layers are used as outputs. While the genetic algorithm produces promising results and requires fewer calculations than traditional search techniques, the neural network approach is not as promising because of the very small size of the training population representing delamination layer numbers.

5.1.5 Support Vector Machines

The Support Vector Machine (SVM) (Vapnik 1998) is a comparatively recent development for learning input/output relationships in data, which can be a powerful tool for general classification and regression problems. When neural networks are applied to classification and regression problems, overfitting often becomes a critical issue. Overfitting occurs when the network reproduces the input/output relationship for the training data but fails to generalize for other testing data sets. To avoid overfitting or to improve generalization, the complexity of the neural network models is generally controlled by introducing a regularization term. In SVM, the generalization is better improved by carefully controlling the complexity of the SVM model using a parameter called Vapnik-Chervonenkis (VC) dimension. Furthermore, SVM is a unified classifier in the sense that many different types of discriminant functions such as linear, nonlinear, neural network, and radial-basis discriminant functions can be put in the framework of SVM with no real modifications.

Worden and Lane (2001) apply the Support Vector Machine (SVM) to damage classification problems. The first is a fault classification for ball bearings, and the second is a damage localization problem within a truss structure. In the ball bearing experiment, the objective is to classify the current condition of the bearing into one of five states based on acceleration records. The classification performance of SVM is compared to those of other conventional pattern classification techniques such as neural network, k-nearest neighbor approaches, and kernel discriminant analysis. The kernel discriminant analysis outperformed all the other methods. In this example, the SVM turned out to be a restricted version of a radial-basis function neural network. For the two-dimensional cantilever truss example with 20 truss elements, novelty analysis was conducted for each element using the displacement transmissibility across the member. Then, a vector of the novelty indices from all 20 members is used as input for SVM, while the target outputs were 20 classes, each of which indicates damage in a specific member. Again, the performances of SVM and a multilayer perceptron network were compared, and they produce a comparable performance.

5.2 Unsupervised Learning

5.2.1 Control Chart Analysis

Control chart analysis has been commonly used for process controls of chemical plants, manufacturing facilities, and nuclear power plants. This control chart analysis continuously monitors the measured quantities or features extracted from the measurements for anomalies. First, the upper and lower control limits for observations are established based on the distribution of the observations, which are obtained from a normal condition of the system. Often the normality of the distribution is assumed. Then, new observations from an unknown condition of the system are monitored against these control limits. When the new observations fluctuate outside the control limits, the monitoring system alarms the abnormality of the system's condition. Sohn and Farrar (2000) apply this control chart analysis to the monitoring of a reinforced concrete bridge column. Acceleration time series are recorded from the vibration tests of the bridge column and Auto-Regressive (AR) prediction models are fit to the time series.

Then, control charts are constructed using the AR coefficients of the AR model as the observation quantities. The upper and lower control limits are set to correspond to the 99% confidence intervals of a normal distribution. The mean and the standard deviation of the normal distribution are derived from the AR coefficients of the normal operational condition. After gradual yielding of the concrete rebars is introduced in the column, new sets of AR coefficients are computed from various levels of damage. These new AR coefficients are plotted on the control charts whose limits are set from the initial undamaged state of the system. If a significant number of the coefficients (at least more than 1% of the coefficients) fall out of the limits, either a state of damage or a significant change in environmental conditions is reached. Because the authors use a third order AR model, there are three control charts for each damage level of the column. The authors determine that the third AR coefficient is most sensitive to damage in this particular experiment.

5.2.2 Outlier Detection

Ruotolo and Surace (1997b) use changes in the rank of a matrix as a means of outlier detection. First, a matrix is formed where each column is the feature vector measured during various environmental and operational conditions of a structure. Singular value decomposition is used to estimate the rank of this matrix. Next, this matrix is augmented by adding an additional column containing a new feature vector from a potential damage state of the structure. If the new feature vector corresponds to a damaged structure, this new vector will be independent from the previously measured vectors, and the rank of the matrix will increase. If the new feature vector is from the undamaged structure, it can be represented as a linear combination of the feature vectors measured during the previous environmental and operational conditions, and the rank will not change. The authors also discuss a method to eliminate the influence of measurement noise on the rank estimates by including several estimates of the feature vector corresponding to each environmental or operational condition. It will be necessary to establish a threshold to distinguish singular values associated with noise from those that correspond to the state of the structure.

Worden et al. (1999) present another study of outlier analysis. The researchers test a 750 × 300 × 3 mm aluminum plate stiffened with two C-channel ribs riveted to the short edges and two 1 in. × 1 in. angle stringers bolted to the long edges of the plate. Damage is introduced as saw cuts in the outside stringer 125 mm from the edge of the panel, and all tests are carried out on the assembly with free-free boundary conditions. Nine levels of damage are investigated, and the depth of the cut ranges from 10% to 90% of the plate thickness. The system is excited with an electrodynamic shaker driven by broadband white noise. The transmissibility frequency response functions (FRFs) between two measurement points are computed at two different paths, and 128 averages of these transmissibilities are taken over each path. The first path is along the line of the damaged stringer, while the other one is parallel to the first one and offset by 100 mm. The following Mahalanobis distance, D, is used as a damage-sensitive feature for novelty analysis,

$$D = (\mathbf{x} - \overline{\mathbf{x}})^T \mathbf{S}^{-1} (\mathbf{x} - \overline{\mathbf{x}}) \ ,$$

where $\mathbf{x}$ is a vector of the current transmissibility FRF under investigation, and $\overline{\mathbf{x}}$ and $\mathbf{S}$ are the mean vector and the sample covariance matrix of the transmissibilities, respectively. When this Mahalanobis index, which is a normalized distance of the new transmissibility FRF from the normal population of the undamaged transmissibilities, becomes larger than a prespecified threshold value, the novelty classifier signals an abnormal condition of the system. Until the cut in the stringer is 30% deep, the outlier analysis applied to the transmissibility directly over the saw cut is unable to detect it. For the other path not directly over the saw cut, the damage is detected when the cut is around 20%. The outlier analysis is demonstrated to be successful in identifying damage to a certain extent, but not overly sensitive to the actual transmissibility path used in the experiment.

A similar study can be found in Worden and Fieller (1999). In this study, a three degree-of-freedom spring-mass-damper system is simulated, and the transmissibility function between masses 1 and 2 is used as a feature considering both amplitude and phase. Harmonic excitation between 0 Hz and 50 Hz is provided. Damage is introduced as a stiffness decrease of 1%, 10%, and 50% of the spring constant value between masses 1 and 2. Four thousand testing data sets are used in this simulation, and Gaussian white noise is added to the simulated data. The method is

unable to classify any of the 1% stiffness reduction cases, whereas the 10% and 50% reductions are correctly classified.

Worden et al. (2000) present three different novelty indices to detect damage in composite plates using Lamb waves. The first one is outlier analysis based on the Mahalanobis distance previously described in Worden et al. (1999). The second one uses an autoassociative neural network. The autoassociative network is trained so that this network can reproduce the input at the output layer. Then, the novelty index corresponding to a new pattern is defined as the Euclidean distance between the target output (or input) and the output from the trained network. The last approach first estimates the probability density function (PDF) of the features over the normal condition set using a kernel density estimation technique (Silverman 1986). Then, once a new feature is obtained, the new feature is classified as either damaged or undamaged by comparing the new feature against the PDF of the normal condition. The methods are demonstrated on experimental data captured from two composite plates. All three methods agreed very well with each other in terms of the experimental results. The author further provided the relative merits and demerits of each approach: The first Mahalanobis distance is the fastest approach, but this method implicitly assumes the Gaussian normality of data. Therefore, if the data significantly depart from normality, this method will eventually break down. The second neural network based approach is the most time consuming to train, but this method has an advantage over the first one in that it imposes no assumption about the distribution type of data. The kernel density based approach is intermediate between the other two methods in terms of training time, and the interpretation of the results is very straightforward. However, this method suffers most if the training set is sparse.

Mevel et al. (2000) use a stochastic subspace approach to determine if damage is present in a structure being monitored. Details of the stochastic subspace approach can be found in Basseville et al. (2000). Recall that the stochastic subspace method first constructs a weighted Hankel matrix consisting of the covariance matrices between measured responses with different time lags. Then, by performing a singular value decomposition (SVD) of the weighted Hankel matrix, the Hankel matrix is factorized into an observability matrix and a controllability matrix. Note that the modal parameters of the system can be extracted from the observability matrix. Next, a basis matrix orthogonal to the output space of the observability matrix is defined. If newly

collected data correspond to the normal condition, the basis matrix should also be orthogonal to the newly computed weighted Hankel matrix,

$$\mathbf{S}_0^T (\mathbf{W}_1 \mathbf{H}_1 \mathbf{W}_2^T) = \mathbf{0} \ ,$$

where $\mathbf{S}_0$ is the basis matrix orthogonal to the observability matrix and computed from the normal condition of the system, $\mathbf{H}_1$ is the Hankel matrix corresponding to the new condition of the system, and $\mathbf{W}_1$ and $\mathbf{W}_2$ are the user defined weighting matrices. In practice, the above equation does not exactly hold and produces a residual vector in the right hand side of the equation. Finally, a two class hypothesis testing using this residual vector as a feature is performed to infer the presence of damage. Essentially, when the residual becomes larger than some threshold value, the null hypothesis, which assumes that there is no damage in the structure, is rejected, thus implying the abnormal state of the system. The authors validate their technique on data from the Z24 Bridge in Switzerland. Ambient response data are measured before and after a damage pattern is introduced in the Z24 Bridge. Two damage cases are considered: either a 20 mm or a 80 mm settlement of a pier. The proposed statistical test successfully indicates the damage in both cases. The authors chart the test statistics from day to day and show that the fluctuations in the test statistics are caused by environmental variables. The authors report that the test statistics variation caused by damage is larger than the fluctuation caused by environmental changes for the Z24 Bridge. However, the authors caution that the environmental variations can be higher than the changes caused by damage in other applications.

Biemans et al. (1999) use wavelet coefficients extracted from sensors on a plate as damage-sensitive features to monitor the crack growth. A rectangular aluminum plate is instrumented with five piezoceramic devices. One of the piezoceramic sensors is used as an actuator. A crack is initiated by spark erosion, and the plate is subjected to static and dynamic tensile loading. The growth of the crack is monitored by the remaining four sensors. The authors calculate a mean vector of the logarithmic variance of the wavelet coefficients and use this vector as a baseline against which the same measure applied to damaged plates can be compared. The Euclidean distance between the mean vectors of the cracked and uncracked plates is used as a damage index. Values of the damage index from measurements on the undamaged plate are used to establish an alarm level above which damage could be considered present. The growths of a

14-mm and a 6-mm crack are well detected, and the damage index and the crack length have almost a linear trend.

Manson et al. (2000) demonstrate the importance of obtaining a valid set of normal condition data from a healthy structure for use in outlier detection. As the authors point out, using an invalid normal condition data set could lead to a healthy structure being labeled damaged, or, a potentially more serious problem, a damaged structure being passed off as healthy. To demonstrate this procedure, experiments were performed with a benchmark monitoring system that uses Lamb-wave inspection to diagnose damage in a composite plate. The two experiments collected data over eighteen hours and eleven days, respectively. Because of the large time durations, temperature significantly affected the response of the plate being monitored. By choosing the normal condition data from different times during testing, the number of outlier data points changed dramatically. The authors plan to perform a more rigorous testing program in order to quantify the effect of important parameters on the normal condition data.

5.2.3 Neural Networks

Chang, Chang, and Xu (1999) propose a model updating and damage detection method based on an adaptive neural network. First, the neural network is trained using simulation data obtained from a finite element model of a structure. The modal parameters computed from the finite element model are used as inputs, and the neural network output consists of structural parameters. Second, when measured modal parameters from the actual structure become available, the neural network is used to calculate the associated structural parameters. Then, the finite element model is updated using these new structural parameters, and the associated modal parameters are computed from the model. If the measured modal parameters are significantly different from those calculated from the finite element model, the network goes through another training until the difference between the measured and calculated quantities becomes acceptable. Finally, the updated structural parameters are used to refine the finite element model or to infer the location and the degree of structural damage. The proposed neural network is applied to the model updating of a suspension bridge model. The finite element model of the bridge consists of 222 nodes, 208 beam elements, 39 rigid elements, and 1,211 degrees of freedom. From this

model, the first eight natural frequencies are calculated in the range of 1.99 Hz to 11.41 Hz. A training set consisting of 33 samples is used in the initial training. The concept of orthogonal array is adopted to reduce the number of training samples required. It is observed that the updating of the weight matrix can stagnate during training. To overcome this problem, an improved back-propagation algorithm with a jump factor and a dynamical learning rate is developed to facilitate the training. The improved back-propagation method demonstrated the fastest and smoothest convergence when compared with the back-propagation method and the dynamic learning rate steepest descent method. In fact, the maximum prediction error of the frequencies is reduced from 17% to 7% within five iterations. However, the authors suggest that further error reduction is not physically meaningful because the parameters determined through the sensitivity analysis are not the only parameters affecting the results.

Sanders et al. (1997) discuss the subject of detecting delamination within composites. In their work, the authors used fiber-optic sensors to measure the first five modal frequencies of several glass/epoxy composite beams. Delamination was introduced into some of the plates by inserting varying widths of Teflon strips into the composite layup. Modal frequencies were also calculated using a classical one-dimensional beam theory approach as well as a finite element model of the beam. Good agreement between the experimental and analytical results was found. The authors developed a feed-forward back-propagation neural network to predict the size and location of delamination within the plates. The input layer of the network consists of five processing units that receive the five modal frequencies of the beam. The network contains three hidden layers that feed into an output layer that contains two processing elements that represent the size and location of the delamination. The network was trained using the classical beam theory approximation that computed modal frequencies for numerous delamination sizes and locations. The experimental modal frequencies were then fed into the trained network that subsequently predicted the size and location of the delamination with good accuracy.

5.2.4 Hypothesis Testing

Todd and Nichols (2002) analyze certain properties of chaotic responses of a structure to look for subtle changes caused by damage. First, a structure is excited using a low-dimensional deterministic chaotic input. Then, attractors are reconstructed from the measured input and

output time series by means of the embedding theorem. Here, the attracter is defined as an invariant subspace of the full state space, and the stability and dimension of the attracter are exploited as indicators of damage. Specifically, the ratio of output attractor variance to input attractor variance is used as a damage-sensitive feature. This attractor variance ratio increases as damage progresses. Then, a single-factor analysis-of-variance (ANOVA) with Bonferroni confidence interval generation (Lapin 1990) was performed on the extracted features. The null hypothesis conjectures that there is no difference between the means of the attractor variance ratios before and after damage occurrence. Assuming that the attractor variance ratio has an F-test distribution, the null hypothesis is rejected when the ratio exceeds a threshold F-test statistic obtained from a specified confidence level. The proposed technique is applied to a beam controlled in a laboratory environment, and damage is introduced by a special elastic clamp at the boundary.

5.3 Other Probability Analyses

Halfpenny (1999) notes that the estimation of fatigue life based on the power spectral density (PSD) of loading was first advanced by Bendat in 1964. Bendat showed that the probability density function (PDF) of loading peaks for a narrow band loading signal converges to a Rayleigh distribution as the bandwidth is reduced. Under the assumption of narrow band signals, Bendat estimated the expected number of loading peaks using moments of areas under the probability density function of loading peaks. This estimation method proved conservative because of its assumption of narrow band signals. Especially for offshore applications, wave and wind excitations could not be assumed to be narrow band. Halfpenny discusses an alternative fatigue life estimation approach that is a function of only four moments of areas of the probability density function and avoids any assumptions on the loading signal bandwidth.

Vanik and Beck (1997) present a global model-based SHM method, which utilizes Bayesian probabilistic inference to determine the existence and location of structural damage in the presence of uncertainties. The stiffness matrix of the structure's finite element model is parameterized so that the elements of the structural model are grouped into substructures. That is, the system stiffness matrix is represented as a linear combination of substructure stiffness matrices. The scaling factor of each substructure ranges from zero to one to simulate damage,

and the collection of these scaling factors is defined as the model parameters. Then, Bayes' theorem is invoked to compute the conditions probability of the model parameters given test data such as frequencies and incomplete mode shapes measured from a structure. From this conditional PDF, a probabilistic damage measure is developed. This damage measure essentially gives the probability that the current scaling factor of a substructure is less than the initial value of the undamaged substructure's scaling factor. This probabilistic damage measure is computed for each substructure. The probabilistic approach is tested on simulations of 2 and 10 degrees-of-freedom shear structures, in which damage takes the form of reduced interstory stiffnesses, and modal noise is taken from a zero-mean Gaussian distribution. Results indicate that there is a danger of false-positive damage indication and that damage could be detected in only a few cases.

In 2000, Vanik and Beck revisited their proposed Bayesian model that identifies damage indicators from sets of modal parameter data. Their goal is to develop damaged and undamaged notification in a real-time monitoring environment. These data sets are also used to discriminate between undamaged states, variations and changes to the undamaged states, and a damaged situation, a term they referred to as the probability of alarm in conjunction with threshold values. The authors illustrate their method with a 10 DOF shear building model that includes story masses and interstory stiffness. Using modal data simulated from a numerical model, they test their algorithms with a 20% stiffness loss in the fifth story. Results are favorable only when the damage indicators are based on the current data set. Any addition of the prior training seems to create an unreal bias towards undamaged states.

Using similar Bayesian inference, Katafygiotis and Lam (1997) build and test a two-story structure made of aluminum bars and plates. They introduce damage by removing column bars in such a way as to avoid torsional motion. The bar removal corresponds to a 25% stiffness reduction. Two stiffness parameters and two damping ratios are used as model parameters. Finite element simulations are used to calculate the model parameters, which are then used to update the analytical model of the structure. The authors also test the case of incomplete data by using measurements taken only from the second story. Their results for this case indicate probable damage at two locations when damage is introduced only at one location.

Katafygiotis, Mickleborough, and Yuen (1999) address the problem of modal parameter identification using measured ambient time histories. The authors follow a Bayesian probabilistic approach similar to Vanik and Beck (1997), and Katafygiotis and Lam (1997), to obtain not only the optimal values of the modal parameters but also the probability distribution of the updated modal parameters. The proposed method provides a basis for differently weighing the various modal parameters based on the differences between the theoretical and experimental modal parameters. The proposed approach is presented on an experiment of the two-story building model previously studied by Katafygiotis and Lam (1997). Two natural frequencies, extracted from the acceleration time histories, are used as modal parameters. Under the assumption of white noise excitation, the statistical properties of the measured spectral density are presented. Based on these statistical results, the probability density function (PDF) of the modal parameters is updated. The updated PDF is well approximated by a Gaussian distribution, and the value of the PDF is maximized at the optimal parameters.

Doebling and Farrar (1997) use measured coherence functions to estimate the uncertainty bounds on the magnitude and phase of the frequency response functions (FRFs), and prorogate the uncertainty to modal parameters. Statistical uncertainty bounds on the magnitude and phase of the measured FRFs are computed from the measured coherence functions according to the following formulas from Bendat and Piersol (1980):

$$\sigma(|H(\omega)|) = \frac{\sqrt{1-\gamma^2(\omega)}}{|\gamma(\omega)|\sqrt{2n_d}}|H(\omega)| \text{ and } \sigma(\angle H(\omega)) = \frac{\sqrt{1-\gamma^2(\omega)}}{|\gamma(\omega)|\sqrt{2n_d}} \angle H(\omega) ,$$

where $|H(\omega)|$ and $\angle H(\omega)$ are the magnitude and phase of the measured FRF, respectively, $\gamma^2(\omega)$ is the coherence function, n_d is the number of measurement averages, and $\sigma(\cdot)$ is the standard deviation operation. Assuming that the probability distribution of the FRF at one frequency value is independent of the FRF distribution in another frequency value, a Monte Carlo simulation procedure is used to generate uncertainty bounds for the resonant frequencies and mode shapes. When statistically significant changes in these modal parameters are identified, these changes could be the result of damage or changes in environmental conditions.

An area that has not received much attention from the SHM community is Fuzzy Logic. Recognizing the complexity of many structures as well as the effects that operational and environmental variability has on the SHM process, it has been suggested by authors such as Yao and Wong (1999) that SHM be formulated in terms of a Fuzzy Logic problem. In Zadeh (1965), a fuzzy set theory makes use of sets, possibly overlapping, whose variables describe the state of a system in much the same way a human would. In particular, one set may correspond to a system in "good" condition whereas another set would correspond to the same system in "better" condition and yet another set to a "worse" condition. Because the sets are not necessarily disjointed, the element of a set describing a system can also be within the intersection with other sets. To overcome this problem, the relations between the sets are put in terms of Boolean operations, and the element in question is designated to a single set with a higher probability as opposed to the others.

Garcia and Osegueda (2000) combine two damage detection methods using pattern recognition techniques with the objective of improving the probability of detecting damage and reducing the probability of false positives. The model utilized is referred to as "decision theoretic" pattern recognition in which damage classification is accomplished via deterministic and statistical means. There are two basic steps to this model: the feature extractor takes measurements and produces feature vectors, and the decision function sorts the feature vectors into classes. The feature extractor not only reduces the number of measurements, but also renders the measurements more suitable for the decision process. An example of feature extraction is processing accelerometer data to obtain mode shapes and frequencies. In the case of damage detection, there are two classes: damaged and undamaged. The experiment consisted of an instrumented aluminum channel that was damaged by saw cutting. Experimental data were collected and analyzed by three damage detection approaches: Damage Index Method, ARMA method, and a Combined method. After being analyzed by each method individually, a single feature vector was formed from the feature vectors from the Damage Index Method and the ARMA methods. The experimental results show that using the combined feature vector to classify the channel as damaged or undamaged has a higher probability of detecting the damage and a lower probability of a false positive.

Structural health monitoring methods often rely on finite element (FE) models of the structural system in question. Results from FE models are then compared to experimental results for validation. There is no general-purpose technique to statistically judge the quality of an FE model. Perez et al. (1997) propose a statistical approach to validate such FE models. The authors apply the "bootstrap" technique to experimental data to develop confidence bounds on the selected measures of the physical system such as natural frequencies and mode shapes. The bootstrap technique is a resampling technique to create numerous artificial samples from limited random samples available. Statistics of interest, such as the mean, standard deviation, and confidence interval, can then be determined from the bootstrap samples. Next, the corresponding physical quantities are extracted from the FE model to determine whether they lie within the confidence interval. In their work, the authors performed vibration testing on a $60.96 \times 60.96 \times 0.95$ cm aluminum plate and extracted mode shape information from the data. A bootstrap analysis was performed on the data to develop 99% confidence intervals for the first two mode shapes. The first two mode shapes were also extracted from an FE model of the plate. It was found that the first two mode shapes predicted by the FE model did not lie completely within the 99% confidence intervals.

In statistical bridge monitoring, Enright et al. (1999) uses a Bayesian expression to find the posterior or current health distribution. The current health prediction of deterioration is developed with baseline or prior deterioration data. As inspection data become available, a conditional probability density function (PDF) for the new health is identified based on the prior degradation and the inspection data using Bayes' Theorem (Laplace 1951). The prior data and inspection data are used to compute the corrosion rate and the main descriptors for the PDF, which then yields the cumulative-time failure distribution. From an analysis of a reinforced concrete (RC) bridge in Pueblo, Colorado, interesting facts about the Bayesian approach are found. The first is that using the prior distribution tends to predict higher failure probabilities than those found by only using inspection data. Secondly, the prior distribution can have a significant effect on the shape of the updated or posterior distribution. Lastly, of the two corrosion damage indicators, the corrosion rate has much more influence on the failure probability than the corrosion initiating time.

6. APPLICATIONS

In this section, the literature that focuses on structural health monitoring application issues is reviewed. The types of structures analyzed include aircraft, civil infrastructures such as bridges and buildings, and laboratory specimens, such as beams and composite plates. As mentioned previously, this review does not address rotating machinery applications. In addition, local nondestructive testing techniques are not covered in this review either. Instead, this section only focuses on global structural health monitoring applications.

6.1 Aerospace Industry

There are a considerable number of studies and corresponding papers dealing with the SHM of aerospace structures. Most present methodologies are used for monitoring and assessing the remaining fatigue life of those structures. Examples of such papers are those by Goranson (1997), and Hunt and Hebden (2000). Goranson describes SHM approaches used by the Boeing Company to assess the integrity of aging jet transport systems. Hunt and Hebden discuss the SHM system implemented on the Eurofighter Typhoon. This SHM system performs real-time fatigue calculations and determines the life consumed by the airframe. A significant amount of structural events and flight performance data are also monitored. A bulk storage device saves strain gauge time histories and other data for future analysis. In fact, the system described by Hunt and Hebden marks the initial phase of an initiative aimed at exploring smart SHM systems for military combat aircraft.

Iglesias and Palomino (2000) introduce the health monitoring system currently in use on Eurofighter-18 and the design guidelines for the monitoring system of Eurofighter-2000. The main objective of these monitoring systems is to gather a high degree of information from the onboard measurements of the aircraft and to predict the remaining fatigue life of the aircraft. The monitoring system for EF-18 primary utilizes the strain records obtained from several critical fatigue points in the aircraft. Other information recorded for ground processing includes altitude, roll rate, normal acceleration, air speed, and so on. Ground processing of the strain data produces stress spectra to assess the remaining fatigue life of the aircraft. The sampling rate of 20 Hz in the current EF-18 strain measurements is restricted by the capacity of onboard magnetic

tape. The authors point out that this limited sampling rate lacks the desired accuracy for the areas subjected to severe dynamic effect. For the monitoring system of EF-2000, the sampling rate will be increased, and additional data beside the typical "g" counts will be considered for fatigue life monitoring. In addition, locations vulnerable to buffeting effects are identified from past experience, and these locations will be directly monitored through specific sensors. Strain gauges with adjustable sampling rates of up to 256 Hz are initially selected, and other alternatives like accelerometers are being investigated. Finally, the results of health monitoring can be used for fleet management such as allocating maintenance resources and manpower management.

Ikegami (1999) describes efforts by NASA, the U.S. Air Force, and Boeing to monitor fatigue life and repair some damage in both military and civilian aircraft. In particular, the U.S. Air Force is exploring the use of a durability patch that is able to repair fatigue cracks and include extra damping into the damaged area. Related to the patch is a damage dosimeter that is battery powered and records three channels of strain as well as temperature to predict the fatigue damage. The data processing functions are performed on the Analog Devices ADSP-2181 chip, which runs at 33 MHz. More information on the damage dosimeter can be found in Johnson, Smith, and Haugse (1999). The authors relate the results of damage dosimeter tests on the B-52H aircraft. In particular, the dosimeter is installed on the B-52H wing panel-to-frame attachment to characterize the magnitude and frequency of the vibrational strain environment as well as the temperature at which the worst vibrations occur in this connection.

Kudva, Grage, and Roberts (1999) give details of the U.S. Air Force Aircraft Structural Integrity Program (ASIP). ASIP can be defined as the design and implementation of engineering, test, and logistics tasks to minimize the possibility of catastrophic structural failure resulting from unanticipated or undetected structural or material degradation. As part of the ASIP program, data such as the Mach number, altitude, weight, strains, and aircraft accelerations are measured to predict the growth of initially assumed cracks. The authors state that there are a number of areas where cost and efficacy of current aircraft SHM procedures can be potentially improved. They include increasing the number, reliability, and fidelity of sensors, performing onboard data processing to provide immediate assessment, reducing the conservatism in current damage tolerance requirements, and substituting direct flaw detection at critical points performed by current procedures with assumed initial flaw sizes and growth rates. The authors further state that

the U.S. Air Force is currently investigating new sensor technologies such as fiber optics to address some of these issues.

Robeson and Thompson (1999) discuss aspects of the Structural Usage Monitoring System (SUMS) program, which is developed jointly by Boeing Corporation and the Army Special Operations Forces community. The Structural Usage Monitoring System (SUMS) is a ground-based computer program for SHM of critical parts on the MH-47E helicopter. In addition to monitoring bearings and rotor shafts on helicopters, the program monitors the Swivel Actuator Bolt and other subassemblies like the aft pitch housing. The main purpose of the SUMS program is to determine the remaining useful life of critical aircraft components based on measurements that characterize the components' length of service as well as the severity of their operating environment. The SUMS program is an alternative to the current SHM methodology for the aircraft where the calculation of the remaining fatigue life is based on the assumed operating conditions rather than the actual measurements of the operating conditions. The SUMS program directly measures these operational conditions, such as the number of turns or ascents the structure makes, to assess the remaining fatigue life. The authors conclude that the SUMS program incorporates a reasonable amount of conservatism based on the fatigue damage estimation from measured loads and that the program can be used to track fatigue in all life-limited parts.

Hall (1999) considers data management issues when implementing a SHM system of aircraft. He states that the initial definition, acquisition, and management of the measurement data for the aircraft SHM is not well understood by those seeking to implement a SHM strategy. Hall expresses the need for data management strategies to be incorporated during the design step of the SHM system and notes that a typical aircraft can currently generate between 3 to 5 Mbytes of data over a four-week period, depending on the parameters monitored. Furthermore, Hall highlights the importance of data validation and error management to ensure that the instrumentation and hardware are measuring certain parameters in a reliable fashion. Hall raises the issue of human factors in decision making regarding the structure's remaining life. Finally, the author points to the Internet as a means for conducting the SHM of aircraft at a central location when those aircraft are dispersed at various locations.

Hammel (2001) reviews the Life Extension Program (LEP) for the British Aerospace (BAe) 146 aircraft. This program refers to a series of procedures, which are implemented to allow for continued operation of an aircraft beyond the originally certificated usage limit. The implementation of the LEP program has been shown to increase the service life of some BAe 146 aircraft components up to 50% (8,000 hours to 12,000 hours). Although specific to the BAe 146 airplanes, the work can be generalized as an overview of similar SHM and fatigue life prediction programs in place throughout the aerospace industry. Hammel discusses the determination of appropriate stress levels as inputs to the monitoring system that executes fatigue and fracture calculations. He details the particular finite element models used to generate the fatigue estimation. Additionally, the author relates the various loads that aircraft typically experience during fleet as well as other flight parameters that are important for fatigue analyses.

Kabashima et al. (2000) first discuss the requirements of a health monitoring system for a satellite structure and advocate the use of optical fiber sensors for the satellite system monitoring. The authors state that the health monitoring system should be utilized during all phases of the satellite structure's life cycle, including manufacturing, environmental testing, launch, and operation in the satellite orbit. Monitoring during manufacturing would make production more efficient by detecting flaws early in the process. Based on data from environmental testing, the remaining service life of the satellite can be estimated, and in-flight monitoring would lead to more efficient operation of a satellite while maintaining reliability. The health monitoring system needs to detect microscopic levels of fractures or cracks at an early stage because even very small cracks near the fuel tank can cause a catastrophic failure of the whole system. Furthermore, the monitoring system should distinguish residual deformation generated during fabrication, thermal deformation, and mechanical distortions caused by external loads. A conventional measurement system using strain gauges and accelerometers typically used during environmental testing is time consuming to install and remove. Furthermore, during operation in the satellite orbit, the structure cannot be equipped with the conventional wired data acquisition system. Fiber-optic sensors have the potential to meet all the requirements of the health monitoring system for the satellite structures. One drawback is that typical optical fibers embedded in laminates like those used to construct satellites can cause swells in the satellite structures and reduce the strength and rigidity of the satellite. The authors propose the use of optical fibers of a smaller diameter (40 μm compared to a typical 125 μm) as a promising

solution to the problems. To test the advantages of the smaller diameter fibers, laminate tensile test specimens were constructed with no fiber-optic sensors, with 125-μm-diameter fibers, and with 40-μm-diameter sensors. The specimens with 125-μm-diameter fibers exhibited the lowest tensile strength and tended to break at the location of the embedded fibers. The specimens containing the 40-μm fibers had no decrease of tensile strength or change in fracture mode. The 40-μm optical fibers were then embedded in a honeycomb sandwich panel for another experiment. The test specimen maintained its flatness, and compressive fracture of the face sheet was successfully monitored with the optical fiber.

Bourasseau et al. (2000) investigated debonding and foam failure of foam core sandwich structures, called Randomes, for airborne equipment. The sandwich structures consist of glass-reinforced skins on both sides of a low-density foam core. Their initial setup involves a toneburst acoustic emitter with a pair of receivers, on the top and bottom surfaces, to gather the resulting Lamb waveform. The foam impedance is nonnegligible, which permits the leaky waves to reflect off the opposite surface and propagate in a different way compared to surface Lamb waves sent by the emitter. Using this information, Bourasseau et al. evaluates this method for the sandwich structures under a low impact velocity caused by a spherical impactor with a 1-kg mass dropping from distances ranging from 0 to 21 cm. Their findings indicate a correlation between reflected wave packets and Lamb waves for damage detection in skin debonding or foam cracking caused by the impact mass.

6.2 Civil Infrastructure

6.2.1 Bridges

Maeck and De Roeck (1999) apply a direct stiffness approach to damage detection, localization, and quantification for the Z24 prestressed concrete bridge in Switzerland. The bridge is a full-scale highway overpass consisting of three post-tensioned box cell girders of spans 14 m, 30 m, and 14 m that rest on four piers. The two central piers are rigidly connected to the girder while the two triplets of piers at both ends are connected via concrete hinges to the girder. Different damage types are introduced into the bridge ranging from concrete spalling, the failure of anchor

heads, the settling of piers between 20 mm and 95 mm, and the rupture of tendons. The authors succeed in localizing and quantifying damage in the bridge for each damage scenario using the direct stiffness approach. Keeping in mind that bending stiffness is defined as the ratio of bending moment to curvature, the direct stiffness approach uses the calculation of modal bending moments and curvatures to derive the bending stiffness at each location. The direct stiffness calculation first uses the experimental frequencies and mode shapes to compute modal curvature. Then, changes in the dynamic stiffness, given by changes in the modal curvature, indicate the presence of damage. However, they note that curvatures are rather small for the side spans and cause numerical difficulties in calculating bending stiffnesses in these spans.

Peeters and De Roeck (2000) compare a classical sensitivity-based updating technique with a direct stiffness calculation approach using data from a prestressed, three-span, 60-m-long concrete bridge. The authors note that a direct calculation of curvatures from measured mode shapes by using a central difference approximation results in oscillations and inaccurate values caused by numerical instabilities. To deal with this problem, the authors utilize a smoothing procedure where a weighted residual penalty-based technique is adopted. Damage in the bridge takes the form of pier settlements between 20 mm to 95 mm and the foundation tilt. Pier settlements of 80 mm and 95 mm seem to yield the most pronounced stiffness changes and thus the best damage resolution. With the 40-mm settlement, damage is less clearly identified, and the small curvatures at the bridge ends for this damage scenario cause numerical instabilities. The authors conclude that the direct stiffness calculation approach offers a reliable alternative to the classical sensitivity-based updating approach.

In a follow-up study of the same Z24 Bridge, Peeters et al. (2000) apply a subspace identification technique to the measured vibration data in order to obtain modal parameters such as frequencies, mode shapes, and damping ratios. The bridge is measured with nine different configurations of 33 accelerometers. Data are sampled at 100 Hz, and the cutoff frequency for antialias filtering is 30 Hz. The number of data points per channel is 65,536 except for a drop weight test, which has 8,192 data points per channel. Both ambient and forced bridge tests are conducted. The forced excitations rely on shakers and drop weights while the ambient excitations are induced by wind and/or traffic loading. The results of the different excitation methods are compared, and it is found that the additional costs of the shaker excitation could not be justified

for bridge testing because ambient excitation results give compatible results with much less cost. Ten vibration modes are extracted from the forced excitation tests, and most of the modes are consistently identified with the ambient excitation tests. It should be noted that extremely low frequency modes are not excitable with shakers whereas wind loading can be.

De Stefano et al. (1997) use Auto-Regressive Moving-Average Vector (ARMAV) models to obtain modal parameters of a three-span bridge girder with unknown random excitation. The frequencies, mode shapes, and damping ratios of the first four vibration modes are extracted under service conditions. Eight accelerometers are placed on the bridge, fixing the locations of three accelerometers and moving the other 5 accelerometers. Spot peaks and high frequency noise are removed by low-pass filtering the acceleration outputs. The extremely low frequency components associated with electrical saturation, integration errors, and the nonstationarity of the inputs are removed by a suitable high-pass filter. In particular, a Butterworth filter is used to obtain a flat magnitude response within the passband. Nonlinear phase distortions are minimized by adopting a forward and backward filtering technique. The filtered signals are then analyzed by means of different time windowing techniques. The time window size is selected to keep portions of the response as locally stationary as possible. The researchers claim that their results are highly reliable, even with highly noisy responses.

Todd et al. (1999) monitor traffic loads on the I-10 Bridge in Southern New Mexico using a 64-channel Fiber Bragg Grating (FBG) strain sensor attached to the bridge's 7 girders. The girders are I-beams and have spans of 36 m. The girder surfaces are stripped of paint and polished. M-Bond 200 adhesive is used to attach the fibers to the girder. The measuring system utilizes four diodes as optical sources, two photodetectors, six couplers, two Fabry-Perot filters, and a laptop computer. Spacing of the mirrors is controlled by piezoelectric actuators, and the spacing itself controls the wavelengths passing through the fibers. The Fabry-Perot filters have a free spectral range of about 45 nm allowing 16 individual sensors, spaced at approximately 2.7 nm, to be interrogated per filter scan. This spacing allows for strains of about 1,300 microstrain. The strain resolution for the system controlled by the piezoelectric voltage ramp and the free spectral resolution is about 1 to 2 microstrain. The sensor array is set to acquire strain data at 45 Hz. It is determined that the dominant frequency is 0.5 Hz, and this frequency corresponds to the passing vehicles. The free modal vibrations appear at 2.6 Hz, 3.7 Hz, and

4.8 Hz. Further tests are undertaken with passing trucks of known weights to extract mode shapes. It is noted that as the truck reaches the midspan of the instrumented span, the average deflection of the girder is almost 30 mm downward. After the truck passes, the average girder deflection returns to zero. Using the same measurement hardware, the authors also instrument a box-girder bridge under construction near Lausanne, Switzerland. They demonstrate the feasibility of monitoring bridges for higher-than-expected loadings during the construction phase.

Abe et al. (1999) utilize ambient vibration measurements of the Hakucho Bridge in Japan to track modal property variations caused by changing wind loads and friction forces. This three span suspension bridge with steel box girders is located at a windy and seismically active area in the northern part of Japan. The total length of the bridge is 1,380 m with a center span of 720 m and each side span of 330 m. Nineteen accelerometers are installed to measure the vertical motions of the girders, and an anemometer is installed at the center of the span to measure the wind velocity. The wind excitation is considered as a stationary white noise process. The response measurements are taken at the center span for the identification of symmetric modes and at the quarter span for the identification of antisymmetric modes. Free decay responses are constructed from the measured responses using the random decrement technique. Then, natural frequencies, mode shapes, and modal damping ratios are extracted from the free decay time series using the Ibraham time domain method. It is observed that the frequencies and damping ratios vary, depending on wind velocities. However, the observed variations of these modal parameters do not match with the predictions observed in wind tunnel testing of the bridge model. The authors attribute the discrepancies in the modal parameter fluctuations to the inability of their Coulomb friction model to represent stick-slip behavior.

Stubbs et al. (1999) employ the damage index method to nondestructively evaluate the structural integrity of bridges. This damage index method utilizes the modal strain energy stored in the undamaged and damaged conditions of a structure to detect damage in the structure. For this study, a four-lane highway bridge that spans Interstate 40 is tested. Vibration measurements are taken at 26 locations on the deck and 4 locations on the column. First, the modal parameter identification and the damage evaluation using the damage index method are conducted using field test data gathered in December 1997 and September 1998. A standard modal analysis is

conducted to determine the resonant frequencies and mode shapes of the lowest five modes. Next, a baseline finite element model is constructed utilizing the data from the as-built plans of the bridge. Modal frequencies and mode shapes are calculated from this model. A comparison of the measured modal properties with those from the finite element model is made, and possible damage locations and severities are estimated using the damage index method. Finally, the diagnosis results from the 1997 and 1998 measurements are compared to the surface crack patterns of the bridge visually inspected in May 1999. It is observed that the damage locations determined with the damage index method correlate with the actual crack patterns.

In a further study using the damage index method, Park, Stubbs, and Bolton (1998) detect damage in a finite element model of a four-story steel frame structure outfitted with 16 accelerometers. This frame structure model stands 3.6 m high and has a width of 2.5 m. All beam-column connections are rigid, and the floors are rigid in the horizontal plane. The damage takes the form of removed braces or reduced vertical stiffness in floors. Frequency response functions are calculated from average cross-power spectra of each input and output pair divided by an average autopower spectrum of the input. The input is random, and the first four bending modes in the two orthogonal directions and the first four torsional modes are extracted. Using the damage index method, the authors are able to locate the damage. Furthermore, using the damage index, the stiffness reduction in the damaged element is also estimated.

Another application of the damage index method can be found in Wang, Satpathi, and Heo (1997). The authors build a scaled model of a single span plate girder bridge and carry out a modal analysis of the structure. Twenty-four accelerometers are mounted on the steel beams of the structure, and a 32-channel data acquisition system is used. Excitation is provided with an impact hammer applied at a fixed point. The effects of the boundary conditions on the modal analysis are investigated. Specifically, fixed-fixed, roller-fixed, and pinned-pinned boundary conditions are considered. Damage is introduced in a girder flange. Assuming that the damage index values are normally distributed, a normalized index is formulated as the actual feature. The first six mode shapes are used to calculate the damage index. The normalized damage index performs quite well although the simulated damage is quite severe. The authors, however, foresee difficulties with the method when multiple damage states are present.

Wang et al. (1999) summarize the preliminary results of the monitoring and damage assessment investigation applied to the Kishwaukee Bridge in Illinois. The bridge consists of two separate bridges each carrying two lanes of northbound and southbound traffic on I-39. The structure is one of the first post-tensioned segmental concrete box girder bridges constructed using a balanced cantilever technique. A large number of cracks originate from the shear key during the construction phase. Diagonal cracking is also observed in interpier segments. Over the past 20-year life span of the bridge, the cracks have propagated further. A finite element analysis has been carried out in conjunction with a modal testing of the actual bridge in the field to assess the effect of these cracks to the overall structural integrity of the bridge. A baseline modal testing of the bridge was carried out about 13 years ago, and it is concluded that the differences between the newly obtained modal parameters and the baseline modal parameters are minimal. However, the finite element simulations indicate that very large localized damage could produce very small changes in the modal parameters. In addition, another numerical simulation indicates that a 30^{o}F decrease in the temperature can result in about a 2% increase in the frequency. Experimental measurements of temperature gradients and strains show that the temperature gradient can produce very large stains and can exceed those introduced by traffic loading. Finally, based on the identified critical damage areas close to the piers, the authors suggest that an inexpensive monitoring system based on a limited number of measurements can be deployed.

Peil and Mehdianpour (1999) monitor a highway bridge under its operating conditions to make life-cycle predictions. The authors state that the conventional life cycle prediction consists of a load model, a system transfer model, and a damage model. However, the final prediction using these models can be unreliable because the uncertainties in the three models can propagate through the final prediction. To minimize the uncertainty in the load model, a structure is monitored in its operating conditions, and strain time histories are measured at critical components. Then, some statistics of the strain time histories are computed, and artificial time series taking into account the past and future loading conditions are generated. The specifics of the employed statistics are not provided. Next, samples of structural components vulnerable to stress concentration are tested in a test rig where the artificially generated time series are used as inputs. In this way, the uncertainties in the system transfer model and the damage model are minimized. Because the test is run to failure, a prediction of the remaining fatigue life can be made. The authors claim that their method can avoid problems associated with unreliable

numerical models because the method only extrapolates time histories statistics of the structure. The remaining fatigue life is then estimated based on these extrapolated statistics.

Doebling, Farrar, and Cornwell (1997) analyze modal data from the Alamosa Canyon Bridge in New Mexico. This bridge has seven independent spans with a common pier between successive spans. Each span consists of a concrete deck supported by six steel girders. The roadway in each span is approximately 7.3 m wide and 15.2 m long. The beams at the pier rest on rollers, and the beams at the abutment are bolted to a half roller to approximate a pin connection. Only the first span of the bridge is instrumented. A total of 31 acceleration measurements are made on the concrete deck and on the girders below the bridge, and force time histories are measured at two points on the bridge. Temperature measurements are made at 9 locations across the bridge to track temperature effects on the test results. Modal tests are conducted every two hours for a total of 24 hours to assess the effects of environmental changes on the results. Damage is introduced by loosening the nuts on the bolted connections that hold the channel-section cross members to the girder, but no changes in the measured modal properties are detected. For this reason, damage cases are simulated using a correlated finite element model. The researchers also evaluate the uncertainties on the measured frequency response functions (FRFs), and propagate the uncertainties to obtain uncertainty bounds on the identified modal parameters using Monte Carlo simulation.

In a similar study, Doebling and Farrar (1997) demonstrate how statistical confidence limits can be defined for measured modal parameters. This statistical analysis is applied to modal data from the I-40 Bridge that is incrementally damaged prior to its demolition. The statistical analysis reveals that, in addition to damage, there are systematic test-to-test variations in the modal parameters of this bridge. For several damage scenarios, these variations are more significant than those produced by the damage. The conclusion of this study is that statistical analysis has to be an integral part of any modal-based damage identification procedure.

An ongoing investigation into using broadband vibration data to monitor the structural integrity and health of an all-composite bridge is presented by Ratcliffe et al. (2000). The bridge consists of two E-Glass/vinyl ester sandwich core sections connected by a longitudinal joint in the traffic direction. Each sandwich core consists of a 28-in.-deep core and 0.4–0.7-in.-thick face sheets.

Accelerometer data are obtained from a mesh of 1,050 test points covering the bridge's upper and lower surfaces. Interactions between the bridge and its abutments, the effectiveness of the longitudinal joint to couple the deck sections, the effectiveness of the core to couple the face sheets, and the structural integrity of the entire structure are investigated. Furthermore, an algorithm is developed to detect local perturbations sensitive to the structure's material state as well as to locate the material defects. A preliminary modal survey shows a frequency resolution of 0.625 Hz with the first natural frequency at approximately 18.74 Hz. It is found that the abutments provide good simply supported boundary conditions up to about 75 Hz, above which some vertical motion of the abutments is detected. Finally, variations over time in the analyses indicate some structural degradation.

Bergmeister and Santa (2000) discuss the instrumentation of one girder box of the Colle di Sarco viaduct in Italy. A description of the various measurement methods and their physical principles as well as their applications for the global monitoring is discussed. The instrumentation includes humidity sensors, wind vanes, strain gauges on the prestressing cables and reinforcements, anemometers, inclinometers, thermocouples, and electrochemical microprobes to measure corrosion. In addition, the bearings are instrumented with load cells and fiber-optic sensors, which are based on the interferometric principle for measuring long-range displacements. The authors state that interpretation of the acquired data and consecutive decision making are equally as important as the measurements. However, the details of the data interrogation and decision making are not provided in the paper.

The Online Alerting of Structural Integrity and Safety (OASIS) system is discussed in Nigbor and Diehl (1997). That system performs four vital functions in real time. First, a remote, real-time alerting feature using visual, on-screen imaging and audible alarms is employed. Second, an event-triggered, high dynamic range, high speed accelerograph, which operates in the background, is present in the system. Third, remote control and the display of system functions through direct control feedback as well as through a Windows-based graphical user interface is accomplished. Last, OASIS can incorporate different types of measurements, such as accelerations, strains, displacements, wind, and temperature. Nigbor and Diehl discuss applications of OASIS to bridges in Korea and Thailand.

Feng et al. (2000) develop an electromagnetic (EM) imaging technology for detecting voids and debonding between fiber reinforced polymer (FRP) composite jackets and reinforced concrete columns. Retrofitting RC columns with FRP composite jackets has been demonstrated to enhance structural performance. However, debonding between the jacket and column caused by seismic damage or poor workmanship can considerably weaken the column, and such damage can remain visually undetected. The proposed damage detection technique is to send a continuous EM wave at the reinforced column and detect the reflected wave energy. A fraction of the wave energy is reflected at each dielectric interface between adjacent layers (e.g., between air and jacket, jacket and column, etc.). An air gap between the jacket and column will form an additional interface, and the energy reflected at this interface should be detectable as evidence of debonding damage. The technique was unsuccessful when plane EM waves were used, so a dielectric lens was used to focus the wave on the bonding interface of the jacketed column. The time gating technique was used to remove unwanted reflections caused by unavoidable obstacles different from air voids. The modified EM wave technique was successfully demonstrated in laboratory tests to detect voids and debonding in a jacketed column with no rebar. Detecting voids in the column with rebar was still under investigation at the time of publication. Seim et al. (1999) used fiber-optic Bragg grating strain sensors for health monitoring of a historic bridge near Portland, Oregon. The Horsetail Falls Bridge is an 18.3-meter reinforced concrete slab span type bridge, consisting of three 6.1-meter spans. The bridge was built in 1914 and was not designed for the traffic loads that it is currently subjected to. To increase the load-carrying capacity of the bridge, the Oregon Department of Transportation used fiber reinforced plastic composite (FRPC) strengthening. Twenty-eight fiber-grating sensors were placed on the bridge in order to monitor the performance of the FRPC additions and the existing concrete structure. After the sensors were positioned, a 26,000-pound dump truck was moved to various locations on the bridge to ensure that the sensors were functioning properly. In parallel with this activity, more rigorous laboratory tests based on this structure are scheduled. Finite element models of the FRCP-reinforced bridge are also being developed. Data taken from the bridge will be used to validate the laboratory work and finite element models.

Fiber-reinforced polymer (FRP) composites are being used frequently to repair or replace many civil structures such as bridges. Shenton and Chajes (1999) discuss the long-term monitoring system that was installed on such a bridge located in Delaware. The Magazine Ditch Bridge is

located on a private road that is owned by the Delaware River and Bay Authority (DRBA). This bridge crosses over a small tidal creek and is used mainly by the DRBA to transport salt and sand. This bridge originally had a two-span, prestressed concrete, flat slab design. The slabs were simply supported by concrete abutments at the end and a central pier. This original design was replaced by a single span, simply supported design. The new design has a FRP composite deck supported by two concrete edge girders. The bridge has a span length of 21 m and a width of 7.5 m. To monitor the performance of the bridge, it was fit with 18 uniaxial foil strain gauges, a temperature sensor, and a humidity sensor. The monitoring system was designed to allow remote access for off-site setup changes by modem. Two types of data are collected from this system; monitoring and event data. Monitoring data are gradually taken at regular intervals. Every hour, the system records five seconds of data at a 100-Hz sample rate. These data are intended to track changes in the system and monitor the health of the system. The event data, on the other hand, are taken at a sample rate of 300 Hz only when a certain strain level of a central strain gauge has been exceeded. The event data record lasts for 9 seconds, including a 0.5-second pretrigger recording period. The purpose of event data is to obtain information while a heavy truck is passing over the bridge.

Ko et al. (1999) discuss the development of a large instrumented bridge project in Hong Kong. Three cable supported bridges, the Tsing Ma Bridge, the Kap Shui Mun Bridge, and the Ting Kau Bridge have been constructed to support the development of a new international airport nearby. A total of 900 sensors, including accelerometers, strain gauges, anemometers, temperature sensors, and displacement transducers, have been placed on the three bridges for structural health monitoring purposes. The authors discuss possible damage scenarios for each bridge and whether or not each scenario could be detected using a measurement of dynamic modal properties. The Tsing Ma Bridge is a suspension bridge with a main span of 1,377 m and an overall length of 2,160 m. The Kap Shui Mun Bridge is a cable-stayed bridge with a main span of 430 m and side spans of 160 m on either side. The Ting Kau Bridge is also a cable-stayed bridge that has two main spans of 448 m and 475 m with two 127 m side spans. For both types of bridges, the main cables are the most important part for the bridge's integrity. These cables are susceptible to damage via corrosion, internal abrasion, and localized faults such as broken wires. If bending stiffness of a cable is negligible, the tension force in the cable is related to the modal frequencies of the cable. Therefore, monitoring the modal characteristics of the

cable will indicate a change in tension. However, it will not reveal any reduction in a cross-sectional area caused by the corrosion or breaking of wires. The authors analyze several other types of damage possible within the three bridges. They claim that dynamic monitoring of the system should be able to detect most forms of damage, excluding corrosion in some parts of the structure.

Because several bridges in California were built prior to the development of modern earthquake design standards, a major initiative to increase the structural integrity of these old bridges has been in place for some time now. A common method for seismic retrofit has been to jacket the columns of the bridges with steel or some type of composite. Although cracks often initiate near the contact surface between the original columns and the jacketing materials, this technique often prevents visual inspection of the contact surface after retrofitting. Feng and Bahng (1999) propose a new method for the monitoring of jacketed columns that employs the combination of vibration testing, neural network, and finite element techniques. The authors constructed a small-scale bridge model based on an old design standard, and the columns of the bridge model were retrofitted with carbon fiber composite. A finite element model was constructed to predict baseline vibration characteristics of the bridge, and the predicted responses were compared with vibration test data taken from the scale model. Damage was then introduced in the bridge model, and vibration tests were repeated for several damage cases. The data taken from the finite element model and the damaged bridge were used to train the neural network using a standard back-propagation algorithm. The trained network is then used to determine the stiffness degradation of the bridge.

Choi and Kwon (2000) developed a neural network damage detection system for a steel truss bridge. The bridge, constructed in 1940, carries one rail road, and is currently healthy. A finite element model of the bridge was developed based on design drawings, and the mass and stiffness of the truss members were updated based on static and dynamic loading tests performed on the real bridge. The refined finite element (FE) model was then used to determine which truss members had the highest stresses during static analysis. This analysis identified eight truss members as most vulnerable to damage. Based on this observation, stiffness reduction in each of these eight truss members is simulated to generate eight damage cases for the subsequent neural network analysis. The first network determines which half, either the left or the right of the

midpoint of the bridge, is damaged. The second network determines which of the eight truss members are damaged. The two-step neural network successfully located the damage in the FE model, and in future studies they will implement the system on the real bridge.

Dunn et al. (1999) discuss a unique opportunity for side-by-side comparison of two bridges built with different design technologies. The 71G and 72G bridges at the Savannah River Site, Department of Energy complex in South Carolina will serve as the test beds. Each bridge handles one-way traffic that results primarily from shift changes at the local facility. The first bridge, 71G, was constructed in the 1950s, and the second bridge, 72G, was completed in 1996 with more modern construction techniques. The old 71G bridge will be demolished and then rebuilt in the future, and the rebuilding of the 71G bridge provides a unique opportunity to compare different aspects of the two bridges built with different construction technologies and design codes. Before the demolition of the bridge, the 71G bridge will be retrofitted with fiber reinforced polymeric (FRP) composite overlays, and strain gauges, and piezoelectric sensors will be installed on both bridges to monitor conditions during and after the retrofitting. Data taken from each bridge during controlled traffic loading will be compared against one another as well as to the numerical results obtained from an analytical model for the bridges. Then, the 71G bridge will be monitored to a complete failure. This test will give a good opportunity to monitor the bridge under overload conditions. A new bridge will be constructed with embedded smart materials. The performance and structural integrity of each bridge will be monitored over the long term, and the overall benefit of using the smart structures/technologies approach will be estimated.

Structural health monitoring systems for bridges are often employed after the completion of the bridges. However, it is possible that bridge girders experience some of the largest loads during transit from the manufacturer and during construction. Kirkpatrick et al. (1999) discuss a project where strains in bridge girders were monitored during shipment and installation. The bridge girders were shipped from Lancaster, Pennsylvania, to Hanover, New Hampshire, to replace the Ledyard Bridge on the New Hampshire/Vermont border. Fiber-Optic Bragg grating sensors were installed to monitor strain in the girders. To ensure the accuracy of the fiber-optic sensors, traditional electrical-resistive type strain gauges were also installed on the structure. Accelerometers and global positioning system (GPS) tracking systems were also installed for the

correlation of measured strain and imposed gravity force. A detailed finite element model of the girders was developed to determine optimum strain gauge locations. Data from all sensors were transmitted via telemetry to a laptop that was located within a chase car that followed the girders during transport. Data revealed that all loads experienced during transit and installation of the bridge girders were within allowable limits.

Kwon et al. (1998) developed a scaled-down laboratory model of a truss bridge to investigate structural health monitoring. The truss bridge model was constructed based on a conventional design practice frequently used for many railways in Korea. The laboratory bridge measured 4.0 × 0.6 × 0.6 m. The authors instrumented the bridge with traditional electric resistance strain gauges as well as four Michelson fiber-optic sensors. A finite element model of the laboratory bridge was also developed for comparison with the measured data. Several damage scenarios were investigated that included the simulated breakage of different combinations of selected structural members. It was found that the Michelson fiber-optic sensors could not exactly measure the structural strain because of signal noise problems. However, the finite element results did match well with the resistance strain gauge data. The authors claim that, if the strain had been measured properly, the damage scenarios could all have been identified from the changes in the strain patterns.

Vurpillot et al. (1997) discuss the use of fiber-optic sensors to monitor displacements of the Versoix Bridge in Switzerland. The Versoix Bridge is a typical concrete bridge that consists of two parallel prestressed concrete beams supporting a concrete deck and two overhangs. To support another lane of traffic, the beams were widened and the width of the overhangs was increased. The authors installed a network of fiber-optic sensors to measure the displacement of the existing bridge components as well as the new bridge components. The authors implemented an algorithm that calculated the spatial displacement of the bridge from the curvature of the bridge. This system will be used for continuous long-term monitoring of the structure. The authors were also interested in differential shrinkage that would occur between the new concrete overhang additions and the existing concrete structure. Results indicated that the differential shrinkage ranged from 0.005% to 0.02%, depending on the climatic conditions during the curing stages of the concrete.

Nellen et al. (1997) use fiber-optic Bragg grating sensors for the monitoring of Storck's Bridge in Winterthur, Switzerland. This bridge is a cable-stayed bridge that is 120 m long and supports 18 railway tracks. Two of the bridge's stay cables are composed of carbon-fiber-reinforced-polymer (CFRP). Each CFRP cable has a length of 35 m and consists of 241 individual 5 mm-diameter wires assembled in a hexagonal pattern and encapsulated in a polymer tube. The CFRP cables were fit with several Bragg grating sensor arrays, and each sensor array consisted of seven sensors. Three of the sensors were adhered to three of the loaded 5-mm wires inside the cable to measure cable tension. The remaining four sensors were placed on "dummy" nonload-bearing wires installed in the vicinity of the loaded wires for temperature compensation. For comparison purposes, the CFRP cables were also fit with resistance strain gauges in a similar fashion. The strain within the cables was monitored during the construction of the bridge and for a 10-month period after construction. The Bragg grating sensor readings were in good agreement with the resistance strain gauge readings.

The University of California, San Diego (UCSD) is leading an effort to design and deploy a fully functional bridge made of advanced composite materials. F.L. di Scalea et al. (2000) describe the bridge and give an overview of the sensing techniques that will be used on the bridge. To answer questions of how advanced composite materials and structures made from these materials perform, the bridge will be monitored in both the short and long term. Component testing and monitoring will take place during construction, at the completion of construction, and during service life. Event monitoring and system recharacterization will also be carried out during the service life of the bridge. Several measurement methods will be implemented during the project. Infrared thermography with active heating will be used at the time of construction for detecting defects, such as delaminations and porosity, and periodically during service life to detect potential structural degradation. Ultrasonic testing will be used to assess failures detected by the thermographic tests. Electrical resistance strain gauges will be used in a variety of locations on the bridge to measure strain and load. Accelerometers will be used for the characterization and monitoring of the bridge's global dynamic behavior. Fiber-optic sensors will be used in conjunction with the electrical-strain gauges and accelerometers to characterize and monitor the bridge response to dynamic loads. A laser position sensor will be used to monitor the position of the bridge midspan. In addition to the redundant sensors installed on the structure, the bridge will be visually inspected periodically.

Based on the knowledge that data from nondestructive methods are difficult to interpret, Enright et al. (1999) use a Bayesian approach to evaluate the effects of corrosion on a reinforced concrete (RC) bridge in Pueblo, Colorado. The RC T-beam highway bridge consists of three simply supported spans, each with 5 girders. The main descriptors for the initial resistance and load effects are initial shear resistance, dead shear, and initial live load. The bridge is subjected to salt spray from passing traffic that causes strength loss in the cross-sectional area of the girders caused by corrosion damage near high shear locations. The resistance and corrosion variables are obtained from site-specific data and previous work (Nowak et al. 1994). The strength degradation is estimated using a probabilistic approach, and strength degradation predictions are updated using Bayesian methods. The expected value of resistance loss increases at a nonlinear rate, as determined by regression analysis. Additionally, a plot of cumulative-time failure probability shows the center girder to have the highest probability of failure.

6.2.2 Buildings

Rytter and Kirkegaard (1997) apply two neural networks to discerning damage in buildings, namely the multilayer perceptron (MLP) network and the radial basis function (RBF) network. Both the MLP and RBF network consist of one hidden layer in addition to the input and output layers. A vibration test of a full-scale four-story reinforced concrete building is performed at the European Laboratory for Structural Assessment (ELSA) to validate the proposed neural network approaches. This building is subjected to an earthquake generated by a pseudo-dynamic testing method. A finite element model of a four-story building is used to generate data sets for the neural network training. Random damage states are generated through finite element simulations, and the associated modal parameters are computed. The relative changes in the frequencies and the mode shapes are used as inputs, and the relative bending stiffness of the beams and columns are used as outputs. The MLP neural network demonstrates the ability to detect damage when trained only with randomly selected damage cases, thus avoiding the need for *a priori* knowledge of the actual damage and its effects. The authors state, however, that the success of the RBF network depends on the damage cases used for training.

Onate, Hanganu, and Miquel (2000) conduct finite element simulations of damaged concrete and reinforced concrete structures such as a housing building and the domes of St. Mark Basilica. The five-story reinforced concrete building has two symmetrical floors per story, and the St. Mark Basilica is a five-domed building in Italy. In particular, the authors investigate the five-story building in order to adjust the safety factor used in its design. They find that the trussed joists in the floors are much more flexible than expected, and other members of the building are unduly carrying loads for which they are not designed. The authors thus conclude that a significant reduction in the design safety factor is in order. Similar results from the St. Mark Basilica substantiate this conclusion.

Fritzen, Bohle, and Stepping (2000) attempt to identify multiple cracks in structures and test a two-story building structure called Steel-quake, which is located at the European Research Center in Ispra, Italy. The dimensions of the building are 8 × 3 × 9 m. The floors are made of corrugated sheets supporting a concrete slab connected by vertical and horizontal welded steel girders. The vertical girders are stiffened with cross bracings in the plane parallel to the wall. The researchers create a finite element model consisting of 1,476 degrees of freedom, 104 4-node shell elements, and 172 2-node beam elements. The authors construct an objective function consisting of Modal Assurance Criterion (MAC) terms and update the model using the measurement data of the undamaged building. A frequency error of 3.98% and a MAC value of 0.99 are achieved on average for the first 10 modes of the updated model. The researchers then identify damage-sensitive parameters by means of an inverse sensitivity formulation and locate damage from changes in these parameters. Finally, the researchers locate the damage by considering only the localized areas, fitting the relevant parameters to the experimental data of the damaged building, and using nonlinear optimization to update the damaged model. For the damaged cases, a mean frequency error of 3.22% and a mean MAC value of 0.95 are obtained. Three crack locations are successfully detected, while the method indicates cracking in one case in which no crack is actually present.

Skjaerbaek, Kirkegaard, and Nielsen (1997) test six-story two-bay test reinforced concrete (RC) frames on a shaker table to extract modal parameters using an Auto-Regressive Moving-Average (ARMA) vector model. The widths of the structures are 2.4 m, and the heights are 3.3 m. Each story deck consists of 8 RC beams (0.12 × 0.12 × 2.0 m). All of the beams and columns in the

frame have identical dimensions of 50 × 60 mm, respectively. The structures are subjected to three sets of simulated earthquakes, and damage takes the form of cracking. The first two earthquakes are artificially generated using a Kanai-Tajimi filter with a center frequency of 10 rad/s and 30 rad/s, respectively. The third earthquake is a scaled acceleration of the 1994 Northridge earthquake. Using an ARMA vector technique, frequencies and decay rates are determined when the undamaged structures are subjected to the shaker table's pullout forces of 0.25 kN, 0.50 kN, and 0.75 kN. Next, after the frames are excited by the three earthquakes, frequencies and damping ratios are determined again from the shaker table's pullout force of 0.50 kN. The frequency decrease and damping ratios increase are observed. The authors then monitor the top story's acceleration time histories and extract the two lowest time-varying frequencies of the structures using a recursive ARMA vector model. The researchers also use the following maximum softening damage index as a useful damage-sensitive feature,

$$\delta_i = 1 - \frac{\mathrm{T}_i^u}{\mathrm{T}_i^d} \ ,$$

where δ_i is the maximum softening damage index for the *i*th vibration mode, T_i^u is a period of the *i*th mode for the undamaged structure, and T_i^d is the maximum value of the *i*th period during an earthquake. As damage progresses, the maximum softening approaches to one. After the frames are subjected to the three earthquakes, the maximum softening damage indices indicate severe damage in the structures, and this result is verified by visual inspection of the cracks.

Hou, Noori, and St. Amand (2000) apply wavelet analysis to acceleration response data recorded from a twelve-story building during the 1971 San Fernando earthquake. The building is a 12-story reinforced concrete moment-resisting structure. The floor dimension is 18.29 × 48.77 m except for the first floor, which is 27.43 × 49.07 m. The building stands 48.46 m above the street level, and it is located approximately 22.53 km from the epicenter of the earthquake. During the San Fernando event, this building suffered both structural and nonstructural damages, and the structural damage mainly consists of cracks and spalling of columns and girder stubs. The wavelet analysis is mainly applied to the acceleration response data recorded at the 7th floor of the building. Characteristics in the Level 1 details of the DB4 wavelet decomposition indicate the presence of some damage attributed to the earthquake occurrence. This result is in agreement

with the field observation in a sense that the cracks and spalling of the columns and stubs might have occurred subsequently during the earthquake. Results of the authors' work also indicate the deleterious effects of signal noise on the analysis. Signals with weak noise coming from heavily damaged structures offer the best hope for wavelet-based SHM.

6.3 Beams

Claiming that most detection techniques for crack damage in a beam are applicable only when there is a single crack in the beam, Ruotolo and Surace (1997a and c) propose a damage assessment method for identifying multiple cracks in beam structures. Using genetic algorithms and simulated annealing for optimization, local minima/maxima are avoided, and global extrema are sought. The objective function is formed as a function of the difference between the measured and calculated frequencies. The proposed method is then applied to numerical data simulated from a beam with multiple cracks and experimental data measured from three cantilever steel beams with two cracks. From these simulations and experiments, it is found that simulated annealing is more efficient than genetic algorithms in finding the correct crack locations and depths.

Cerri and Vestroni (2000) identify the location, size, and amount of damage in a reinforced concrete beam specimen tested in a laboratory by solving an inverse problem. The beam is 2,450 mm long and has a cross section of 100 × 150 mm. Static tests of a simply supported beam are conducted to characterize the mechanical behavior of the beams above an elastic limit. For dynamic testing, the beam is suspended by flexible springs to simulate free-free boundary conditions, and frequencies are extracted from acceleration measurements. An inverse problem is formulated using the following objective function, $l(s,b,\beta)$,

$$l(s,b,\beta) = \sum_r \left| \frac{f_r^d - f_r^a(s,b,\beta)}{f_r^u} \right|^2 ,$$

where f_r^d and f_r^u represent the rth damaged and undamaged experimental frequency, respectively, and $f_r^a(s,b,\beta)$ represents the rth analytical frequency associated with the damage location along the beam s, the extent of the cracked zone b, and the degree of bending stiffness

reduction β. The authors first minimize the objective function with respect to b and β. Then, the objective function becomes only a function of s. Using only the first three frequencies, all three variables, s, b, and β, in the objective function are correctly identified.

Nandwana and Maiti (1997) identify the location and size of a crack in a stepped cantilever beam using natural frequencies. The crack is modeled as a rotating spring, and the spring constant is estimated as a function of the crack location for each natural frequency. This stiffness vs crack location curve is plotted for each of the first three natural frequencies, and the point of intersection of the three curves gives the crack location. The crack size is then computed from the estimated stiffness at the intersection by solving a characteristic equation between the stiffness and the crack size. The method based on the rotational spring has previously applied to beams of a uniform cross section, and this paper is an extension of the previous method to a stepped cantilever beam. The effectiveness of the proposed method is illustrated by a finite element model of a two-step beam.

Lin et al. (2000) evaluate the effectiveness of the electrical time domain reflectometry (ETDR) technique in monitoring shear deformation and detecting shear crack damages in concrete beams. The ETDR technique derives information from the reflections of a voltage pulse sent through a transmission medium. It is a well-developed technique that has been widely used in electrical engineering applications. The method can measure the deformation of the whole structure as well as pinpoint the location of disturbances. The authors use an embedded high-sensitivity coaxial sensor prototype to monitor the transverse shear response of a concrete cylinder. The capacitance of the cable is increased in the sheared section, where the diameter of the cable changes. The authors claim that the maximum capacitance change occurs at the center of the shear couple where the cable is deformed the most. Single and double shear tests were conducted with the coaxial sensor embedded through the concrete cylinders. No noticeable signal response was observed before the onset of the shear crack damage in the cylinders, but once the shear crack was induced, a shear deformation pattern of the sensor signal was apparently shown at the location of the shear plane of the specimen. As the deformation continued, the deformation pattern increased. It is concluded that the ETDR prototype sensor is capable of detecting the onset as well as monitoring the growth of shear-induced crack damages in concrete cylinders. Crack damages were clearly captured by the ETDR signal waveforms. Also, it is determined that

the sensor is rugged enough for concrete structure application because it remains intact and continues to function after the failure of a concrete specimen.

Kwon et al. (2000) constructed four reinforced concrete beams to investigate failure detection using fiber-optic sensors. Fiber-optic Michelson sensors were attached to the surface of the rebar before the concrete was poured to form the beams. Electric resistance strain gauges were attached at the same time as the fiber-optic sensors so the measurements of the fiber-optic sensors could be checked for accuracy. The beams were loaded in bending until fracture occurred. The authors found that the measurements from the fiber-optic sensors did not match the measurements from the electric resistance strain gauges. However, the fiber-optic sensors were successful in detecting the failure of the beam.

Huang and Yang (1996) evaluate the effect of corrosion on reinforced concrete (RC) beams. While RC is a durable infrastructure material, soluble chlorides from road salts or marine exposure can destroy the passive oxide layer, inducing corrosion of the reinforced steel. The authors attempt to develop a relationship between the corrosion condition and the structural performance for repair and replacement. Electrochemical measurements are conducted before and after 3-point static loading tests of the RC beams to relate the load capacity of the RC beams to corrosion rates or cross section loss of the reinforced steel bars. Thirty-two RC beams of dimensions 150 × 150 × 500 cm and 48 cylinders of a 300-cm length and a 150-cm diameter are cast. The specimens are split into four design groups, a combination of low or high water content concrete with or without an impressed crack. The beams are placed in a sea-water bath, and a current is applied to the steel reinforcement. A potentiostat/galvanostat is used to measure the open circuit potential and the DC polarization current. All the specimens are then tested for middle deflection and surface strains in 3-point loading. The DC polarization value gives the corrosion current density, which is then used to calculate the instantaneous corrosion rate. Integrating the corrosion rate over time yields a monotonically increasing function of the steel thickness loss, which is defined as a corrosion index. The findings show that the load capacity of the beam decreases as the corrosion index increases and as the steel thickness decreases. The rate at which stiffness loss occurs is dependent on the design type of the beam. For example, the greatest stiffness loss is shown for the higher strength concrete made out of less water with the

induced surface cracks. This result is indicative that the load capacity and stiffness of the RC beam is dependent on the concrete quality and the predetermined cracks.

6.4 Composites

Cawley (1997) applies Lamb wave testing to detect delamination in a 600-mm-long composite plate. A 10-cycle 0.5 MHz tone burst is applied to the plate with a conventional ultrasonic transducer. In Lamb wave testing, the measurements are limited to the short time period between the generation of the wave and the onset of the first reflection signal at the boundaries. For an example of a plate, a wave is generated at one end of the plate, and the echoes from the boundary of the plate are monitored. Any additional reflection signals other than arriving from the boundary would indicate the presence of damage. For the undamaged plate, the time delay between the transmitted and reflected pulse corresponds well with the theoretical prediction. A 20-mm delamination located 100 mm from the far end of the plate is identified by monitoring an additional reflected signal that arrives ahead of the reflection from the end of the plate.

Badcock and Birt (2000) also employ Lamb wave testing for the detection of delamination damage in composite plates. Ultrasonic Lamb waves are generated and measured using piezocomposite sensors, which can potentially be embedded within the fiber composites. Hitchen and Kemp (1995) have shown that a residual energy is linearly related to the total area of delamination in the composite laminate. Here, the residual energy is the energy absorbed by the process of delamination extension, and it is the difference between the maximum energy absorbed and the energy absorbed at damage initiation. Badcock and Birt show that this residual energy is linearly related to signal loss of the ultrasonic Lamb waves and attempt to provide a quantitative estimate of the degree of damage by measuring this Lamb wave signal loss.

Zak et al. (1999) describes experiments on an eight-layer graphite/epoxy composite plate with dimensions of 250 × 90 × 8 mm. The delamination is introduced at the midplane by placing a Teflon foil between layers of the composite. Delamination sizes and locations are varied for each test specimen. Changes in the delamination lengths and locations result in a reduction of the natural frequencies and changes in the mode shapes. In addition, delamination produces additional modes of vibration and additional natural frequencies. With the addition of contact

forces in a finite element model, the additional modal frequencies could be reproduced in the numerical simulation. It is also observed that all simulations as well as the experimental results depend heavily on the boundary conditions.

Foedinger et al. (1999) present a collaborative effort to develop an *in situ* SHM system for filament wound composite pressure vessels and rocket motorcases using embedded fiber-optic sensor arrays. Standard ASTM (American Society of Testing Materials) filament wound pressure vessels with embedded Fiber Bragg Grating (FBG) sensor arrays are tested. The FBG sensors are embedded in the composite pressure vessels to measure the internal strain during curing and pressurization. The measured strains show an increase in strain upon the expansion of the vessel until the cure temperature is reached. Strain relaxation then occurs during the cooldown. Impact and burst strength tests are also undertaken to detect impact events and measure postimpact internal residual strain. The multiplexing instrumentation is developed for the real-time measurements of the strains and temperatures throughout the pressure vessel. They note that continuous improvements in the grating sensors as well as in the optical switch are needed to provide a faster sampling rate and to incorporate more sensors. The authors show that the sensor arrays can provide meaningful measurements of internal strain for cure monitoring, impact damage detection, and other SHM concerns, and demonstrate that the presence of these sensor arrays does not adversely affect the burst strength of the pressure vessels.

The use of composite structures is prevalent in the aerospace industry. Several of these composite structures are embedded with various sensors and actuators to provide the optimal performance of the structures. Composites provide better specific stiffness and strength properties than metal. However, the use of composites also leads to new types of failure modes such as delamination. Kaiser et al. (1999) discussed using the sensors and actuators that are already in place to perform dynamic structural health monitoring. The authors performed several tests on undamaged and delaminated composite plates to show that delamination in composites can be detected through the identification of modal parameters. In their work, the authors use MX filters to obtain modal parameters, such as eigenfrequencies and damping values, for the structure. For their test setup, the structure and the modal model receive the same excitation. The MX filters are used to reduce the error between the output of the structure and that of the

model to some predefined convergence criteria. Their test results gave good evidence that delamination can indeed be detected using modal methods.

Smart composite structures commonly contain embedded sensors such as piezoelectric wafers and optical fibers for sensing and monitoring purposes. These embedded sensors may introduce several disadvantages because of incompatibility with the organic host composite. Also, composite processing methods often do not facilitate the incorporation of such sensors into the composite structure. Blanas et al. (1999) discuss the use of thin ferroelectric ceramic/polymer sheets for embedded sensing of composite structures. The authors claim that these sheets achieve optimum electroactive properties while maintaining good compatibility with the host composite. The ferroelectric sheets consisted of particles of ferroelectric calcium modified lead titanate ceramic dispersed into a ferrelectric thermoplastic or a thermoset epoxy. These sheets were embedded within a $56 \times 56 \times 0.3175$ cm unidirectional composite plate. The polymer sheets formed a 10-cm-square array at the center of the composite plate and were embedded two layers below the surface. Acoustic emission (AE) sources were generated by breaking pencil lead on the surface of the composite plate. The authors indicate that extensional plate waves (often called Lamb waves) can be used to detect damage in composite structures. In their work, the authors show that the polymer sheet sensing elements readily detect extensional plate waves.

Maseras-Gutierrez et al. (1998) discuss the detection of impacts within a composite structure. The authors instrumented a rectangular composite specimen with piezoceramic sensors. The test specimen was then impacted in several locations. Data from the sensors was used to train two multilayer perceptron neural networks. These networks could then be used to predict impact intensity and location within the test structure.

Chen et al. (1997) discuss a technique that can be used to detect damage within glass-fiber reinforced polymer (GFRP) composite C-channels. The technique consists of embedding ferromagnetic particles into the GFRP composite matrix. An alternating magnetic field is then passed over the composite C-channel that causes the magnetic particles to vibrate. A Laser Doppler Vibrometer records the resulting vibration of the composite. The authors tested this idea by creating several $7.62 \times 2.54 \times 0.254$ cm C-channel specimens. Damage was introduced into some of the specimens by introducing central delaminations during the layup procedure.

Vibration signatures from the undamaged and damaged specimens were recorded and used to train a perceptron neural network. The network can be used to determine whether a vibration signature is from a damaged specimen or an undamaged specimen.

Furrow, Brown, and Mott (2000) developed an optical fiber system for monitoring strain in composite bridge decks. The system was designed to monitor deformation or strain in real time as well as periodically over a period of years. The steps taken during the research include (1) choosing one sensing system after investigating several measurement options, (2) demonstrating the sensing system on a scale model, (3) installing fiber-optic sensors in four bridge decks, (4) performing laboratory three-point bend tests on two of the bridge decks, and (5) obtaining field test data from a composite bridge deck. The extrinsic Fabry-Perot interferometer (EFPI) was selected as the most suitable sensor system to measure displacement in this study. The authors' investigation showed that the EFPI sensor was the only sensor sensitive to the axial strain components and relatively insensitive to temperature variations. In the scale model test of the composite bridge, the EFPI sensors were attached to the surface of a specimen to demonstrate the measurement capabilities of the sensors. Next, two three-point bend tests were performed on the composite bridge test specimens. Each bridge specimen was composed of a top face sheet, a bottom face sheet, and a support structure made up of triangular sections. Sensors were embedded in both face sheets and in the support structure. In both cases, the sensors embedded in the top and bottom face sheets were damaged during installation, and no data could be taken from them. The sensors in the supports survived installation, and the measurements agreed with those from electrical strain gauges and were as expected. Finally, two 3.048×6.096 m composite bridge decks were instrumented for field testing. Again, the face sheet sensors were damaged and were unusable. The sensors in the support structure were operational. Data were taken for about six hours on two days, one week apart, with the composite bridge installed into an on ramp of a truck weigh station. The data were consistent from one week to the next. A slight drift in the data was observed, and further testing was planned to determine if this variation was caused by increasing temperature throughout the day or actual permanent damage to the bridge deck.

Composite materials commonly used in the design of lightweight structures are susceptible to transverse impacts that can cause significant damage such as delamination. Delaminations are difficult to detect and can have a detrimental effect on the residual strength of the composite material. Most NDE techniques for detecting delamination are cost ineffective and require extensive human labor. Wang and Chang (2000) present an active diagnostic technique for identifying the impact damage in composites. This method uses a built-in network of piezoelectrics that act both as actuators and sensors for detecting impact damage. A signal generator produces diagnostic signals that are emitted from the piezoelectric ceramic wafers, and the waves propagate through the material and are measured by the other wafers. Damage is identified by analyzing differences in sensor measurements, which are mainly caused by a change in local material properties, before and after the damage is introduced. The differences can be related to the location and size of the delamination. The arrival times of waves to each sensor are recorded, and this information is used to determine the damage location. In this research, the delamination was approximated as an ellipse. Experiments were conducted on various graphite/epoxy plates with four piezoelectric wafers mounted on the surface with conductive epoxy. Damage was introduced to the plates by means of a quasi-static impact. Damage location and size estimated with the described technique were comparable to x-ray images of the damaged plates. The estimated damage centers were within 5.08 mm of the actual ones in 68.8% of the cases, and 90.1% were within 10.16 mm. The presented technique often overestimated the actual size of the damage.

Osmont et al. (2000) present a passive technique to identify the location of a damaging impact on a composite plate using piezoelectric sensors. The authors propose a technique based on the analysis of the acoustic emission produced during the impacts on carbon-epoxy structures. The parameter used is the High-Frequency Root Mean Square (HF-RMS) value of the electric signal registered by the piezoelectric sensors,

$$S = \left(\int_0^T x^2(t)\, dt / T \right)^{1/2},$$

where S is the HF-RMS value, $x(t)$ is the electrical signal measured by the piezoelectric sensors, and T is the duration of the signal. The authors established a "linear relation" between the HF-RMS value and the delamination area. To determine the location of damage, they used an optimization process based on the S values from each sensor. They also conclude that it should be possible to give estimates of the damaged areas for plates similar to the reference plate used in experiments.

Elvin and Leung (1997) discuss the feasibility of detecting delamination within composite cantilever beam structures using fiber-optic sensors. In their method, a single fiber-optic sensor will be embedded within the composite structure. A separate fiber-optic sensor, outside of the structure, will serve as a reference fiber. As loading is applied to the composite structure, the optical path length of the embedded fiber will change, which will create a phase shift between the output of the embedded fiber and the reference fiber. The authors claim that by applying a moving point load to the composite structure, it is possible to detect and characterize delamination within the structure. As the point load is moved over a delaminated region, the total extension of the embedded fiber will jump significantly. By noting the position of the load as well as the magnitude of the change in total extension, the position and relative magnitude of the delamination can be determined. The authors studied the feasibility of this approach by modeling a cantilever beam using the boundary-element method (BEM). Delamination in the beam was modeled as an elliptical hole within the beam. The authors analyzed how the total extension of a certain path where the optical fiber is embedded changed with different elliptical hole sizes and locations. Based on their analysis, the authors concluded that the change in total extension of the fiber-optic sensor within the composite structure could indeed be used to detect and characterize delamination.

Two approaches to calculate the stiffness degradation within reinforced concrete beams are discussed by Maeck et al. (2000) as methods that require few sensor measurements but large computational power. The first technique, model updating, is an attempt to find degradation in numerical modal parameters using eigenfrequencies for symmetric beam damage and modeshapes for asymmetric damage. Minimizing the differences between numerical and experimental parameters yields a least-squares problem that is solved with the Gauss-Newton method. The employment of a predetermined damage function reduces the number of updating

parameters, simplifying the optimization problem and the identification of damage locations. Their second technique, direct stiffness calculation, uses the modeshapes that are required in the asymmetric updating case. The dynamic bending stiffness is found by dividing the modal bending moments by the corresponding curvature. One drawback of this approach is that an inaccurate estimate of the bending stiffness is obtained near elements with either zero moments or curvatures. This difficulty causes problems in estimating the stiffness degradation but little hindrance in locating damage. These two techniques are applied to reinforced concrete beam tests. First, the finite element models are updated and validated using the test data from the concrete beams. Then, destructive three-point and four-point loading tests are performed. The damage location and extent are successfully identified under a four-point bending test. However, the three-point loading test, in which more concentrated loading is applied to the beams, produced dynamic stiffness values higher than expected. The authors attribute this unforeseen result to the inappropriate selection of the optimization function as well as a potential creeping effect that might have occurred during the extended testing period of the three-point loading test.

Beard et al. (1997) propose an experiment that takes the common procedure of damage detection by measuring the arrival times of scattered waves and applies it to an uncommon filament wound composite tube. The tube itself is a graphite epoxy helix/hoop/helix/hoop filament tube with a radius of 6.35 cm, a length of 31.75 cm, and a nominal wall thickness of 0.14 cm. The propagating waves are generated in cylindrical Lamb modes by a piezoelectric transducer. The authors integrate a network of Lead Zirconate Titanate (PZT) ceramic wafer sensors into the tube with 2 sets of 6 sensors spaced 60 degrees apart and 5 cm from each end. A function generator permits one set to produce the Lamb waves while the other set monitors the time response at the other end. In an undamaged structure, data are recorded for each actuator-sensor path to determine the amplitude envelope and evaluate the arrival time with the known distance to find wave velocity. Damage is introduced by a quasi-static impact to induce delamination and small matrix cracks. Data on wave propagation are collected and analyzed to determine damage location. Isolated into a region identified by six sensors, the damage is found on the path with the fastest scattered wave arrival time. Using the geometry of the tube and triangulation, a best-fit intersection point yields the final location. Further evidence shows that an assumption of an elliptical damage shape may lead to damage extent evaluations in addition to location.

Staszewski et al. (2000) employ an artificial neural network to estimate the impact location and amplitude on a composite panel, and they use a genetic algorithm to determine the optimal sensor locations. A box-like structure composed of aluminum channels and a composite plate was used as the test specimen to simulate the skin panel of an airplane. The impacts to the composite plate were applied on the top surface while the bottom surface was instrumented with 17 piezoceramics to record strain data. The force of the impact was kept below 0.1 N to prevent damage to the plate. A standard Multi-Layer Perception (MLP) neural network trained with the back-propagation learning rule was used for this experiment. The x and y coordinates of the impact were identified using the time after the impact of maximum response and magnitude of response as inputs to the neural network. The overall relative error of the impact location estimation was 2.5% when the training data set for the network was contaminated by noise. The level of noise was set to 20% of the root-mean-square (RMS) of the measured strains. The same features were used to predict the impact amplitude, but a different noise level, 5% of the RMS of the strain data, was used to predict the amplitude of the impact force. The mean percentage error for the impact amplitude prediction was 28%. A modified genetic algorithm (GA) was used to generate suboptimal fail-safe sensor placement. The performance of this suboptimal sensor configuration was compared with the optimal sensor placement found by exhaustive search.

6.5 Others

Corrosion in pipeline systems is a major problem in the oil, gas, and chemical industries. Particularly, because many of the industrial pipelines are buried underground and/or insulated, visual inspection cannot readily be conducted. Cawley (1997) applies Lamb wave testing to the detection of corrosion in insulated pipeline systems. The author is provided with a unique opportunity to apply the Lamb wave technique to a real insulated pipeline system with 50-mm-thick insulation covered with galvanized steel sheeting. The insulation of the pipelines is removed, the pipelines are visually inspected, and new insulation is wrapped round the pipeline. The Lamb wave test is conducted before the removal of the insulation, and the diagnosis results are correlated with the visual inspection later. A 550-m-long pipeline is inspected, and 1-m sections of insulation are removed at a minimum of 20-m intervals to accommodate the transducer placement. In all tests, a 5 cycle tone burst signal with a central frequency of 64 kHz

is applied to excite the pipeline in both forward and backward directions. Corrosion is evident from the attenuation of reflected pulse amplitudes relative to the undamaged portions of pipe and by time delays associated with the reflected pulses that do not correspond to welds or supports. All corrosion areas are successfully identified except one area of corrosion, which is located downstream from the other major corrosion areas. The author notes that the Lamb wave method has trouble picking up defects downstream of large defective areas, but this would not be a problem in practice because, once the major corrosion area is identified, the insulation near the troubled area should be removed anyway. The author states that the reliable range for detection is about 12 to 15 m in either direction implying that successive tests could be set up for 25 to 30 m apart.

Zimmerman (1999) discusses the application of Ritz vector extraction for the identification of damage in Vertical Stabilizer Assemblies (VSAs) of the Space Shuttle Orbiter. Fifty-six accelerometer measurement points are used to analyze damage in the VSAs. An MB500 shaker with a root mean square force input of 100 N is used, providing 25 ensembles of burst random excitation to the VSAs. To minimize unnecessary feedback from the stabilizer to the shaker, the shaker is suspended 10 ft above the excitation point from a platform. This configuration of the sensors and the shaker is compliant to the Shuttle Modal Inspection System (SMIS). A scanning laser vibrometer is also used to obtain additional measurements. The Ritz vectors are extracted from both accelerometers and a laser scanning vibrometer. The Ritz vectors represent an alternative to modal vectors spanning the response space of dynamic systems. He shows that Ritz vectors are more efficient in identifying damage than modal vectors because fewer Ritz vectors are required to identify the damage than modal vectors.

The design and analysis of nuclear containment vessels have recently attracted a lot of research attention because of the criticality of these vessels. Onate, Hanganu, and Miquel (2000) construct a three-dimensional finite element model of a reinforced concrete containment vessel, accounting for the lack of symmetry in the prestress forces, the nonlinear material behavior, the presence of three buttresses, as well as the uncertainties in some material parameters. They consider internal pressure loading caused by an accident, external pressure caused by prestressing, and the container self-weight. They also employ a damage model that accounts for cracking. The main

findings of the work are that the foundation slab has negligible effect on the failure of the vessel and that safety factors accounting for the slabs' effects are overestimated.

Pirner and Fischer (1997) explore the possibility of extrapolating measured data from a radio tower for the identification of damage and for the estimate of the residual life of the structure. The response of a TV tower in Prague, the Czech Republic, is monitored for 3 to 4 years. The measurements include vibrations of the tower-shaft caused by wind, stresses in the cylindrical extension supporting the antennae, and the temperature distribution along the circumference of the cylinder. The dynamic response of the tower is measured by a pair of mutually perpendicular absolute displacement transducers located at a height of 198 m aboveground. These transducers have a maximum amplitude measuring capability of ± 40 mm within a frequency range of 0.2 to 15 Hz. The researchers use 2 active and 2 passive electric resistance strain gauges to measure even slow varying strains as well. At certain sections of the tower, the authors compute the number of stress cycles at a given stress level, which are produced by dynamic/static loading and thermal effects. Based on the stress vs the number of cycles curve obtained from 411 days of observations and a laboratory fatigue test of a sample cut out of the TV tower after 20 years of use, the stress vs the number of cycle curves for 20 years is extrapolated. This curve can provide invaluable information to estimate the remaining fatigue life of the towers.

Ruotolo, Sorohan, and Surace (2000) address the issue of refining a numerical model of structures, given experimental data. The authors perform experiments on a three-dimensional truss structure, which is 4 m long and composed of eight equally spaced cubic bays. The truss structure uses a total of 109 aluminum tubes connected with standard meroform nodes. Each tube is fit with specifically designed connectors at both ends to permit clamping with the nodes. The truss also incorporates 0.7-m-long diagonal elements to increase the torsional stiffness. The truss is suspended by four elastic cords to simulate a free-free boundary condition. The dynamic response of the structure is acquired in three translational directions of all 36 nodes, and excitation is provided by an instrumented hammer. Classical modal analysis is conducted to estimate the frequencies and mode shapes of the first five modes from the measured frequency response functions. The authors note that, at frequencies higher than 170 kHz, the motion of local truss members becomes dominant and prevents the accurate calculation of the higher mode

shapes. Three finite element models of the truss are refined using an eigensensitivity based model updating method. The updating procedure is performed using only frequencies while the accuracy of the updated models is evaluated using both the Modal Assurance Criterion and the cross orthogonality check between the experimental and numerical mode shapes. The three models include a simple model with truss elements, a model created with a Euler-Bernoulli beam element for a truss member, and a model with three beam elements for each truss member. The most refined last model provides the best agreement between experimental and numerical results.

Frosch and Matamoros (1999) show that internal strain gauge measurements can be used to assess the health of beam-column joints in reinforced concrete moment-resisting frame structures. They use a 2/3-scale model of a typical reinforced concrete moment-resisting frame structure, and load the structure with actuators to simulate an earthquake. The loading is intended to induce deformations into the columns and beams well into the nonlinear range while providing the typical effects of cyclic loading. The load-deformation history is traced using the load cells attached to the actuators and displacement transducers mounted at the inflection point. Strain gauge readings on the longitudinal reinforcements are used to monitor the formation of a plastic hinge in the longitudinal reinforcement. Strain gauges on the transverse reinforcements can provide an indication that the structure has experienced post-yield responses and large deformations. The authors state that significant flexural cracking should be evident in the structure when the longitudinal reinforcement yields. Frosch and Matamoros note that an increase in the strength of the concrete will, in general, decrease the measured transverse strains and thus lower the potential for transverse strain measurements to be used as features. Via a network of strain gauges installed in a structure, the authors conclude that it is possible to locate beam-column joints that have experienced inelastic behavior.

Fukuda and Osaka (1999) state that mechanical properties of molded products strongly depend on the molding conditions such as temperature, pressure, timing, rates, and so on. The ultimate goal of this study is to establish an optimal cure condition, which can automatically adapt to various moldings based on the measured data of the degree of matrix cure, residual stress and strain, void content, etc. During the autoclave molding process, the internal and residual strains in graphite fiber reinforced plastics (GFRP) laminates are measured with Extrinsic Fabry-Perot

Interferometric (EFPI) optical fiber strain sensors, and the resin curing is monitored by embedded piezoceramic sensors/actuators. First, real-time measurements of internal and residual strains in graphite fiber reinforced plastics (GFRP) laminates are recorded using optical fiber strain sensors while the GFRP is undergoing the autoclave process. They note that the structure of the sensor plays an important role in that sensor's sensitivity to internal strains. Second, the researchers develop a thin piezoelectric film having sensing and actuating functions for observing the gelation point of resins.

Chung (1998) reviews self-monitoring structural materials such as concrete with short carbon fibers, continuous carbon fiber polymer-matrix composites, and carbon-carbon composites with continuous carbon fibers. Tests are undertaken on these materials to evaluate their SHM ability. For the first material, cracking causes pullout of the electrically conducting short carbon fibers, which thereby increases the electrical resistivity of the composite. For the second, strains cause the fibers to align, causing the electrical resistivity in the fiber direction to decrease and in the transverse direction to increase. For the last composite, the dimensional change caused by elastic deformation causes the electrical resistance (not resistivity) to increase. Chung finds that cement containing short carbon fibers (0.24% vol %) is a highly sensitive strain sensor with a gauge factor of up to 700. The polymer matrix composite containing continuous carbon fibers is a sensitive strain and damage sensor with a gauge factor of up to 38 in magnitude with the capability to detect fiber fracture and delamination. The detection of fiber fracture is based on relations between the fraction of broken fibers and resistivity. Last, the carbon-carbon composite with continuous carbon fibers is found to be an extremely good damage indicator detecting damage even after the first cycle of tensile loading within the elastic range. Such composites hold promise for fatigue SHM.

Similar to the previous work, Nishimura et al. (2000) investigate the performance of self-diagnosis composites embedded in concrete piles subjected to cyclic bending tests. Specifically, carbon powder and carbon fiber are introduced into glass fiber reinforced plastic composites to obtain good electrical conductivity. It is found that the electrical resistance of the carbon powder increases markedly at 200 microstrain, which is a much smaller strain than required for crack formation. The strain is inferred from the change in the resistance of the glass fiber reinforced plastic composite doped with carbon powder normalized by a reference resistance. When the

piles are subjected to 12 cycles at various load levels, crack formation, growth, and final fracture are clearly detected. The authors surmise that the percolation structure of the carbon powder dispersed in the plastic matrix phase exhibits a higher sensitivity to strains than carbon fibers. However, they note that prestressing the concrete pile generally dulls the sensitivity of the embedded carbon powder-doped composites.

Wang and Pran (2000) emphasize the need for SHM systems to ensure structural integrity of structures designed with optimization methods that attempt to achieve an optimal balance between the ship's strength and weight. This design philosophy is prevalent in the marine industry where engineers are trying to design strong lightweight ships. They note the tradeoff between weight reduction and strength and demonstrate the usefulness of fiber-optic Bragg grating strain gauges in monitoring ship hulls. This program is a part of the Composite Hull Embedded Sensor System (CHESS) undertaken jointly by the U.S. Navy and Norwegian Defense Research Initiative. In this program, the KNM Skjols, a twin hull surface-effect ship made from sandwich panels with fiber reinforced polymer skins, is monitored. The authors look at global bending moments and forces acting on the ship's hull during operation and note that the vertical bending moment dominates the strain gauge signals. While they show that fiber-optic strain gauge systems can be used effectively in the SHM of ship hulls, they note that more parameters are needed to accurately characterize the seaworthiness of ships. In turn, more efficient signal processing techniques would also be required to deal with the extra data needed for monitoring more parameters. The CHESS program continues to investigate these problems.

Microelectro-mechanical systems (MEMS) are being used for a large number of scientific and industrial applications. Ruffin (1999) discusses several applications of MEMS for Army missile systems, including system health monitoring. After Desert Storm, maintenance checks of several missile systems revealed large amounts of corrosion. Undetected degradation of system components can lead to significant problems. Ruffin discusses the Remote Readiness Asset Prognostic/Diagnostic System (RRAPDS) program that was initiated to develop onboard missile health monitoring systems. This system will utilize MEMS technology to remotely monitor critical components of missile systems to prevent possible problems and reduce costs associated with maintenance and inspection. The system will feature low-power, high bandwidth communications; miniature, low-power sensors, and sensor embedding technologies. Ruffin also

discusses an application of MEMS technology to the structural integrity monitoring of both the mechanical components and the propellant grain and to the service life of solid propellant rocket motors.

Cohen et al. (1999) discuss the development of a fiber-optic sensor system that will detect wear of water lubricated shaft bearings on Naval marine propulsion systems. The sensor system helps eliminate the amount of downtime needed for traditional inspection methods. These bearings are comprised of nitrile rubber staves that support a shaft, which has a copper nickel sleeve. By embedding plastic fiber optics within the nitrile rubber staves, the amount of wear present within the staves can be detected. As the sacrificial fiber-optic sensors wear, their optical power transmission characteristics change. The plastic fiber-optic sensors are chosen because of the similarity of their material properties with the host nitrile rubber. Currently, a simple underwater indicator is being considered for monitoring wear, and this indicator requires a diver with a light source to interrogate the fiber-optic sensors occasionally. At the time of the report, work was under way to develop a means to route the fiber-optic sensors to the ships' onboard data systems for real-time measurement.

Nellen et al. (1997) discuss the development of a steel sensor rod to monitor the stress and temperature during the expansion of the Luzzone electrical power dam in the Swiss Alps. The height of this dam is to be increased from 17 m to 225 m, and it is desired to monitor the effects of thermal stresses during the curing process of the concrete as well as the stresses during the operation of the dam. The steel sensor rod is 2 m long and contains three "gauge sections" for strain and temperature measurements. In each gauge section, one fiber-optic Bragg grating sensor is attached to the inside surface of the hollow steel rod, and the other sensor is attached to a small dummy steel plate within the rod that only experiences thermal strain. Resistance strain gauges were also mounted next to the Bragg grating sensors to provide a means for comparison. To test the steel rod sensor, it was embedded into a $0.5 \times 0.5 \times 3$ m concrete prism. The strain transfer from the concrete to the Bragg grating sensor was then verified by loading the prism in compression from 0 to 1,000 kN. Strain measurements from the Bragg gratings and the resistance strain gauges were simultaneously taken and showed good agreements. At the time of the paper, plans were in place to use the steel sensor rod during the expansion of the Luzzone dam.

Kronenberg et al. (1997) use the same methodology to monitor the Emosson Dam in the Swiss Alps. The Emosson Dam is 180 m high and at its coping (top layer), it is 550 m long. The authors developed a fiber-optic-based system to replace the original mechanical extensometers that were embedded in the dam. This sensor development was accomplished through a multitube device, similar to the one discussed in Nellen et al. (1997). At the time of the paper, the fiber-optic system had been successfully installed. However, the system had not produced enough measurements to draw any conclusions as to the accuracy of the system.

Kiddy and Pines (1997) develop a finite-element-based methodology for damage detection and characterization in helicopter main rotor blades. The authors use a sensitivity-based, element-by-element (SB-EBE) method for damage detection. The SB-EBE method updates the design parameters of the numerical model to closely reproduce the measured dynamic response. First, mass, stiffness in the lag direction, and stiffness in the flap direction are selected as the design parameters. Second, the sensitivity of the global mass and stiffness matrices with respect to these design parameters is computed from the numerical model. Third, the values of the design parameters are updated by minimizing the difference between the measured vibration data and the ones simulated from the finite element model in an iterative manner. Finally, the perturbation of these design parameters can be directly related to damage in one of the selected design parameters. The authors validated the SB-EBE method with the use of numerical simulations. A FEM of a rotor blade was developed, and three types of damage were introduced into the model. The first type of damage is ballistic damage that is characterized by a reduction in stiffness and mass of a given element. The second type of damage is delamination that is characterized by a reduction in stiffness only. The third type of damage is simply the loss of mass within an element. For all three types of damage, the SB-EBE method identifies the correct amount of changes in these design parameters.

Zheng and Ellingwood (1998) provide probability-based assessment for two damage detection techniques, magnetic particle and ultrasonic inspection. They apply these methods to a time-dependent fatigue study in order to evaluate the health of a steel miter gate. Uncertainty for reliable assessment is represented by flaw detection and flaw measurement. The probability of flaw detection is a logistic regression function with an asymptotic factor. The flaw measurement error, the measurement noise with respect to true size, is described as a linear function

determined through regression analysis. While modeling can give insight into failure mechanisms, they argue that decisions regarding maintenance or repair should be based on analytical predictions in combination with inspection data and uncertainties in the inspection techniques. The probability appraisal of a steel miter gate on a river lock system gives an example for each of the detection methods. Initially, a probability distribution function is assumed for the damage. A detected crack is projected for forty years of growth, and then flaw measurement uncertainties are used to bound the size for more accurate health monitoring. In the case where no crack is detected, the probability of detection determines whether a crack may exist, and if so, references a distribution where the crack size follows a stochastic crack growth law.

7. RELATED INFORMATION

A list of SHM projects, web sites, conferences, and technical journals of interest to the SHM community is identified using the commonly available Internet search engines. Note that posting in this list does not imply any judgment, good or bad, about the quality of the site or the organization/person posting the information. The only purpose of this listing is to inform the SHM community of any SHM related information. Although every effort is made to ensure up-to-date content, some lost links or out-of-date web sites might be found. If you can provide any information on these failed sites or would like to add your site to our list, please contact sohn@lanl.gov.

7.1 Structural Health Monitoring Projects

Alexiou (2000) presents a brief outline of Accurate Modeling and Damage Detection in the High Safety and Cost Structures (AMADEUS) project funded by the Commission of the European Union under the Brite-EuRam Framework III. The ultimate industrial objective of AMADEUS is to develop methods, procedures and guidelines for routine, nondestructive, in-service maintenance, health monitoring, and damage detection in high safety and cost structures. This knowledge will be incorporated into an autonomous PC-based expert system capable of on-site structural assessment. The development of such a system requires advances in various technical fields. First advances will be made in model reduction techniques such as Guyan, Dynamic, Improved Reduced System, Modal, and Hybrid. Second, fatigue life prediction of structures is another issue that will be analyzed by the AMADEUS group. Third, a computer program called MODPLAN is implemented to determine the best measurement, suspension, and excitation points to be used during the modal testing of structures. Finally, various damage detection criteria are considered. Collaborators on this project include Imperial College in United Kingdom, Construcciones Aeronáuticas S.A. (CASA) in Spain, Transport Research & Development (TRD) in Greece, Alenia Spazio Turin in Italy, Ziegler Instruments in Germany, and Centro Recerche Fiat in Italy.

Other European programs in SHM are described in Foote (1999). The author notes that, of the European institutions conducting research in SHM, 37% cited aerospace applications, 20% cited civil applications, and the remaining are of generic applicability. Among some of the specific programs discussed is the SHODOS (Structural Health Monitoring Using Distributed Optical Fibre Sensors) program, which concerns itself with transferring optical fiber technology to other areas. In particular, the SHODOS program is attempting to use fiber-optic sensors for distributed sensing of concrete bridges. He also mentions the FOSMET (Fiber-Optic Strain Monitoring at Elevated Temperatures) program, whose goal is to develop an optical fiber based distributed strain measurement system to monitor high temperature (up to 600^{o}C) components in power generation plants. The FOSMET program is a 5-nation consortium that includes 6 industrial partners, 3 research organizations, and 1 academic institution.

Mita (1999) discusses two 5-year programs instituted by the Japanese government to address SHM needs for civil structures. The first is sponsored by the Ministry of International Trade and Industries (MITI), and consists of universities as well as industrial partners. Some of the collaborators are the University of Tokyo, Hitachi, and Shimizu Corporation in Japan. The research efforts include investigating fiber-optic sensor systems, developing composite materials that can suppress damage using shape memory alloy fibers/films, developing smart patch sensors with maximum strain memory, and developing new design methodologies for tall structures. The second program is through government-industry collaboration between the Building Research Institute and the Ministry of Construction whose purpose is to conduct research in smart structures. This research deals with sensor and actuator technologies as well as performance verification procedures.

Vandiver (1997) discusses some SHM techniques related to damage detection in U.S. Army missile systems, such as the determination of propellant separation. In particular, he talks briefly about sensing methods such as interferometric, ultrasonic, and fiber-optic methods. Vandiver also gives some information on where these sensing methods have been employed and where further research is being conducted.

Bartelds (1997) gives some information concerning the European Union's SHM research objectives and programs. For example, the development of integrated automated systems for damage detection and for load path monitoring is funded by the European Unions Directorate General for Research. The potential end user community consists of aircraft manufacturers, and operations are involved very early on in the project to clarify the monitoring options considered in the project. Programs supported by agencies such as the Western European Armament Group and the Group for Aeronautical Research and Technology are also mentioned.

Melvin et al. (1997) discussed the Integrated Vehicle Health Monitoring (IVHM) system, which intended to provide reliable and low-cost maintainability for the X-33 Reusable Launch Vehicle (RLV). The X-33 shown in Figure 10 was a half-scale, suborbital experimental flight test vehicle that was a collaborative effort between NASA and Lockheed Martin. The objective of IVHM was to provide automated collection of measured data, easy repair access, expedited maintenance, and a logistic decision-making system. To achieve this goal, Lockheed Martin developed a smart distributed health-management system for both the vehicle and the ground systems that included an automated, computerized, paperless ground computer environment using the latest commercial off-the-shelf workstation, software, and internet tools. However, the X-33 project was completely shut down on March 2001.

Figure 10. X-33 Reusable Launch Vehicle: On March 1, 2001, NASA announced that the X-33 Program has been scrapped. (NASA concept art: Courtesy of NASA)

Chong (1997) describes National Science Foundation (NSF) initiatives for SHM activities in the field of civil infrastructure systems. The NSF initiative identifies the following four key areas: (1) Deterioration Science that examines how materials and structures break down and wear out, (2) Assessment Technologies that determines durability, safety, and environmental conditions of structures, (3) Renewal Engineering that extends and enchances the life of civil infrastructures, and (4) Institutional Effectiveness and Productivity that maximized the impact of civil infrastructure investments on the productivity, economic, and social well-being of the public. An example of NSF-funded projects includes developing self-healing concrete, the development of optical-fiber-based SHM systems, active bucking and damage control in structures, and the use of a shape memory alloy for a fiber reinforcement.

The Department of Defense has pledged support for the Multi-University Center for Integrated Diagnostics (M-URI) at the Georgia Institute of Technology. The program's chief goals are described in Cowan and Winer (1999). The main goal of the center is to understand the physics and chemistry of moving components subjected to high loads, high temperatures, and corrosive environments. The authors state that novel sensors and signal processing methodologies are needed for recording and transmitting pertinent information. Basic research into understanding deterioration mechanisms and identifying the means to detect the initiation of flaws and other potential failure locations will be undertaken. Additionally, M-URI will develop methodologies for failure prediction in real time, including modeling fault initiation and failure signatures and observing the fracture phases of fatigue-based failure. Finally, the program will seek to design and develop sensors that can be placed at critical locations on mechanical systems for response to changes in variables of state or vibration.

Staszewski (2002b) presents an overview of the European Union supported project, Monitoring ON-Line Integrated Technologies for Operational Reliability (MONITOR). They identified the continual aging of aircraft fleets, the increased use of larger capacity aircraft, and a more common use of composite materials as major challenges to inspection and maintenance of airframe structures. In this context, the objective of the MONITOR program was to review and translate aircraft end-user requirements into health and usage monitoring system specifications, to monitor actual in-flight operational loading and to quantify the performance of the emerging damage detection technologies. Finally, a series of ground and flight tests were conducted to

validate the operational load monitoring and damage detection systems. The MONITOR consortium consisted of major European aircraft manufacturers with research and academic institutions. The MONITOR partners include Aeronautical Research Institute, Sweden; Aerospatiale Matra, France; Association for Research, Technology, and Training, Greece; BAE Systems, UK; Centre National de la Recherche Scientifique, France; DaimlerChrysler Aerospace, Germany; Defense and Evaluation Research Agency, UK; Finmeccanica SpA Ramo Aziedale Alenia, Italy; Institute of Optical Research, Sweden; Stichting National Lucht-en Ruimtevaartlaboratorium, The Netherlands; University of Sheffield, UK.

7.2 Web Sites

The Structures and Composites Laboratory (http://structure.Stanford.edu) is part of the Department of Aeronautics and Astronautics at Stanford University. Research encompasses composite design, including vibration, stability, impact damage, and environmental effects; biological applications of composites, manufacturing; fiber-optic and piezoelectronic sensors; and smart structures. Especially, this web site provides several FORTRAN 77 codes for computing crack initiation and delamination propagation in laminates' composite plates, and predicts the future strength and life of a composite structure based on that structure's previous load-strain history.

The Damage Identification web site (http://ext.lanl.gov/projects/damage_id/) operated by Engineering Sciences and Applications Division in Los Alamos National Laboratory provides information regarding the SHM project conducted by LANL personnel. This page is dedicated to serving the research community in the field of vibration-based structural health monitoring and damage detection. Visual inspection methods and local nondestructive methods such as acoustic or ultrasonic methods, magnetic field methods, radiographs, eddy-current methods, and thermal field methods are not covered in this page. The actual experimental test data relevant to these projects as well as project reports and related publications can be downloaded from this web.

The Nondestructive Testing Information Analysis Center (NTIAC: http://www.ntiac.com/) is a full-service Information Analysis Center sponsored by the Defense Technical Information Center (DTIC) and operated under contract by Texas Research Institute Austin, Inc., (TRI/Austin) in Austin, Texas. NTIAC's primary goal is to provide users with in-depth and up-to-date information on issues related to nondestructive testing and evaluation. This web site offers a computerized, bibliographic database with over 50,000 NDT articles, reports, and an extensive list of other NDE websites, and it provides quarterly NTIAC newsletters to subscribers anywhere in the world.

The primary objective of the ASCE, Structural Health Monitoring Committee (http://wusceel.cive.wustl.edu/asce.shm/default.htm) is to address fundamental issues for health monitoring using structural response data that are needed to improve its effectiveness in detecting, locating, and assessing damage produced by severe loading events and by progressive environmental deterioration. The U.S. task group solidified in 1999 jointly under the auspices of the International Association for Structural Control (IASC) and the dynamic committee of the ASCE Engineering Mechanics Division with Prof. James L. Beck from California Institute of Technology as chair. The task group is charged with studying the efficacy of various structural health monitoring methods. Several meetings have been held over the last few years. The IASC-ASCE SHM Task Group has developed a series of benchmark structural health monitoring problems, beginning with a relatively simple problem and proceeding on to more realistic and more challenging problems. This site describes the task group activities. The benchmark problems proposed by the committee are contained herein, as well as recent papers and reports on the members' research activities.

SINOPSYS (model based Structural monitoring using IN-OPeration SYStem identification, http://www.irisa.fr/sigma2/sinopsys) mainly describe stochastic subspace-based modal identification techniques based on only output response measurements. It also contains the application of the stochastic subspace method to damage detection of the Z24 Bridge benchmark test and the Steel-quake benchmark test.

The Society for Machinery Failure Prevention Technology (MFPT: http://www.mfpt.org) was organized in 1967 under the leadership and sponsorship of the Office of Naval Research as the Mechanical Failures Prevention Group (MFPG). The objectives of MFPG are to gain a better understanding of the processes of mechanical failures, to reduce the incidence of mechanical failures by improving design methodology, and to devise methods of accurately predicting mechanical failures or prevention. The Society meets annually in the spring and provides a forum for the exchange of ideas and accomplishments in such areas as sensors technology, failure modes and mechanisms, root-cause failure analysis, condition monitoring, predictive maintenance, prognostics technology, nondestructive evaluation and testing, life extension and integrated diagnostics, and condition based maintenance.

Structural Health Monitoring Central (http://shm.celeris.ca) is an initiative of Celeris Aerospace Canada, Inc., to provide a central location on the World Wide Web for all issues pertaining to the acquisition, validation, analysis, and management of operational load data acquired from vehicles or machinery. The site includes contributions from experts in different fields, discussion groups where you can post questions to recognized experts in a number of relevant disciplines to address your problems. Copies of links to papers with practical information pertaining to the implementation of SHM programs are provided. Access is currently free of charge, but you have to register.

Structural Dynamics Research Laboratory (http://www.sdrl.uc.edu) is within the Mechanical, Industrial, and Nuclear Engineering Department at the University of Cincinnati. The function of this laboratory is to develop, investigate, and evaluate experimental approaches to the estimation of the dynamic properties of structural systems. The direction of this activity over the last twenty years has centered on research related to the experimental determination of modal parameters. The focus of recent work has broadened to include the identification of general systems for control design, active vibration control, rotating machinery modeling, and signature analysis, vibroacoustic interaction in structures, and acoustic noise source identification utilizing microphone arrays.

The World-Wide Web virtual library for Acoustics and Vibrations (http://www.ecgcorp.com) is operated by Edge Consulting Group, LLC., and this site provides extensive information regarding audio, noise control, measurement and testing, and architectural acoustics. This site has very useful links to papers, software, consulting firms, and books.

The Center for Nondestructive Evaluation (CNDE: http://www.cnde.iastate.edu) at Iowa State University is a National Science Foundation Industry/University Cooperative Research Center that focuses on the research and development of new theories and techniques for use in quantitative NDE.

The Center for Intelligent Material Systems and Structures (CIMSS: http://www.cimss.vt.edu/) is part of the Mechanical Engineering Department of Virginia Tech. The Center focuses on theoretical and experimental research associated with intelligent material systems, adaptive structures, and smart structures to integrate structures, actuators, sensors, and control systems, allowing them to adaptively change or respond to external conditions. Examples of these mechatronic structures include buildings, bridges, and roadways that can sense and control damage, aircraft that can actively monitor structural integrity, and automotive components that use active materials to reduce vibrations and enhance performance. Current research areas at CIMSS include the design and analysis of smart systems and structures, active control and health monitoring techniques for civil infrastructure systems and aerospace structures, the design of actuators, sensors, and hybrid control systems, and the development of sensory systems for health monitoring.

The Monosys group (http://www.aguide.net) issues a free quality business-to-business magazine called Guide to Monitoring distributed worldwide every three months to assist the needs and interests of civil engineers in respect to systems, control processes, equipment, and instrumentation used for materials technology and monitoring applications in the built infrastructure. This site also has an online database, which lists manufacturers, specialist companies, and interested parties in the Monitoring Industry.

The AMADEUS (http://www.me.ic.ac.uk/dynamics/struct/AMADEUS/amadeus.html) web site describes the Accurate Modeling and Damage Detection in High Safety and Cost Structures (AMADEUS) project funded by the Commission of the European Union under the Brite-EuRam Framework III. This site is constructed and currently maintained by Dr. Chaoping Zang and Dr. Mehmet Imregun at the Mechanical Engineering Department of the Imperial College of Science, Technology, & Medicine, UK. The site describes the ultimate industrial objective of AMADEUS as developing methods, procedures, and guidelines for routine, nondestructive, in-service maintenance monitoring and damage detection in high safety and cost structures. The previous meeting schedules and some of the past presentation materials are available for download.

The Drexel Intelligent Infrastructure and Transportation Safety Institute (http://www.di3.drexel.edu) is a university-government-industry partnership, established in 1997. The primary objective of this institute is exploring and understanding the issues involved in objectively evaluating, integrating, and managing all the components of a transportation system from one single platform. It is intended to serve as a multidisciplinary generator for knowledge and products for infrastructure health monitoring and management by capitalizing on information and other technologies. This web site also provides a link to Drexel Intelligent Infrastructure Laboratory that supports several ongoing field research projects and facilitates advances in structural health monitoring research areas. Two physical laboratory models (Demonstrator and Test Beam) were created along with controlled load input systems, extensive instrumentation, data acquisition, and online monitoring capabilities to serve as a tool to develop, evaluate, demonstrate, and validate structural health monitoring, damage assessment techniques, integration of experimental systems, and intelligent-automated control systems in structural engineering. Online live web camera provides real-time data from the demonstrator and the test beam.

The main objective of the structural dynamics group in COST (http://www.belspo.be/cost) Action F3 is to increase the knowledge required for improving the structural design, the mechanical reliability and the safety of structures in the field of linear and nonlinear dynamics. As model updating procedures are used to build a representative model of dynamic systems, they can also be used to detect damage on structures and monitor health conditions in general.

Updating methods open new possibilities in the field of predictive maintenance, default diagnosis, and characterization of the mechanical signature of structures. Furthermore, the complexity of today's mechanical systems and their increased level of performance make it necessary to model nonlinear effects that were not of as much importance in previous analyses. These effects include nonlinear dynamics, mechanisms for damping and dissipation of energy, and the phenomena of energy localization. The research action is divided into three working groups dealing respectively with the following issues: (1) finite element model updating methods; (2) health monitoring and damage detection; and (3) the identification of nonlinear systems.

7.3 Conferences

There have been an increasing number of conferences to bring together researchers, customers, industrial partners, and government agencies in diverse disciplines to study this emerging structural health monitoring problem.

Annual Symposium on Smart Structures and Materials (San Diego, 1997; San Diego, 1998, Newport Beach, 1999; Newport Beach, 2000; Newport Beach, 2001) and *Non-Destructive Evaluation Techniques for Aging Infrastructure & Manufacturing* (San Antonio, 1998; Newport Beach, 1999; Newport Beach, 2000; Newport Beach, 2001) are two annual conferences organized by the Society of Optical Engineering (SPIE). These two conferences have been carried on jointly for the last few years, and they are annually held on the west coast of the United States in March. More information can be found at the SPIE's web site (www.spie.org).

Another annual conference for the structural dynamics community is the *International Modal Analysis Conference* (IMAC 1982–2001) organized by the Society of Experimental Mechanics (www.sem.org). Although the first few IMACs were devoted to experimental modal analysis, the recent IMACs encompass a variety of subjects in the general structural dynamics field. The theme of the latest IMAC was "Smart Structures and Transducers," and it was held in February 4–7, 2002, Los Angeles, California.

Starting in September 1997, *the International Workshop on Structural Health Monitoring* has been held at Stanford University (1997, 1999, 2001) every other year. This workshop is organized by Prof. F. K. Chang at Stanford, and further information for the upcoming 2003 workshop can be found at http://structure.stanford.edu/workshop.

The *DAMAS Conference* has also been held on alternate years, and this conference is mainly targeting the research community in Europe. The first one was held at Pescara, Italy, in 1995, and the subsequent ones have been held at the University of Sheffield, UK, 1997; Dublin, Ireland, 1999; Cardiff University, Wales, UK, 2001; and South Hampton, UK, 2003, respectively. The next conference is scheduled to take place in 2005 at Gdansk, Poland.

Other European conferences include *1st-5th European Conferences on Smart Structures & Materials* (Scotland, 1992; United Kingdom 1994; France, 1996; United Kingdom 1998; United Kingdom, 2000), *European COST F3 Conferences* (Identification in Engineering Systems, University of Wales Swansea, UK, 1999; System Identification and Structural Health Monitoring, Universidad Politécnica de Madrid, Spain, 2000; Structural System Identification, University of Kassel, Germany, 2001), and the *International Seminar on Modal Analysis* (Katholieke Universiteit Leuven in Belgium, 1996, 1998, and 2000).

The *World Conference on Structural Control* is another resource for structural health monitoring and damage detection research activities. The first two conferences were held at Pasadena, California (August 3–5, 1994), and Kyoto, Japan (July 28–July 1, 1998), respectively. This conference takes place every four years, and the last one was held in April 7–11, 2002, in Como, Italy.

The *International Congress on Condition Monitoring and Diagnostic Engineering Management (COMADEM)* is an annual congress organized by the Society for Machinery Failure Prevention Technology (MFPT). COMADEM provides a forum for the exchange of ideas and accomplishments in such areas as sensors technology, failure mode and mechanisms, root-cause failure analysis, condition monitoring, predictive maintenance, prognostics technology, tribology, condition-based maintenance, nondestructive evaluation and testing, life extension and integrated diagnostics, mainly for rotation machinery.

In addition, two new conferences have been recently established that specifically address the structural health monitoring problems. The *European Workshop on Structural Health Monitoring* will take place in Europe every two years alternatively with the aforementioned Stanford Workshop. The first workshop (http://www.onera.fr/congres/shm2002) was held at Paris, France, in July 10–12, 2002. The next European workshops will be held at Munich, Germany, in 2004. Another new SHM conference, *the First International Workshop on Structural Health Monitoring of Innovative Structures*, was also held in September 19–20, 2002, at Winnipeg, Manitoba, Canada. This conference is sponsored by Intelligent Sensing for Innovative Structures (ISIS) in Canada, and more details regarding the conference can be found at http://www.isiscanada.com/Conference/SHM_Conference/SHM_conference.htm.

7.4 Technical Journals

The Journal of Intelligent Material Systems and Structures, which is published by SAGE Publications (http://www.sagepub.co.uk), is an independent journal devoted to the prompt publication of original papers reporting the results of experimental or theoretical work on any aspect of intelligent materials systems and/or structures research such as fiber-optic sensors, structural health monitoring, MEMS, biomimetics, the applied mathematics of phase transitions and materials science, neural networks, structural dynamic control, adaptive and sensing materials, distributed control, parallel processing, organic chemistry, composite mechanics and processing, biomaterials, and electronic materials.

The Smart Materials and Structures Journal is dedicated to technical advances in smart materials and structures, and this journal covers both basic and applied research in physics, engineering, and materials science, and industrial applications. Particularly, this journal has some of the most popular articles from the 2001 Structural Health Monitoring special issue. The electronic version of the articles can be downloaded from the publishers web site: http://www.iop.org/Journals/sm.

The *Shock and Vibration Digest* presents information about current and emerging vibration technology for researchers and practicing engineers. This journal also includes timely abstracts from a wide range of current literature, proceedings, and conferences related to vibration. The abstracts are arranged in technical categories that allow the reader to follow specific areas of

interest with minimal effort. Specific areas of interest include machines, computational techniques, testing systems, smart structures, structural components, vehicles, experimental tests, mechanical components, design, control techniques, structures, modeling techniques, human response, health monitoring, and predictive maintenance. This journal is available electronically to members of institutions with a print subscription. More information about electronic access can be found at http://www.sagepub.co.uk.

Articles from the *Journal of Sound and Vibration* are also available online through the Academic Press' online library called IDEA (http://www.academicpress.com/jsv) free of charge. Another SHM-related journal maintained by the Academic Press Publisher is *Mechanical Systems and Signal Processing* (http://www.academicpress.com/mssp). This journal facilitates the application and integration of advances in instrumentation and associated computing power with systems theory, signal processing, control theory, and statistics.

Application-specific journals where SHM articles can be found include *AIAA Journal* (www.aiaa.org) for the advancement of the science and technology of astronautics and aeronautics, *ASME Journal of Vibration and Acoustics* (www.asme.org) for the application of the physical principles of acoustics to the solution of noise control problems and to industrial and medical applications, *ASCE Journal of Structural Engineering* (www.asce.org) for the design, analysis, safety, and fabrication of structures ranging from bridges to transmission towers and tall buildings.

Earthquake Engineering and Structural Dynamics (http://www.interscience.wiley.com), *Sound and Vibration* (http://www.sandvmag.com), *P/PM Technology* (http://www.ppmtech.com), *Test Engineering & Management* (http://www.mattingley-publ.com) also have valuable articles related to SHM and condition-based monitoring.

Finally, *An International Journal of Structural Health Monitoring* (www.sagepub.co.kr) is being launched in July 2002 to publish peer-reviewed papers that contain theoretical, analytical, and experimental investigations that will advance the body of knowledge and its application in the discipline of structural health monitoring. It was published twice in 2002 and will be issued quarterly from 2003 on.

8. SUMMARY

Many damage detection methods that we have reviewed attempt to identify damage by solving an inverse problem, which often requires the construction of analytical models. In particular, the finite element model based techniques first construct an objective function based on the measured quantities and the predicted response from the analytical model. Then, an optimization problem is solved to minimize or maximize the object function. This dependency on prior analytical models, which often have significant uncertainties and are not fully validated with experimental data, makes these approaches less attractive for certain applications. This issue was already identified in the previous review and a lot of work is still needed in the field of model updating and validation. None of the reviewed literature thoroughly verified their numerical models nor quantified the associated uncertainties before employing these models for damage detection applications. In addition, this approach to damage identification will have specific difficulties when trying to handle operational and environmental variability as well as when systems exhibit significant nonlinear responses.

Some researchers try to avoid this dependency on the numerical models by performing signal-based unsupervised learning. These approaches include novelty/outlier analysis, statistical process control charts, and simple hypothesis testing. These approaches are demonstrated to be very effective for identifying the onset of damage growth, and they are identified as one of the most significant improvements since the previous literature review. Although these signal-based approaches only identify the existence and location of damage, this level one and two damage identification might be sufficient for many practical applications. However, if one is interested in identifying damage types and amounts, techniques based on a supervised learning mode are most likely adapted.

Another way of solving the inverse problem is the employment of neural network approaches. A neural network can be used to map the inverse relationship between the measured responses and the structural parameters of interest based on training data sets. Various derivations of this basic neural network approach have been reported in both this and the previous literature reviews. However, most of the reviewed neural-network-based approaches suffer from a single common drawback that the training is performed in a supervised mode and that this training

requires a large amount of training data sets from both the undamaged and damaged structures. Because the acquisition of data sets from the damaged structure is prohibitive for most applications, many studies attempt to generate the training data sets associated with various damage cases from numerical simulations. Therefore, the success of these neural network approaches again depends on the fidelity of the employed analytical models.

One of the main obstacles for deploying a monitoring system on-site is the environmental and operational variation of structures. Although many damage detection techniques are successfully applied to scaled models or specimen tests in controlled laboratory environments, the performance of these techniques in real operational environments is still questionable and needs to be validated. Often the so-called damage-sensitive features employed in these damage detection techniques are also sensitive to changes of the environmental and operational conditions of the structures. Currently various sensors are available to measure parameters relevant to these ambient conditions of the structure and, in fact, several structures in the field are reported to have various instrumentations such as thermocouples, anemometers, and humidity sensors. However, the information gathered from these sensors is not directly tied to the existing damage detection algorithms. Therefore, these ambient variations of the system need to be explicitly considered in the process of structural health monitoring. Based on this review, it is the author's opinion that very little work has been conducted in this area.

Another area of future work is statistical model development. Compared to the previous review, a larger number of works is reported to have some form of statistical approach in their damage decision-making process. However, most of the statistical approaches stay in very primitive forms. For instance, almost all of the damage detection techniques reviewed in this and the previous reports assume the Gaussian distribution of a feature space and establish decision-making threshold values based on this normality assumption. The validity of this normality assumption should first be evaluated before the subsequent establishment of the decision boundaries. Even if the actual feature distribution is close to a normal distribution, the parameter estimation of the assumed normal distribution mainly weighs the central population of the feature distribution. It should be noted that one is most likely interested in the tails of the distribution for damage detection applications because it is anomalies from the rest of the population that are related to damage occurrence. Recent work is underway in Los Alamos to

establish damage decision criteria parameterizing the maximum and minimum values of the feature distribution using Extreme Value Statistics (Castillo 1988 and Worden et al. 2002).

The majority of the reviewed damage detection techniques are still based on linearity assumptions of models that are fit to measured data, in spite of the fact that many researchers point out the inherent nonlinear nature of structural damage. Linear system models fail particularly when the systems operate over wide ranges. For instance, a linear model of the rigid body modes of an aircraft might be accurate most of the time. However, if the aircraft experiences strange aerodynamic loads occasionally, the linear model breaks down and this is when damage is most likely accumulated. A handful of researchers take advantage of the nonlinear characteristics of damage in the identification process. For instant, several nonlinearity identification techniques are successfully applied to damage detection problems.

Another issue frequently addressed in this review is the development of an autonomous monitoring system. The recent advances in sensing technologies and hardware make this development feasible, but much work is needed to automate system identification and damage diagnosis algorithms. To date, the majority of the reviewed damage detection techniques require user-interaction to make a final decision regarding the damage state of the structure. In addition, it is well accepted by the modal testing community that the variation of extracted modal parameters attributed to different analyst and extraction algorithms can often be larger that the changes of these modal parameters caused by damage. Therefore, the automation of the damage detection algorithms is necessary to remove the uncertainty involved by user interfaces and to make autonomous decisions. An example of such an automation is the Sequential Probability Ratio Test (Ghosh 1970). This method is proven to be useful for process monitoring in nuclear power plants, and this test can be applied to damage diagnosis problems by automating the decision-making process.

As a related issue, significant progress has been made in modal parameter identification techniques when input measurements are not available. As mentioned in the previous review, the need to reduce the dependence upon measurable excitation forces is critical for the long-term monitoring of structures such as bridges and offshore platforms. Therefore, this modal parameter extraction technique without an input record is an important issue for civil structure monitoring

because their loading conditions under normal operation are often unknown. Furthermore, several promising research works are reported to automate this identification process. This development of an automated system identification process will be a prerequisite for many robust monitoring systems.

To date, interactions between global vibration-based damage-detection methods and local nondestructive testing techniques have been missing. Because of the conventional practice taken where the global monitoring is accomplished with a limited number of sensors dispersed over a relatively large area of a structure, such sensing systems provide the spatial resolution that can only detect fairly significant damage. The use of a few sparsely located sensors to determine the location and degree of damage present is not adequate to fully assess the condition of the structure when damage is local. On the other hand, many local nondestructive techniques require *a priori* knowledge of potential damage locations for damage assessment. Therefore, it is the authors' opinion that multiscale monitoring that integrates local nondestructive inspection and global vibration testing will be beneficiary for many applications. For instance, a local active sensing system such as the Lamb wave propagation method or the impedance method can be used to detect the formation of incipient damage. Then, a global vibration test can be performed to quantify the effects of the local damage on the global system response (e.g., how local debonding in a composite wing near a fuselage affects the flutter characteristic of the aircraft).

This integration of the local active sensing and global vibration-based monitoring also demands better sensor technologies. Recent advances in MEMS, fiber optics, and piezoceramic sensors are making it feasible to deploy nonintrusive, ubiquitous, multipurpose sensors at affordable costs. Furthermore, as a new generation of sensing technologies pushes the limits of scale, the cabling and bookkeeping of multiple sensors has become an issue. Although wireless communication technology can provide a partial solution to this problem, unwavering power supply to the transmitter remains largely unsolved, and the functionality of the sensors themselves needs to be diagnosed for long-term continuous monitoring applications.

Conventional engineering practice in SHM is replete with studies that focus on the development of either new hardware for the sensing aspect of SHM or new software for the data interrogation portion of the problem. Few studies have addressed both the hardware and software aspects of

SHM in an integrated manner. The basic problem is that no sensing system has been developed with the intent of specifically addressing issues related to SHM. To date, the standard practice in the SHM community has been to adapt off-the-shelf sensing technologies to a particular proof-of-concept experiment. However, our goal of developing a SHM system that goes beyond the laboratory demonstration and can be deployed in the field on real-world structures necessitates that new sensing hardware must be developed in conjunction with the data interrogation algorithms. Little work has been reported on this subject.

The ultimate goal of structural health monitoring will be *damage prognosis*, which estimates the remaining service life of a structure given the measurement and assessment of its current damaged state and accompanying its predicted performance in the anticipated future loading environments. Every industry is interested in detecting degradation and deterioration in its structural and mechanical infrastructure at the earliest possible state and in predicting the remaining useful life of the systems. Industry's desire to perform such damage diagnosis and prognosis is based on the tremendous economic and life-safety benefits that these technologies can offer. Damage diagnosis and prognosis solutions can be used to monitor systems to confirm system integrity in normal and extreme loading environments, to estimate the probability of mission completion and personnel survivability, to determine the optimal time needed for preventive maintenance, and to develop appropriate design modifications that present observed damage propagation. Many industries are moving towards selling maintenance service rather than final products. This paradigm shift in business practice is imposing a heavy reliance on reducing maintenance cost through condition-based monitoring and performance prediction. The ESA-WR group in Los Alamos National Laboratory recently initiated a three-year damage prognosis project mainly to investigate the onset of delamination in composite materials and to predict the propagation of fatigue and crack damage afterward. More details on our damage prognosis efforts can be found in Farrar et al. (2003).

Finally, it is our plan to update this literature review every 5 or 6 years. Therefore, if the readers are interested in having your and your colleagues' research work included in our future literature reviews, please send emails to sohn@lanl.gov.

ACKNOWLEDGMENTS

Support for this project was provided by Los Alamos National Laboratory through the Laboratory Directed Research and Development (LDRD) program (8M05-X1MV-0000-0000), which makes investments in innovative science and technology in areas of science and technology at the discretion of the Laboratory Director, as opposed to those determined by an external funding agency.

REFERENCES

1. Abe, M., Fujino, Y., Kajimura, M., Yanagihara, M., and Sato, M. (1999) "Monitoring of a Long Span Suspension Bridge by Ambient Vibration Measurement," *Structural Health Monitoring 2000*, Stanford University, Palo Alto, California, pp. 400–407.

2. Adams, D.E., and Farrar, C.R. (2002) "Application of Frequency Domain ARX Features for Linear and Nonlinear Structural Damage Identification," Proceedings of SPIE's 9th Annual International Symposium on Smart Structures and Materials, San Diego, California.

3. Agneni, A., Crema, L.B., and Mastroddi, F. (2000) "Damage Detection from Truncated Frequency Response Functions," *European COST F3 Conference on System Identification and Structural Health Monitoring*, Madrid, Spain, pp. 137–146.

4. Ahmadian, H., Mottershead, J.E., and Friswell, M.I. (1997) "Substructure Modes for Damage Detection," *Structural Damage Assessment Using Advanced Signal Processing Procedures*, Proceedings of DAMAS '97, University of Sheffield, UK, pp. 257–268.

5. Aktan, A.E., Catbas, F.N., Grimmelsman, K.A., and Tsikos, C.J. (2000) "Issues in Infrastructure Health Monitoring for Management," *Journal of Engineering Mechanics*, Vol. 126, No. 7, pp. 711–724.

6. Aktan, A.E., Tsikos, C.J., Catbas, F.N., Grimmelsman, K., and Barrish, R. (1999) "Challenges and Opportunities in Bridge Health Monitoring," *Structural Health Monitoring 2000*, Stanford University, Palo Alto, California, pp. 461–473.

7. Alexiou, K. (2000) "Accurate Modeling and Damage Detection in High Safety and Cost Structures (AMADEUS)," *European COST F3 Conference on System Identification and Structural Health Monitoring*, Madrid, Spain, pp. 667–675.

8. Alexiou, K., Luengo Martin, P., Zang, C., and Imregun, M. (2000) "Two Frequency-Domain Criteria for Test/Analysis Correlation and Finite Element Model Updating," *European COST F3 Conference on System Identification and Structural Health Monitoring*, Madrid, Spain, pp. 731–740.

9. Al-Khalidy, A., Noori, M., Hou, Z., Yamamoto, S., Masuda, A., and Sone, A. (1997) "Health Monitoring Systems of Linear Structures Using Wavelet Analysis," *Structural Health Monitoring, Current Status and Perspectives*, Stanford University, Palo Alto, California, pp. 164–175.

10. Austin, T., Singh, M., Gregson, P., Dakin, J., and Powell, P. (1999) "Damage Assessment in Hybrid Laminates Using an Array of Embedded Fibre Optic Sensors," *Smart Structures and Materials 1999: Smart Systems for Bridges, Structures, and Highways*, Proceedings of SPIE, Vol. 3,671, pp. 281–288.

11. Ayres, J.W., Rogers, C.A., and Chaudhry, Z.A. (1996), "Qualitative Health Monitoring of a Steel Bridge Joint via Piezoelectric Acutator/Sensor Patches," Proceedings of SPIE, Vol. 2,719, pp. 123–131.

12. Badcock, R.A., and Birt, E.A. (2000) "The Use of 0-3 Piezocomposite Embedded Lamb Wave Sensors for Detection of Damage in Advanced Fibre Composite," *Smart Materials and Structures*, Vol. 9, pp. 291–297.

13. Balis Crema, L., and Mastroddi, F. (1998) "A Direct Approach for Updating and Damage Detection by Using FRF Data," *Proceedings of ISMA23, Noise and Vibration Engineering*, Leuven, Belgium.

14. Barai, S.V., and Pandey, P.C. (1997) "Time-Delay Neural Networks in Damage Detection of Railway Bridges," *Advances in Engineering Software*, Vol. 28, pp. 1–10.

15. Barnett, V., and Lewis, T. (1994) *Outliers in Statistical Data*, John Wiley & Sons, Chichester, England.

16. Bartelds, G. (1997) "Aircraft Structural Health Monitoring, Prospects for Smart Solutions from a European Viewpoint," *Structural Health Monitoring, Current Status and Perspectives*, Stanford University, Palo Alto, California, pp. 293–300.

17. Basseville, M., Abdelghani, M., and Benveniste, A. (2000) "Subspace-Based Fault Detection Algorithms for Vibration Monitoring," *Autometica*, Vol. 36, No. 1, pp. 101–109.

18. Beard, S., and Chang, Fu-Kuo (1997) "Active Damage Detection in Filament Wound Composite Tubes Using Built-In Sensors and Actuators," *Journal of Intelligent Material Systems and Structures*, Vol. 8, pp. 891–897.

19. Beardsley, P.J., Hemez, F.M., and Doebling, S.W. (1999) "Updating Nonlinear Finite Element Models in the Time Domain," *Structural Health Monitoring 2000*, Stanford University, Palo Alto, California, pp. 774–783.

20. Beck, J., Papdimitriou, C., Au, S., and Vanik, M. (1998) "Entropy-Based Optimal Sensor Location for Structural Damage Detection," *Smart Systems for Bridges, Structures, and Highways*, Proceedings of SPIE, Vol. 3,325, pp. 161–172.

21. Beck, J.L., Chan, E., and Papadimitriou, C. (1998) "Statistical Methodology for Optimal Sensor Locations for Damage Detection in Structures," *Proceedings of the International Modal Analysis Conference*, pp. 349–355.

22. Beck, J.L., Chan, E., and Papadimitriou, C. (1998) "Statistical Methodology for Optimal Sensor Locations for Damage Detection in Structures," *Proceedings of the International Modal Analysis Conference*, pp. 349–355.

23. Bendat, J.S., and Piersol, A.G. (1980) *Engineering Applications of Correlation and Spectral Analysis*, John Wiley and Sons, New York, pp. 274.

24. Bendat, J.S. (1964) "Vibration-Data Analysis," J. Acoust. Soc. Am., Vol. 36, No. 5, p. 1,020.

25. Bennett, R., Hayes-Gill, B., Crowe, J., Armitage, R., Rodgers, D., and Hendroff, A. (1999) "Wireless Monitoring of Highways," *Smart Structures and Materials 1999: Smart Systems for Bridges, Structures, and Highways,* Proceedings of SPIE, Vol. 3,671, pp. 173–182.

26. Bergmeister, K., and Santa, U. (2000) "Global Monitoring for Bridges," *Nondestructive Evaluation of Highways, Utilities, and Pipelines*, Proceedings of SPIE, Vol. 3,995, pp. 14–25.

27. Bernal, D. (2000a) "Extracting Flexibility Matrices from State-Space Realizations," *European COST F3 Conference on System Identification and Structural Health Monitoring*, Madrid, Spain, pp. 127–135.

28. Bernal, D. (2000b) "Damage Localization Using Load Vectors," *European COST F3 Conference on System Identification and Structural Health Monitoring*, Madrid, Spain, pp. 223–231.

29. Biemans, C., Staszewski, W.J., Boller, C., and Tomlinson, G.R. (1999) "Crack Detection in Metallic Structures Using Piezoceramic Sensors," *Damage Assessment of Structures*, Proceedings of the International Conference on Damage Assessment of Structures (DAMAS 99), Dublin, Ireland, pp. 112–121.

30. Blanas, P., Wenger, M., Rigas, E., and Das-Gupta, D. (1999) "Active Composite Materials as Sensing Elements for Fiber Reinforced Smart Composite Structures," *Smart Structures and Integrated Systems,* Proceedings of SPIE, Vol. 3,329, pp. 482–490.

31. Bodeux, J.B., and Golinval, J.C. (2000) "ARMAV Model Technique for System Identification and Damage Detection," *European COST F3 Conference on System Identification and Structural Health Monitoring*, Madrid, Spain, pp. 303–312.

32. Boller, C. (2000) "Ways and Options For Aircraft Structural Health Management," *European COST F3 Conference on System Identification and Structural Health Monitoring*, Madrid, Spain, pp. 71–82.

33. Bonato, P., Ceravolo, R., De Stefano, A., and Molinari, F. (1999) "Modal Identification by Cross-Time-Frequency Estimators," *Damage Assessment of Structures*, Proceedings of the International Conference on Damage Assessment of Structures (DAMAS 99), Dublin, Ireland, pp. 363–372.

34. Borinski, J., Meller, S.A., Pulliam, W., Murphy, K.A., and Schetz, J. (2000) "Optical Fiber Sensors for In-Flight Health Monitoring," *Smart Structures and Materials 2000: Sensory Phenomena and Measurement Instrumentation,* Proceedings of SPIE, Vol. 3,986, pp. 445–454.

35. Bourasseau, N., Moulin, E., Delebarre, C., and Bonniau, P. (2000) "Radome Health Monitoring with Lamb Waves: Experimental Approach," *NDT&E International*, Vol. 33, pp. 393–400.

36. Brandon, J.A. (1997) "Structural Damage Identification of Systems with Strong Nonlinearities: A Qualitative Identification Methodology," *Structural Damage Assessment Using Advanced Signal Processing Procedures*, Proceedings of DAMAS '97, University of Sheffield, UK, pp. 287–298.

37. Brandon, J.A. (1999) "Towards a Nonlinear Identification Methodology for Mechanical Signature Analysis," *Damage Assessment of Structures*, Proceedings of the International Conference on Damage Assessment of Structures (DAMAS 99), Dublin, Ireland, pp. 265–272.

38. Brandon, J.A., Stephens, A.E., Lopes, E.M.O., and Kwan, A.S.K. (1999) "Spectral Indicators in Structural Damage Identification: A Case Study," *Proceedings of the Institute of Mechanical Engineers*, Vol. 213, Part C, pp. 1–5.

39. Brownjohn, J.M.W. (1997) "Vibration Characteristics of a Suspension Footbridge," *Journal of Sound and Vibration*, Vol. 202, No. 1, pp. 29–46.

40. Burton, T.D., Farrar, C.R., and Doebling, S.W. (1998) "Two Methods for Model Updating Using Damage Ritz Vectors," *Proceedings of the International Modal Analysis Conference*, pp. 973–979.

41. Calcada, R., Cunha, A., and Delgado, R. (2000) "A Project for the Experimental and Numerical Assessment of Dynamic Effects of Road Traffic on Bridges," *European COST F3 Conference on System Identification and Structural Health Monitoring*, Madrid, Spain, pp. 313–322.

42. Campanile, L.F., and Melcher, J. (1994) "Modal Damage Diagnosis and Adaptive Filter Technique: A Strategy for Smart Structural Health Monitoring," *Conference on Adaptive Structures*, Sendai, Japan.

43. Carrasco, C., Osegueda, R., Ferregut, C., and Grygier, M. (1997) "Localization and Quantification of Damage in a Space Truss Model Using Modal Strain Energy," *Smart Systems for Bridges, Structures, and Highways*, Proceedings of SPIE, Vol. 3,043, pp. 181–192.

44. Castillo, E. (1988) *Extreme Value Theory in Engineering*, Academic Press, Inc., New York, New York.

45. Catbas, F.N., Grimmelsman, K.A., Barrish, R.A., Tsikos, C.J., and Aktan, A.E. (1999) "Structural Identification and Health Monitoring of a Long-Span Bridge," *Structural Health Monitoring 2000*, Stanford University, Palo Alto, California, pp. 417–429.

46. Cawley, P. (1997) "Long Range Inspection of Structures Using Low Frequency Ultrasound," in *Structural Damage Assessment Using Advanced Signal Processing Procedures*, Proceedings of DAMAS '97, University of Sheffield, UK, pp. 1–17.

47. Cawley, P., and Adams, R.D. (1979) "The Location of Defects in Structures from Measurements of Natural Frequencies," *Journal of Strain Analysis*, Vol. 14, No. 2, pp. 49–57.

48. Celebi, M. (1999) "GPS in Dynamic Monitoring of Long-Period Structures," *Structural Health Monitoring 2000*, Stanford University, Palo Alto, California, pp. 337–345.

49. Cerri, M.N., and Vestroni, F. (2000) "Identification of Damage in Reinforced Concrete Beams," *European COST F3 Conference on System Identification and Structural Health Monitoring*, Madrid, Spain, pp. 179–189.

50. Chan, T.H., Ni, Y.Q., and Ko, J.M. (1999) "Neural Network Novelty Filtering for Anomaly Detection of Tsing Ma Bridge Cables," *Structural Health Monitoring 2000*, Stanford University, Palo Alto, California, pp. 430–439.

51. Chang, C.C., Chang, T.Y.P, Xu, Y.G., and Wang, M.L. (2000) "Structural Damage Detection Using an Iterative Neural Network," *Journal of Intelligent Material Systems and Structures*, Vol. 11, pp. 32–42.

52. Chang, F.K. (1999) "Structural Health Monitoring: A Summary Report on the First International Workshop on Structural Health Monitoring, September 18–20, 1997," *Structural Health Monitoring 2000*, Stanford University, Palo Alto, California.

53. Chang, T.Y.P., Chang, C.C., and Xu, Y.G. (1999) "Updating Structural Parameters: An Adaptive Neural Network Approach," *Structural Health Monitoring 2000*, Stanford University, Palo Alto, California, pp. 379–389.

54. Chattopadhyay, A., Dragomir-Daescu, D., and Gu (1997) "Dynamic Response of Smart Composites with Delaminations," *Structural Health Monitoring, Current Status and Perspectives*, Stanford University, Palo Alto, California, pp. 729–740.

55. Chaudhari, T.D., and Maiti, S.K. (1999) "Crack Detection in Geometrically Segmented Beams," *Damage Assessment of Structures*, Proceedings of the International Conference on Damage Assessment of Structures (DAMAS 99), Dublin, Ireland, pp. 343–353.

56. Chen, G., and Ewins, D.J. (2000) "Verification of FE Models for Model Updating," *European COST F3 Conference on System Identification and Structural Health Monitoring*, Madrid, Spain, pp. 709–720.

57. Chen, Z., Cudney, H., Giurgiutiu, V., Rogers, C., Quattrone, R., and Berman, J. (1997) "Full-Scale Ferromagnetic Active Tagging Testing of C-Channel Composite Elements," *Smart Systems for Bridges, Structures, and Highways*, Proceedings of SPIE, Vol. 3,043, pp. 169–180.

58. Choi, M.Y., and Kwon, I.B. (2000) "Damage Detection System of a Real Steel Truss Bridge by Neural Networks," *Smart Structures and Materials 2000: Smart Systems for Bridges, Structures, and Highways*, Proceedings of SPIE, Vol. 3,988, Newport Beach, California, pp. 295–306.

59. Choi, S., and Stubbs, N. (1997) "Nondestructive Damage Detection Algorithms for 2D Plates," *Smart Systems for Bridges, Structures, and Highways*, Proceedings of SPIE, Vol. 3,043, pp. 193–204.

60. Chong, K.P. (1997) "Health Monitoring of Civil Structures," *Structural Health Monitoring, Current Status and Perspectives*, Stanford University, Palo Alto, California, pp. 339–350.

61. Chouaki, A., and Ladeveze, P. (2000) "Application of a Modelling Error Estimator for Health Monitoring and Damage Detection," *Proceedings of ISMA25, Noise and Vibration Engineering*, Leuven, Belgium.

62. Chung, D.D.L. (1998) "Self-Monitoring Structural Materials," *Materials Science & Engineering,* Vol. 22, No. 2, pp. 57–78.

63. Cioara, T.G., and Alampalli, S. (2000) "Extracting Reliable Modal Parameters for Monitoring Large Structures," *European COST F3 Conference on System Identification and Structural Health Monitoring*, Madrid, Spain, 333–340.

64. Cohen, E., Mastro, S., Nemarich, C., Korczynski, J., Jarrett, A., and Jones, W. (1999) "Recent Developments in the Use of Plastic Optical Fiber for an Embedded Wear Sensor," *Smart Structures and Materials 1999: Sensory Phenomena and Measurement Instrumentation for Smart Structures and Materials*, Proceedings of SPIE, Vol. 3,670, pp. 256–267.

65. Cover, T.M., and Thomas, J.A. (1991) *Elements of Information Theory*, John Wiley & Sons, Inc., New York, New York.

66. Cowan, R.S., and Winer, W.O. (1999) "Research Developments in Integrated Diagnostics and Prognostics," *Structural Health Monitoring 2000*, Stanford University, Palo Alto, California, pp. 237–246.

67. Davis, M., Bellemore, D., Berkoff, T., Kersey, A., Putnam, M., Idriss, R., and Kodinduma, M. (1996) "Fiber-Optic Sensor System for Bridge Monitoring with Both Static Load and Dynamic Modal Sensing Capabilities," *Nondestructive Evaluation of Bridges and Highways*, Proceedings of SPIE, Vol. 2,946, pp. 219–232.

68. De Callafon, R.A. (1999) "On-Line Damage Identification Using Model Based Orthonormal Functions," *Structural Health Monitoring 2000*, Stanford University, Palo Alto, California, pp. 912–920.

69. De Stefano, A., Sabia, D., and Sabia, L. (1997) "Structural Identification Using ARMAV Models from Noisy Dynamic Response under Unknown Random Excitation," *Structural Damage Assessment Using Advanced Signal Processing Procedures*, Proceedings of DAMAS '97, University of Sheffield, UK, pp. 419–428.

70. di Scalea, F.L., Karbhari, V.M., and Seible, F. (2000) "The I-5/Gilman Advanced Technology Bridge Project," *Smart Structures and Materials 2000: Smart Systems for Bridges, Structures, and Highways*, Proceedings of SPIE, Vol. 3,988, Newport Beach, California, pp. 10–17.

71. Doebling, S.W., and C.R. Farrar (1997) "Using Statistical Analysis to Enhance Modal-Based Damage Identification," in *Structural Damage Assessment Using Advanced Signal Processing Procedures*, Proceedings of DAMAS '97, University of Sheffield, UK, pp. 199–210.

72. Doebling, S.W., C.R. Farrar, M.B. Prime, and DW. Shevitz (1996) "Damage Identification and Health Monitoring of Structural and Mechanical Systems from Changes in their Vibration Characteristics: A Literature Review," Los Alamos National Laboratory report LA-13070-MS.

73. Doebling, S.W., C.R. Farrar, M.B. Prime, and D.W. Shevitz (1998) "A Review of Damage Identification Methods that Examine Changes in Dynamic Properties," *Shock and Vibration Digest* 30 (2), pp. 91–105.

74. Doebling, S.W., Farrar, C.R., and Cornwell, P.J. (1997) "A Computer Toolbox for Damage Identification Based on Changes in Vibration Characteristics," *Structural Health Monitoring, Current Status and Perspectives*, Stanford University, Palo Alto, California, pp. 241–254.

75. Dubow, J., Zhang, W., Bingham, J., Syammach, F., Krantz, D., Belk, J., Bierman, P., Harjani, R., Mantell, S., Polla, D., and Troyk, P. (1999) "Embedded Cure Monitor, Strain Gauge, and Mechanical State Estimator," *Smart Electronics and MEMS*, Proceedings of SPIE, Vol. 3,673, pp. 336–350.

76. Dunn, K., Louthan, M., Iyer, N., Giurgiutiu, V., Petrou, M., and Laub, D. (1999) "Application of Smart Materials/Technology at the Savannah River Site," *Smart Structures and Materials 1999: Smart Systems for Bridges, Structures, and Highways*, Proceedings of SPIE, Vol. 3,671, pp. 64–75.

77. Efroymson, M.A. (1960) "Multiple Regression Analysis," *Mathematical Methods for Digital Computers*, A. Ralston, and H.S. Wilf, Editors, John Wiley and Sons, New York, pp. 291–302.

78. Elvin, N., and Leung, C. (1997) "Feasibility of Delamination Detection with Embedded Optical Fibers," *Smart Structures and Integrated Systems*, Proceedings of SPIE, Vol. 3,041, pp. 627–634.

79. Enright, Michael P., and Frangopol, Dan M. (1999) "Condition Prediction of Deteriorating Concrete Bridges Using Bayesian Updating," *Journal of Structural Engineering*, Vol. 125, No. 10, pp. 1,118–1,125.

80. Ettouney, M., Daddazio, R., and Hapij, A. (1999) "Optimal Sensor Locations for Structures with Multiple Loading Conditions," *Smart Structures and Materials 1999: Smart Systems for Bridges, Structures, and Highways*, Proceedings of SPIE, Vol. 3,671, pp. 78–89.

81. Ettouney, M., Daddazio, R., Hapij, A., and Aly, A. (1998) "Health Monitoring of Complex Structures," *Smart Structures and Materials 1999: Industrial and Commercial Applications of Smart Structures Technologies*, Proceedings of SPIE, Vol. 3,326, pp. 368–379.

82. Faravelli, L., and Pisano, A.A. (1997) "Damage Assessment Toward Performance Control," *Structural Damage Assessment Using Advanced Signal Processing Procedures*, Proceedings of DAMAS '97, University of Sheffield, UK, pp. 185–198.

83. Farrar, C.R., and Doebling, S.W. (1999). "Vibration-Based Structural Damage Identification," accepted for publication by *Philosophical Transactions: Mathematical, Physical and Engineering Sciences*, Royal Society, London, UK.

84. Farrar, C.R., Baker, W.E., Bell, T.M., Cone, K.M., Darling, T.W, Duffey, T.A., Eklund, A., and Migliori, A. (1994) "Dynamic Characterization and Damage Detection in the I-40 Bridge over the Rio Grande," Los Alamos National Laboratory report LA-12767-MS.

85. Farrar, C.R., Sohn, H., Hemez, F.M., Anderson, M.C., Bement, M.T., Cornwell, P.J., Doebling, S.D., Lieven, N., Robertson, A.N., and Schultze, J.F. (2003) "Damage Prognosis: Current Status and Future Needs," Los Alamos National Laboratory report, LA-14051-MS.

86. Felber, A. (1997) "Practical Aspects of Testing Large Bridges for Structural Assessment," *Structural Health Monitoring, Current Status and Perspectives*, Stanford University, Palo Alto, California, pp. 577–588.

87. Feng, M., and Bahng, E. (1999) "Damage Assessment of Bridges with Jacketed RC Columns Using Vibration Test," *Smart Structures and Materials 1999: Smart Systems for Bridges, Structures, and Highways*, Proceedings of SPIE, Vol. 3,671, pp. 316–327.

88. Feng, M.Q., De Flaviis, F., Kim, Y.J., and Diaz, R. (2000) "Application of Electromagnetic Waves in Damage Detection of Concrete Structures," *Smart Structures and Materials 2000: Smart Systems for Bridges, Structures, and Highways*, Proceedings of SPIE, Newport Beach, California, pp. 118–126.

89. Feroz, K.T., and Oyadiji, S.O. (1997) "Damage Assessment of Slotted Bars Using Auto-Correlation Technique," *Structural Damage Assessment Using Advanced Signal Processing Procedures*, Proceedings of DAMAS '97, University of Sheffield, UK, pp. 337–348.

90. Foedinger, R., Rea, D., Sirkis, J., Troll, J., Grande, R., and Vandiver, T.L. (1999) "Structural Health Monitoring and Impact Damage Detection for Filament Wound Composite Pressure Vessels," *Structural Health Monitoring 2000*, Stanford University, Palo Alto, California, pp. 159–169.

91. Foote, P.D. (1999) "Structural Health Monitoring: Tales from Europe," *Structural Health Monitoring 2000*, Stanford University, Palo Alto, California, pp. 24–35.

92. Friswell, M.I., and Penny, J.E.T. (1997) "Is Damage Location Using Vibration Measurements Practical?" *Structural Damage Assessment Using Advanced Signal Processing Procedures*, Proceedings of DAMAS '97, University of Sheffield, UK, pp. 351–362.

93. Fritzen, C.P., and Bohle, K. (1999a) "Identification of Damage in Large Scale Structures by Means of Measured FRFs-Procedure and Application to the I40-Highway Bridge," *Damage Assessment of Structures*, Proceedings of the International Conference on Damage Assessment of Structures (DAMAS 99), Dublin, Ireland, pp. 310–319.

94. Fritzen, C.P., and Bohle, K. (1999b) "Parameter Selection Strategies in Model-Based Damage Detection," *Structural Health Monitoring 2000*, Stanford University, Palo Alto, California, pp. 901–911.

95. Fritzen, C.P., Bohle, K., and Stepping, A. (2000) "Damage Detection in Structures with Multiple Cracks Using Computational Models," *European COST F3 Conference on System Identification and Structural Health Monitoring*, Madrid, Spain, pp. 191–200.

96. Frosch, R.J., and Matamoros, A.B. (1999) "Monitoring and Assessment of Reinforced Concrete Structures," *Structural Health Monitoring 2000*, Stanford University, Palo Alto, California, pp. 494–501.

97. Fukuda, T., and Osaka, K. (1999) "In situ Measuring and Cure Monitoring of Composite Materials in Autoclave Molding," *Structural Health Monitoring 2000*, Stanford University, Palo Alto, California, pp. 247–264.

98. Furrow, P.C., Brown, R.T., and Mott, D.B. (2000) "Fiber Optic Health Monitoring System for Composite Bridge Decks," *Smart Structures and Materials 2000: Smart Systems for Bridges, Structures, and Highways*, Proceedings of SPIE, Vol. 3,988, Newport Beach, California, pp. 380–391.

99. Garcia, G., and Osegueda, R. (2000) "Combining Damage Detection Methods to Improve Probability of Detection," *Smart Structures and Materials 2000: Smart Systems for Bridges, Structures, and Highways*, Proceedings of SPIE, Vol. 3,988, Newport Beach, California, pp. 135–142.

100. Garcia, G., and Stubbs, N. (1997) "Application and Evaluation of Classification Algorithms to a Finite Element Model of A Three-Dimensional Truss Structure for Nondestructive Damage Detection," *Smart Systems for Bridges, Structures, and Highways*, Proceedings of SPIE, Vol. 3,043, pp. 205–216.

101. Garcia, G., Osegueda, R., and Meza, D. (1998) "Comparison of the Damage Detection Results Utilizing an ARMA Model and a FRF Model to Extract the Modal Parameters," *Smart Systems for Bridges, Structures, and Highways*, Proceedings of SPIE, Vol. 3,325, pp. 244–252.

102. Garcia, G.V., and Osegueda, R. (1999) "Damage Detection Using ARMA Model Coefficients," *Smart Structures and Materials 1999: Smart Systems for Bridges, Structures, and Highways*, Proceedings of SPIE, Vol. 3,671, pp. 289–296.

103. Garibaldi, L., Giorcelli, E., Marchesiello, S., and Ruzzene, M. (1999) "CVA-BR Against ARMAV: Comparison over Real Data from an Ambient Noise Excited Bridge," *Damage Assessment of Structures*, Proceedings of the International Conference on Damage Assessment of Structures (DAMAS 99), Dublin, Ireland, pp. 423–431.

104. Garibaldi, L., Marchesiello, S., and Gorman, D.J. (1999) "Bridge Dynamics Misinterpretations due to Low Spatial Resolution and Closeness of Frequencies," *Damage Assessment of Structures*, Proceedings of the International Conference on Damage Assessment of Structures (DAMAS 99), Dublin, Ireland, pp. 411–422.

105. Gaul, L., and Hurlebaus, S. (1999) "Wavelet-Transform to Identify the Location and Force-Time-History of Transient Load in a Plate," *Structural Health Monitoring 2000*, Stanford University, Palo Alto, California, pp. 851–860.

106. Gause, L., Krantz, D., Biermann, P., and Belk, J. (1999) "Early Demonstration of Remotely Queried Microsensors," *Smart Structures and Materials 1999: Smart Electronics and MEMS*, Proceedings of SPIE, Vol. 3,673, pp. 190–194.

107. Gawronski, W. (1998) *Dynamics and Control of Structures: A Modal Approach*, Springer, New York, New York.

108. Gawronski, W., and Sawicki, J.T. (2000) "Structural Damage Detection Using Modal Norms," *Journal of Sound and Vibration,* Vol. 229, pp. 194–198.

109. Ghosh, B.K. (1970) Sequential Test of Statistical Hypotheses, Addison-Wesley Publishing Company, Menlo Park, California.

110. Giles, I., Mondanos, M., Badcock, R., and Lloyd, P. (1999) "Distributed Optical Fibre Based Damage Detection in Composites," *Sensory Phenomena and Measurement Instrumentation for Smart Structures and Materials*, Proceedings of SPIE, Vol. 3,670, pp. 311–321.

111. Giurgiutiu, V., and Rogers, C. (1997) "The Electro-Mechanical (E/M) Impedance Method for Structural Health Monitoring and Non-Destructive Evaluation," International Workshop on Structural Health Monitoring, Stanford University, California, September 18–20, 1997.

112. Giurgiutiu, V., Redmond, J., Roach, D., and Rackow, K. (2000) "Active Sensors for Health Monitoring of Aging Aerospace Structures," *Smart Structures and Materials 2000: Smart Structures and Integrated Systems*, Proceedings of SPIE, Vol. 3,985, pp. 294–305.

113. Goranson, U.G. (1997) "Jet Transport Structures Performance Monitoring," Proceedings of the Stanford Workshop on Structural Health Monitoring, Palo Alto, California, pp. 3–17.

114. Graue, R., and Reutlinger, A. (2000) "Importance and Methods of Structural Health Monitoring For Future Launchers," *European COST F3 Conference on System Identification and Structural Health Monitoring*, Madrid, Spain, pp. 83–94.

115. Gregory, O., Euler, W., Crisman, E., Mogawer, H., and Thomas, K. (1999) "Smart Optical Waveguide Sensors for Cumulative Damage Assessment," *Smart Structures and Materials 1999: Smart Systems for Bridges, Structures, and Highways*, Proceedings of SPIE, Vol. 3,671, pp. 100–108.

116. Halfpenny, A. (1999) "A Frequency Domain Approach for Fatigue Life Estimation from Finite Element Analysis," *Damage Assessment of Structures*, Proceedings of the International Conference on Damage Assessment of Structures (DAMAS 99), Dublin, Ireland, pp. 401–410.

117. Hall, S.R. (1999) "The Effective Management and Use of Structural Health Data," *Structural Health Monitoring 2000*, Stanford University, Palo Alto, California, pp. 265–275.

118. Hammel, I.G. (2001) "Development of a Life Extension Programme for the Bae 146 Regional Aircraft," Masters Thesis in the Department of Aerospace Design, Manufacture and Management at the University of Bristol, UK.

119. Hanagud, S., and Luo, H. (1997) "Damage Detection and Health Monitoring Based on Structural Dynamics," *Structural Health Monitoring, Current Status and Perspectives*, Stanford University, Palo Alto, California, pp. 715–726.

120. Hanselka, H., Melcher, M., Campanile, L.F., and Kaiser, S. (1997) "A Demonstrator for On-line Health Monitoring of Adaptive Structures," *Structural Damage Assessment Using Advanced Signal Processing Procedures*, Proceedings of DAMAS '97, University of Sheffield, UK, pp. 225–236.

121. Haywood, J., Staszewski, W.J., Worden, K. (2001) "Impact Location in Composite Structures Using Smart Sensor Technology and Neural Networks," The 3rd International Workshop on Structural Health Monitoring, Stanford, California, September 12–14, pp. 1,466–1,475.

122. Helmicki, A., Hunt, V., Shell, M., Lenett, M., Turer, A., Dalal, V., and Aktan, A. (1999) "Multidimensional Performance Monitoring of a Recently Constructed Steel-Stringer Bridge," *Proceedings of the 2nd International Workshop on Structural Health Monitoring*, Stanford University, Palo Alto, California, pp. 408–416.

123. Hermann, H.-G., and Streng, J. (1997) "Problem-Specific Neural Networks for Detecting Structural Damage," *Structural Health Monitoring, Current Status and Perspectives*, Stanford University, Palo Alto, California, pp. 267–278.

124. Hermans, L., and Van der Auweraer, H. (1998) "Modal Testing and Analysis of Structures under Operational Conditions: Industrial Applications," *NATO-ASI Modal Analysis and Testing*, Sesimbra, Portugal, May 3–15, pp. 549–563.

125. Heylen, W., and Trendafilova, I. (2000) "Measurement Point Selection in Damage Detection Using the Average Mutual Information," *European COST F3 Conference on System Identification and Structural Health Monitorin*g, Madrid, Spain, pp. 147–156.

126. Heyns, P.S. (1997) "Structural Damage Assessment Using Response-Only Meaurements," *Structural Damage Assessment Using Advanced Signal Processing Procedures*, Proceedings of DAMAS '97, University of Sheffield, UK, pp. 213–223.

127. Hickinbotham, S.J., and Austin, J. (2000) "Novelty Detection for Flight Data from Airframe Strain Gauges," *European COST F3 Conference on System Identification and Structural Health Monitoring*, Madrid, Spain, pp. 773–780.

128. Hitchen, S.A., and Kemp, R.M.J. (1995) "The Effect of Stacking Sequence on Impact Damage in a Carbon Fibre/Epoxy Composite," *Composites*, Vol. 26, pp. 207–214.

129. Ho, Y.K., and Ewins, D.J. (1999) "Numerical Evaluation of the Damage Index," *Structural Health Monitoring 2000*, Stanford University, Palo Alto, California, pp. 995–1,011.

130. Ho, Y.K., and Ewins, D.J. (2000) "On the Structural Damage Identification with Mode Shapes," *European COST F3 Conference on System Identification and Structural Health Monitoring*, Madrid, Spain, pp. 677–686.

131. Hou, Z., Noori, M., and St. Amand, R. (2000) "Wavelet-Based Approach for Structural Damage Detection," *Journal of Engineering Mechanics*, July 2000, pp. 677–683.

132. Huang, R., and Yang, C.C. (1996) "Condition Assessment of Reinforced Concrete Beams Relative to Reinforcement Corrosion," *Cement and Concrete Composites*, Vol. 19, pp. 131–137.

133. Huang, S., Zhao, T., and Chen, W. (1997) "The Evaluation of the Bridge Pavement Samples Using an Optical Fiber Sensor System," *Smart Materials, Structures, and Integrated Systems*, Proceedings of SPIE, Vol. 3,241, pp. 347–352.

134. Hunt, S.R., and Hebden, I.G. (2000) "Validation of the Eurofighter Typhoon Structural Health and Usage Monitoring System," *European COST F3 Conference on System Identification and Structural Health Monitoring*, Madrid, Spain, pp. 743–753.

135. Hyland, D. (1997) "Connectionist Algorithms for Structural System Identification and Anamoly Detection," *Structural Health Monitoring, Current Status and Perspectives*, Stanford University, Palo Alto, California, pp. 18–29.

136. Iglesias, M.J., and Palomino, A. (2000) "SHMS, A Good Chance to Gain Experience to Optimise the Aircraft Structural Capability," *European COST F3 Conference on System Identification and Structural Health Monitoring*, Madrid, Spain, pp. 753–771.

137. Ihler, E., Zaglauer, W., Herold-Schmidt, U., Dittrich, K.W., and Wiesbeck, W. (2000) "Integrated Wireless Piezoelectric Sensors," *Smart Structures and Materials 2000: Industrial and Commercial Applications of Smart Structures Technologies*, Proceedings of SPIE, Vol. 3,991, Newport Beach, California, pp. 44–51.

138. Ikegami, R. (1999) "Structural Health Monitoring: Assessment of Aircraft Customer Needs," *Structural Health Monitoring 2000*, Stanford University, Palo Alto, California, pp. 12–23.

139. Inada, T., Shimamura, Y., Todoroki, A., Kobayashi, H., and Nakamura, H. (1999) "Damage Identification Method for Smart Composite Cantilever Beams with Piezoelectric Materials," *Structural Health Monitoring 2000*, Stanford University, Palo Alto, California, pp. 986–994.

140. Jacob, P.J., Desforges, M.J., and Ball, A.D. (1997) "Analysis of Suitable Wavelet Coefficients for Identificaiton of the Simulated Failure of Composite Materials," *Structural Damage Assessment Using Advanced Signal Processing Procedures*, Proceedings of DAMAS '97, University of Sheffield, UK, pp. 31–40.

141. Jenkins, C. H., Kjerengtroen, L., and Oestensen, H. (1997) "Sensitivity of Parameter Changes in Structural Damage Detection," *Shock and Vibration*, Vol. 4, No. 1, pp. 27–37.

142. Jenq, S.T., and Lee, W.D. (1997) "Identification of Hole Defect for GFRP Woven Laminates Using Neural Network Scheme," *Structural Health Monitoring, Current Status and Perspectives*, Stanford University, Palo Alto, California, pp. 741–751.

143. Johnson, G.A., Pran, K., Wang, G., Havsgard, G.B., and Vohra, S.T. (1999) "Structural Monitoring of a Composite Hull Air Cushion Catamaran with a Multi-Channel Fiber Bragg Grating Sensor System," *Structural Health Monitoring 2000*, Stanford University, Palo Alto, California, pp. 190–198.

144. Johnson, P.S., Smith, D.L., and Haugse, E.D. (1999) "Characterizing Aircraft High-Cycle Fatigue Environment Using the Damage Dosimeter," *Structural Health Monitoring 2000*, Stanford University, Palo Alto, California, pp. 513–522.

145. Jones, A., Noble, R., Bozeat, R., and Hutchins, D. (1999) "Micromachined Ultrasonic Transducers for Damage Detection in CFRP Composites," *Smart Electronics and MEMS*, Proceedings of SPIE, Vol. 3,673, pp. 369–378.

146. Juang, J.N., and Pappa, R.S. (1985) "An Eigensystem Realization Algorithm for Modal Parameter Identification and Modal Reductions," *Journal of Guidance and Control Dynamics*, Vol. 8, pp. 620–627.

147. Kabashima, S., Ozaki, T., and Takeda, N. (2000) "Damage Detection of Satellite Structures by Optical Fiber with Small Diameter," *Smart Structures and Materials 2000: Smart Structures and Integrated Systems*, Proceedings of SPIE, Vol. 3,985, pp. 343–351.

148. Kaiser, S., Melcher, J., Breitbach, E., and Sachau, D. (1999) "Structural Health Monitoring of Adaptive CFRP-Structures," *Industrial and Commercial Applications of Smart Structures Technologies*, Proceedings of SPIE, Vol. 3,674, pp. 51–59.

149. Katafygiotis, L.S., and Lam, H.F. (1997) "A Probabilistic Approach to Structural Health Monitoring Using Dynamic Data," *Structural Health Monitoring, Current Status and Perspectives*, Stanford University, Palo Alto, California, pp. 152–163.

150. Katafygiotis, L.S., Mickleborough, N.C., and Yuen, K.-V (1999) "Statistical Identification of Structural Modal Parameters Using Ambient Response Data," *Computational Stochastic Mechanics*, pp. 93–102.

151. Kawiecki, G. (2000) "Modal Damping Measurements for Damage Detection," *European COST F3 Conference on System Identification and Structural Health Monitoring*, Madrid, Spain, pp. 651–658.

152. Kiddy, J., and Pines, D. (1997) "Damage Detection of Main Rotor Faults Using a Sensitivity Based Approach," *Smart Structures and Integrated Systems*, Proceedings of SPIE, Vol. 3,041, pp. 611–618.

153. Kim, J., Ryu, Y., Lee, B., and Stubbs, N. (1997a) "Smart Baseline Model for Nondestructive Evaluation of Highway Bridges," *Smart Systems for Bridges, Structures, and Highways*, Proceedings of SPIE, Vol. 3,043, pp. 217–226.

154. Kim, K., and Paik, S.-H (1997) "Optical Fiber Monitoring System of Bridges in Korea," *Structural Health Monitoring, Current Status and Perspectives*, Stanford University, Palo Alto, California, pp. 555–563.

155. Kim, K., Ryu, J., Lee, S., and Choi, L. (1997b) "In-Situ Monitoring of Sungsan Bridge in Han River with a Optical Fiber Sensor System," *Smart Systems for Bridges, Structures, and Highways*, Proceedings of SPIE, Vol. 3,043, pp. 72–76.

156. Kirkpatrick, T., Peterson, D., Rossi, P., Ray, L., and Livingston, R. (1999) "Preliminary Study to Facilitate Smart Structure Systems in Bridge Girders," *Smart Structures and Materials 1999: Smart Systems for Bridges, Structures, and Highways*, Proceedings of SPIE, Vol. 3,671, pp. 152–160.

157. Klein, L.A. (1999) *Sensor and Data Fusion: Concepts and Application,* Second Edition, SPIE, Press., Vol. TT14, Bellingham, Washington.

158. Ko, J., Ni, Y., and Chan, T. (1999) "Dynamic Monitoring of Structural Health in Cable-Supported Bridges," *Smart Structures and Materials 1999: Smart Systems for Bridges, Structures, and Highways*, Proceedings of SPIE, Vol. 3,671, pp. 161–172.

159. Krawczuk, M., Ostachowicz, W., and Kawiecki, G. (2000) " Detection of Delaminations in Cantilevered Beams Using Soft Computing Methods," *European COST F3 Conference on System Identification and Structural Health Monitoring*, Madrid, Spain, pp. 243–252.

160. Kronenberg, P., Casanova, N., Inaudi, D., and Vurpillot, S. (1997) "Dam Monitoring with Fiber Optics Deformation Sensors," *Smart Systems for Bridges, Structures, and Highways*, Proceedings of SPIE, Vol. 3,043, pp. 2–11.

161. Kudva, J.N., Grage, M.J., and Roberts, M.M. (1999) "Aircraft Structural Health Monitoring and Other Smart Structures Technologies-Perspectives on Development of Future Smart Aircraft," *Structural Health Monitoring 2000*, Stanford University, Palo Alto, California, pp. 106–119.

162. Kulcu, E., Qin, X., Barrish, R.A., Jr., and Aktan, A.E. (2000) "Information Technology and Data Management Issues for Health Monitoring of the Commodore Barry Bridge," *Nondestructive Evaluation of Highways, Utilities, and Pipelines IV*, Proceedings of the SPIE, Vol. 3,995, pp. 98–111.

163. Kurashima, T., Usu, T., Tanaka, K., and Nobiki, A. (1997) "Application of Fiber Optic Distributed Sensor for Strain Measurement in Civil Engineering," *Smart Materials, Structures, and Integrated Systems*, Proceedings of SPIE, Vol. 3,241, pp. 247–258.

164. Kwon, I., Choi, D., Choi, M., and Moon, H. (1998) "Real-Time Health Monitoring of a Scaled-Down Steel Truss Bridge by Passive-Quadrature 3X3 Fiber Optic Michelson Sensors," *Smart Systems for Bridges, Structures, and Highways*, Proceedings of SPIE, Vol. 3,325, pp. 253–261.

165. Kwon, I.B., Park, P., Huh, Y.H., Kim, D.J., Hong, S.H., Lee, D.C., Titin, C., and Moon, H. (2000) "Failure Detection of Reinforced Concrete Beams with Embedded Fiber Optic Michelson Sensors," *Smart Structures and Materials 2000: Smart Systems for Bridges, Structures, and Highways*, Proceedings of SPIE, Vol. 3,988, Newport Beach, California, pp. 400–411.

166. Lakshmanan, K., and Pines, D. (1997) "Detecting Crack Size and Location in Composite Rotorcraft Flexbeams," *Smart Structures and Integrated Systems*, Proceedings of SPIE, Vol. 3,041, pp. 408–416.

167. Lapin, L.L. (1990) *Probability and Statistics for Modern Engineering*, PWS-Kent Publishing, 2nd Edition, Boston, Massachusetts.

168. Laplace, P.S. (1951) *A Philosophical Essay on Probabilities*, Dover Publications, Inc., New York.

169. Lau, C.K., Mak, P.N., Wong, K.Y., Chan, W.Y.K., and Man, K.L.D. (1999) "Structural Health Monitoring of Three Cable-Supported Bridges in Hong Kong," *Structural Health Monitoring 2000*, Stanford University, Palo Alto, California, pp. 450–460.

170. Lee, G.C., and Liang, Z. (1999) "Development of a Bridge Monitoring System," *Structural Health Monitoring 2000*, Stanford University, Palo Alto, California, pp. 349–358.

171. Leung, C.K.Y., Elvin, N., Olson, N., and Morse, T., and He, Y.F. (1997) "Optical Fiber Crack Sensor for Concrete Structures," *Structural Health Monitoring, Current Status and Perspectives*, Stanford University, Palo Alto, California, pp. 765–776.

172. Leutenegger, T., Schlums, D.H., and Dual, J. (1999) "Structural Testing of Fatigued Structures," *Smart Structures and Integrated Systems*, Proceedings of SPIE, Vol. 3,668, pp. 987–997.

173. Lew, J.-S, and Juang, J.-N (2001) "Structural Damage Detection Using Virtual Passive Controllers," Proceedings of the *International Modal Analysis Conference*, Kissimmee, Florida, pp. 1,219–1,225.

174. Lhermet, N., Claeyssen, F., and Bouchilloux, P. (1998) "Electromagnetic Stress Sensor and its Applications: Monitoring Bridge Cables and Prestressed Concrete Structures," *Smart Systems for Bridges, Structures, and Highways*, Proceedings of SPIE, Vol. 3,325, pp. 46–52.

175. Lichtenwalner, P.F., and Sofge, D.A. (1998) "Local Area Damage Detection in Composite Structures Using Piezoelectric Transducers," *Industrial and Commercial Applications of Smart Structures Technologies*, Proceedings of SPIE, Vol. 3,326, pp. 509–515.

176. Lichtenwalner, P.F., White, E., and Baumann, E. (1998) "Information Processing for Aerospace Structural Health Monitoring," *Industrial and Commercial Applications of Smart Structures Technologies*, Proceedings of SPIE, Vol. 3,326.

177. Lin (1990), "Location of Modeling Errors Using Modal Test Data," *AIAA Journal,* Vol. 28, pp. 1650–1654.

178. Lin, C. (1998) "Unity Check Method for Structural Damage Detection," *Journal of Spacecraft and Rockets*, Vol. 35, No. 4, pp. 577–579.

179. Lin, M. (1999) "Development of SMART Layer for Built-In Structural Diagnostics," *Structural Health Monitoring 200*0, Stanford University, Palo Alto, California, pp. 603–611.

180. Lin, M., Abatan, A., and Zhang, W. (1999) "Crack Damage Detection of Concrete Structures Using Distributed Electrical Time Domain Reflectometry (ETDR) Sensors," *Smart Structures and Materials 1999: Smart Systems for Bridges, Structures, and Highways*, Proceedings of SPIE, Vol. 3,671, pp. 297–304.

181. Lin, M.W., Abatan, A.O., and Zhou, Y. (2000) "Transverse Shear Response Monitoring of Concrete Cylinder Using Embedded High-Sensitivity ETDR Sensor," *Smart Structures and Materials 2000: Smart Systems for Bridges, Structures, and Highways*, Proceedings of SPIE, Vol. 3,988, Newport Beach, California, pp. 319–328.

182. Liu, P., and Rao, V.S. (2000) "Structural Health Monitoring Using Parameter Identification Methods," *Smart Structures and Materials 2000: Smart Structures and Integrated Systems*, Proceedings of SPIE, Vol. 3,985, pp. 792–805.

183. Liu, P., Sana, S., and Rao, V.S. (1999) "Structural Damage Identification Using Time-Domain Parameter Estimation Techniques," *Structural Health Monitoring 2000*, Stanford University, Palo Alto, California, pp. 812–820.

184. Liu, P.L., and Chen, C.C. (1996) "Parametric Identification of Truss Structures by Using Transient Response," *Journal of Sound and Vibration*, Vol. 191, No. 2, pp. 273–287.

185. Liu, P.L., and Sun, S.C. (1997) "The Application of Artificial Neural Networks on the Health Monitoring of Bridges," *Structural Health Monitoring, Current Status and Perspectives*, Stanford University, Palo Alto, California, pp. 103–110.

186. Ljung, L. (1999) *System Identification: Theory for the Users*, Second Edition, Prentice-Hall, New Jersey.

187. Lloret, S., Inaudi, D., Glisic, B., Kronenberg, P., and Vurpillot, S. (2000) "Optical Set-Up Development for the Monitoring of Structural Dynamic Behavior Using SOFO Sensors," *Smart Structures and Materials 2000: Sensory Phenomena and Measurement Instrumentation*, Proceedings of SPIE, Vol. 3,986, pp. 199–205.

188. Lo, Y., and Shaw F. (1998) "Development of Corrosion Sensors Using a Single-Pitch Bragg Grating Fiber with Temperature Compensations*," Smart Systems for Bridges, Structures, and Highways*, Proceedings of SPIE, Vol. 3,325, pp. 64–72.

189. Loh, C., Lin, C., and Huang, C. (2000) "Time Domain Identification of Frames under Earthquake Loadings," *Journal of Engineering Mechanics*, Vol. 126, No. 7, pp. 693–703.

190. Loh, C.H., and Huang, C.C. (1999) "Damage Identification of Multi-Story Steel Frames Using Neural Networks," *Structural Health Monitoring 2000*, Stanford University, Palo Alto, California, pp. 390–399.

191. Loh, C.H., and Lin, H.M. (1996) "Application of Off-Line and On-Line Identification Techniques to Building Seismic Response Data," *Earthquake Engineering and Structural Dynamics*, Vol. 25, pp. 269–290.

192. Lopes, V. Jr., Pereira, J.A., and Inman, D.J. (2000) "Structural FRF Acqisition via Electric Impedance Measurement Applied to Damage Location," Proceedings of SPIE, Vol. 4,062, pp. 1,549–1,555.

193. Lopez-Diez, J., Cuerno-Rejado, C., Luengo, P., and Alexiou, K. (2000) "Error Location in Mass and Stiffness Distribution for Finite Element Models of Spacecraft Structures," *European COST F3 Conference on System Identification and Structural Health Monitoring*, Madrid, Spain, pp. 699–708.

194. Lovell, P., and Pines, D. (1997) "A Remote Wireless Damage Detection System for Monitoring the Health of Large Civil Structures," *Smart Systems for Bridges, Structures, and Highways*, Proceedings of SPIE, Vol. 3,043, pp. 12–22.

195. Lovell, P., and Pines, D. (1998) "Damage Assessment in a Bolted Lap Joint," *Smart Structures and Materials 1999: Smart Systems for Bridges, Structures, and Highways*, Proceedings of SPIE, Vol. 3,325, pp. 112–126.

196. Luo, H., and Hanagud, S. (1997) "Dynamic Learning Rate Neural Networks Training and Composite Structural Damage Detection," *AIAA*, Vol. 35, No. 9, pp. 1,522–1,527.

197. Ma, J., and Pines, D. (2000) "The Concept of Dereverberation and Its Applications to Damage Detection in Civil Structures," *Smart Structures and Materials 2000: Smart Systems for Bridges, Structures, and Highways*, Proceedings of SPIE, Vol. 3,988, Newport Beach, California, pp. 127–134.

198. Maeck, J., and De Roeck, G. (1999) "Damage Detection on a Prestressed Concrete Bridge and RC Beams Using Dynamic System Identification," *Damage Assessment of Structures*, Proceedings of the International Conference on Damage Assessment of Structures (DAMAS 99), Dublin, Ireland, pp. 320–327.

199. Maeck, J., Abdel Wahab, M., Peeters, B., De Roeck, G., Visscher, J., De Wilde, W.P., Ndambi, J.M., and Vantomme, J. (2000) "Damage Identification in Reinforced Concrete Structures by Dynamic Stiffness Determination," *Engineering Structures (Elsevier Science Ltd.)*, Vol. 22, pp. 1,339–1,349.

200. Maeck, J., Abdel Wahab, M., and De Roeck, G. (1998) "Damage Detection in Reinforced Concrete Structures by Dynamic System Identification," *Proceedings of ISMA23, Noise and Vibration Engineering*, Leuven, Belgium.

201. Manson, G., Pierce, G., Worden, K., Monnier, T., Guy, P., and Atherton, K. (2000) "Long-Term Stability of Normal Condition Data for Novelty Detection," *Smart Structures and Materials 2000: Smart Structures and Integrated Systems*, Proceedings of SPIE, Vol. 3,985, pp. 323–334.

202. Manson, G., Worden, K., Martin, A., and Tunnicliffe, D. L. (1999) "Visualization and Dimension Reduction of Acoustic Emission Data for Damage Detection," *Key Engineering Materials*, Vols. 167–168, pp. 64–75.

203. Mares, C., Mottershead, J.E., and Friswell, M.I. (1999a) "Damage Location in Beams by Using Rigid-Body Constraints," *Damage Assessment of Structures*, Proceedings of the International Conference on Damage Assessment of Structures (DAMAS 99), Dublin, Ireland, pp. 381–390.

204. Mares, C., Ruotolo, R., and Surace, C. (1999b) "Using Transmissibility Data to Assess Structural Damage," *Damage Assessment of Structures*, Proceedings of the International Conference on Damage Assessment of Structures (DAMAS 99), Dublin, Ireland, pp. 236–245.

205. Martin, A., Hudd, J., Wells, P., Tunnicliffe, D., and Das-Gupta, D. (1999) "Development and Comparison of Low Profile Piezoelectric Sensors for Impact And Acoustic Emission (AE) Detection in CFRP Structures," *Damage Assessment of Structures*, Proceedings of the International Conference on Damage Assessment of Structures (DAMAS 99), Dublin, Ireland, pp. 102–111.

206. Maseras-Gutierrez, M., Staszewski, W., Found, M., and Worden, K. (1998) "Detection of Impacts in Composite Materials Using Piezoceramic Sensors and Neural Networks," *Smart Structures and Materials 1999: Smart Structures and Integrated Systems*, Proceedings of SPIE, Vol. 3,329, pp. 491–497.

207. Masri, S.F., Smyth, A.W., Chassiakos, A.G., Caughey, T.K., and Hunter, N.F. (2000) "Application of Neural Networks for Detection of Changes in Nonlinear Systems," Journal of Engineering Mechanics, July, pp. 666–676.

208. Masuda, A., Yamamoto, S., and Sone, A. (1999) "Adaptive Identification of Time-Varying Systems with Application to the Structural Health Monitoring," Proceedings of the Second World Conference on Structural Control, Kyoto, Japan, pp. 2,203–2,211.

209. Matrat, J., Levin, K., and Jarlas, R. (1999) "Effect of Debonding on Strain Measurement of Embedded Bragg Grating Sensors," *Structural Health Monitoring 2000*, Stanford University, Palo Alto, California, pp. 651–660.

210. McKee, B., Dahl, S., and Shkarlet, K. (1999) "Smart Coatings for In-Situ Monitoring of Engine Components," *Industrial and Commercial Applications of Smart Structures Technologies*, Proceedings of SPIE, Vol. 3,674, pp. 461–468.

211. Mehrabi, A.B, Tabatabai, H., and Lotfi, H.R. (1998) "Precursor Transformation Method for Damage Detection in Structures," *Smart Systems for Bridges, Structures, and Highways*, Proceedings of SPIE, Vol. 3,325, pp. 161–172.

212. Melvin, L., Childers, B., Rogowski, R., Prosser, W., Moore, J., Frogatt, M., Allison, S., Wu, M.C., Bly, J., Aude, C., Bouvier, C., Zisk, E., Enright, E., Cassadaban, Z., Reightler, R., Sirkis, J., Tang, I., Peng, T., Wegreich, R., Garbos, R., Mouyos, W., Aibel, D., and Bodan, P. (1997) "Integrated Vehicle Health Monitoring (IVHM) for Aerospace Vehicles," *Structural Health Monitoring, Current Status and Perspectives*, Stanford University, Palo Alto, California, pp. 705–714.

213. Messina, A., Williams, E.J., and Contursi, T. (1998) "Structural Damage Detection by a Sensitivity and Statistical-Based Method," *Journal of Sound and Vibration*, Vol. 216, No. 5, pp. 791–808.

214. Mevel, L., Benveniste, A., Basseville, M., Goursat, M. (2000) "In Operation Structural Damage Detection and Diagnosis," *European COST F3 Conference on System Identification and Structural Health Monitoring*, Madrid, Spain, pp. 641–650.

215. Mita, A. (1999) "Emerging Needs in Japan for Health Monitoring Technologies in Civil and Building Structures," *Structural Health Monitoring 2000*, Stanford University, Palo Alto, California, pp. 56–67.

216. Mitchell, K., Sana, S., Balakrishnan, V., Rao, V., and Pottinger, H. (1999) "Micro Sensors for Health Monitoring of Smart Structures," *Smart Electronics and MEMS*, Proceedings of SPIE, Vol. 3,673, pp. 351–358.

217. Mitchell, K., Sana, S., Liu, P., Cingirikonda, K., Rao, V.S., and Pottinger, H.J. (2000) "Distributed Computing and Sensing for Structural Health Monitoring Systems," *Smart Structures and Materials 2000: Smart Electronics and MEMS*, Proceedings of SPIE, Vol. 3,990, pp. 156–166.

218. Modena, C., Sonda, D., and Zonta, D. (1999) "Damage Localization in Reinforced Concrete Structures by Using Damping Measurements," *Damage Assessment of Structures*, Proceedings of the International Conference on Damage Assessment of Structures (DAMAS 99), Dublin, Ireland, pp. 132–141.

219. Moerman, W., Taerwe, L., De Waele, W., Degrieck, J., and Baets, R. (1999) "Remote Monitoring of Concrete Elements by Means of Bragg Gratings," *Structural Health Monitoring 2000*, Stanford University, Palo Alto, California, pp. 369–378.

220. Monaco, E., Calandra, G., and Lecce, L. (2000) "Experimental Activities on Damage Detection Using Magnetostrictive Actuators and Statistical Analysis," *Smart Structures and Materials 2000: Smart Structures and Integrated Systems*, Proceedings of SPIE, Vol. 3,985, pp. 186–196.

221. Morassi, A. (1997) "Damage Detection and Fourier Coefficients," *Structural Damage Assessment Using Advanced Signal Processing Procedures*, Proceedings of DAMAS '97, University of Sheffield, UK, pp. 387–397.

222. Mroz, Z., and Lekszycki, T. (2000) "Identification of Damage in Structures Using Parameter Dependent Modal Response," *Proceedings of ISMA25, Noise and Vibration Engineering*, Leuven, Belgium.

223. Nakamura, M., Masri, S.F., Chassiakos, A.G., and Caughey, T.K. (1998) "A Method for Non-Parametric Damage Detection Through the Use of Neural Networks," *Earthquake Engineering and Structural Dynamics*, Vol. 27, pp. 997–1,010.

224. Naldi, G., and Venini, P. (1997) "Postprocessing Singular Solutions by the Wavelet Transform," *Structural Damage Assessment Using Advanced Signal Processing Procedures*, Proceedings of DAMAS '97, University of Sheffield, UK, pp. 109–120.

225. Nandwana, B.P., and Maiti, S.K. (1997) "Detection of the Location and Size of a Crack in Stepped Cantilever Beams Based on Measurements of Natural Frequencies," *Journal of Sound and Vibration*, Vol. 203, No. 3., pp. 434–446.

226. Natke, H.G., and Cempel, C. (1997) "Model-Aided Diagnosis Based on Symptoms," *Structural Damage Assessment Using Advanced Signal Processing Procedures*, Proceedings of DAMAS '97, University of Sheffield, UK, pp. 363–375.

227. Negro, P., Verzeletti, G., Magonette, G.E., and Pinto, A.V. (1994) "Tests on a Four-Story Full-Scale R/C Frame Designed According to Eurocodes 8 and 2: Preliminary Report, EUR 15879 EN, European Laboratory for Structural Assessment (ELSA)," Joint Research Center, Ispra, Italy.

228. Nellen, P., Anderegg, P., Brönnimann, R., and Sennhauser, U. (1997) "Application of Fiber Optical and Resistance Strain Gauges for Long-Term Surveillance of Civil Engineering Structures," *Smart Systems for Bridges, Structures, and Highways*, Proceedings of SPIE, Vol. 3,043, pp. 77–86.

229. Nigbor, R.L., and Diehl, J.G. (1997) "Two Years' Experience Using OASIS Real-Time Remote Condition Monitoring System on Two Large Bridges," *Structural Health Monitoring, Current Status and Perspectives*, Stanford University, Palo Alto, California, pp. 410–417.

230. Nishimura, H., Sugiyama, T., Okuhara, Y., Shin, S-G., Matsubara, H., and Yanagida, H. (2000) "Application of Self-Diagnosis FRP to Concrete Pile for Health Monitoring," *Smart Structures and Materials 2000: Smart Structures and Integrated Systems*, Proceedings of SPIE, Vol. 3,985, pp. 335–342.

231. Nowak, A. S., Yamani, A. S., and Tabsh, S. W. (1994) "Probabilistic Models for Resistance of Concrete Bridge Girders," *ACI Structural Journal*, Vol. 91, No. 3, pp. 269–276.

232. Oka, K., Ohno, H., Kurashima, T., Matsumoto, M., Kumagai, H., Mita, A., and Sekijima, K. (1999) "Fiber Optic Distributed Sensor for Structural Monitoring," *Structural Health Monitoring 2000*, Stanford University, Palo Alto, California, pp. 672–679.

233. Okabe, Y., Yashiro, S., Kosaka, T., and Takeda, N. (2000) "Detection of Transverse Cracks in Composites by Using Embedded FBG Sensors," *Smart Structures and Materials 2000: Sensory Phenomena and Measurement Instrumentation*, Proceedings of SPIE, Vol. 3,986, pp. 282–291.

234. Onate, E., Hanganu, A., and Miquel, J. (2000) "Prediction of Damage and Failure in Civil Engineering Structures Using a Finite Element Model," *European COST F3 Conference on System Identification and Structural Health Monitoring*, Madrid, Spain, pp. 53–70.

235. Osmont, D., Dupont, M., Gouyon, R., Lemistre, M., and Balageas, D. (2000) "Damage and Damaging Impact Monitoring by PZT Sensors-Based HUMS," *Smart Structures and Materials 2000: Sensory Phenomena and Measurement Instrumentation*, Proceedings of SPIE, Vol. 3,986, pp. 85–92.

236. Pai, P.F., and Jin, S. (2000) "Locating Structural Damage Using Operational Deflection Shapes," *Smart Structures and Materials 2000: Smart Structures and Integrated Systems*, Proceedings of SPIE, Vol. 3,985, pp. 271–282.

237. Paolozzi, A., Felli, F., and Caponero, M.A. (1999) "Global Temperature Measurements of Aluminum Alloy Specimens with Embedded Optical Fibers," *Structural Health Monitoring 2000*, Stanford University, Palo Alto, California, pp. 257–264.

238. Paolozzi, A., Ivagnes, M., and Lecci, U. (1999) "Qualification Tests of Aerospace Composite Materials with Embedded Optical Fibers," *Structural Health Monitoring 2000*, Stanford University, Palo Alto, California, pp. 661–671.

239. Papadimitriou, C., Katafygiotis, L.S., and Yuen, K.-V. (1999) "Optimal Instrumentation Strategies for Structural Health Monitoring Applications," *Structural Health Monitoring 2000*, Stanford University, Palo Alto, California, pp. 543–552.

240. Papadimitriou, C., Levine-West, M., and Milman, M. (1997) "Structural Damage Detection Using Modal Test Data," *Structural Health Monitoring, Current Status and Perspectives*, Stanford University, Palo Alto, California, pp. 678–689.

241. Pardo de Vera, C., and Guemes, J. (1997) "Embedded Self-Sensing Piezoelectrics for Damage Detection," *Proceedings of the International Workshop on Structural Health Monitoring*, Stanford University, California, September 18–20, 1997, pp. 445–455.

242. Park, G., Cudney, H., and Inman, D.J. (1999a) "Impedance-Based Health Monitoring Technique for Civil Structures," *Structural Health Monitoring 2000*, Stanford University, Palo Alto, California, pp. 523–532.

243. Park, G., Cudney, H., and Inman, D. (1999b) "Impedance-Based Health Monitoring Technique for Massive Structures and High-Temperature Structures," *Smart Structures and Materials 1999: Sensory Phenomena and Measurement Instrumentation for Smart Structures and Materials*, Proceedings of SPIE, Vol. 3,670, pp. 461–469.

244. Park, G., Kabeya, K., Cudney, H., and Inman, D.J. (1999) "Impedance-Based Structural Health Monitoring for Temperature Varying Applications," *JSME International Journal*, Vol. 42, No. 2, pp. 249–258.

245. Park, K.C., and Reich, G.W. (1999) "Model-Based Health Monitoring of Structural Systems: Progress, Potential and Challenges," *Structural Health Monitoring 2000*, Stanford University, Palo Alto, California, pp. 82–95.

246. Park, K.C., Reich, G.W., and Alvin, K.F. (1997) "Structural Damage Detection Using Localized Flexibilities," *Structural Health Monitoring, Current Status and Perspectives*, Stanford University, Palo Alto, California, pp. 125–139.

247. Park, S., Stubbs, N., and Bolton, R.W. (1998) "Damage Detection on a Steel Frame Using Simulated Modal Data," *Proceedings of the International Modal Analysis Conference*, pp. 616–622.

248. Peeters, J.M.B., and De Roeck, D. (2000) "Damage Identification on the Z24-Bridge Using Vibration Monitoring," *European COST F3 Conference on System Identification and Structural Health Monitoring*, Madrid, Spain, pp. 233–242.

249. Peeters, J.M.B., Maeck, J., and De Roeck, G. (2000) "Excitation Sources and Dynamic System Identification in Civil Engineering," *European COST F3 Conference on System Identification and Structural Health Monitoring*, Madrid, Spain, pp. 341–350.

250. Peil, U., and Mehdianpour, M. (1999) "Life Cycle Prediction via Monitoring," *Structural Health Monitoring 2000*, Stanford University, Palo Alto, California, pp. 723–730.

251. Perez, L., Ferregut, C., Carrasco, C., Paez, T., Barney, P., and Hunter, N. (1997) "Statistical Validation of a Plate Finite-Element Model for Damage Detection," *Smart Systems for Bridges, Structures, and Highways*, Proceedings of SPIE, Vol. 3,043, pp. 134–144.

252. Pierce, S., Staszewski, W., Gachagan, A., James, I., Philp, W., Worden, K., Culshaw, B., McNab, A., Tomlinson, G., and Hayward, G. (1997) "Ultrasonic Condition Monitoring of Composite Structures Using a Low Profile Acoustic Source and an Embedded Optical Fibre Sensor," *Smart Systems for Bridges, Structures, and Highways*, Proceedings of SPIE, Vol. 3,043, pp. 437–448.

253. Pines, D.J., and Salvino, L.W. (2002) "Structural Health Monitoring Using Empirical Mode Decomposition and Hilbert-Juang Transform on One-Dimensional Structures," *Smart Structures and Integrated Systems*, Proceedings of SPIE, Vol. 4,701.

254. Pines, D.J. (1997) "The Use of Wave Propagation Models for Structural Damage Identification," *Structural Health Monitoring, Current Status and Perspectives*, Stanford University, Palo Alto, California, pp. 665–677.

255. Pirner, M., and Fischer, O. (1997) "Monitoring Stresses in GRP Extension of the Prague TV Tower," *Structural Damage Assessment Using Advanced Signal Processing Procedures*, Proceedings of DAMAS '97, University of Sheffield, UK, pp. 451–460.

256. Purekar, A., Lakshmanan, A., and Pines, D. (1998) "Detecting Delamination in Composite Rotorcraft Flexbeams using the Local Wave Response," *Smart Structures and Integrated Systems*, Proceedings of SPIE, Vol. 3,329, pp. 523–535.

257. Rao, Y.J., Henderson, P.J., Jackson, D.A., Zhang, L., and Bennion, I. (1997) "Simultaneous Strain, Temperature, and Vibration Measurement Using a Multiplexed In-Fibre-Bragg-Grating/Fibre-Fabry-Perot Sensor System," Electronics Letters, Vol. 33, No. 24, pp. 2,063–2,064.

258. Ratcliffe, C.P., Gillespie, J.W., Heider, D., Eckel, D.A., Crane, R.M. (2000), "Experimental Investigation into the Use of Vibration Data for Long Term Monitoring of an All Composite Bridge," Proceedings of SPIE, Vol. 3,995, p.64–75.

259. Reich, G.W., and Park, K.C. (2000) "Experimental Applications of a Structural Health Monitoring Methodology," *Smart Structures and Materials 2000: Smart Systems for Bridges, Structures, and Highways*, Proceedings of SPIE, Vol. 3,988, Newport Beach, California, pp. 143–153.

260. Rizkalla, S., Benmokrane, B., and Tadros, G. (2000) "Structural Health Monitoring Bridges with Fibre Optic Sensors," *European COST F3 Conference on System Identification and Structural Health Monitoring*, Madrid, Spain, pp. 501–510.

261. Robeson, E., and Thompson, B. (1999) "Tools for the 21st Century: MH-47E SUMS," *Structural Health Monitoring 2000*, Stanford University, Palo Alto, California, pp. 179–189.

262. Rohrmann, R.G., Baessler, M., Said, S., Schmid, W., and Ruecker, W.F. (1999) "Structural Causes of Temperature Affected Modal Data of Civil Structures Obtained by Long Time Monitoring," *Proceedings of the XVII International Modal Analysis Conference*, Kissimmee, Florida, pp. 1–6.

263. Ruffin, P. (1999) "Opportunities and Challenges for MEMS Technology in Army Missile Systems Applications," *Smart Structures and Materials 1999: Smart Electronics and MEMS*, Proceedings of SPIE, Vol. 3,673, pp. 34–44.

264. Ruotolo, R., and Surace, C. (1997a) "Damage Assessment of Multi-Cracked Beams Using Combinatorial Optimisation," *Structural Damage Assessment Using Advanced Signal Processing Procedures*, Proceedings of DAMAS '97, Univeristy of Sheffield, UK, pp. 77–86.

265. Ruotolo, R., and Surace, C. (1997b) "Damage Detection Using Singular Value Decomposition," *Structural Damage Assessment Using Advanced Signal Processing Procedures*, Proceedings of DAMAS '97, University of Sheffield, UK, pp. 87–96.

266. Ruotolo, R., and Surace, C. (1997c) "Damage Assessment of Multiple Cracked Beams: Results and Experimental Validation," *Journal of Sound and Vibration*,Vol. 206, No. 4, pp. 567–588.

267. Ruotolo, R., and Surace, C. (1998) "Diagnosis of Damage in a Steel Frame," *Proceedings of the International Modal Analysis Conference*, pp. 609–615.

268. Ruotolo, R., Sorohan, S., and Surace, C. (2000) "Analysis of the Behavior of a Three-Dimensional Truss Structure," *European COST F3 Conference on System Identification and Structural Health Monitoring*, Madrid, Spain, pp. 169–178.

269. Rytter, A. (1993) "Vibration Based Inspection of Civil Engineering Structures," Ph. D. Dissertation, Dept. of Building Technology and Structural Eng., Aalborg University, Denmark.

270. Rytter, A., and Kirkegaard, P. (1997) "Vibration Based Inspection Using Neural Networks," *Structural Damage Assessment Using Advanced Signal Processing Procedures*, Proceedings of DAMAS '97, University of Sheffield, UK, pp. 97–108.

271. Sadeghi, M.H., and Fassois, S.D. (1998) "Reduced Dimensionality Geometric Approach to Fault Identification in Stochastic Structural Systems," *AIAA Journal*, Vol. 36, pp. 2,250–2,256.

272. Safak, E. (1997) "New Directions in Seismic Monitoring of Multi-Story Buildings," *Structural Health Monitoring, Current Status and Perspectives*, Stanford University, Palo Alto, California, pp. 418–430.

273. Said, W.M., and Staszewski, W.J. (2000) "Optimal Sensor Location for Damage Detection Using Mutual Information," 11th International Conference on Adaptive Structures and Technologies, Nagoya, Japan, October 23–26, pp. 428–435.

274. Sakellariou, J.S., and Fassois, S.D. (2000) "Parametric Output Error Based Identification and Fault Detection in Structures Under Earthquake Excitation," *European COST F3 Conference on System Identification and Structural Health Monitoring*, Madrid, Spain, pp. 323–322.

275. Sanders, W., Akhavan, F., Watkins, S., and Chandrashekhara, K. (1997) "Fiber Optic Vibration Sensing and Neural Networks Methods for Prediction of Composite Beam Delamination," *Smart Structures and Integrated Systems*, Proceedings of SPIE, Vol. 3,041, pp. 858–867.

276. Satori, K., Ikeda, Y., Kurosawa, Y., Hongo, A., and Takeda, N. (2000) "Development of Small-Diameter Optical Fiber Sensors for Damage Detection in Composite Laminates," *Smart Structures and Materials 2000: Sensory Phenomena and Measurement Instrumentation*, Proceedings of SPIE, Vol. 3,986, pp. 104–111.

277. Satpathi, D., Victor, J., Wang, M., Yang, H., and Shih, C. (1999) "Development of a PVDF Film Sensor for Infrastructure Monitoring," *Smart Structures and Materials 1999: Smart Systems for Bridges, Structures, and Highways*, Proceedings of SPIE, Vol. 3,671, pp. 90–99.

278. Schueler, R., Joshi, S., and Schulte, K. (1997) "Conductivity of CFRP as a Tool for Health and Usage Monitoring," *Smart Structures and Integrated Systems*, Proceedings of SPIE, Vol. 3,041, pp. 417–426.

279. Schulz, M.J., Naser, A.S., Thyagarajan, S.K., Mickens, T., and Pai, P.F. (1998) "Structural Health Monitoring Using Frequency Response Functions and Sparse Measurements," *Proceedings of the International Modal Analysis Conference*, pp. 760–766.

280. Seim, J., Udd, E., Schulz, W., and Laylor, H. (1999) "Health Monitoring of an Oregon Historical Bridge with Fiber Grating Strain Sensors," *Smart Structures and Materials 1999: Smart Systems for Bridges, Structures, and Highways*, Proceedings of SPIE, Vol. 3,671, pp. 128–134.

281. Shah, S.P., Popovics, J.S., Subramaniam, K.V., and Aldea, C. (2000) "New Directions in Concrete Health Monitoring Technology," *Journal of Engineering Mechanics*, Vol. 126, No. 7, pp. 754–760.

282. Shenton, H., and Chajes, M. (1999) "Long-Term Health Monitoring of an Advanced Polymer Composite Bridge," *Smart Structures and Materials 1999: Smart Systems for Bridges, Structures, and Highways*, Proceedings of SPIE, Vol. 3,671, pp. 143–151.

283. Shinozuka, M., and Rejaie, S.A. (2000) "Analysis of Remotely Sensed Pre- and Post-Disaster Images for Damage Detection," *Smart Structures and Materials 2000: Smart Systems for Bridges, Structures, and Highways*, Proceedings of SPIE, Vol. 3,988, Newport Beach, California, pp. 307–318.

284. Shinozuka, M., Ghanem, R., Houshmand, B., and Mansouri, B. (2000) "Feasibility of Damage/Change Detection in Civil Structures by SAR Imagery: Proof of Concept Study Using SAR Simulation," *Smart Structures and Materials 2000: Smart Systems for Bridges, Structures, and Highways*, Proceedings of SPIE, Vol. 3,988, Newport Beach, California, pp. 165–175.

285. Side, S., Staszewski, W.J., Wardle, R., and Worden, K. (1997) "Fail-Safe Sensor Distributions for Damage Detection," *Structural Damage Assessment Using Advanced Signal Processing Procedures*, Proceedings of DAMAS '97, University of Sheffield, UK, pp. 135–146.

286. Sikorsky, C., and Stubbs, N. (1997) "Improving Bridge Management Using NDE and Quality Management," *Structural Damage Assessment Using Advanced Signal Processing Procedures,* Proceedings of DAMAS '97, University of Sheffield, UK, pp. 399–408.

287. Sikorsky, C. (1997) "Integrating Modal Based NDE Techniques and Bridge Management Systems Using Quality Management," *Smart Systems for Bridges, Structures, and Highways*, Proceedings of SPIE, Vol. 3,043, pp. 31–42.

288. Sikorsky, C. (1999) "Development of a Health Monitoring System for Civil Structures Using a Level IV Nondestructive Damage Evaluation Method," *Structural Health Monitoring 2000*, Stanford University, Palo Alto, California, pp. 68–81.

289. Silverman, B.W. (1986) *Density Estimation for Statistics and Data Analysis*, Chapman and Hall, New York, New York.

290. Skjaerbaek, P.S., Kirkegaard, P.H., and Nielsen, S.R.K. (1997) "Shaking Table Tests of Reinforced Concrete Frames," *Structural Damage Assessment Using Advanced Signal Processing Procedures*, Proceedings of DAMAS '97, University of Sheffield, UK, pp. 441–450.

291. Sohn, H, Worden, K., and Farrar, R.C. (2001) "Novelty Detection Using Auto-Associative Neural Network," *Symposium on Identification of Mechanical Systems: International Mechanical Engineering Congress and Exposition*, November 11–16, New York, New York, 2001.

292. Sohn, H., and Farrar, C. R. (2000) "Statistical Process Control and Projection Techniques for Damage Detection," *European COST F3 Conference on System Identification and Structural Health Monitoring*, Madrid, Spain, pp. 105–114.

293. Sohn, H., and Law, K.H. (1999a) "Extraction of Ritz Vectors from Vibration Test Data," *Structural Health Monitoring 2000*, Stanford University, Palo Alto, California, pp. 840–850.

294. Sohn, H., and Law, K.H. (1998b) "Application of Load-Dependent Ritz Vectors to Probabilistic Damage Detection," *Smart Systems for Bridges, Structures, and Highways*, Proceedings of SPIE, Vol. 3,325, pp. 149–160.

295. Sohn, H., Dzwonczyk, M., Straser, E.G., Law, K.H., Meng, T., and Kiremidjian, A.S. (1998a) "Adaptive Modeling of Environmental Effects in Modal Parameters For Damage Detection in Civil Structures," *Smart Systems for Bridges, Structures, and Highways*, Proceedings of SPIE, Vol. 3,325, pp. 127–138.

296. Sohn, H., Farrar, C.R., Hunter, N.F., and Worden, K. (2001) "Structural Health Monitoring Using Statistical Pattern Recognition Techniques," *ASME Journal of Dynamic Systems, Measurement and Control: Special Issue on Identification of Mechanical Systems,* Vol. 123, No. 4, pp. 706–711.

297. Solomon, I, Cunnane, J., and Stevenson, P. (2000) "Large-Scale Structural Monitoring Systems," Proceedings of SPIE, Vol. 3,995, pp. 276–287.

298. Sophia, H., and Karolos, G. (1997) "Damage Detection Using Impulse Response," *Nonlinear Analysis, Theory, Methods & Applications*, Vol. 30, No. 8, pp. 4,757–4,764.

299. Stanbridge, A.B., Khan, A.Z., and Ewins, D.J. (1997) "Fault Identification in Vibrating Structures Using a Scanning Laser Doppler Vibrometer," *Structural Health Monitoring, Current Status and Perspectives*, Stanford University, Palo Alto, California, pp. 56–65.

300. Staszewski, W.J. (2000a) "Advanced Data Pre-Processing for Damage Identification Based on Pattern Recognition," *International Journal of Systems Science*, Vol. 31, No. 11, pp. 1,381–1,396.

301. Staszewski, W. (2000b) "Monitoring ON-Line Integrated Technologies for Operational Reliability—MONITOR," Air & Space Europe, Vol. 2, No. 4.

302. Staszewski, W.J., Biemans, C., Boller, C., and Tomlinson, G.R. (1999) "Impact Damage Detection in Composite Structures-Recent Advances," *Structural Health Monitoring 2000*, Stanford University, Palo Alto, California, pp. 754–763.

303. Staszewski, W.J., Read, I., and Foote, P.D. (2000) "Damage Detection in Composite Materials Using Optical Fibres—Recent Advances in Signal Processing," *Smart Structures and Materials 2000: Smart Structures and Integrated Systems*, Proceedings of SPIE, Vol. 3,985, pp. 261–270.

304. Staszewski, W.J., Worden, K., and Tomlinson, G.R. (1998) "Optimal Sensor Placement for Neural Network Fault Diagnosis," Proceedings of Adaptive Computing in Engineering Design and Control '96, pp. 92–99.

305. Staszewski, W.J. (1998) "Structural and Mechanical Damage Detection Using Wavelets," *The Shock and Vibration Digest*, Vol. 30, No. 6, pp. 457–472.

306. Staszewski, W.J., Worden, K., Wardle, R., and Tomlinson, G.R. (2000) "Fail-Safe Sensor Distributions for Impact Detection in Composite Materials," *Smart Materials and Structures*, Vol. 9., pp. 298–303.

307. Straser, E.G., Kiremidjian, A.S., Meng, T.H., and Redlefsen, L. (1998) "A Modular, Wireless Network Platform for Monitoring Structures," *Proceedings of the International Modal Analysis Conference*, pp. 450–456.

308. Strock, O.J., and Rueger, S.M. (1995) *Telemetry System Architecture*, 3rd Edition, Instrument Society of America, Research Triangle Park, North Carolina.

309. Stubbs, N., Sikorsky, C., Park, S.C., and Bolton, R. (1999) "Verification of a Methodology to Nondestructively Evaluate the Structural Properties of Bridges," *Structural Health Monitoring 2000*, Stanford University, Palo Alto, California, pp. 440–449.

310. Su, M. (1998) "TDR Monitoring Systems for the Integrity of Infrastructures," *Smart Structures and Materials 1999: Smart Systems for Bridges, Structures, and Highways*, Proceedings of SPIE, Vol. 3,325, pp. 93–103.

311. Takeda, N., Kosaka, T., and Ichiyama, T. (1999) "Detection of Transverse Cracks by Embedded Plastic Optical Fiber in FRP Laminates," *Smart Structures and Materials 1999: Sensory Phenomena and Measurement Instrumentation for Smart Structures and Materials*, Proceedings of SPIE, Vol. 3,670, pp. 248–255.

312. Tennyson, R.C., and Mufti, A.A. (2000) "Monitoring Bridge Structures Using Fiber Optic Sensors," *European COST F3 Conference on System Identification and Structural Health Monitoring*, Madrid, Spain, pp. 511–520.

313. Teral, S., Kleinerman, M., and Malavieille, P. (1998) "Power Cable Fault Management with Fiber Optic Distributed Sensors: Future Technological Trends," *Industrial and Commercial Applications of Smart Structures Technologies*, Proceedings of SPIE, Vol. 3,326, pp. 380–389.

314. Todd, M., Johnson, G., and Vohra, S. (2000) "Progress Towards Deployment of Bragg Grating-Based Fiber Optic Systems in Structural Monitoring Applications," *European COST F3 Conference on System Identification and Structural Health Monitoring*, Madrid, Spain, pp. 521–530.

315. Todd, M.D., Johnson, G., and Vohra, S., Chen-Chang, C., Danver, B., and Malsawma, L. (1999) "Civil Infrastructure Monitoring with Fiber Optic Bragg Grating Sensor Arrays," *Structural Health Monitoring 2000*, Stanford University, Palo Alto, California, pp. 359–368.

316. Todd, M.D., and Nichols, J.M. (2002) "Structural Damage Assessment Using Chaotic Dynamic Interrogation," *Proceedings of 2002 ASME International Mechanical Engineering Conference and Exposition*, New Orleans, Louisiana.

317. Todd, M.D., Nichols, J.M., Pecora, L.M., and Virgin, L.N. (2001) "Vibration-Based Damage Assessment Utilizing State Space Geometry Changes: Local Attractor Variance Ratio," Smart Materials and Structures, Vol. 10, No. 5, pp. 1,000–1,008.

318. Todoroki, A., Shimamura, Y., and Inada, T. (1999) "Plug and Monitor System via Ethernet with Distributed Sensors and CCD Cameras," *Structural Health Monitoring 2000*, Stanford University, Palo Alto, California, pp. 571–580.

319. Topole, K. (1997) "Damage Evaluation via Flexibility Formulation," *Smart Systems for Bridges, Structures, and Highways*, Proceedings of SPIE, Vol. 3,043, pp. 145–154.

320. Tracy, Michael, and Chang, Fu-Kuo (1998) "Identifying Impacts in Composite Plates with Piezoelectric Strain Sensors, Part I: Theory," *Journal of Intelligent Material Systems and Structures*, Vol. 9, pp. 920–928.

321. Trendafilova, I. (1998) "Damage Detection in Structures from Dynamic Response Measurements. An Inverse Problem Perspective," *Modeling and Simulation Based Engineering*, Technical Science Press, pp. 515–520.

322. Tsyfansky, S.L., and Beresnevich, V.I. (1997) "Vibrodiagnosis of Fatigue Cracks in Geometrically Nonlinear Beams," *Structural Damage Assessment Using Advanced Signal Processing Procedures*, Proceedings of DAMAS '97, University of Sheffield, UK, pp. 299–311.

323. Valente, C., and Spina, D. (1997) "Crack Detection in Beam Elements Using the Gabor Transform," *Proceedings of Adaptive Computing in Engineering Design and Control '96*, pp. 147–156.

324. Valentin-Sivico, J., Rao, V.S., and Koval, L.R. (1997) "Health Monitoring of Bridge-Like Structures Using State Variable Models," *Smart Systems for Bridges, Structures, and Highways*, Proceedings of SPIE, Vol. 3,043, pp. 205–216.

325. Vandiver, T.L. (1997) " Health Monitoring of US Army Missile Systems," *Structural Health Monitoring, Current Status and Perspectives*, Stanford University, Palo Alto, California, pp. 191–196.

326. Vanik, M. W., Beck, J. L., and Au, S. K. (2000) "Bayesian Probabilistic Approach to Structural Health Monitoring*," Journal of Engineering Mechanics*, Vol. 126, No. 7, pp. 738–745.

327. Vanik, M.W., and Beck, J.L. (1997) "A Bayesian Probabilistic Approach to Structural Health Monitoring," *Structural Health Monitoring, Current Status and Perspectives*, Stanford University, Palo Alto, California, pp. 140–152.

328. Vapnik, V. (1998), *Statistical Learning Theory*, John Wiley & Sons, Inc., New York, New York.

329. Varadan, V.K., and Varadan, V.V. (1999) "Wireless Remotely Readable and Programmable Microsensors and MEMS for Health Monitoring of Aircraft Structures," *Structural Health Monitoring 2000*, Stanford University, Palo Alto, California, pp. 96–105.

330. Varadan, V.K., and Varadan, V.V. (2000) "Conformal and Embedded IDT Micro Sensors for Health Monitoring of Structures," *Smart Structures and Materials 2000: Smart Electronics and MEMS,* Proceedings of SPIE, Vol. 3,990, pp. 167–177.

331. Vill, W. (1947) "Theorie et Applications de la Notion de Signal Analytique," Cables et Transmission, Vol. 2a, pp. 61–74. (Translated into English by I. Selin, RAND Corp. Report T-92, Santa Monica, California, August, 1958.)

332. Vincent, H.T., Hu, S.-L.J., and Hou, Z. (1999) "Damage Detection Using Empirical Mode Decomposition Method and a Comparison with Wavelet Analysis," *Structural Health Monitoring 2000*, Stanford University, Palo Alto, California, pp. 891–900.

333. Vurpillot, S., Casanova, N., Inaudi, D., and Kronenburg, P. (1997) "Bridge Spatial Displacement Monitoring with 100 Fiber Optic Sensors Deformations: Sensors Network and Preliminary Results," *Smart Systems for Bridges, Structures, and Highways*, Proceedings of SPIE, Vol. 3,043, pp. 51–57.

334. Walter, P.L. (1998) "Shock and Vibration Measurements via Space Telemetry," *Shock and Vibration Digest*, September, pp. 18–23.

335. Wang, C.S., and Chang, F.K. (2000) "Diagnosis of Impact Damage in Composite Structures with Built-in Piezoelectrics Network," *Smart Structures and Materials 2000: Smart Electronics and MEMS*, Proceedings of SPIE, Vol. 3,990, Newport Beach, California, pp. 13–19.

336. Wang, G., and Pran, K. (2000) "Ship Hull Structure Monitoring Using Fiber Optic Sensors," *European COST F3 Conference on System Identification and Structural Health Monitoring*, Madrid, Spain, pp. 15–27.

337. Wang, M.L., Xu, F.L., and Lloyd, G.M. (2000) "A Systematic Numerical Analysis of the Damage Index Method Used for Bridge Diagnostics," *Smart Structures and Materials 2000: Smart Systems for Bridges, Structures, and Highways*, Proceedings of SPIE, Vol. 3,988, Newport Beach, California, pp. 154–164.

338. Wang, M., Xu, F., Satpathi, D., and Chen, Z. (1999) "Modal Testing for a Multispans Continuous Segmental Prestressed Concrete Bridge," *Smart Structures and Materials 1999: Smart Systems for Bridges, Structures, and Highways*, Proceedings of SPIE, Vol. 3,671, pp. 328–336.

339. Wang, M.L., Satpathi, D., and Heo, G. (1997) "Damage Detection of a Model Bridge Using Modal Testing," *Structural Health Monitoring, Current Status and Perspectives*, Stanford University, Palo Alto, California, pp. 589–600.

340. Wang, M.L., Satpathi, D., Lloyd, Chen, Z.L., and Xu (1999) "Monitoring and Damage Assessment of the Kishwaukee Bridge," A Preliminary Investigative Report submitted to the Illinois Department of Transportation, Bridge Research Center, University of Illinois at Chicago.

341. Wang, Q., and Deng, X. (1999) "Damage Detection with Spatial Wavelets," *International Journal of Solids and Structures*, Vol. 36, No. 3, pp. 3,443–3,468.

342. Westermo, B., and Thompson, L.D. (1997) "A Peak Strain Sensor for Damage Assessment and Health Monitoring," *Structural Health Monitoring, Current Status and Perspectives*, Stanford University, Palo Alto, California, pp. 515–526.

343. Wiese, S., Kowalsky, W., Wichern, J., and Grahn, W. (1999) "Fiberoptical Sensors for On-Line Monitoring of Moisture in Concrete Structures," *Structural Health Monitoring 2000*, Stanford University, Palo Alto, California, pp. 643–650.

344. Wilcox, P.D., Dalton, R.P., Lowe, M.J.S., and Cawley, P. (1999) "Mode Selection and Transduction for Structural Monitoring Using Lamb Waves," *Structural Health Monitoring 2000*, Stanford University, Palo Alto, California, pp. 703–712.

345. Williams, E.J., and Messina, A. (1999) "Applications of the Multiple Damage Location Assurance Criterion," Proceedings of the International Conference on Damage Assessment of Structures (DAMAS 99), Dublin, Ireland, pp. 256–264.

346. Wong, KY; Chan, WYK; Man, KL; Mak, WPN; Lau, CK (2000) "Structural Health Monitoring Results on Tsing Ma, Kap Shui Mun, and Ting Kau Bridges," Proceedings of SPIE, Vol. 3,995, pp. 288–299.

347. Worden, K., and Fieller, N.R.J. (1999) "Damage Detection Using Outlier Analysis," *Journal of Sound and Vibration*, Vol. 229, No. 3, pp. 647–667.

348. Worden, K., and Lane, A.J. (2001) "Damage Identification Using Support Vector Machines," *Smart Materials and Structures*, Vol. 10, pp. 540–547.

349. Worden, K., Allen, D., Sohn, H., and Farrar, C.R. (2002) "Damage Detection in Mechanical Structures using Extreme Values Statistics," Los Alamos National Laboratory report LA-13903-MS.

350. Worden, K., Manson, G., Wardle, R., Staszewski, W., and Allman, D. (1999) "Experimental Validation of Two Structural Health Monitoring Methods," *Structural Health Monitoring 2000*, Stanford University, Palo Alto, California, pp. 784–799.

351. Worden, K., Pierce, S.G., Manson, G., Philp, W.R., Staszewski, W.J., and Culshaw, B. (2000) "Detection of Defects in Composite Plates Using Lamb Waves and Novelty Detection," *International Journal of Systems Science*, Vol. 31, pp. 1,397–1,409.

352. Yamakawa, H., Iwaki, H., Mita, A., and Takeda, N. (1999) "Health Monitoring of Steel Structures Using Fiber Bragg Grating Sensors," *Structural Health Monitoring 2000*, Stanford University, Palo Alto, California, pp. 502–510.

353. Yamaura, T., Inque, Y., Kino, H., and Nagai, K. (1999) "Development of Structural Health Monitoring System Using Brillouin Optical Time Domain Reflectometry," *Structural Health Monitoring 2000*, Stanford University, Palo Alto, California, pp. 533–542.

354. Yang, S.M., and Lee, G.S. (1999) "Effects of Modeling Error on Structure Damage Diagnosis by Two-Stage Optimization," *Structural Health Monitoring 2000*, Stanford University, Palo Alto, California, pp. 871–880.

355. Yao, J.T.P., and Wong, F.S. (1999) "Symptom Based Reliability and Structural Health Monitoring," *Structural Health Monitoring 2000*, Stanford University, Palo Alto, California, pp. 743–753.

356. Zadeh, L.A. (1965) "Fuzzy Sets*," Information and Control*, Vol. 8, pp. 338–353.

357. Zak, A., Krawczuk, M., and Ostachowicz, W. (1999) "Vibration of a Laminated Composite Plate with Closing Delamination," *Structural Damage Assessment Using Advanced Signal Processing Procedures*, Proceedings of DAMAS '99, University College, Dublin, Ireland, pp. 17–26.

358. Zeng, T., Du, W., Zhang, F., Rosidian, A., Claus, R.O., Liu, Y., and Cooper, K.L. (1999) "Fabrication of Piezoelectric Ultrathin Films for MEMs and Sensors by the Electrostatic Self-Assembly Process," *Structural Health Monitoring 2000*, Stanford University, Palo Alto, California, pp. 625–634.

359. Zhang, D., Venkatesan, G., Kaveh, M., Tewfik, A. (1999) "Fault Monitoring Using Acoustic Emissions," *Smart Structures and Materials 1999: Sensory Phenomena and Measurement Instrumentation for Smart Structures and Materials*, Proceedings of SPIE, Vol. 3,670, pp. 392–402.

360. Zhang, L., Quiong, W., and Link, M. (1998) "A Structural Damage Identification Approach Based on Element Modal Strain Energy," *Proceedings of ISMA23, Noise and Vibration Engineering*, Leuven, Belgium.

361. Zheng, R., and Ellingwood, B. R. (1998) "Role of Non-Destructive Evaluation in Time-Dependent Reliability Analysis," *Structural Safety*, Vol. 20, pp. 325–339.

362. Zimmerman, D.C., and Kaouk, M. (1994) "Structural Damage Detection Using a Minimum Rank Update Theory," *ASME Journal of Vibration and Acoustics*, Vol. 116, No. 2, pp. 222–231.

363. Zimmerman, D.C. (1999) "Looking into the Crystal Ball: The Continued Need for Multiple Viewpoints in Damage Detection," *Damage Assessment of Structures*, Proceedings of the International Conference on Damage Assessment of Structures (DAMAS 99), Dublin, Ireland, pp. 76–90.

364. Zonta, D., Modena, C., and Bursi, O.S. (2000) "Analysis of Dispersive Phenomena in Damaged Structures," *European COST F3 Conference on System Identification and Structural Health Monitoring*, Madrid, Spain, pp. 801–810.

REFERENCES FOR ROTATING MACHINERY

1. Barron, R. (Editor) (1997) *Engineering Condition Monitoring: Practice, Methods and Applications*, Pierson Education.

2. Basaraba, B.M., and Archer, J. A. (1995) *IPT's Rotating Equipment Training Manual*, *and IPT's Rotating Equipment Handbook*, IPT Publishing and Training Ltd.

3. Boving, K.G. (Editor) (1989) *NDE Handbook: Nondestructive Examination Methods for Condition Monitoring*, Woodhead publishing.

4. Braun. S. (Editor) (1986) *Mechanical Signature Analysis: Theory and Application*, Academic Press, London.

5. Cempel, C., and Haddad, S.D. (Editors) (1991) *Vibroacoustic Condition Monitoring*, Ellis Horwood Series in Mechanical Engineering, Ellis Horwood, New York.

6. Chow, M-Y. (1997) *Methodologies of Using Neural Network and Fuzzy Logic Technologies for Motor Incipient Fault Detection*, World Scientific.

7. Collacott, R.A. (1977) *Mechanical Fault Diagnosis and Condition Monitoring,* Chapman and Hall, London.

8. Collacott, R.A. (1985) *Structural Integrity Monitoring*, Kluwer Academic Publishing, Dordrecht.

9. Crawford, A.W. (1992) *The Simplified Handbook of Vibration Analysis*, Computational Systems, Inc., Knoxville, Tennessee.

10. Davies, A. (Editor) (1997) *Handbook of Condition Monitoring—Techniques and Methodology*, Chapman & Hill.

11. Hewlett Packard (1997) *Effective Machinery Measurements Using Dynamic Signal Analyzers*, Application Note 243-1, Hewlett Packard Company.

12. Eisenmann, R.C., Sr., and Eisenmann, R.C., Jr. (1997) *Machinery Malfunction Diagnosis and Correction: Vibration Analysis and Troubleshooting for the Process Industries*, Hewlett-Packard Professional books, Prentice-Hall, Upper Saddle River, New Jersey.

13. Goldman, S. (1999) *Vibration Spectrum Analysis : A Practical Approach*, Industrial Press Inc., New York.

14. Hunt, T. (1996) *Condition Monitoring of Mechanical and Hydraulic Plant - A Concise Introduction and Guide*, Chapman & Hall.

15. Lipovszky, G., Solyomvari, K., and Varga, G. (1990) *Vibration Testing of Machines and their Maintenance*, Elsevier, New York.

16. Lyon, R.H. (1987) *Machinery Noise and Diagnostics*, Butterworths, Boston.

17. Mitchell, J.S. (1993) *Introduction to Machinery Analysis and Monitoring*, PenWel Books, Tulsa, Oklahoma.

18. Mobley, K. (1999) *Vibration Fundamentals*, Butterworth Heinemann.

19. Poulienzos, A., Stavrakakis, G. (1994) *Real Time Fault Monitoring in Industrial Processes*, Kluwer Academic Publishers.

20. Rao, J.S. (2000) *Vibratory Condition Monitoring of Machines*, CRC Press/Narosa Pub. House, Boca Raton, Florida.

21. Rao, B.K.N. (1996) *Handbook of Condition Monitoring*, Elsevier Science.

22. Rao, B.K.N. (Editor) (1993) *Profitable Condition Monitoring*, Kluwer Academic Publishers, Boston.

23. Tavner, P. (1987) *Condition Monitoring of Electrical Machines*, Research Studies Press Ltd., 1987.

24. Taylor, J.I. (2000) *Gear Analysis Handbook*, Vibration Consultants, Inc., Tampa Bay, Florida.

25. Taylor, J.I. (1994) *The Vibration Analysis Handbook*, Vibration Consultants, Inc.

26. Vas, P. (1993) *Parameter Estimation, Condition Monitoring, and Diagnosis of Electrical Machines*, Series title: Monographs in Electrical and Electronic Engineering No. 27. Oxford University Press, New York.

27. Watton, J. (1992) *Condition Monitoring and Fault Diagnosis in Fluid Power Systems*, Series Title: Ellis Horwood Series in Mechanical Engineering, E. Horwood, New York.

28. Wild, P. (1994) *Industrial Sensors and Applications for Condition Monitoring*, Mechanical Engineering Publications, London.

29. Williams, J., Davies, A., and Drake, P.R. (1994) *Condition-Based Maintenance and Machine Diagnostics*, Chapman & Hall.

30. Wouk, V. (1991) *Machinery Vibration Measurement and Analysis*, McGraw-Hill, New York.

DISTRIBUTION LIST

Los Alamos National Laboratory
Frank Addessio MS B-216
Mark Anderson MS P-946
Tony Andrade MS A-107
Bill Baker MS P-946
Matt Bement MS T-080
Irene Beyerlein MS B-216
Tom Butler MS P-946
Amanda Cundy MS P-946
Scott Doebling MS T-080
Chuck Farrar MS T-006
Mike Fugate MS B-265
Steve Girrens MS P-946
Earle Marie Hanson MS P-945
Francois Hemez MS T-006
Norm Hunter MS P-946
Don Hush MS B-265
Paul Johnson MS D-443
Cheng Liu MS G-775
Richard Mah MS A-107
Tom Meyer MS A-127
Albert Migliori MS E-536
Brett Nadler MS T-006
Gyuhae Park MS T-006
Bill Press MS A-121
Dan Prono MS F-613
John Schultze MS P-946
Devin Shunk MS P-946
Hoon Sohn MS T-006
Fred Smith MS P-946
Daniel Stinemates MS P-946
David Watkins MS M-708
Todd Williams MS B-216

Masato Abe
University of Tokyo
Dept. of Civil Engineering
Hongo 7-3-1, Bunkyo-ku
Tokyo 113-8656, Japan

Doug Adams
Purdue University
School of Mechanical Engineering,
West Lafayette, IN 47907-1077
Yoshio Akimune
Smart Structure Research Center
1-1-1 Umezono Tsukuba, Ibaraki
305-8568 Japan

Emin Aktan
Drexel University
3201 Arch Street, Suite 240
Philadelphia, PA 19104

David Alexander
General Atomics Aerospace Systems
16761 Via Del Campo Court
San Diego, CA 92127-1713

Ken Alvin
Sandia National Laboratories
M/S 0439
Albuquerque, NM 87185-5800

Grahem Archer
School of Civil Engineering
1284 Civil Engineering Building
Purdue University
West Lafayette, IN 47907-1284

Koji Asakura
Engineering Advancement Association of
Japan (ENAA)
CYD Bldg.
1-4-6 Nishi-Shinbashi
Minato-ku, Tokyo, Japan 105-0003

Doo Byong Bae
Dept. of Civil and Environmental Eng.
Kookmin University
861-1 Chongnung-dong Songbuk-gu
Seoul,136-702, Korea
Daniel Balageas

ONERA
29, Avenue de la Division Leclerc
BP 72, 92322 Chatillon, France

Etienne Balmès
Laboratoire de Mécanique des Sols,
Structures et Matériaux (MSSMat)
Ecole Centrale de Paris
92295 Chatenay-Malabry, France

Luciana Barroso
CE/TTI Building, Room 705-L
Department of Civil Engineering
Texas A&M University
College Station, TX 77845

Dominique Barthe
Aérospatiale EADS
59, Route de Verneuil
78130 Les Mureaux, France

Janice Barton
University of SouthHampton
Dept. of Ship Science
SouthHampton SO17 1BJ
UK

Jim Beck
Applied Mechanics and Civil Engineering
Caltech 104-44
Pasadena, CA 91125

Albert Benveniste
IRISA, Campus de Beaulieu
35042 Rennes, France

Mrinmay Biswas
Duke University
Dept. of Civil Engineering
Durham, NC 27706

Christian Boller
Daimler Chrysler Aerospace
Munich, D-81663
Germany

James Brownjohn
Nanyang Technological University
School of Civil and Structural Engineering
Nanyang Avenue
Singapore 639798.
Rune Brinker
Department of Building Technology and
Structural Engineering
Aalborg University
Sohngaardsholmsvej 57, DK-9000
Aalborg, Denmark

Dave Brown
University of Cincinnati
Mail Drop 72
Cincinnati, OH 45221-0072

Thomas Burton
Dept. of Mech. Engineering
Texas Tech University
Lubbock, TX, 79409-1021

John Cafeo
GM R&D Center,
Mail Code 480.106.256
30500 Mound Road
Warren, MI 48090

R. Cantieni
Uberlandstrasse 129
Dubendorf, CH-8600 Switzerland

Tom Carne
Dept. 2741
Sandia National Laboratory
Albuquerque, NM 87185-5800

Peter Cawley
Dept. of Mechanical Engineering
Imperial College
Exhibition Rd
London, SW7 2BX
UK

Sung-Pil Chang
Dept. of Civil Engineering
Seoul National University
Shilimdong, Kwanaku,
Seoul, Korea 151-742

Chih Chen Chang
Department of Civil Engineering
Hong Kong University of Science & Technology
Clear Water Bay, Kowloon
Hong Kong

Steve Chase
Federal Highway Administration
6300 Georgetown Pike
McLean, VA 22101-2296

Eu Kyeung Cho
Hyundai Engineering & Construction Co.
San1-1, Mabuk-Ri, Goosung-Myun,Yongin-Si
Kyunggi-Do, Korea, 449-910

Fu-Kuo Chang
Dept. of Aeronautics and Astronautics
Stanford University
Stanford, CA 94305

Tse-Yung Chang
Hong Kong University of Science and Technology
Civil Engineering
Clear Water Bay
Kowloon, Hong Kong

Weiling Chiang
President's Office
National Central University
Chungli, Taiwan

Franklin Cheng
University of Missouri Rolla
Dept. of Civil Eng.
Rolla, MO 65401

Dara Childs
Texas A&M University,
Mechanical Engineering Dept.,
College Station, TX 77843

Chang Keun Choi
Dep. of Civil Engineering
Korean Institute of Advanced Science and Technology
373-1, Kusong-dong, Yusong-gu,
Taejon ,KOREA, 305-701

Ken Chong
National Science Foundation
4201 Wilson Blvd., Rm. 545
Arlington, VA 22230

Anil Chopra
Earthquake Engineering Research Center
University of California
1301 South 46th St.
Richmond, CA 94804

Leo Christodoulou
DARPA,
3701 N. Fairfax Drive,
Arlington, VA 22203-1714

Scott Cogan
Laboratoire de Mécanique Appliquée Raymond Chaléat (LMARC)
Université de Franche-Comté
24, Rue de l'Epitaphe
25030 Besancon, France

Jerry Conner
Room 1-290
Massachusetts Institute of Technology
77 Massachusetts Avenue
Cambridge, MA 02139

Joel Conte
Department of Structural Engineering
Jacobs School of Engineering
University of California, San Diego
9500 Gilman Dr.
La Jolla, CA 92093-0085

Fred Costanzo
Naval Surface Warfare Center
Code 661
9500 MacArthur Blvd.
West Bethesda, MD 20817

Roy Craig, Jr.
University of Texas at Austin
Aerospace Engineering and Engineering
Mechanics Dept., Mail Code C0600
Austin, TX 78712Ð1085

Eddie Crow
Penn State Applied Research Laboratory,
P. O. Box 30,
State College, PA 16804-0030

Shirley Dyke
Washington University
One Brookings Hall 1130
St. Louis, MO 63130

Dave Ewins
Imperial College
Mechanical Engineering Dept.
Exhibition Road
London SW7 2BX, UK

Andrew Facciano
Raytheon Missile Systems
Bldg 805/MS E4
1151 E. Hermans Rd.
Tucson, AZ 85706

Spilios D. Fassois
Stochastic Mechanical Systems (SMS)
Department of Mechanical and
Aeronautical Engineering
University of Patras
265 00 Patras, Greece

Gregory Fenves
Department of Civil and Environmental
Engineering, MC 1710
University of California
Berkeley, CA 94720-1710

Mike Friswell
Dept. of Mechanical Engineering
University of Wales, Swansea
Singleton Park,
Swansea, SA2 8PP
UK

Claus-Peter Fritzen
Institute of Mechanics and Automatic Control
University of Siegen
Paul-Bonatz-Str. 9-11
D-57068 Siegen, Germany

Ephrahim Garcia
DARPA
Dense Science Office
3701 N. Fairfax Dr.
Arlington, VA 22203-1714

Luigi Garibaldi
Dipartimento di Meccanica
Politecnico di Torino
Corso Duca degli Abruzzi, 24
10129 Torino, Italy

Lothar Gaul
Institut A fur Mechanik
Universitat Stuttgart
Pfaffenwaldring 9
70550 Stuttgart, Germany

Michel Géradin
Joint Research Center
European Laboratory for Structural
Assessment (ELSA)
TP 480, IPSC
21020 Ispra, Italy

Steve Glaser
University of California, Berkeley,
Dept of Civil & Environmental Eng.
Berkeley, CA 94720-1710

Jean-Claude Golinval
Université de Liège
Département d'Aérospatiale, Mécanique
et Matériaux
Institut de Mécanique et Génie Civil
1, Chemin des Chevreuils, B52/3
4000 Liège, Belgium

Christian U. Grosse
Dept. of Construction Materials
University of Stuttgart
Pfaffenwaldring 4
D-70550 Stuttgart
Germany

Michael Grygier
NASA Johnson Space Center ES43
Houston, TX 77058

Alfredo Guemes
UPM
ETSI Aeronautics
Madrid, 28016
Spain

Edward F. Hart
Advanced MicroMachines
Goodrich Corporation
11000 Cedar Av. #240
Cleveland, OH 44106-3052

Joe Hammond
Inst. of Sound and Vibration Research
University of SouthHampton
SO17 1BJ
SouthHampton, UK

Kurt Hansen
Dept. of Energy Engineering
Technical University of Denmark
Building 404, DTU
DK 2800 Lyngby
Denmark

Nicholas Haritos
Dept. of Civil and Environment Eng.
University of Melbourne
Parkville, Victoria 3052
Australia

Tim Hasselman
ACTA Inc.
2790 Skypark Drive, Suite 310
Torrance, CA 90505

Jon C. Helton
Sandia National Laboratories
P.O. Box 5800, Mail Stop 0779
Albuquerque, NM 87185-0779

Lawrence Hjelm
Hjelm Engineering, Consultant,
2030 W. Alex Bell Rd.,
Dayton, OH 45459-1164

Dan Inman
Virginia Polytechnic Institute of State Univ.310
New Engineering Building
Mail code 0261
Blacksburg, VA 24061-0219

Bill Hardmen
Naval Air Systems Command
Building 106, Unit 4
22195 Elmer Road
Patuxent River, MD 29670-1534

Gary F. Hawkins
Space Materials Laboratory
Aerospace Corporation
2350E. El Segundo Bl.
El Segundo, CA 90245-4691

Andy Hess
Suite 600
1214 Jefferson Davis Highway
Arlington, VA 22202-4303

Roy Ikegami
The Boeing Company
POB. 3707 MC 84-09
Seattle, WA 98124-2207

Jeong Hwan Jang
EJTECH CO. LTD.
5th Floor, Seoweon Building, 2-44
YangJae-Dong, Seocho-Gu, Seoul, Korea
Daniel Kammer
University of Wisconsin-Madison
Dept. of Engr. Mech. and Astronautics
3352 Engr. Hall, 1415 Johnson Drive
Madison, WI 53706

Tom Kashanganki
University of Maryland
SMART Materials and Structures Res. Center
College Park, MD 20742

Tom Kenny
Stanford University,
Department of Mechanical Engineering,
Terman 540, MC 4021,
Stanford, CA 94305-4021

Klaus Kerkhoff
Staatliche Materialprufungsanstalt
Universitat Stuttgart
D-70569 Stuttgart (Vailhingen)
Germany

Chul Young Kim
Dept. of Civil & Environmental Engineering
Myong Ji University
San 38-2, Nam-dong, Yongin-si
Kyunggi-do, 449-728, Korea

Hyoung-Man Kim
The Boeing Company
M/S: HB2-10
13100 Space Center Blvd
Houston, TX 77059

Jae Kwan Kim
Dept. of Civil Engineering
Seoul National University
Shilimdong, Kwanaku,
Seoul, Korea 151-742

Nam Sik Kim
Hyundai Eng. & Construction Co. Ltd.
San1-1, Mabuk-Ri, Goosung-Myun, Yongin-Si
Kyunggi-Do, Korea, 449-910

Anne Kiremidjian
Department of Engineering
Stanford University
Terman Engineering Center 238
Stanford, CA 94305-4020

Hyun Moo Koh
Dept. of Civil Engineering
Seoul National University
Shilimdong, Kwanaku,
Seoul, Korea 151-742

John Kosmatka
University of California San Diego
Department of AMES
San Diego, CA 92093-0085

Christian Kot
Argonne National Laboratory
9700 South Cass Ave. RE/331
Argonne, IL 60439-4817

Paul Kulowitch
Naval Air Systems Command,
Naval Air Warfare Center Aircraft Division,
48066 Shaw Rd., Bldg. 2188, Unit 5,
Patuxent, MD 20670

Everett Kuo
Ford Research Laboratory
P.O. Box 2053/MD2122
Dearborn, MI 48121

Pierre Ladevèze
Laboratoire de Mécanique et Technologie de Cachan (LMT)
61, Avenue du Président Wilson
94235 Cachan, France

Tom Lang
Proctor and Gamble Co.
8256 Union Centre Blvd.
West Chester, OH 45069

Charles Larson
Boeing
MS.H013-C326
5301 Bolsa Avenue
Huntington Beach, CA 92649

Jim Larson
Air Force Research Laboratory,
AFRL/MLLMN
Wright-Patterson Air Force Base, OH 45433
Kincho Law
Dept. of Civil Engineering
Stanford University
Stanford, CA 94305-4020

Eui Lee
Naval Air Systems Command,
MS-5, Bldg. 2188,
Patuxent River, MD 20670

George Lee
Multidisciplinary Center for Earthquake Engineering Research
SUNY at Buffalo
Red Jacket Quadrangle
Buffalo, NY 14261-0025

H. S. Lew
NIST
Bldg. 226, Rm B168
Gaithersburg, MD 20899

Zhong Liang
University of Buffalo
Dept. of Mechanical and Aerospace Eng.
141 Ketter Hall
Buffalo, NY 14260

Nick Lieven
Dept. of Aerospace Engineering
University of Bristol, Queen's Bldg.
Bristol, BS8 1TR, UK

Tae W. Lim
University of Kansas
Dept. of Aerospace Engineering
2004 Learned Hall
Lawrence, KS 66045

Michael Link
Universitat Gesamthochschule Kassal
Fachbereich 14
Bauingenienurwesen, Fachgebiet Leichtbau
Monchebergstr. 7
D-34109 Kassal
Germany

Shih-Chi Liu
National Science Foundation
4201 Wilson Blvd.
Arlington, VA 22230

Richard Livingston
Federal Highway Administration
6300 Georgretown Pike, HRD1-12
McLean, Va 22101

Yevgeny Macheret
Science and Technology Division
Institute for Defense Analyses
4850 Mark Center Drive
Alexandria, Virginia 22311-1882

Georges Magonette
European Laboratory for Structural Assessment (ELSA)
Institute for the Protection and Security of the Citizen
T.P. 480 1-21020 (VA), Italy

Nuno Maia
IDME/IST
Av. Rovisco Pais
1096 Lisboa Codex
Portugal

Fred Mannering
Civil Engineering Department
Purdue University
550 Stadium Mail Drive
West Lafayette, IN 47907-1284

Dave Martinez
Sandia National Laboratories
M/S 0439
Albuquerque, NM, 87185-5800

Sami Masri
University of Southern California
Department of Civil Engineering
MC 2531
Los Angeles, CA 90089-2531

Peter Matic
Naval Research Laboratory, Multifunctional
Materials Branch
Code 6350
Washington, DC 20375

Randy Mayes
Sandia National Laboratories
MS0557
PO Box 5800
Albuquerque, NM 87185

David McCallen
Center for Complex Distributed Systems
Lawrence Livermore National Laboratory
Livermore, CA 94550

Ken McConnell
Iowa State University
3017 Black Eng. Bldg.
Ames, Iowa 50011

Ray Meilunas
Naval Air Systems Command,
Unit 5.Bldg. 2188,
Patuxent River, MD 20670

Laurent Mevel
Université de Valenciennes et du
Hainaut-Cambrésis
LAMIH—DEV, Le Mont Houy
59313 Valenciennes, France

Akira Mita
Graduate School of Science and Technology,
Keio University
8-14-1 Hiyoshi, Kohoku-ku
Yokohama 223-8522
Japan

Jack Moehle
University of California
Department of Civil Engineering
775 Davis Hall
Berkeley, CA 94720

Julio M. Montalvao e Silva
IDME/IST
Av. Rovisco Pais
1096 Lisboa Codex
Portugal

Denby Morrison
Shell E&P Technology Company
Ocean R&D, Bellarie Technology Center
P.O. Box 481
Houston, TX 7700

John Mottershead
Dept. of Engineering
Brownlow Hill
University of Liverpool
Liverpool, L69 3GH
UK

Yi-qing Ni
Department of Civil and Structural Engineering
Hung Hom, Kowloon, Hong Kong

Robert Nigbor
Department of Civil Engineering
University of Southern California
Los Angeles, CA 90089-2531

Ozden Ochoa
Offshore Technology Research Center
1200 Mariner Dr.
Texas A&M University
College Station, TX 77845

Roger Ohayon
Conservatoire National des Arts et Métiers (CNAM)
Laboratoire de Mécanique des Structures et Systèmes Couplés
2, Rue Conté
75003 Paris, France

Wally Orisamolu
United Technologies Research Center
411 Silver Lane, MS 129-73
East Hartford, CT

Roberto Osegueda
The University of Texas at El Paso
Department of Civil Engineering
El Paso, TX 79912

Yves Ousset
ONERA
29, Avenue de la Division Leclerc
BP 72, 92322 Chatillon, France

Tom Paez
Sandia National Laboratories,
MS0557, Departments 9124,
9126
Albuquerque, NM 87185

Richard Pappa
NASA Langley Research Center
MS 230
Hampton, VA 23681

Gerard Pardoen
University of California-Irvine
101 ICEF-Civil Eng.
Irvine, CA 92717

K. C. Park
Center for Aerospace Structures
University of Colorado, Boulder
Campus Box 429
Boulder, CO 80309-0429

Alexander Parlos
Texas A&M University,
Mechanical Engineering,
Mail Stop 3123
College Station, TX 77843

Airan Perez
Office of Naval Research
ONR 332
800 North Quincy St.
Arlington, VA 22217-5660

Lee Peterson
Center for Aerospace Structures
University of Colorado, Boulder
Campus Box 429
Boulder, CO 80309-0429

Chris L. Pettit
AFRL/VASD
2210 Eighth Street, Building 146
Wright-Patterson Air Force Base
Wright-Patterson AFB, OH 45433-7532

Charlie Pickrel
Structural Dynamics Laboratory
Boeing Commercial Airplanes Group
Mail Code 1W-06, P.O. Box 3707
Seattle, WA 98124-2207

Christophe Pierre
Mechanical Engineering Department
The University of Michigan
1014-D Rackham
Ann Arbor, MI 48109-1070

Darryll J. Pines
Dept. of Aerospace Engineering
Rm 3154 Engineering Classroom Bldg
University of Maryland
College Park, MD 20742

Don Rabern
Embry-Riddle Aeronautical University
3700 Willow Creek Road
Prescott, AZ 86301

Bob Randall
School of Mechanical/Manufacturing Engineering
University of New South Wales,
Sydney 2052 Australia

Bruce Rasmussen
Air Force Research Laboratory
AFRL/MLLMN
2941 P. St., B652, R121,
Wright-Patterson Air Force Base, OH 45433

Erik Rasmussen
Naval Surface Warfare Center
Code 65
9500 MacArthur Blvd.
West Bethesda, MD 20817

Mark Richardson
Vibrant Technology, Inc.
18141 Main Street
Jamestown, CA 95327

Jim Ricles
Lehigh University
Department of Civil Engineering
117 ATLSS Drive, H Building
Bethlehem, PA 18015-4729

Amy Robertson
Hytec, Inc.
4735 Walnut, Suite W-100
Boulder, CO 80301

Romualdo Ruotolo
Dip. Ingegneria Aeronautica e Spaziale
Politecnico di Torino
10100 Torino
Italy

Erdal Safak
U.S. Geological Survey
DFC, Box 25046, MS.966
Denver, CO 80225

Masoud Sanayei
Tufts University
Dept. of Civil and Env. Engineering
Medford, MA 02155

Paul Sas
Katholieke Universiteit Leuven
Mechanical Engineering Dept.
Celestijnenlaan 300B
B-3001 Herverlee
Belgium

Buc Schreyer
1105 Lawrence, NE,
Albuquerque, NM 87123

Len Schwer
Schwer Engineering and Consulting
6122 Aaron Court
Windsor, CA 95492

Frieder Seible
Jacobs School of Engineering
University of California, San Diego
9500 Gilman Dr.
La Jolla, CA 92093-0085

Bob Shumway
Division of Statistics
Univ. of California, Davis
Davis, CA 95616

Suzanne Smith
University of Kentucky
Department of Engineering Mechanics
467 Anderson Hall
Lexington, KY 40506-0046

Jay R. Snyder
Victory Systems
POB 2191
Woodbridge, VA 22195
Cecily Sobey
Earthquake Engineering Research Center
Library
Gift & Exchange Dept.
University of California/RFS 453
1306 South 46th Street
Richmond, CA 94804-4698

Ian Stanley
Kinemetrics, Inc.
222 Vista Ave.
Pasadena, CA91107

David Stoffer
University Of Pittsburgh
Department of Statistics
Pittsburgh, PA 15260

Norris Stubbs
Texas A&M University
Department of Civil Engineering
Mechanics & Materials Center
College Station, TX 77843-3136

David Swanson
Penn State Applied Research Laboratory,
P.O. Box 30, N. Atherton Street,
State College, PA 16804-0030

Mike Todd
Dept. of Structural Engineering
University of California, San Diego
409 University Center
Mail Code 0085
La Jolla, CA 92093-0085

Geoff Tomlinson
The University of Sheffield
Dept. of Mechanical and Process Engineering
PO Box 600
Mappin St, Sheffield S1 4DU UK

Pavel Trivailo
RMIT University
226 Lorimer St.
Fishermen's Bend 3207 Victoria
GPO Box 2476V
Melbourne 3001 Victoria Australia

Ward Turner
Exxon Production Research Company
P.O. Box 2189
Houston, TX 77252

Herman Van Der Auweraer
LMS International
Interleuvenlaan 68
B-3001 Leuven, Heverlee
Belgium

C. E. Ventura
The University of British Columbia
Dept. of Civil Engineering
2324 Main Mall
Vancouver, B.C.
Canada, V6T 1Z4

Tim Vik
Caterpillar, Inc.
Tech Center Bld K, P.O. Box 1875
Peoria, IL 61656-1875

Sara Wadia-Fascetti
Northeastern University
Dept. of Civil Engineering
443 Shell Engineering Center
Boston, MA 02115

Gunnar Wang
Norwegian Defense Research Est.
P.O. Box 25
N-2007 Kjeller, Norway

Ming Wang
Dept. of Civil and Material Engineering (M/C 246)
College of Engineering
842 West Taylor St.
Chicago, Illinois 60607-7023

Semyung Wang
Aerospace System Design Lab
School of Aerospace Engineering Technology
Georgia Institute of Technology
Atlanta, GA 30332-0150

W. Jason Weiss
School of Civil Engineering
Purdue University
550 Stadium Mall Drive
West Lafayette, IN 47907-2051

Ed White
Boeing
P.O. Box 516
St. Louis, MO 63166

Al Wicks
Mechanical Engineering Department
Virginia Tech. Univ.
Blacksburg, VA 24061-0238

Felix S. Wong
Weidlinger Associates
4410 El Camino Real, Suite 110
Los Altos, CA 94022-1049

Shi-Chang Wooh
Room 1-272
Massachusetts Institute of Technology
77 Massachusetts Avenue
Cambridge, MA 02139

Keith Worden
The University of Sheffield
Department of Mechanical and Process Engineering
PO Box 600
Mappin St
Sheffield, S1 3JD UK

Fan Wu
Risk Management & Solutions, Inc.
149 Commonwealth Drive
Menlo Park, CA 94025

J. T. P. Yao
Dept. of Civil Engineering
Texas A&M University
College Station, TX 77843-3136

T. Glenn Yuguchi
Raytheon Missile Systems
POB 11337
TU/807/C5
Tucson, Arizona 85734-1337

Chung-Bang Yun
Dept. of Civil Engineering
Korean Institute of Advanced Science and Technology
373-1, Kusong-dong, Yusong-gu,
Taejon, KOREA, 305-701

Dave Zimmerman
University of Houston
Department of Mechanical Engineering
Houston, TX 77204-4792

Andrei Zagraia
Davidson Laboratory, Stevens Institute of Technology
711 Hudson St. Hoboken, NJ 07030